

final report

Project code: B.FLT.0147

Prepared by: Nigel Perkins – AusVet Animal Health Services Pty Ltd
Peter Watts – FSA Consulting
Shahbaz Mushtaq, Torben Marcussen, Roger Stone -
University of Southern Queensland
John Gaughan – University of Queensland
Ian Perkins - Livestock and Property Management QLD
Richard Shephard - Herd Health Pty Ltd

Date published: July 2015

ISBN: 9781741919288

PUBLISHED BY

Meat & Livestock Australia Limited
Locked Bag 991
NORTH SYDNEY NSW 2059

Impact of increased climate variability on Australian feedlots

Meat & Livestock Australia acknowledges the matching funds provided by the Australian Government to support the research and development detailed in this publication.

This publication is published by Meat & Livestock Australia Limited ABN 39 081 678 364 (MLA). Care is taken to ensure the accuracy of the information contained in this publication. However MLA cannot accept responsibility for the accuracy or completeness of the information or opinions contained in the publication. You should make your own enquiries before making decisions concerning your interests. Reproduction in whole or in part of this publication is prohibited without prior written consent of MLA.

Abstract

This project was undertaken to investigate the effects of possible future climate scenarios for each of the five major feedlot regions in Australia with a particular focus on management of effluent and water reticulation and on excessive heat load events (EHL). The project involved generation of predicted climate data for five locations across Australia representing the geographic distribution of feedlots within the country, and comparing patterns of change to historic climate data for the same locations.

All climate models showed a gradual and progressive rise in temperature over time (2010-2099) at all locations with the increase generally being higher as the severity of climate change was increased from mild to severe at each location. Rainfall changes were less consistent and some locations showed a reduction in average annual rainfall over time while others showed some increase and generally more variability. There was little evidence of any increase in risk of pond overtopping under any predicted climate scenario with the exception of one location (northern NSW) and under the most severe climate change scenario when pond overtopping rates increased.

There was a progressive rise in the risk of excessive heat load events and associated heat stress in feedlot animals over time, at all locations. When current risk mitigation strategies were applied these effects were all reduced to the levels similar to historic patterns. Drinking water requirements rose at all locations over time and under all climate change scenarios while water runoff volumes tended to decline and become more variable. These findings indicate that heat load management and prevention and water security will become more important in the future.

Executive summary

This project was undertaken to investigate the effects of possible future climate scenarios for each of the five major feedlot regions in Australia with a particular focus on management of effluent and water reticulation and on excessive heat load events (EHL).

Objectives

1. Provide descriptions of the future climate scenarios for the five major feedlot regions of Australia to 2050 through:
 - a. Assessment of the various models used to predict climate change.
 - b. Selection of a small number of models that best fit the requirements of the study.
 - c. Utilising these models to develop predicted climate data for a range of future global warming scenarios (low, medium, high).
2. Model the impact of these scenarios on the three study aspects for feedlots located in the five regions:
 - a. Size requirements for effluent ponds, to ensure that they continue to meet the regulatory requirements that apply to pond overflows for the various states.
 - b. Requirements for cattle drinking and effluent dilution/irrigation water.
 - c. Frequency and severity of heat stress events.
3. Provide recommendations on actions that the feedlot industry should take to adapt to increasing climate variability in areas of effluent pond design, stock and reticulated water, and heat stress mitigation and management.

Methods

Selection of five locations

Five representative point locations across Australia were selected to represent the geographic distribution of Australian feedlots.

Table 1: Selected locations used in climate modelling

Region	Representative Location	Climate Zone	Seasonal Rainfall Zone	Mean Annual Rainfall
Northern New South Wales	Caroona	Warm summer, cool winter	Summer	600 mm
Central Queensland	Comet	Hot dry summer, mild winter	Summer	589 mm
Southern Queensland	Dalby	Warm summer, cool winter	Summer	632 mm
Central New South Wales	Leeton	Warm dry summer, cool winter	Uniform	421 mm
South-West Western Australia	Narrogin	Warm dry summer, cool winter	Winter	522 mm

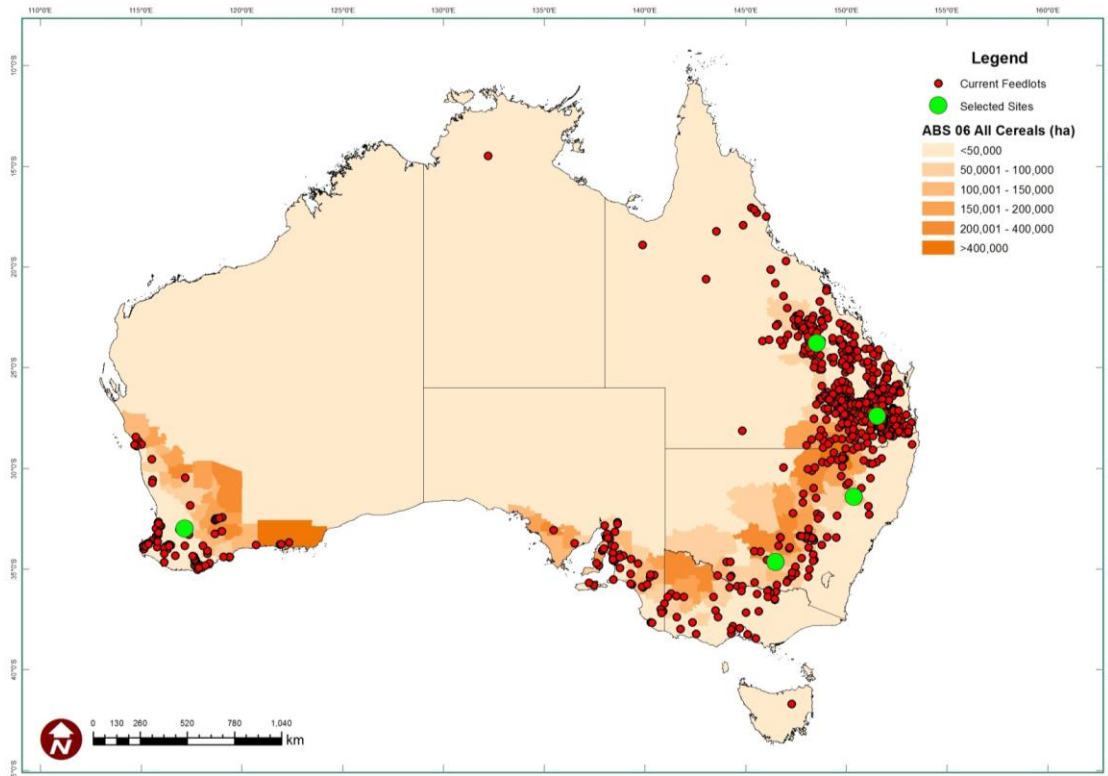


Figure 4.1: Map of Australia showing the grain belt (shading), locations of feedlots (red dots) and selected modelling locations (green circles).

Selection of climate models

Climate models developed through the 5th Assessment Report (AR5), of the Intergovernmental Panel on Climate Change (IPCC) were reviewed in detail by team members from the Australian Centre for Sustainable Catchments (ACSC).

Five General Circulation Models (GCMs) were selected for use in this study based on suitability for representing Australian climate change and ability to generate predicted climate data at the level of

detail required for feedlot hydrology (daily climate data) and heat load (hourly climate data) modelling.

The five GCMs selected for generation of all predicted climate data for this report included:

- **HadGEM2-ES:** Hadley Centre for Climate Prediction and Research/Met Office (Exeter, United Kingdom);
- **CNRM-CM5:** Centre National de Recherches Meteorologiques (Toulouse, France);
- **GFDL-ESM2G:** Geophysical Fluid Dynamics Laboratory (Princeton, USA);
- **MIROC5:** Atmosphere and Ocean Research Institute (The University of Tokyo, Japan);
- **MRI-CGCM3:** Meteorological Research Institute (Tsukuba-city, Ibaraki, Japan).

Each GCM was parameterised at each of three different *scenarios* to represent different levels of greenhouse gas concentration trajectories derived from the IPCC AR5 report, called Representative Concentration Pathways (RCPs). The RCPs are based on possible ranges of radiative forcing measured in watts per square meter (W/m^2) in the year 2100 and represent mild (RCP2.6), moderate (RCP4.5) and high (RCP8.5) greenhouse gas concentrations. These three scenarios are intended to represent mild, moderate or severe levels of adverse effects of climate change into the future.

Historic SILO data

Historic SILO records for climate variables recorded at daily intervals for each of the five selected locations for the period from 1900-2009 were sourced from The Long Paddock website maintained by the Science Delivery Division of the Queensland Department of Science, Information Technology, Innovation and the Arts (DSITIA). These historic data were used for preliminary assessments of GCM suitability and for comparative historic runs to assess impacts of climate change.

Generation of climate datasets

Predicted climate datasets were generated at each combination of the following factors:

- Location: Caroon, Comet, Dalby, Leeton, Narrogin;
- GCM: five models (CNRM, GFDL, HAD, MIR, MRI);
- RCP scenarios: RCP2.6, RCP4.5, RCP8.5; and,
- Time periods: two time periods (2010-2049, 2050-2099).

Predicted daily climate data were combined with historic SILO data for each location for the period 1900-2010 to generate a daily climate dataset for each location that spanned the period from 1900-2099. This allowed comparisons at each location between historic data (1900-2010) with predicted future data for each of three RCP scenarios across two future time periods (2010-2049 and 2050-2099).

Historic SILO records do not provide data at hourly time steps. As a result, hourly data used for heat load modelling and for water intake modelling, were generated through the GCMs for both historic (1960-1999) and future time windows (2010-2049, 2050-2099).

General summary of future climate scenarios

Summary plots and tables of rainfall and temperature were generated for historic periods (1900-2009) and predicted climate periods (2010-2049 and 2050-2099) to provide general indications of likely future changes in these measures at each location and for each RCP scenario.

Feedlot hydrology modelling

Feedlot hydrology modelling was completed by Feedlot Services Australia (FSA) staff using the feedlot module within the Model for Effluent Disposal using Land Irrigation or MEDLI model.

MEDLI models the effluent cycle from effluent production in an enterprise through to disposal. The feedlot module allows detailed parameterisation of cattle feedlots to model feedlot pad moisture and runoff. These data are exported from the feedlot module into the main MEDLI program which then uses feedlot waste as an effluent stream input into a treatment pond / effluent irrigation system.

The initial setup of MEDLI required development of a representative “standard”, Class 1, 10 000 SCU feedlot for each location, based on industry knowledge and existing datasets on individual feedlots at each modelled location. Input parameters included specification of diet inputs and manure generation for each feedlot, and incorporated location-specific knowledge concerning likely markets, cattle types and common feedstuffs. Manure excretion rates were estimated using a spreadsheet tool called BEEFBAL, as a component of modelling runoff volumes.

Once the feedlot parameters were defined the MEDLI model was ready to be run with daily climate data as inputs (rainfall, minimum and maximum daily temperature, solar radiation and evapotranspiration).

Initial iterations of the MEDLI modelling were run at each location using the feedlot parameters for that location and using historic SILO climate data for a 100-year period (1910-2009) also for that location. Iterations were run with adjustment of effluent pond dimensions until pond overtopping occurred on fewer than ten occasions in the 100-year period, indicating compliance with the National Guidelines for Beef Cattle Feedlots in Australia (MLA, 2012). All MEDLI parameters were then fixed for that location and then modelling was run with the predicted climate datasets to determine the effect of future climate scenarios on overtopping frequency and runoff estimates.

MEDLI modelling required 100 years of daily data and the GCMs generated 90 years of future climate data (2010-2099) for each location-scenario combination. Datasets covering 100 years (2000-2099) were constructed by adding ten years of daily data from the SILO historic data for each location (2000-2009) to the 90 year data from GCM models for each scenario (2010-2099).

Feedlot hydrology (MEDLI) model outputs included overtopping frequency and summary statistics on rainfall, evaporation and runoff. There was particular interest in comparative measures of pond

overtopping frequency and effluent runoff between the historic period for each location (1910-2009) and the future period (2000-2099) for each of the three RCP scenarios.

Accumulated heat load modelling

Accumulated heat load modelling was completed by Dr John Gaughan, University of Queensland (Gaughan et al, 2008).

The five selected GCMs were used to generate predicted climate data at hourly time-steps for each combination of location and RCP scenario for two future time periods (2010-2049 and 2050-2099). In addition, GCM models were used to predict climate data at hourly time steps under a control RCP scenario equivalent to the existing 20th century levels of radiative forcing for the time period 1960-1999. This provided a 40-year predicted historic dataset used for comparative purposes to assess the impact of future climate change on heat load measures.

Hourly predicted climate data were generated for black globe temperature, relative humidity, solar radiation and wind speed. Wind speed was calculated from the Northward Near-Surface Wind and the Eastward Near-Surface Wind values and could only be generated in GCM output at a daily time step. Post-processing by ACSC was used to derive hourly wind speed values for each dataset.

Hourly climate data were then processed to generate heat load index (HLI) values (Gaughan et al. 2008) and these in turn were used to generate accumulated heat load (AHL) values. Baseline thresholds for heat accumulation and dissipation were based on industry standards (healthy, black Angus steer, 100 days on feed with a body condition score of 4+ and no access to shade).

AHL estimates were generated under each of four different heat load mitigation strategies based on modifying the upper and lower HLI thresholds which in turn influence accumulation and dissipation of heat by animals. The four heat load mitigation strategies were defined as:

- Control: the standard reference animal defined in HLI development as having a lower HLI threshold of 77 and an upper HLI threshold of 86.
- Mild mitigation: HLI lower=84 and HLI upper=89, representing the standard baseline animal with 1-2 m²/SCU shade provided in the feedlot pens.
- Moderate mitigation: HLI lower=84 and HLI upper = 93, representing an increase in HLI upper of +7 units, achievable through extra shade (3-5 m²/SCU) or by other strategies such as heat tolerant genotypes.
- Maximal mitigation: HLI lower=84 and HLI upper=96, representing maximum possible mitigation either through any combination of shade and other management strategies or by switching genotype from *Bos taurus* to purebred *Bos indicus*.

Outputs were presented in summary plots showing the median days per year when AHL exceeded a defined threshold under various scenarios and mitigation strategies, and tables of summary statistics.

Water intake modelling

Water intake (litres per head per day) was predicted using a formula published by Parker et al (2000) and requiring climate data inputs (maximum daily temperature and minimum daily relative humidity) derived from predicted hourly climate datasets generated for AHL modelling. This approach was selected based on previous Australian work assessing water intake in cattle feedlots and on preliminary model assessment performed in this study.

Output summaries are presented in graphical and tabular form using median daily water intake (L/hd/day) and maximal daily water intake (L/hd/day) as the primary measures and comparing historic values (1960-1999) to future predictions for different RCP scenarios. Larger-scale trends in water usage over time were summarised as megalitres of water per 1,000 head per year.

Feedlot runoff

The MEDLI model runs used for feedlot hydrology modelling generated a daily estimate of feedlot runoff (mm / day) as part of the standard model outputs. Comparative assessment of feedlot runoff changes over time under different climate change scenarios were analysed in this report to provide an indication of the broad direction and magnitude of future changes in surface water availability. This information is useful in considering design options for effluent ponds in the future against varying uses such as managing effluent to avoid overtopping and providing water that may be used in the feedlot (following appropriate recycling and treatment programs) or used in land-irrigation systems.

Annual runoff measures are presented in graphical and tabular form to provide an indication of whether feedlot runoff is increasing over time or decreasing over time (change in annual mean measures). In addition the coefficient of variation (CoV) is presented as a measure of variability. When the CoV is rising it suggests that variation in summary runoff measures is increasing relative to the mean and conversely when CoV is declining it indicates that variation is reducing relative to the mean.

Results

General summary of future climate scenarios

The mean temperature anomaly provides an indication of the expected rise in average temperature over time, compared to the average temperature for the period from 1961-1990. For the period 2010-2049, mean temperature anomaly estimates ranged from under +0.7 °C to +1.3 °C with most values clustering around +1 °C.

Compared to the 1961-1990 period the mean temperature anomaly for the period from 2050-2099 showed a rise of +0.9 to +3.6 °C depending on the scenario and location with most values ranging between +1.5 and +2 °C..

There were also rises in the number of days where the maximum daily temperature was greater than 35 °C or 40 °C when the future climate periods were compared to the 1961-1990 baseline reference period.

Rainfall patterns showed more variability over time. There were some situations where rainfall increased substantially and others where rainfall appeared to decline.

Some locations showed consistent changes in rainfall. Comet and Narrogin showed a decline in average rainfall that appeared to get progressively worse from historic to 2010-2049 and then to 2050-2099.

Dalby and Leeton also showed a decline in rainfall over time that was less obvious than Comet and Narrogin.

Feedlot hydrology modelling

The key output from feedlot hydrology modelling using the MEDLI modelling framework was the estimates of pond overtopping frequency under different levels of climate change.

Table 2: Summary of pond overtopping occurrence in the historic period and at each of the five locations under different combinations of model and scenario.

Source	Period	Scenario	Caroona	Comet	Dalby	Leeton	Narrogin
			Overtopping events per 100 years				
SILO (1910-2009)	1910-2009	Historic control	9	9	9	9	9
CNRM-CM5	2000-2099	RCP2.6	4	9	4	0	0
GFDL-ESM2G	2000-2099	RCP2.6	4	6	4	0	0
HadGEM2-ES	2000-2099	RCP2.6	10	3	8	0	0
MIROC5	2000-2099	RCP2.6	10	3	9	0	0
MRI-CGCM3	2000-2099	RCP2.6	9	3	5	2	0
CNRM-CM5	2000-2099	RCP4.5	8	9	10	0	1
GFDL-ESM2G	2000-2099	RCP4.5	4	7	6	0	0
HadGEM2-ES	2000-2099	RCP4.5	11	6	5	0	0
MIROC5	2000-2099	RCP4.5	14	7	12	0	0
MRI-CGCM3	2000-2099	RCP4.5	7	4	7	0	0
CNRM-CM5	2000-2099	RCP8.5	22	5	5	0	1
GFDL-ESM2G	2000-2099	RCP8.5	17	6	7	0	0
HadGEM2-ES	2000-2099	RCP8.5	32	5	5	0	0
MIROC5	2000-2099	RCP8.5	43	5	17	0	0
MRI-CGCM3	2000-2099	RCP8.5	39	3	8	1	0

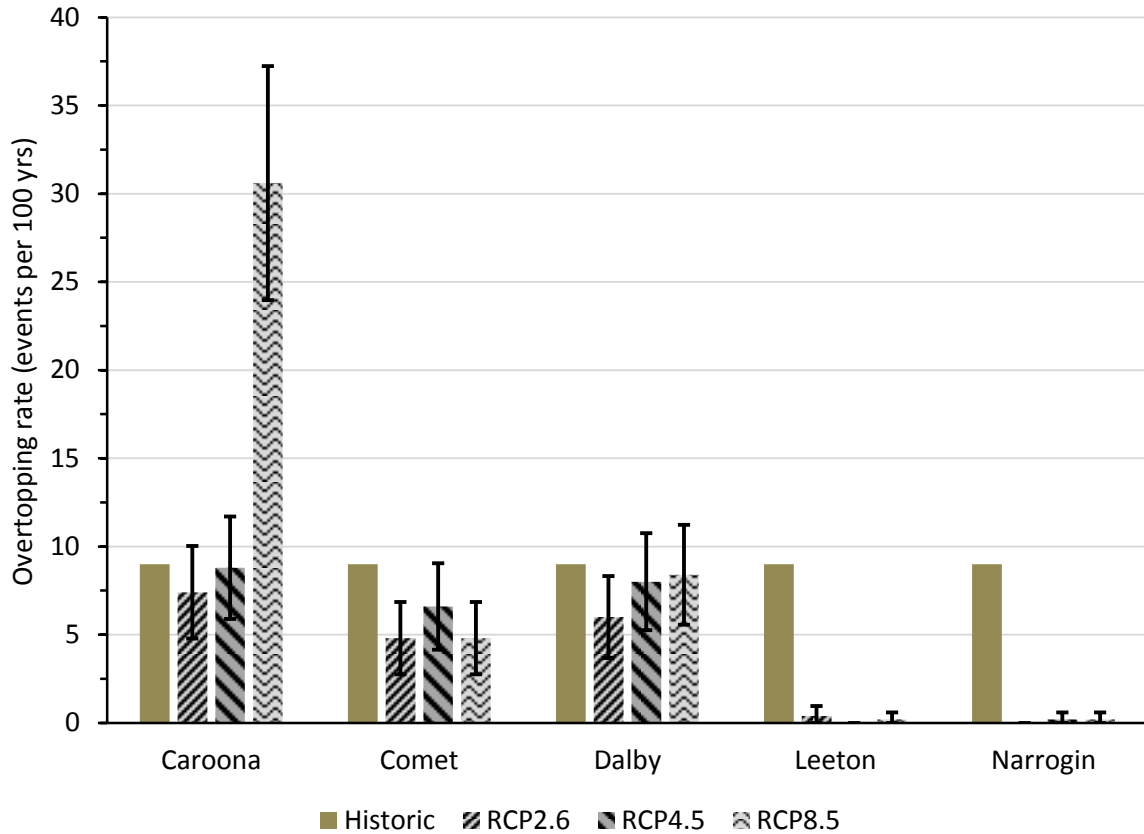


Figure 1: Plot of mean overtopping rate (events per 100 years) for each location and scenario (historic, RCP2.6, RCP4.5 and RCP8.5). Bars represent 95% confidence intervals either side of the mean.

There was no difference in overtopping rate over time at Comet and Dalby, suggesting that current approaches to determining pond dimensions are likely to be appropriate for the foreseeable future.

There was a substantial decline in pond overtopping rates at Leeton and Narrogin over time.

The pond overtopping rate at Caroona showed no change in overtopping rate from the historic control for the RCP2.6 and 4.5 scenarios but there was a large increase in the rate of pond overtopping under the RCP8.5 scenario (from 9 per 100 years to 31 per 100 years, $p < 0.05$).

Rainfall records for Caroona show that average annual rainfall increased in the 2050-2099 period and there was an increase in the number of days when heavier falls of rain were recorded compared to the historic period and this may explain the increased frequency in overtopping events under this scenario.

The findings suggest that there is little evidence to support changes in the guidelines with respect to holding pond dimensions. If the level of climate change experienced in the future is more consistent with the RCP8.5 scenario then there may be justification in revisiting the guidelines for some areas such as northern NSW (Caroona) because of possible risks of overtopping.

Accumulated heat load modelling

There was considerable variation in heat load risk between the five different locations and the three different scenarios. At all locations there was a progressive rise in AHL measures from RCP2.6 through RCP4.5 and to RCP8.5. A large amount of detailed results for locations, models and scenarios is presented in the main report and further details are provided in the separate report of Appendices to the main report.

The number of days per year when AHL was greater than a defined threshold was used as a simple summary measure for comparisons. Expressing the heat load as the number of days of AHL>100 per 10-year period in each of the time periods of interest (historic, 2010-2049 and 2050-2099), allowed direct comparison of the risk of heat load between locations and scenarios and under different mitigation strategies.

Table 3: Summary of number of heat load days per 10-year period for each combination of location, scenario, time period and mitigation strategy.

Location	1960-99					2050-2099				
	Mitigation strategies					Mitigation strategies				
	None	Mild	Mod	Max	None	Mild	Mod	Max		
Number of days per 10 years when AHL>100, across all models										
Caroona										
RCP2.6	0.8	6.7	0.7	0.2	0.2	28.8	7.3	1	0.3	
RCP4.5	0.8	7.1	1.1	0.4	0.2	54.8	13.7	2.6	0.4	
RCP8.5	0.8	101.7	37.8	14.5	3.2	682.6	354.5	195.6	89.3	
RCP8.5, no CNRM-CM5		4.7	1.1	0.1	0.1	71.9	19.7	5.2	0.5	
Comet										
RCP2.6	15.2	82.8	13.4	3	0	129.2	24.8	5.6	0.1	
RCP4.5	15.2	64.5	11.6	2.3	0	339.6	82.9	15.9	1.4	
RCP8.5	15.2	596.6	247.6	94.9	23.1	2166.9	1212.4	764.3	370.1	
RCP8.5, no CNRM-CM5		45.4	9.3	2.1	0.1	470.5	146.8	51.2	5.3	
Dalby										
RCP2.6	0.6	2	0	0	0	8.4	1.8	0.2	0	
RCP4.5	0.6	2.1	0.4	0	0	60.2	15.1	3.2	0.2	
RCP8.5	0.6	1.4	34	9.3	1.9	684.3	338.1	174.3	66.4	
RCP8.5, no CNRM-CM5		2.9	0.4	0	0	41.4	10	3.5	0.4	
Leeton										
RCP2.6	13.2	46.7	14.1	2.3	0.1	96.7	35.2	8.6	1.2	
RCP4.5	13.2	64.6	18.6	3.5	0.8	175.3	71.1	20.8	5.6	
RCP8.5	13.2	183	84.5	42.7	17.6	826.5	468.6	269.8	135.2	
RCP8.5, no CNRM-CM5		29.7	9	1.9	0.1	182.7	85.4	37.3	12.2	
Narrogin										
RCP2.6	0.2	0.8	0.2	0	0	1.4	0.2	0	0	
RCP4.5	0.2	1	0.2	0	0	2.4	0.4	0.1	0	
RCP8.5	0.2	19	6.6	1.8	0	100.3	44.3	18.1	7	
RCP8.5, no CNRM-CM5		0.6	0.1	0	0	4.2	0.7	0.2	0.1	

One GCM (CNRM-CM5) produced AHL estimates for some scenarios and locations that were substantially higher than other models. In these cases summary statistics were generated with and without CNRM-CM5 data included.

In all locations there was a rise in the number of heat load days per 10 years when moving from historic to RCP2.6, 4.5 and 8.5. In all cases mitigation at some level (mild, moderate or maximal) was sufficient to bring the heat load risk down to levels that were equivalent to or lower than the historic level. It is noteworthy that in several situations this required the exclusion of CNRM-CM5.

At Dalby and Narrogin, there was very little change in heat load under RCP2.6 and RCP4.5 scenarios for the period from 2010-2049 and there was a relatively small rise in heat load risk in the 2050-2099 period. For RCP8.5 at these locations there was an increased rise in heat load particularly after 2050 but much of this effect was due to the influence of the CNRM-CM5 model and when this model was filtered the rise was much less marked.

For Narrogin, the results indicate that mild or moderate mitigation strategies will be sufficient to reduce heat load effects to historic levels, depending on the RCP scenario that is being considered.

The results for all other locations suggest that moderate or maximal mitigation strategies will be required to effectively manage heat load for the period from 2050-2099, and this is only effective when the results from CNRM-CM5 models are removed from the estimations.

These findings provide useful information for revising guidelines and providing advice to feedlot managers.

Water intake modelling

Median estimated water intake levels for the historic period (1960-1999) ranged from a low in winter of 35-45 L/hd/day to a summer high of 55-65 L/hd/day. There was least variability in water intake ranges in the winter and most variability in the summer. In summer months daily water intake varied from lows around 35-40 L/hd/day to maximal daily intakes of 85-95 L/hd/day.

There was a progressive rise in predicted daily water intake from historic to 2010-49 periods and again to the 2050-99 period at each location, though the amount of the rise varied between locations and scenarios.

The median daily water intake values for the period 2010-49 rose by 1-8% across all locations when compared to the 1960-99 period. Peak water intake (represented by maximal daily intake estimates) rose by less than 10% compared to the historic period.

The same pattern was viewed in the 2050-99 period when compared to the historic period but the amount of increase in water intake was larger in the 2050-99 period compared to the increase in the 2010-49 period. There was a 3-17% increase in median daily water intake and peak daily water intake levels rose by up to 34% compared to historic levels.

Median annual water intake estimates ranged from 17-22 ML/'000 hd/yr across all scenarios and both time periods with the highest requirements occurring in the 2050-99 period and the RCP8.5 scenario.

The findings of this report indicate that water requirements will progressively rise over time under all scenarios. The rise in annual water requirements is progressively approaching 24 ML/'000 hd/yr level, particularly for the 2050-99 period.

The national guidelines currently state that, as a guide, a proposed feedlot would normally need to demonstrate access to approximately 24 ML of high-security water per annum per 1,000 SCU of feedlot capacity. These recommendations are based on total water requirements which include uses other than cattle water intake. Our findings suggest that this requirement will need to be increased in the future.

Feedlot runoff

The daily volume of runoff was used as an indicator of the potential change over time in runoff water availability at each location, by comparing runoff under various climate change scenarios for future time periods to the runoff estimates generated for the same location and using historic climate input data.

The findings suggest that with the exception of Carroona, all locations appear likely to experience a decline in annual runoff volumes over time and most of the locations are likely to have increased uncertainty about annual runoff volumes in any one year. Findings for Carroona suggest a small increase in runoff over time along with an increase in variability.

These findings are likely to be of value to feedlots considering future development plans that may involve potential land application of holding pond water (irrigation) or recycling of holding pond water for use within the feedlot.

Recommendations

- 1. It is recommended that current guidelines for management of waste and water runoff be maintained.***
- 2. It is recommended that efforts be directed at continuing to raise awareness amongst the feedlot industry about excessive heat load (EHL) and the importance of preventive and response measures including heat load mitigation strategies, monitoring and early detection of heat events and response plans to deal with short term heat events.***
- 3. It is recommended that the feedlot industry review the national guidelines with respect to requirements for access to high-security water per 1,000 SCU of feedlot capacity for future feedlot developments.***

Contents

Abstract	2
Executive Summary	3
List of Tables	21
List of Figures	31
List of Abbreviations and Terms	39
1 Introduction	41
1.1 Background	41
1.2 Project Objectives	41
2 Literature review	42
3 General overview of methodology	42
3.1 Methodology overview	42
3.2 Selection of Modelling Locations	43
3.3 Predicted climate datasets	44
3.4 Feedlot hydrology modelling	47
3.4.1 Introduction to feedlot hydrology	47
3.4.2 National feedlot guidelines for runoff control	47
3.4.3 Introduction to MEDLI	48
3.4.4 Feedlot parameterisation in MEDLI	49
3.4.4.1 Animals and feedlot diet	50
3.4.4.2 Waste Estimation	51
3.4.4.3 Waste Management	52
3.4.4.4 Controlled drainage area components	53
3.4.4.5 Holding pond design and management	53
3.4.5 Hydrology modelling using predicted climate data	55

3.5	Accumulated heat load (AHL) modelling.....	56
3.5.1	Background	56
3.5.2	Heat load index (HLI)	56
3.5.3	Accumulated heat load (AHL).....	57
3.5.4	AHL modelling.....	58
3.6	Water intake	60
3.7	Feedlot runoff.....	67
4	Results	69
4.1	Summaries of future climate scenarios.....	69
4.1.1	Temperature summaries	69
4.1.1.1	Average temperature anomaly.....	71
4.1.1.2	Caroona.....	72
4.1.1.3	Comet.....	77
4.1.1.4	Dalby	82
4.1.1.5	Leeton	86
4.1.1.6	Narrogin	90
4.1.2	Rainfall summaries	95
4.1.2.1	Caroona.....	96
4.1.2.2	Comet.....	100
4.1.2.3	Dalby	104
4.1.2.4	Leeton	108
4.1.2.5	Narrogin	112
4.2	Feedlot hydrology modelling.....	116
4.2.1	Pond overtopping rate.....	116
4.2.2	Rainfall	119
4.2.2.1	Caroona.....	119
4.2.2.2	Comet.....	122

4.2.2.3	Dalby	124
4.2.2.4	Leeton	126
4.2.2.5	Narrogin	128
4.2.3	Evaporation.....	130
4.2.3.1	Caroona.....	130
4.2.3.2	Comet.....	131
4.2.3.3	Dalby	132
4.2.3.4	Leeton	133
4.2.3.5	Narrogin	134
4.2.4	Runoff	135
4.2.4.1	Caroona.....	135
4.2.4.2	Comet.....	136
4.2.4.3	Dalby	137
4.2.4.4	Leeton	138
4.2.4.5	Narrogin	139
4.3	Accumulated heat load (AHL) modelling outputs.....	140
4.3.1	Plots of median heat load days per year	140
4.3.1.1	Caroona, RCP2.6.....	141
4.3.1.2	Caroona, RCP4.5.....	142
4.3.1.3	Caroona, RCP8.5.....	143
4.3.1.4	Comet, RCP2.6	144
4.3.1.5	Comet, RCP4.5	145
4.3.1.6	Comet, RCP8.5	146
4.3.1.7	Dalby, RCP2.6.....	147
4.3.1.8	Dalby, RCP4.5	148
4.3.1.9	Dalby, RCP8.5	149
4.3.1.10	Leeton, RCP2.6.....	150

4.3.1.11	Leeton, RCP4.5.....	151
4.3.1.12	Leeton, RCP8.5.....	152
4.3.1.13	Narrogin, RCP2.6.....	153
4.3.1.14	Narrogin, RCP4.5.....	154
4.3.1.15	Narrogin, RCP8.5.....	155
4.3.2	Tables of summary statistics for heat load days per year	156
4.3.2.1	Caroona, RCP2.6.....	159
4.3.2.2	Caroona, RCP4.5.....	163
4.3.2.3	Caroona, RCP8.5.....	167
4.3.2.4	Comet, RCP2.6	171
4.3.2.5	Comet, RCP4.5	175
4.3.2.6	Comet, RCP8.5	179
4.3.2.7	Dalby, RCP2.6.....	183
4.3.2.8	Dalby, RCP4.5.....	187
4.3.2.9	Dalby, RCP8.5.....	191
4.3.2.10	Leeton, RCP2.6.....	195
4.3.2.11	Leeton, RCP4.5.....	199
4.3.2.12	Leeton, RCP8.5.....	203
4.3.2.13	Narrogin, RCP2.6.....	207
4.3.2.14	Narrogin, RCP4.5.....	211
4.3.2.15	Narrogin, RCP8.5.....	215
4.4	Daily water intake.....	219
4.4.1	Caroona.....	219
4.4.2	Comet	226
4.4.3	Dalby.....	232
4.4.4	Leeton	238
4.4.5	Narrogin.....	244

4.5	Effluent water runoff	250
4.5.1	Caroona.....	252
4.5.2	Comet	255
4.5.3	Dalby	258
4.5.4	Leeton	261
4.5.5	Narrogin	264
5	Discussion	266
5.1	Changes to climate	267
5.2	Feedlot hydrology.....	267
5.3	Heat load.....	268
5.4	Water intake	269
5.5	Effluent water runoff	271
6	Recommendations	272
7	References	273
8	Appendices	278

List of Tables

Table 3.1: Description of selected locations used for modelling.....	43
Table 3.2: Summary of feedlot modelling locations.....	49
Table 3.3: Descriptive summary of market type and basic performance details for each location	50
Table 3.4: Description of dietary breakdown by location.....	51
Table 3.5: Manure production parameters for each location	52
Table 3.6: Pen cleaning details applied for each feedlot location	52
Table 3.7: Input values for area estimates for pen, hard and soft areas, used for all feedlot locations in MEDLI models	53
Table 3.8: Holding pond parameters at each location required to achieve an overtopping frequency of 9 events per 100 years when using a 100-year SILO climate file for each site.....	55
Table 4.1: Minimum, mean and maximum temperature anomaly based on difference between the average of five model values for each predicted climate year and the historic average for 1961-1990, reported for each location and scenario and for two different future time periods (2010-2049 and 2050-2099).....	71
Table 4.2: Summary of the count of the number of days per year when the maximum daily temperature record was greater than 35 C at location=Caroona. Based on SILO records for the period from 1900-2009 and GCM outputs for 2010-2049 & 2050-2099 from five different models run under three RCP scenarios. Location = Caroona.	74
Table 4.3: Summary of the count of the number of days per year when the maximum daily temperature record was greater than 40 C at location=Caroona. Based on SILO records for the period from 1900-2009 and GCM outputs for 2010-2049 & 2050-2099 from five different models run under three RCP scenarios. Location = Caroona.	76
Table 4.4: Summary of the count of the number of days per year when the maximum daily temperature record was greater than 35 C. Based on SILO records for the period from 1900-2009 and GCM outputs for 2010-2049 & 2050-2099 from five different models run under three RCP scenarios. Location = Comet.	80
Table 4.5: Summary of the count of the number of days per year when the maximum daily temperature record was greater than 40 C. Based on SILO records for the period from 1900-2009 and GCM outputs for 2010-2049 & 2050-2099 from five different models run under three RCP scenarios. Location = Comet.	81
Table 4.6: Summary of the count of the number of days per year when the maximum daily temperature record was greater than 35 C. Based on SILO records for the period from 1900-2009 and GCM outputs for 2010-2049 & 2050-2099 from five different models run under three RCP scenarios. Location = Dalby.....	84

Table 4.7: Summary of the count of the number of days per year when the maximum daily temperature record was greater than 40 C. Based on SILO records for the period from 1900-2009 and GCM outputs for 2010-2049 & 2050-2099 from five different models run under three RCP scenarios. Location = Dalby.....	85
Table 4.8: Summary of the count of the number of days per year when the maximum daily temperature record was greater than 35 C. Based on SILO records for the period from 1900-2009 and GCM outputs for 2010-2049 & 2050-2099 from five different models run under three RCP scenarios. Location = Leeton.....	88
Table 4.9: Summary of the count of the number of days per year when the maximum daily temperature record was greater than 40 C. Based on SILO records for the period from 1900-2009 and GCM outputs for 2010-2049 & 2050-2099 from five different models run under three RCP scenarios. Location = Leeton.....	89
Table 4.10: Summary of the count of the number of days per year when the maximum daily temperature record was greater than 35 C. Based on SILO records for the period from 1900-2009 and GCM outputs for 2010-2049 & 2050-2099 from five different models run under three RCP scenarios. Location = Narrogin.	93
Table 4.11: Summary of the count of the number of days per year when the maximum daily temperature record was greater than 40 C. Based on SILO records for the period from 1900-2009 and GCM outputs for 2010-2049 & 2050-2099 from five different models run under three RCP scenarios. Location = Narrogin.	94
Table 4.12: Monthly and annual average rainfall (mm) based on historic SILO records and on GCM outputs for five models and three scenarios for the period 2010-2049. Location = Caroona.....	98
Table 4.13: Monthly and annual average rainfall (mm) based on historic SILO records and on GCM outputs for five models and three scenarios for the period 2050-2099. Location = Caroona.....	99
Table 4.14: Monthly and annual average rainfall (mm) based on historic SILO records and on GCM outputs for five models and three scenarios for the period 2010-2049. Location = Comet.....	102
Table 4.15: Monthly and annual average rainfall (mm) based on historic SILO records and on GCM outputs for five models and three scenarios for the period 2050-2099. Location = Comet.....	103
Table 4.16: Monthly and annual average rainfall (mm) based on historic SILO records and on GCM outputs for five models and three scenarios for the period 2010-2049. Location = Dalby.	106
Table 4.17: Monthly and annual average rainfall (mm) based on historic SILO records and on GCM outputs for five models and three scenarios for the period 2050-2099. Location = Dalby.	107
Table 4.18: Monthly and annual average rainfall (mm) based on historic SILO records and on GCM outputs for five models and three scenarios for the period 2010-2049. Location = Leeton.	110
Table 4.19: Monthly and annual average rainfall (mm) based on historic SILO records and on GCM outputs for five models and three scenarios for the period 2050-2099. Location = Leeton.	111

Table 4.20: Monthly and annual average rainfall (mm) based on historic SILO records and on GCM outputs for five models and three scenarios for the period 2010-2049. Location = Narrogin.	114
Table 4.21: Monthly and annual average rainfall (mm) based on historic SILO records and on GCM outputs for five models and three scenarios for the period 2050-2099. Location = Narrogin.	115
Table 4.22: Pond overtopping frequency at each location, reported as events per 100 years, for the SILO dataset serving as an historic control and for each combination of GCM and scenario.	117
Table 4.23: Summary statistics for rainfall at Carroona derived from MEDLI modelling datasets. GCM ave / SILO is the ratio of the average across all GCM outputs for that scenario to the SILO mean value.	120
Table 4.24: Count of the number of days when daily rainfall (mm) fell within each 100-year interval at Carroona. GCM ave / SILO is the ratio of the average across all GCM outputs for that scenario to the SILO value.	121
Table 4.25: Summary statistics for rainfall at Comet derived from MEDLI modelling datasets. GCM ave / SILO is the ratio of the average across all GCM outputs for that scenario to the SILO mean value.	122
Table 4.26: Count of the number of days when daily rainfall (mm) fell within each interval at Comet. GCM ave / SILO is the ratio of the average across all GCM outputs for that scenario to the SILO value.	123
Table 4.27: Summary statistics for rainfall at Dalby derived from MEDLI modelling datasets. GCM ave / SILO is the ratio of the average across all GCM outputs for that scenario to the SILO mean value.	124
Table 4.28: Count of the number of days when daily rainfall (mm) fell within each interval at Dalby. GCM ave / SILO is the ratio of the average across all GCM outputs for that scenario to the SILO value.	125
Table 4.29: Summary statistics for rainfall at Leeton derived from MEDLI modelling datasets. GCM ave / SILO is the ratio of the average across all GCM outputs for that scenario to the SILO mean value.	126
Table 4.30: Count of the number of days when daily rainfall (mm) fell within each interval at Leeton. GCM ave / SILO is the ratio of the average across all GCM outputs for that scenario to the SILO value.	127
Table 4.31: Summary statistics for rainfall at Narrogin derived from MEDLI modelling datasets. GCM ave / SILO is the ratio of the average across all GCM outputs for that scenario to the SILO mean value.	128
Table 4.32: Count of the number of days when daily rainfall (mm) fell within each interval at Narrogin. GCM ave / SILO is the ratio of the average across all GCM outputs for that scenario to the SILO value.	129

Table 4.33: Summary statistics for evaporation (mm per year for annual summaries and mm per day for maximum daily evaporation) at Caroona, derived from MEDLI modelling datasets. GCM ave / SILO is the ratio of the average across all GCM outputs for that scenario to the SILO mean value. . 130

Table 4.34: Summary statistics for evaporation (mm per year for annual summaries and mm per day for maximum daily evaporation) at Comet, derived from MEDLI modelling datasets. GCM ave / SILO is the ratio of the average across all GCM outputs for that scenario to the SILO mean value. 131

Table 4.35: Summary statistics for evaporation (mm per year for annual summaries and mm per day for maximum daily evaporation) at Dalby, derived from MEDLI modelling datasets. GCM ave / SILO is the ratio of the average across all GCM outputs for that scenario to the SILO mean value. 132

Table 4.36: Summary statistics for evaporation (mm per year for annual summaries and mm per day for maximum daily evaporation) at Leeton, derived from MEDLI modelling datasets. GCM ave / SILO is the ratio of the average across all GCM outputs for that scenario to the SILO mean value. 133

Table 4.37: Summary statistics for evaporation (mm per year for annual summaries and mm per day for maximum daily evaporation) at Narrogin, derived from MEDLI modelling datasets. GCM ave / SILO is the ratio of the average across all GCM outputs for that scenario to the SILO mean value. . 134

Table 4.38: Summary statistics for evaporation (mm per year for annual summaries and mm per day for maximum daily evaporation) at Caroona, derived from MEDLI modelling datasets..... 135

Table 4.39: Summary statistics for evaporation (mm per year for annual summaries and mm per day for maximum daily evaporation) at Comet, derived from MEDLI modelling datasets..... 136

Table 4.40: Summary statistics for evaporation (mm per year for annual summaries and mm per day for maximum daily evaporation) at Dalby, derived from MEDLI modelling datasets 137

Table 4.41: Summary statistics for evaporation (mm per year for annual summaries and mm per day for maximum daily evaporation) at Leeton, derived from MEDLI modelling datasets 138

Table 4.42: Summary statistics for evaporation (mm per year for annual summaries and mm per day for maximum daily evaporation) at Narrogin, derived from MEDLI modelling datasets 139

Table 4.43: Summary of number of days per 10 years when AHL >100 for each location and RCP, averaged across all five models, and reported for the historic time period and for two future time periods with no mitigation and with mild, moderate and maximal mitigation strategies implemented. RCP8.5, no CNRM-CM5 refers to an average across four models with all data from one model (CNRM-CM5) removed..... 158

Table 4.44: Summary statistics for count of the number of days per year when AHL>100. Location=Caroona, RCP2.6, time periods= 1960-1999, 2010-2049, 2050-2099. No mitigation implemented..... 159

Table 4.45: Summary statistics for count of the number of days per year when AHL>100. Location=Caroona, RCP2.6, time periods= 2010-2049, 2050-2099. Mild mitigation implemented. . 160

Table 4.46: Summary statistics for count of the number of days per year when AHL>100. Location=Caroona, RCP2.6, time periods= 2010-2049, 2050-2099. Moderate mitigation implemented.....	161
Table 4.47: Summary statistics for count of the number of days per year when AHL>100. Location=Caroona, RCP2.6, time periods= 2010-2049, 2050-2099. Maximal mitigation implemented.	162
Table 4.48: Summary statistics for count of the number of days per year when AHL>100. Location=Caroona, RCP4.5, time periods= 1960-1999, 2010-2049, 2050-2099. No mitigation implemented.....	163
Table 4.49: Summary statistics for count of the number of days per year when AHL>100. Location=Caroona, RCP4.5, time periods= 2010-2049, 2050-2099. Mild mitigation implemented. .	164
Table 4.50: Summary statistics for count of the number of days per year when AHL>100. Location=Caroona, RCP4.5, time periods= 2010-2049, 2050-2099. Moderate mitigation implemented.....	165
Table 4.51: Summary statistics for count of the number of days per year when AHL>100. Location=Caroona, RCP4.5, time periods= 2010-2049, 2050-2099. Maximal mitigation implemented.	166
Table 4.52: Summary statistics for count of the number of days per year when AHL>100. Location=Caroona, RCP8.5, time periods= 1960-1999, 2010-2049, 2050-2099. No mitigation implemented.....	167
Table 4.53: Summary statistics for count of the number of days per year when AHL>100. Location=Caroona, RCP8.5, time periods= 2010-2049, 2050-2099. Mild mitigation implemented. .	168
Table 4.54: Summary statistics for count of the number of days per year when AHL>100. Location=Caroona, RCP8.5, time periods= 2010-2049, 2050-2099. Moderate mitigation implemented.....	169
Table 4.55: Summary statistics for count of the number of days per year when AHL>100. Location=Caroona, RCP8.5, time periods= 2010-2049, 2050-2099. Maximal mitigation implemented.	170
Table 4.56: Summary statistics for count of the number of days per year when AHL>100. Location=Comet, RCP2.6, time periods= 1960-1999, 2010-2049, 2050-2099. No mitigation implemented.....	171
Table 4.57: Summary statistics for count of the number of days per year when AHL>100. Location= Comet, RCP2.6, time periods= 2010-2049, 2050-2099. Mild mitigation implemented.	172
Table 4.58: Summary statistics for count of the number of days per year when AHL>100. Location= Comet, RCP2.6, time periods= 2010-2049, 2050-2099. Moderate mitigation implemented.	173

Table 4.59: Summary statistics for count of the number of days per year when AHL>100. Location= Comet, RCP2.6, time periods= 2010-2049, 2050-2099. Maximal mitigation implemented. 174

Table 4.60: Summary statistics for count of the number of days per year when AHL>100. Location= Comet, RCP4.5, time periods= 1960-1999, 2010-2049, 2050-2099. No mitigation implemented..... 175

Table 4.61: Summary statistics for count of the number of days per year when AHL>100. Location= Comet, RCP4.5, time periods= 2010-2049, 2050-2099. Mild mitigation implemented. 176

Table 4.62: Summary statistics for count of the number of days per year when AHL>100. Location= Comet, RCP4.5, time periods= 2010-2049, 2050-2099. Moderate mitigation implemented. 177

Table 4.63: Summary statistics for count of the number of days per year when AHL>100. Location= Comet, RCP4.5, time periods= 2010-2049, 2050-2099. Maximal mitigation implemented. 178

Table 4.64: Summary statistics for count of the number of days per year when AHL>100. Location= Comet, RCP8.5, time periods= 1960-1999, 2010-2049, 2050-2099. No mitigation implemented..... 179

Table 4.65: Summary statistics for count of the number of days per year when AHL>100. Location= Comet, RCP8.5, time periods= 2010-2049, 2050-2099. Mild mitigation implemented. 180

Table 4.66: Summary statistics for count of the number of days per year when AHL>100. Location= Comet, RCP8.5, time periods= 2010-2049, 2050-2099. Moderate mitigation implemented. 181

Table 4.67: Summary statistics for count of the number of days per year when AHL>100. Location= Comet, RCP8.5, time periods= 2010-2049, 2050-2099. Maximal mitigation implemented. 182

Table 4.68: Summary statistics for count of the number of days per year when AHL>100. Location=Dalby, RCP2.6, time periods= 1960-1999, 2010-2049, 2050-2099. No mitigation implemented..... 183

Table 4.69: Summary statistics for count of the number of days per year when AHL>100. Location= Dalby, RCP2.6, time periods= 2010-2049, 2050-2099. Mild mitigation implemented..... 184

Table 4.70: Summary statistics for count of the number of days per year when AHL>100. Location= Dalby, RCP2.6, time periods= 2010-2049, 2050-2099. Moderate mitigation implemented..... 185

Table 4.71: Summary statistics for count of the number of days per year when AHL>100. Location= Dalby, RCP2.6, time periods= 2010-2049, 2050-2099. Maximal mitigation implemented. 186

Table 4.72: Summary statistics for count of the number of days per year when AHL>100. Location= Dalby, RCP4.5, time periods= 1960-1999, 2010-2049, 2050-2099. No mitigation implemented. 187

Table 4.73: Summary statistics for count of the number of days per year when AHL>100. Location= Dalby, RCP4.5, time periods= 2010-2049, 2050-2099. Mild mitigation implemented..... 188

Table 4.74: Summary statistics for count of the number of days per year when AHL>100. Location= Dalby, RCP4.5, time periods= 2010-2049, 2050-2099. Moderate mitigation implemented..... 189

Table 4.75: Summary statistics for count of the number of days per year when AHL>100. Location= Dalby, RCP4.5, time periods= 2010-2049, 2050-2099. Maximal mitigation implemented.	190
Table 4.76: Summary statistics for count of the number of days per year when AHL>100. Location= Dalby, RCP8.5, time periods= 1960-1999, 2010-2049, 2050-2099. No mitigation implemented.	191
Table 4.77: Summary statistics for count of the number of days per year when AHL>100. Location= Dalby, RCP8.5, time periods= 2010-2049, 2050-2099. Mild mitigation implemented.....	192
Table 4.78: Summary statistics for count of the number of days per year when AHL>100. Location= Dalby, RCP8.5, time periods= 2010-2049, 2050-2099. Moderate mitigation implemented.....	193
Table 4.79: Summary statistics for count of the number of days per year when AHL>100. Location= Dalby, RCP8.5, time periods= 2010-2049, 2050-2099. Maximal mitigation implemented.	194
Table 4.80: Summary statistics for count of the number of days per year when AHL>100. Location=Leeton, RCP2.6, time periods= 1960-1999, 2010-2049, 2050-2099. No mitigation implemented.....	195
Table 4.81: Summary statistics for count of the number of days per year when AHL>100. Location= Leeton, RCP2.6, time periods= 2010-2049, 2050-2099. Mild mitigation implemented.....	196
Table 4.82: Summary statistics for count of the number of days per year when AHL>100. Location= Leeton, RCP2.6, time periods= 2010-2049, 2050-2099. Moderate mitigation implemented.....	197
Table 4.83: Summary statistics for count of the number of days per year when AHL>100. Location= Leeton, RCP2.6, time periods= 2010-2049, 2050-2099. Maximal mitigation implemented.	198
Table 4.84: Summary statistics for count of the number of days per year when AHL>100. Location= Leeton, RCP4.5, time periods= 1960-1999, 2010-2049, 2050-2099. No mitigation implemented. ...	199
Table 4.85: Summary statistics for count of the number of days per year when AHL>100. Location= Leeton, RCP4.5, time periods= 2010-2049, 2050-2099. Mild mitigation implemented.....	200
Table 4.86: Summary statistics for count of the number of days per year when AHL>100. Location= Leeton, RCP4.5, time periods= 2010-2049, 2050-2099. Moderate mitigation implemented.....	201
Table 4.87: Summary statistics for count of the number of days per year when AHL>100. Location= Leeton, RCP4.5, time periods= 2010-2049, 2050-2099. Maximal mitigation implemented.	202
Table 4.88: Summary statistics for count of the number of days per year when AHL>100. Location= Leeton, RCP8.5, time periods= 1960-1999, 2010-2049, 2050-2099. No mitigation implemented. ...	203
Table 4.89: Summary statistics for count of the number of days per year when AHL>100. Location= Leeton, RCP8.5, time periods= 2010-2049, 2050-2099. Mild mitigation implemented.....	204
Table 4.90: Summary statistics for count of the number of days per year when AHL>100. Location= Leeton, RCP8.5, time periods= 2010-2049, 2050-2099. Moderate mitigation implemented.....	205

Table 4.91: Summary statistics for count of the number of days per year when AHL>100. Location= Leeton, RCP8.5, time periods= 2010-2049, 2050-2099. Maximal mitigation implemented.	206
Table 4.92: Summary statistics for count of the number of days per year when AHL>100. Location=Narrogin, RCP2.6, time periods= 1960-1999, 2010-2049, 2050-2099. No mitigation implemented.....	207
Table 4.93: Summary statistics for count of the number of days per year when AHL>100. Location= Narrogin, RCP2.6, time periods= 2010-2049, 2050-2099. Mild mitigation implemented.....	208
Table 4.94: Summary statistics for count of the number of days per year when AHL>100. Location= Narrogin, RCP2.6, time periods= 2010-2049, 2050-2099. Moderate mitigation implemented.....	209
Table 4.95: Summary statistics for count of the number of days per year when AHL>100. Location=Narrogin, RCP2.6, time periods= 2010-2049, 2050-2099. Maximal mitigation implemented.	210
Table 4.96: Summary statistics for count of the number of days per year when AHL>100. Location= Narrogin, RCP4.5, time periods= 1960-1999, 2010-2049, 2050-2099. No mitigation implemented.	211
Table 4.97: Summary statistics for count of the number of days per year when AHL>100. Location= Narrogin, RCP4.5, time periods= 2010-2049, 2050-2099. Mild mitigation implemented.....	212
Table 4.98: Summary statistics for count of the number of days per year when AHL>100. Location= Narrogin, RCP4.5, time periods= 2010-2049, 2050-2099. Moderate mitigation implemented.....	213
Table 4.99: Summary statistics for count of the number of days per year when AHL>100. Location= Narrogin, RCP4.5, time periods= 2010-2049, 2050-2099. Maximal mitigation implemented.....	214
Table 4.100: Summary statistics for count of the number of days per year when AHL>100. Location= Narrogin, RCP8.5, time periods= 1960-1999, 2010-2049, 2050-2099. No mitigation implemented.	215
Table 4.101: Summary statistics for count of the number of days per year when AHL>100. Location= Narrogin, RCP8.5, time periods= 2010-2049, 2050-2099. Mild mitigation implemented.....	216
Table 4.102: Summary statistics for count of the number of days per year when AHL>100. Location= Narrogin, RCP8.5, time periods= 2010-2049, 2050-2099. Moderate mitigation implemented.....	217
Table 4.103: Summary statistics for count of the number of days per year when AHL>100. Location= Narrogin, RCP8.5, time periods= 2010-2049, 2050-2099. Maximal mitigation implemented.....	218
Table 4.104: Summary statistics for daily water intake (L/hd/day) by month of year for Carooona for the historic period (1960-1999) and for each of three scenarios in 2010-2049. Summary statistics for the future period are derived from all five model outputs within each scenario. % changes are based on comparison to the same statistics from the historic period.....	222
Table 4.105: Summary statistics for daily water intake (L/hd/day) by month of year for Carooona for the historic period (1960-1999) and for each of three scenarios in 2050-2099. Summary statistics for the future period are derived from all five model outputs within each scenario. % changes are based on comparison to the same statistics from the historic period. perc=percentile.	223

Table 4.106: summary statistics for water intake at Caroona expressed as ML per thousand head per year, based on aggregating daily water intake estimates to produce an annual estimate.....	224
Table 4.107: Summary statistics for daily water intake (L/hd/day) by month of year for Comet for the historic period (1960-1999) and for each of three scenarios in 2010-2049. Summary statistics for the future period are derived from all five model outputs within each scenario. % changes are based on comparison to the same statistics from the historic period. perc = percentile.....	228
Table 4.108: Summary statistics for daily water intake (L/hd/day) by month of year for Comet for the historic period (1960-1999) and for each of three scenarios in 2050-2099. Summary statistics for the future period are derived from all five model outputs within each scenario. % changes are based on comparison to the same statistics from the historic period. perc= percentile.	229
Table 4.109: summary statistics for water intake at Comet expressed as ML per thousand head per year, based on aggregating daily water intake estimates to produce an annual estimate.....	230
Table 4.110: Summary statistics for daily water intake (L/hd/day) by month of year for Dalby for the historic period (1960-1999) and for each of three scenarios in 2010-2049. Summary statistics for the future period are derived from all five model outputs within each scenario. % changes are based on comparison to the same statistics from the historic period. perc = percentile.....	234
Table 4.111: Summary statistics for daily water intake (L/hd/day) by month of year for Dalby for the historic period (1960-1999) and for each of three scenarios in 2050-2099. Summary statistics for the future period are derived from all five model outputs within each scenario. % changes are based on comparison to the same statistics from the historic period. perc = percentile.....	235
Table 4.112: summary statistics for water intake at Dalby expressed as ML per thousand head per year, based on aggregating daily water intake estimates to produce an annual estimate.....	236
Table 4.113: Summary statistics for daily water intake (L/hd/day) by month of year for Leeton for the historic period (1960-1999) and for each of three scenarios in 2010-2049. Summary statistics for the future period are derived from all five model outputs within each scenario. % changes are based on comparison to the same statistics from the historic period. perc = percentile.....	240
Table 4.114: Summary statistics for daily water intake (L/hd/day) by month of year for Leeton for the historic period (1960-1999) and for each of three scenarios in 2050-2099. Summary statistics for the future period are derived from all five model outputs within each scenario. % changes are based on comparison to the same statistics from the historic period. perc = percentile.....	241
Table 4.115: summary statistics for water intake at Leeton expressed as ML per thousand head per year, based on aggregating daily water intake estimates to produce an annual estimate.....	242
Table 4.116: Summary statistics for daily water intake (L/hd/day) by month of year for Narrogin for the historic period (1960-1999) and for each of three scenarios in 2010-2049. Summary statistics for the future period are derived from all five model outputs within each scenario. % changes are based on comparison to the same statistics from the historic period. perc = percentile.	246
Table 4.117: Summary statistics for daily water intake (L/hd/day) by month of year for Narrogin for the historic period (1960-1999) and for each of three scenarios in 2050-2099. Summary statistics for	

the future period are derived from all five model outputs within each scenario. % changes are based on comparison to the same statistics from the historic period. perc = percentile. 247

Table 4.118: summary statistics for water intake at Narrogin expressed as ML per thousand head per year, based on aggregating daily water intake estimates to produce an annual estimate..... 248

Table 4.119: Summary statistics for annual runoff at Caroona, CoV=coefficient of variation. The change in coefficient of variation is provided for 2050-2099 and is expressed as a % of the 2010-2049 values. The change in mean runoff is expressed as a % of the historic mean runoff..... 252

Table 4.120: Summary statistics for annual runoff at Comet, CoV=coefficient of variation. The change in coefficient of variation is provided for 2050-2099 and is expressed as a % of the 2010-2049 values. The change in mean runoff is expressed as a % of the historic mean runoff..... 255

Table 4.121: Summary statistics for annual runoff at Dalby, CoV=coefficient of variation. The change in coefficient of variation is provided for 2050-2099 and is expressed as a % of the 2010-2049 values. The change in mean runoff is expressed as a % of the historic mean runoff..... 258

Table 4.122: Summary statistics for annual runoff at Leeton, CoV=coefficient of variation. The change in coefficient of variation is provided for 2050-2099 and is expressed as a % of the 2010-2049 values. The change in mean runoff is expressed as a % of the historic mean runoff..... 261

Table 4.123: Summary statistics for annual runoff at Narrogin, CoV=coefficient of variation. The change in coefficient of variation is provided for 2050-2099 and is expressed as a % of the 2010-2049 values. The change in mean runoff is expressed as a % of the historic mean runoff..... 264

List of Figures

Figure 4.1: Map of Australia showing the grain belt (shading), locations of feedlots (red dots) and selected modelling locations (green circles).....	4
Figure 4.2: Map of Australia showing the grain belt (shading), locations of feedlots (red dots) and selected modelling locations (green circles).....	44
Figure 4.3: Predicted daily water intake (L/hd/day) over the course of a one year period (1985) from the middle of the historic time period. Different lines represent model outputs from the three predictive equations.	63
Figure 4.4: Predicted daily water intake (L/hd/day) over the course of a one year period (2099) from the end of the future climate runs. Different lines represent model outputs from the three predictive equations.	63
Figure 4.5: Diagrammatic representation of a box plot.....	64
Figure 4.6: Daily water intake over a one-year period (2035) at Caroona, with different lines for each of five models, all run under the same scenario (RCP2.6).....	65
Figure 4.7: Daily water intake over a one-year period (2099) at Caroona, with different lines for each of five models, all run under the same scenario (RCP8.5).....	65
Figure 4.8: Plot showing median daily water intake for each month of the year for the period 2050-2099 at Caroona. The blue solid line shows the monthly median from the historic period for comparison.	66
Figure 4.1: Annual average of maximum daily temperature (a) and of daily average temperature (b) from SILO data (1900-2009) and GCM predictions (2010-2099). The shaded area covers the range from minimum to maximum values of five GCMs and the dark line is the average of the five models. Separate plots are shown for each of three RCP scenarios: 8.5 (top), 4.5 (middle) and 2.6 (bottom). Location = Caroona.	72
Figure 4.2: Annual maximum temperature (a) and average temperature (b) anomaly based on difference between the daily value calculated from 1961-1990 and the average of five GCMs from 2010-2099. Separate plots are shown for RCP 8.5 (top), 4.5 (middle) and 2.6 (bottom) in each Figure. Blue shows an increase compared to 1961-1990 and red is a decrease. Location = Caroona.....	73
Figure 4.3: Annual average of maximum daily temperature (a) and of daily average temperature (b) from SILO data (1900-2009) and GCM predictions (2010-2099). The shaded area covers the range from minimum to maximum values of five GCMs and the dark line is the average of the five models. Separate plots are shown for each of three RCP scenarios: 8.5 (top), 4.5 (middle) and 2.6 (bottom). Location = Comet.	78
Figure 4.4: Annual maximum temperature (a) and average temperature (b) anomaly based on difference between the daily value calculated from 1961-1990 and the average of five GCMs from 2010-2099. Separate plots are shown for RCP 8.5 (top), 4.5 (middle) and 2.6 (bottom) in each Figure. Blue shows an increase compared to 1961-1990 and red is a decrease. Location = Comet.....	79

Figure 4.5: Annual average of maximum daily temperature (a) and of daily average temperature (b) from SILO data (1900-2009) and GCM predictions (2010-2099). The shaded area covers the range from minimum to maximum values of five GCMs and the dark line is the average of the five models. Separate plots are shown for each of three RCP scenarios: 8.5 (top), 4.5 (middle) and 2.6 (bottom). Location = Dalby..... 82

Figure 4.6: Annual maximum temperature (a) and average temperature (b) anomaly based on difference between the daily value calculated from 1961-1990 and the average of five GCMs from 2010-2099. Separate plots are shown for RCP 8.5 (top), 4.5 (middle) and 2.6 (bottom) in each Figure. Blue shows an increase compared to 1961-1990 and red is a decrease. Location = Dalby. 83

Figure 4.7: Annual average of maximum daily temperature (a) and of daily average temperature (b) from SILO data (1900-2009) and GCM predictions (2010-2099). The shaded area covers the range from minimum to maximum values of five GCMs and the dark line is the average of the five models. Separate plots are shown for each of three RCP scenarios: 8.5 (top), 4.5 (middle) and 2.6 (bottom). Location = Leeton..... 86

Figure 4.8: Annual maximum temperature (a) and average temperature (b) anomaly based on difference between the daily value calculated from 1961-1990 and the average of five GCMs from 2010-2099. Separate plots are shown for RCP 8.5 (top), 4.5 (middle) and 2.6 (bottom) in each Figure. Blue shows an increase compared to 1961-1990 and red is a decrease. Location = Leeton. 87

Figure 4.9: Annual average of maximum daily temperature (a) and of daily average temperature (b) from SILO data (1900-2009) and GCM predictions (2010-2099). The shaded area covers the range from minimum to maximum values of five GCMs and the dark line is the average of the five models. Separate plots are shown for each of three RCP scenarios: 8.5 (top), 4.5 (middle) and 2.6 (bottom). Location = Narrogin..... 91

Figure 4.10: Annual maximum temperature (a) and average temperature (b) anomaly based on difference between the daily value calculated from 1961-1990 and the average of five GCMs from 2010-2099. Separate plots are shown for RCP 8.5 (top), 4.5 (middle) and 2.6 (bottom) in each Figure. Blue shows an increase compared to 1961-1990 and red is a decrease. Location = Narrogin. 92

Figure 4.11: Average annual rainfall (a) and rainfall anomaly (difference between average of five GCMs and 1961-1990 average rainfall, b). Data derived from SILO records and GCM predictions (2010-2099). The shaded area to the right of 2010 in plot (a) covers the range from minimum to maximum values of five GCMs and the dark line is the average of the five models. Separate plots are shown for each of three RCP scenarios: 8.5 (top), 4.5 (middle) and 2.6 (bottom). Location = Caroona. 96

Figure 4.12: Monthly rainfall anomaly based on difference between historic monthly average (1961-1990) and the monthly average of the five GCM outputs. Shaded area is the anomaly between historic and minimum or maximum value of the five GCM estimates in each month. Separate plots are shown for each of three RCP scenarios: 8.5 (top), 4.5 (middle) and 2.6 (bottom). Location = Caroona..... 97

Figure 4.13: Average annual rainfall (a) and rainfall anomaly (difference between average of five GCMs and 1961-1990 average rainfall, b). Data derived from SILO records (1900-2009) and GCM

predictions (2010-2099). The shaded area to the right of 2010 in plot (a) covers the range from minimum to maximum values of five GCMs and the dark line is the average of the five models. Separate plots are shown for each of three RCP scenarios: 8.5 (top), 4.5 (middle) and 2.6 (bottom). Location = Comet. 100

Figure 4.14: Monthly rainfall anomaly based on difference between historic monthly average (1961-1990) and the monthly average of the five GCM outputs. Shaded area is the anomaly between historic and minimum or maximum value of the five GCM estimates in each month. Separate plots are shown for each of three RCP scenarios: 8.5 (top), 4.5 (middle) and 2.6 (bottom). Location = Comet..... 101

Figure 4.15: Average annual rainfall (a) and rainfall anomaly (difference between average of five GCMs and 1961-1990 average rainfall, b). Data derived from SILO records (1900-2009) and GCM predictions (2010-2099). The shaded area to the right of 2010 in plot (a) covers the range from minimum to maximum values of five GCMs and the dark line is the average of the five models. Separate plots are shown for each of three RCP scenarios: 8.5 (top), 4.5 (middle) and 2.6 (bottom). Location = Dalby..... 104

Figure 4.16: Monthly rainfall anomaly based on difference between historic monthly average (1961-1990) and the monthly average of the five GCM outputs. Shaded area is the anomaly between historic and minimum or maximum value of the five GCM estimates in each month. Separate plots are shown for each of three RCP scenarios: 8.5 (top), 4.5 (middle) and 2.6 (bottom). Location = Dalby. 105

Figure 4.17: Average annual rainfall (a) and rainfall anomaly (difference between average of five GCMs and 1961-1990 average rainfall, b). Data derived from SILO records (1900-2009) and GCM predictions (2010-2099). The shaded area to the right of 2010 in plot (a) covers the range from minimum to maximum values of five GCMs and the dark line is the average of the five models. Separate plots are shown for each of three RCP scenarios: 8.5 (top), 4.5 (middle) and 2.6 (bottom). Location = Leeton..... 108

Figure 4.18: Monthly rainfall anomaly based on difference between historic monthly average (1961-1990) and the monthly average of the five GCM outputs. Shaded area is the anomaly between historic and minimum or maximum value of the five GCM estimates in each month. Separate plots are shown for each of three RCP scenarios: 8.5 (top), 4.5 (middle) and 2.6 (bottom). Location = Leeton. 109

Figure 4.19: Average annual rainfall (a) and rainfall anomaly (difference between average of five GCMs and 1961-1990 average rainfall, b). Data derived from SILO records (1900-2009) and GCM predictions (2010-2099). The shaded area to the right of 2010 in plot (a) covers the range from minimum to maximum values of five GCMs and the dark line is the average of the five models. Separate plots are shown for each of three RCP scenarios: 8.5 (top), 4.5 (middle) and 2.6 (bottom). Location = Narrogin..... 112

Figure 4.20: Monthly rainfall anomaly based on difference between historic monthly average (1961-1990) and the monthly average of the five GCM outputs. Shaded area is the anomaly between historic and minimum or maximum value of the five GCM estimates in each month. Separate plots

are shown for each of three RCP scenarios: 8.5 (top), 4.5 (middle) and 2.6 (bottom). Location = Narrogin.	113
Figure 4.21: Plot of mean overtopping rate (events per 100 years) for each location and scenario (historic, RCP2.6, RCP4.5 and RCP8.5). Bars represent 95% confidence intervals either side of the mean.	118
Figure 4.22: Number of days per year when AHL > threshold, showing historic (1960-99) and future runs (2010-2099), under each of four mitigation strategies. Location= Caroona, scenario=RCP2.6. Y-scale maximum=20.	141
Figure 4.23: Number of days per year when AHL > threshold, showing historic (1960-99) and future runs (2010-2099), under each of four mitigation strategies. Location= Caroona, scenario=RCP4.5. Y-scale maximum=30.	142
Figure 4.24: Number of days per year when AHL > threshold, showing historic (1960-99) and future runs (2010-2099), under each of four mitigation strategies. Location= Caroona, scenario=RCP8.5. Y-scale maximum=50.	143
Figure 4.25: Number of days per year when AHL > threshold, showing historic (1960-99) and future runs (2010-2099), under each of four mitigation strategies. Location= Comet, scenario=RCP2.6. Y-scale maximum=30.	144
Figure 4.26: Number of days per year when AHL > threshold, showing historic (1960-99) and future runs (2010-2099), under each of four mitigation strategies. Location= Comet, scenario=RCP4.5. Y-scale maximum=100.	145
Figure 4.27: Number of days per year when AHL > threshold, showing historic (1960-99) and future runs (2010-2099), under each of four mitigation strategies. Location= Comet, scenario=RCP8.5. Y-scale maximum=140.	146
Figure 4.28: Number of days per year when AHL > threshold, showing historic (1960-99) and future runs (2010-2099), under each of four mitigation strategies. Location= Dalby, scenario=RCP2.6. Y-scale maximum=10.	147
Figure 4.29: Number of days per year when AHL > threshold, showing historic (1960-99) and future runs (2010-2099), under each of four mitigation strategies. Location= Dalby, scenario=RCP4.5. Y-scale maximum=10.	148
Figure 4.30: Number of days per year when AHL > threshold, showing historic (1960-99) and future runs (2010-2099), under each of four mitigation strategies. Location= Dalby, scenario=RCP8.5. Y-scale maximum=30.	149
Figure 4.31: Number of days per year when AHL > threshold, showing historic (1960-99) and future runs (2010-2099), under each of four mitigation strategies. Location= Leeton, scenario=RCP2.6. Y-scale maximum=30.	150

Figure 4.32: Number of days per year when AHL > threshold, showing historic (1960-99) and future runs (2010-2099), under each of four mitigation strategies. Location= Leeton, scenario=RCP4.5. Y-scale maximum=50.	151
Figure 4.33: Number of days per year when AHL > threshold, showing historic (1960-99) and future runs (2010-2099), under each of four mitigation strategies. Location= Leeton, scenario=RCP8.5. Y-scale maximum=50.	152
Figure 4.34: Number of days per year when AHL > threshold, showing historic (1960-99) and future runs (2010-2099), under each of four mitigation strategies. Location= Narrogin, scenario=RCP2.6. Y-scale maximum=10.	153
Figure 4.35: Number of days per year when AHL > threshold, showing historic (1960-99) and future runs (2010-2099), under each of four mitigation strategies. Location= Narrogin, scenario=RCP4.5. Y-scale maximum=10.	154
Figure 4.36: Number of days per year when AHL > threshold, showing historic (1960-99) and future runs (2010-2099), under each of four mitigation strategies. Location= Narrogin, scenario=RCP8.5. Y-scale maximum=10.	155
Figure 4.37: Box plot showing median water usage (L/hd/day) at Caroona by month from daily predictions over the period 1960-1999.	219
Figure 4.38: Predicted median daily water intake by month of year at Caroona for the period from 2010-2049 (solid lines). The solid blue line is the median predicted water intake from the historic period (1960-1999), provided for comparative purposes. Dashed lines shows the maximum daily water intake for each month.	220
Figure 4.39: Predicted median daily water intake by month of year at Caroona for the period from 2050-2099 (solid lines). The solid blue line is the median predicted water intake from the historic period (1960-1999), provided for comparative purposes. Dashed lines shows the maximum daily water intake for each month.	221
Figure 4.40: Plot of annual water intake (ML/1000 head/year) at Caroona by year for each of three scenarios over two periods (1960-1999 and 2010-2099). Water intake for 2010-2099 shows the range from minimum to maximum annual values across the five models (shaded area) and the median (black line). The blue line shows a smoothed long-term average.	225
Figure 4.41: Box plot showing median water usage (L/hd/day) at Comet by month from daily predictions over the period 1960-1999.	226
Figure 4.42: Predicted median daily water intake by month of year at Comet for the period from 2010-2049 (solid lines). The solid blue line is the median predicted water intake from the historic period (1960-1999), provided for comparative purposes. Dashed lines shows the maximum daily water intake for each month.	227
Figure 4.43: Predicted median daily water intake by month of year at Comet for the period from 2050-2099 (solid lines). The solid blue line is the median predicted water intake from the historic	

period (1960-1999), provided for comparative purposes. Dashed lines shows the maximum daily water intake for each month. 227

Figure 4.44: Plot of annual water intake (ML/1000 head/year) at Comet by year for each of three scenarios over two periods (1960-1999 and 2010-2099). Water intake for 2010-2099 shows the range from minimum to maximum annual values across the five models (shaded area) and the median (black line). The blue line shows a smoothed long-term average. 231

Figure 4.45: Box plot showing median water usage (L/hd/day) at Dalby by month from daily predictions over the period 1960-1999. 232

Figure 4.46: Predicted median daily water intake by month of year at Dalby for the period from 2010-2049 (solid lines). The solid blue line is the median predicted water intake from the historic period (1960-1999), provided for comparative purposes. Dashed lines shows the maximum daily water intake for each month. 233

Figure 4.47: Predicted median daily water intake by month of year at Dalby for the period from 2050-2099 (solid lines). The solid blue line is the median predicted water intake from the historic period (1960-1999), provided for comparative purposes. Dashed lines shows the maximum daily water intake for each month. 233

Figure 4.48: Plot of annual water intake (ML/1000 head/year) at Dalby by year for each of three scenarios over two periods (1960-1999 and 2010-2099). Water intake for 2010-2099 shows the range from minimum to maximum annual values across the five models (shaded area) and the median (black line). The blue line shows a smoothed long-term average. 237

Figure 4.49: Box plot showing median water usage (L/hd/day) at Leeton by month from daily predictions over the period 1960-1999. 238

Figure 4.50: Predicted median daily water intake by month of year at Leeton for the period from 2010-2049 (solid lines). The solid blue line is the median predicted water intake from the historic period (1960-1999), provided for comparative purposes. Dashed lines shows the maximum daily water intake for each month. 239

Figure 4.51: Predicted median daily water intake by month of year at Caroon for the period from 2050-2099 (solid lines). The solid blue line is the median predicted water intake from the historic period (1960-1999), provided for comparative purposes. Dashed lines shows the maximum daily water intake for each month. 239

Figure 4.52: Plot of annual water intake (ML/1000 head/year) at Leeton by year for each of three scenarios over two periods (1960-1999 and 2010-2099). Water intake for 2010-2099 shows the range from minimum to maximum annual values across the five models (shaded area) and the median (black line). The blue line shows a smoothed long-term average. 243

Figure 4.53: Box plot showing median water usage (L/hd/day) at Narrogin by month from daily predictions over the period 1960-1999. 244

Figure 4.54: Predicted median daily water intake by month of year at Narrogin for the period from 2010-2049 (solid lines). The solid blue line is the median predicted water intake from the historic

period (1960-1999), provided for comparative purposes. Dashed lines shows the maximum daily water intake for each month. 245

Figure 4.55: Predicted median daily water intake by month of year at Narrogin for the period from 2050-2099 (solid lines). The solid blue line is the median predicted water intake from the historic period (1960-1999), provided for comparative purposes. Dashed lines shows the maximum daily water intake for each month. 245

Figure 4.56: Plot of annual water intake (ML/1000 head/year) at Narrogin by year for each of three scenarios over two periods (1960-1999 and 2010-2099). Water intake for 2010-2099 shows the range from minimum to maximum annual values across the five models (shaded area) and the median (black line). The blue line shows a smoothed long-term average. 249

Figure 4.57: Scatterplots of annual rainfall (y-axis) and annual runoff (x-axis) for two representative modelling runs. The left plot shows average rainfall and runoff estimates derived from all model outputs at Narrogin for RCP8.5 and the right plot shows estimates derived from all model outputs at Leeton for RCP2.6. Lines are fitted quadratic regression lines. 250

Figure 4.58: Plot of annual rainfall (left axis) and annual runoff (right axis) over time with smoothed averages of rainfall (thick blue line) and runoff (thick black line) overlaid. 251

Figure 4.59: Example plot of annual runoff over time, from Narrogin and for RCP8.5. 252

Figure 4.60: Plot showing the annual runoff (mm/yr) at Caroona for the historic and predicted time periods. The predicted period incorporates a shaded area showing the range from the minimum to maximum value from the five models for each year and the block line shows the annual average for the five models. The blue line is a smoothed long-term average runoff estimate. 253

Figure 4.61: Plot showing annual runoff at Caroona from historic climate records (black line) and annual runoff for each of the three RCP levels. The thick coloured lines show smoothed long-term average runoff for each RCP. 254

Figure 4.62: Plot showing the annual runoff (mm/yr) at Comet for the historic and predicted time periods. The predicted period incorporates a shaded area showing the range from the minimum to maximum value from the five models for each year and the block line shows the annual average for the five models. The blue line is a smoothed long-term average runoff estimate. 256

Figure 4.63: Plot showing annual runoff at Comet from historic climate records (black line) and annual runoff for each of the three RCP levels. The thick coloured lines show smoothed long-term average runoff for each RCP. 257

Figure 4.64: Plot showing the annual runoff (mm/yr) at Dalby for the historic and predicted time periods. The predicted period incorporates a shaded area showing the range from the minimum to maximum value from the five models for each year and the block line shows the annual average for the five models. The blue line is a smoothed long-term average runoff estimate. 259

Figure 4.65: Plot showing annual runoff at Dalby from historic climate records (black line) and annual runoff for each of the three RCP levels. The thick coloured lines show smoothed long-term average runoff for each RCP. 260

Figure 4.66: Plot showing the annual runoff (mm/yr) at Leeton for the historic and predicted time periods. The predicted period incorporates a shaded area showing the range from the minimum to maximum value from the five models for each year and the block line shows the annual average for the five models. The blue line is a smoothed long-term average runoff estimate. 262

Figure 4.67: Plot showing annual runoff at Leeton from historic climate records (black line) and annual runoff for each of the three RCP levels. The thick coloured lines show smoothed long-term average runoff for each RCP. 263

Figure 4.68: Plot showing the annual runoff (mm/yr) at Narrogin for the historic and predicted time periods. The predicted period incorporates a shaded area showing the range from the minimum to maximum value from the five models for each year and the block line shows the annual average for the five models. The blue line is a smoothed long-term average runoff estimate. 265

Figure 4.69: Plot showing annual runoff at Narrogin from historic climate records (black line) and annual runoff for each of the three RCP levels. The thick coloured lines show smoothed long-term average runoff for each RCP. 266

List of Abbreviations and Terms

ACSC	Australian Centre for Sustainable Catchments
AHL	Accumulated Heat Load
AHLU	Accumulated Heat Load Units
AR5	Assessment Report 5
ASCII	American Standard Code for Information Interchange
BCS	Body condition score
BGT	Black globe temperature
BOM	Bureau of meteorology
C	Celsius
CI	Confidence interval
CMIP5	Coupled Model Intercomparison Project Phase 5
CNRM-CM5	GCM from Centre National de Recherches Meteorologiques, France
CoV	Coefficient of variation
CRC	Co-operative Research Centre
DAFF	Department of Agriculture, Fisheries and Forestry
DMI	Dry matter
DMI	Dry matter intake
DMI	Dry matter intake
DOF	Days on feed
DSITIA	Department of Science, Information Technology, Innovation and the Arts
EHL	Excessive heat load
FCE	Feed conversion efficiency
FSA	Feedlot Services Australia
GCM	General Circulation Model
GFDL-ESM2G	GCM from Geophysical Fluid Dynamics Laboratory, USA
ha	Hectare
HadGEM2-ES	GCM from Hadley Centre for Climate Prediction and Research, UK
hd	Head
HLI	Heat Load Index
HLIACC	Actual heat load index at a point in time
IPCC	Intergovernmental Panel on Climate Change
IQR	Inter-quartile range
kg	Kilogram

L	Litre
MEDLI	Model for Effluent Disposal using Land Irrigation
MIROC5	GCM from Atmosphere and Ocean Research Institute, Japan
ml	millilitre
ML	Megalitre
MLA	Meat and Livestock Australia
mm	millimetre
MRI-CGCM3	GCM from Meteorological Research Institute, Japan
MWI	Median water intake
NSW	New South Wales
QCCCE	Queensland Climate Change Centre for Excellence
QLD	Queensland
Radn	Radiation
RCP	Representative Concentration Pathway
RH	Relative humidity
SCU	Standard cattle unit
SILO	An internet website that provides a source of meteorological data
T	Temperature
UQ	University of Queensland
USA	United States of America
Vict	Victoria
WA	Western Australia
WC	Water consumption
WS	Wind speed
yr	year

1 Introduction

1.1 Background

Climate scientists are predicting changes to climate that may have considerable impacts on feedlots. Scientists predict increasing temperature, variation in the amount and intensity of rainfall, changing humidity, solar radiation and other aspects of climate. Feedlots will need to adapt to these changes through changing practices. Climate variability may be different in each region of Australia and this means that there is a need for information on the possible impact of future climate change in each of the major lotfeeding regions in Australia.

This project has used relevant climate models to predict possible climate scenarios for each of the five major lotfeeding regions in Australia.

The project has involved the identification and use of appropriate climate models to provide future daily climate data under different scenarios ranging from no change to the current conditions, mild change, moderate change and severe change.

1.2 Project objectives

1. Provide descriptions of the future climate scenarios for the five major feedlot regions of Australia to 2050 through:
 - a. Assessment of the various models used to predict climate change.
 - b. Selection of a small number of models that best fit the requirements of the study.
 - c. Utilising these models to develop predicted climate data for a range of future global warming scenarios (low, medium, high).
2. Model the impact of these scenarios on the three study aspects for feedlots located in the five regions:
 - a. Size requirements for effluent ponds, to ensure that they continue to meet the regulatory requirements that apply to pond overflows for the various states.
 - b. Requirements for cattle drinking and effluent dilution/irrigation water.
 - c. Frequency and severity of heat stress events.
3. Provide recommendations on actions that the feedlot industry should take to adapt to increasing climate variability in areas of effluent pond design, stock and reticulated water, and heat stress mitigation and management.

2 Literature review

A brief literature review was completed and published as a separate report to accompany this report. The review was intended to provide a brief review of scientific literature on climate change and its potential impact on the Australian cattle feedlot industry.

Increasing evidence indicates that the climate is changing, and that human activity is a major contributing cause. Globally, the annual mean temperature has increased in the past 130 years, and this is consistent with changes observed in Australia. Each decade since 1950 has recorded warmer temperatures than the previous decade. It is more difficult to identify long-term changes in Australia's already variable rainfall. Apparent trends appear to be a general increase in Spring and Summer monsoonal rainfall to the north, higher than normal rainfall in central Australia, and decreased late Autumn and Winter rainfall in the south of the country.

Climate scientists are acknowledging that extreme weather events, such as the increasing number of record hot days experienced in Australia, are linked to climate change. Effects of climate change on the world's oceans include an average sea-surface temperature increase of 0.8°C since 1910. The rise in sea level differs around the globe – the sea level to the north and north-west of Australia have risen 7-11mm every year since 1993. This is two to three times greater than the global average.

The effects of climate change on animal health and productivity are likely to be both direct and indirect. Examples of direct effects include temperature related deaths and morbidity during extreme weather events, with indirect effects including changes in vector-borne diseases, feed and water shortages, and changes in pest populations. Climate change will also affect cropping enterprises, including changes in grain production and supply that will impact feedlot operations. Changes in climate will also impact water requirements and availability. Hot weather dramatically increases the water requirements of cattle, and access to secure water is the more significant limitation on the expansion of the feedlot industry.

The impacts of climate change on the feedlot industry will vary by region as it is anticipated that each feedlot region will experience a slightly different range of climatic changes.

These changes will require adaption and mitigation if the industry is to continue to thrive and development of recommendations, strategies and action plans will need to consider social, cultural and economic implications as well as biophysical impacts.

3 General overview of methodology

3.1 Methodology overview

The methodology used to determine the effect of climate change on feedlot hydrology was as follows:

1. Selection of five representative feedlot locations
2. Generation of predicted climate-change data files for each selected location
3. Generation of historic (observed) climate data for the selected locations in two general formats:

- a. Daily data suitable for use in MEDLI models
 - b. Sub-daily data suitable for use in heat load models
4. Completion of preliminary validation assessment of the predicted climate-change data files.
 5. Completion of analyses to assess impacts of predicted climate data in the two modelling systems
 - a. MEDLI
 - i. Design runoff control systems for a “standard” 10 000 head feedlot at each location and assess its performance.
 - ii. Assess the performance the performance of the runoff control system at each location under different climate change scenarios.
 - b. Heat load modelling

A brief summary of each of the methodology steps is provided in this section of the body of the report. More detailed descriptions of each of the methodology steps is provided in Appendices.

3.2 Selection of modelling locations

There were approximately 450 accredited feedlots throughout Australia at the time this project was undertaken¹. The project required that five representative locations for feedlots were to be modelled for future climate change scenarios. Table 4.1 and Figure 4.2 show the locations that were chosen for modelling.

Table 4.1: Description of selected locations used for modelling

Region	Representative Location	Climate Zone	Seasonal Rainfall Zone	Mean Annual Rainfall
Northern New South Wales	Caroona	Warm summer, cool winter	Summer	600 mm
Central Queensland	Comet	Hot dry summer, mild winter	Summer	589 mm
Southern Queensland	Dalby	Warm summer, cool winter	Summer	632 mm
Central New South Wales	Leeton	Warm dry summer, cool winter	Uniform	421 mm
South-West Western Australia	Narrogin	Warm dry summer, cool winter	Winter	522 mm

¹ www.feedlots.com.au

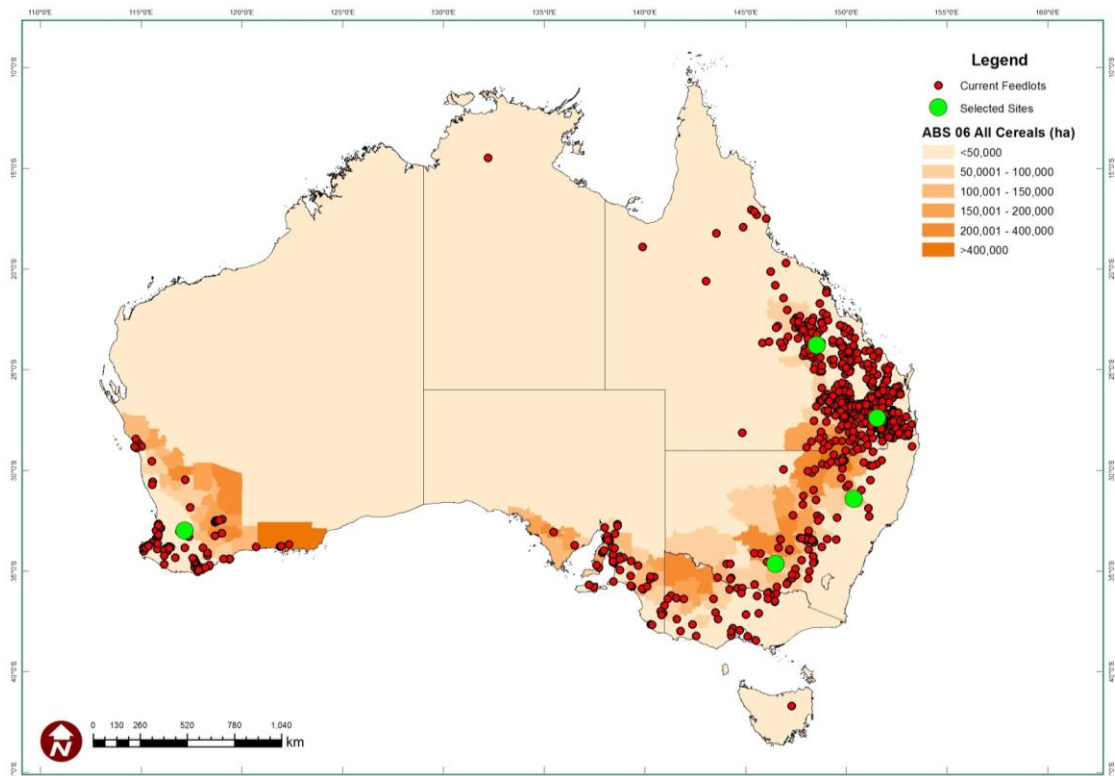


Figure 4.2: Map of Australia showing the grain belt (shading), locations of feedlots (red dots) and selected modelling locations (green circles).

The selection criteria for these locations included consideration of:

- current feedlot zones;
- climatic zones;
- annual rainfall zones;
- season rainfall zones; and,
- potential for heat load in cattle.

A detailed description of the selection criteria is provided in a separate volume of Appendices that accompanies this report.

3.3 Predicted climate datasets

A detailed description of selection of climate models, preliminary assessment and downscaling approaches is provided in a separate volume of Appendices that accompanies this report. This section presents a brief summary of the processes involved in selecting climate models and generating climate data for use in feedlot hydrology modelling and animal heat stress modelling.

Team members from the Australian Centre for Sustainable Catchments (ACSC) were involved in generating predicted climate datasets for use in this project. ACSC researchers are world leaders in climate and meteorological science².

As part of this component of the project, ACSC researchers completed a detailed review of available computer models used for generating global climate data through the Intergovernmental Panel on Climate Change (IPCC). These models are described as General Circulation Models (GCMs) and model development and validation is undertaken in a collaborative manner with attention to validation and review. These processes are managed through the IPCC and outlined in the Coupled Model Intercomparison Project Phase 5 (CMIP5), a framework to guide development and improvement of climate models.

A decision was made to focus on the most recent GCMs which were developed as part of the 5th Assessment Report (AR5) of the IPCC, because these models represented the most advanced approach to date in modelling predicted climate change (compared to earlier AR4 models). In addition AR5 models provided opportunities to generate climate data at finer time scales, of specific interest in this project since the climate datasets were to be used in feedlot hydrology models and in heat load index models, requiring data at daily or sub-daily time scales.

Available AR5 GCMs were subjected to a detailed desktop performance evaluation to select those GCMs that were assessed as being most suitable to modelling under Australian conditions and that were capable of producing datasets meeting specifications for the two subsequent modelling steps. This review process identified seven candidate GCMs.

The seven GCMs were then used to generate predicted climate datasets for an historic time period (1960-1999) and these data were further assessed by comparison to actual observed climate records for the same period and locations, and by comparing results from MEDLI modelling of the predicted and observed datasets for the selected feedlot locations.

Two of the seven GCMs were subsequently discarded as unsuitable following this preliminary assessment process.

The preliminary assessment process also identified problems with scaling that required development of additional downscaling techniques as part of this component of the project. Predicted climate data generated from GCMs tended to be predicted across relatively large area scales and in some cases involved averaging over time. There were also issues associated with modelling dependencies amongst related climate variables. In developing effective downscaling methods the ACSC team has developed and validated novel methodologies to re-calibrate GCM datasets in order to downscale data to daily or sub-daily time steps, incorporate dependencies between different climate variables and produce datasets that can be used to represent fine-scale variation in future climate variables (daily or sub-daily changes in temperature and rainfall for example).

This downscaling approach enabled the generation of predicted climate data for historic time periods at a daily time-step that had a high level of agreement when compared to observed historic

² www.usq.edu.au/acsc

data from the same locations. The same approach was then applied to the generation of predicted future climate data.

Following completion of model selection and preliminary testing, five models were selected as being most appropriate for the specific requirements of this project. These five models were used for generation of all predicted climate data for this report:

- **HadGEM2-ES:** Hadley Centre for Climate Prediction and Research/Met Office (Exeter, United Kingdom);
- **CNRM-CM5:** Centre National de Recherches Meteorologiques (Toulouse, France);
- **GFDL-ESM2G:** Geophysical Fluid Dynamics Laboratory (Princeton, USA);
- **MIROC5:** Atmosphere and Ocean Research Institute (The University of Tokyo, Japan);
- **MRI-CGCM3:** Meteorological Research Institute (Tsukuba-city, Ibaraki, Japan).

Each GCM was then parameterised at each of four different *scenarios* to represent different levels of climate change. The baseline scenario was a no-change, control level for comparative purposes, equivalent to 20th century historic levels. There were then three additional scenarios based on three greenhouse gas concentration trajectories derived from the IPCC AR5 report, called Representative Concentration Pathways (RCPs). These three RCPs represented mild (RCP2.6), moderate (RCP4.5) and high (RCP8.5) greenhouse gas concentrations. The RCPs are based on possible ranges of radiative forcing measured in watts per square meter (W/m^2) in the year 2100.

Daily predicted climate datasets were generated at each combination of the following factors:

- Location: five selected locations representing the major feedlot areas of Australia (Caroona, Comet, Dalby, Leeton, Narrogin);
- GCM: five models (CNRM, GFDL, HAD, MIR, MRI);
- Scenarios: three greenhouse gas concentration levels (RCP2.6, RCP4.5, RCP8.5); and,
- Time periods: two time periods (2010-2049, 2050-2099).

Predicted daily climate data were combined with historic SILO data for each location for the period 1900-2010 to generate a daily climate dataset for each location that spanned the period from 1900-2099. This allowed comparisons at each location between historic data (1900-2010) with predicted future data for each of three RCP scenarios across two future time periods (2010-2049 and 2050-2099).

Historic SILO records do not provide data at hourly time steps. As a result hourly data used for heat load modelling and for water intake modelling, were generated through the GCMs for both historic and future time windows. A decision was made to limit historic predictions to the period 1960-1999 in order to provide sufficient data for comparative purposes (40 years) while limiting the size of the generated data.

Hourly predicted climate datasets were generated at each combination of the following factors:

- Location: five selected locations representing the major feedlot areas of Australia (Caroona, Comet, Dalby, Leeton, Narrogin);
- GCM: five models (CNRM, GFDL, HAD, MIR, MRI);
- Scenarios: three greenhouse gas concentration levels (RCP2.6, RCP4.5, RCP8.5); and,
- Time periods: three time periods (1960-1999, 2010-2049, 2050-2099).

Datasets were made available through a custom web-link for download as ASCII files for use in MEDLI and HLI models.

3.4 Feedlot hydrology modelling

Feedlot hydrology modelling was completed using the Model for Effluent Disposal using Land Irrigation or MEDLI model (Gardner and Davis 1998; Atzeni et al 2001). Details of the feedlot module within MEDLI are poorly documented. Hence, a detailed description of the feedlot module and a brief overview of the MEDLI modelling process is provided here. A more detailed overview of the MEDLI model is provided in the separate volume of Appendices that accompanies this report.

Predicted climate-change data files were provided as daily time-step files for each combination of GCM-scenario-location.

3.4.1 Introduction to feedlot hydrology

Feedlots involve high density livestock production with consequent production of significant amounts of organic matter, nutrients, salts and pathogens contained in pen runoff.

Feedlot runoff is managed through structural design to minimise catchment areas that generate runoff and through construction of holding ponds to prevent runoff entering local surface or groundwater systems.

3.4.2 National feedlot guidelines for runoff control

The design objective for feedlot runoff control systems is to size the holding pond so that pond overflows to natural watercourses only occur at an acceptable frequency.

The National Guidelines for Beef Cattle Feedlots in Australia³ (MLA 2012) recommend the use of daily-step hydrological modelling of the controlled drainage area and holding pond to establish that the proposed holding pond would spill less frequently than an average of one in ten years (or one in 20 years in the case of an evaporation pond).

³ <http://www.mla.com.au/News-and-resources/Publication-details?pubid=5939>

The National Guidelines stipulate that holding ponds should have sufficient storage capacity so that:

- Normal holding ponds (*i.e.* those from which wastewater is routinely extracted for land application) spill no more frequently than an average of 1 in 10 years; and,
- Evaporation ponds (*i.e.* those from which there is normally no land application of captured wastewater) spill no more frequently than an average of 1 in 20 years.

According to the National Guidelines, an acceptable design method is to use daily-step hydrological modelling of the controlled drainage area and holding pond to establish that the proposed holding pond would spill less frequently than an average of 1 in 10 years (or 1 in 20 years in the case of an evaporation pond). The meteorological data set used should be representative of the site and cover a period of at least 100 years (*i.e.* a data set covering $\geq 36\,524$ days).

The National Guidelines indicate that runoff calculations should be applied in a water balance for the holding pond that accounts for the following:

- Evaporative losses
- Seepage losses
- Any extractions made for the land application of wastewater
- The pond capacity utilised in storing sludge.

Modelled wastewater applications should be based on calculating the soil moisture deficit and meeting plant nutrient needs based on their growth stage. Assumptions made about the timing of applications (*e.g.* application only made in fine weather in the 'x' weeks prior to seasonal cropping) should be explicitly stated. In addition, reasonable expectations of cropping activity and the yields in that location should be used (*i.e.* the modelled wastewater applications must realistically reflect expected management practices).

The holding pond water balance will typically have to be run through a number of times to determine a pond capacity that notionally spills at the required frequency (*i.e.* no more often than an average of 1 in 10 years for a 'normal' holding pond and 1 in 20 years for an evaporation pond). The 1 in 10 year frequency is not determined by statistical analysis. It is determined by counting the number of spill events in 100 years and ensuring that this is 10 or less.

It is acknowledged that, once a pond has 'spilled' in this type of modelling, the likelihood of another modelled spill occurring within the next few days is quite high. The National Guidelines indicate that modelled spill events within 30 days of one another should be treated as a single spill. In reality, it is more likely that a feedlot manager would be able to intervene in these circumstances, and possibly avert secondary spills.

An allowance of at least an additional 10% of pond storage capacity should be made to accommodate sludge that will progressively build up in the pond.

In this project, the MEDLI model with an integrated feedlot module was used for daily-step hydrological modelling.

3.4.3 Introduction to MEDLI

MEDLI® is a Windows®-based computer model developed jointly by the CRC for Waste Management and Pollution Control, the Queensland Department of Natural Resources (now Department of

Science, Information Technology, Innovation and the Arts - DSITIA) and the Department of Primary Industries (now Department of Agriculture, Fisheries and Forestry - DAFF), Queensland.

MEDLI models the effluent cycle from effluent production in an enterprise through to the disposal area and predicts the fate of the water, nitrogen, phosphorus, and soluble salts. In this project, only water balance modelling is relevant.

Feedlot hydrology was modelled using Version 2.0 of MEDLI, developed specifically for modelling feedlot pad moisture and runoff (Atzeni et al. 2001). The feedlot component of the model generates the runoff details (date, volume, concentrations) from the feedlot and then exports these data into the main MEDLI program. The main MEDLI program then uses the feedlot waste as an effluent stream input into a treatment pond / effluent irrigation system.

The feedlot module of MEDLI requires considerable parameterisation to define the population of animals in the feedlot and feedlot design attributes. The design of a feedlot enterprise in MEDLI is extremely flexible with provision for defining animal types, stocking density, occupancy rates, catchment and runoff characteristics of both pen areas and non-pen areas of the feedlot and details of pen maintenance and cleaning.

3.4.4 Feedlot parameterisation in MEDLI

The initial setup of MEDLI required development of a representative “standard”, Class 1, 10 000 SCU feedlot for each location, based on industry knowledge and existing datasets on individual feedlots at each modelled location. Input parameters included specification of diet inputs and manure generation for each feedlot, also developed using location specific knowledge concerning likely markets, cattle types, common feedstuffs and other location specific knowledge.

Table 4.2: Summary of feedlot modelling locations

Location	Nearest Town	Latitude	Longitude	Elevation (m ASL)	Mean annual rainfall (mm)
Northern New South Wales	Caroona	-31.40°	150.35°	317	600
Central Queensland	Comet	-23.75°	148.50°	164	589
Southern Queensland	Dalby	-27.15°	151.25°	343	632
Central New South Wales	Leeton	-34.55°	146.40°	150	421
South-West Western Australia	Narrogin	-32.90°	117.15°	358	522

For each “standard” feedlot, data on the following components was developed:

1. Herd and diet details (market types and proportion in the feedlot)
2. Waste estimation (based on daily intake and ration components)
3. Controlled drainage area catchment components

4. Holding pond design and management.

3.4.4.1 Animals and feedlot diet

Each “standard” feedlot was created with a capacity expressed as 10 000 Standard Cattle Units (SCU’s), recognising that the actual number of cattle at any site would depend on the breakdown of market types and liveweights at that location.

Herd data was obtained using existing datasets for each location, in particular an aggregated dataset (EconSearch Pty Ltd et al. 2009). For simplicity, and to allow direct comparison, the entry and exit weights, days on feed and average daily weight gain varied for each market type, but were considered to be the same for each location. For example at Carroona and Leeton, mid-fed and long-fed cattle made up 57% (27% and 30% respectively) of the total herd, whereas, at Narrogin, the entire herd is either domestic or short-fed cattle. Table 4.3 gives typical entry and exit weights, average daily gain and dry matter intakes for different market types. Diet composition data used for each location are provided in Table 4.4.

Table 4.3: Descriptive summary of market type and basic performance details for each location

	Market type			
	Domestic	Short-fed	Mid-fed	Long-fed
Typical days on feed (days)	60	100-140	150-180	220-240
DOF modelled (days)	60	120	165	230
Entry weight (kg)	359	431	433	413
Exit weight (kg)	455	659	714	712
Net gain (kg)	96	228	281	299
Average daily gain (kg/d)	1.6	1.9	1.7	1.3
DM Intake (kg/hd/d)	9.3	10.3	10.9	10.5
FCE (kg DM/hd/d)	5.8	5.4	6.6	9.3
Mortality rate (%)	1	1	1	1
% of feedlot capacity by market type	Domestic	Short-fed	Mid-fed	Long-fed
Carroona	19	24	27	30
Comet	37	30	14	19
Dalby	47	40	6	7
Leeton	19	24	27	30
Narrogin	40	60	0	0

Table 4.4: Description of dietary breakdown by location

Diet parameter	Type	Units	Location				
			Caroona	Comet	Dalby	Leeton	Narrogin
Grain	Summer	% of diet	25	50	43		
	Winter	% of diet	50	25	32	75	75
Protein	Cottonseed	% of diet	10	10	10	10	
	Canola	% of diet					5
	Lupins	% of diet					5
	Other	% of diet					
Roughage	Straw/Hay	% of diet	3.5	2	3.5	3.5	9.5
	Silage	% of diet	5	4	5	5	
Liquids		% of diet	1.5	4	1.5	1.5	0.5
Supplements		% of diet	5	5	5	5	5

3.4.4.2 Waste Estimation

The herd composition, along with the diet and feeding data, affects the total amount of manure added to the pad. This in-turn affects the amount of water that can be stored in the pad, which affects the volume of runoff generated. Manure excretion rates were estimated using a spreadsheet tool called BEEFBAL (Davis et al 2012) and the data inputs as described in Table 4.3 and Table 4.4.

The BEEFBAL spreadsheet tool generated estimates of manure output per head per year expressed as total solids, volatile solids and water. The BEEFBAL outputs were then used as input values in MEDLI modelling. Summaries of these values are presented in the following table.

Table 4.5: Manure production parameters for each location

Location	Manure parameter	Domestic	Short-fed	Mid-fed	Long-fed
		kg/head/ year	kg/head/ year	kg/head/ year	kg/head/ year
Caroona	Total Solids	499	553	585	534
	Volatile Solids	327	362	383	349
	Water	4,994	5,531	5,854	5,338
Comet	Total Solids	614	680	719	656
	Volatile Solids	440	487	515	470
	Water	6,136	6,795	7,191	6,558
Dalby	Total Solids	562	623	659	601
	Volatile Solids	390	432	457	417
	Water	5,622	6,226	6,589	6,008
Leeton	Total Solids	374	414	438	400
	Volatile Solids	200	222	235	214
	Water	3,740	4,142	4,384	3,997
Narrogin	Total Solids	366	406	429	392
	Volatile Solids	185	205	217	198
	Water	3,664	4,058	4,295	3,916

3.4.4.3 Waste Management

It was assumed that the “standard” feedlot was a Class 1 feedlot (Skerman, 2000) and that the maximum depths of manure (above soil – manure interface layer) present in the pens should not exceed 50 mm. Pens are cleaned every seven weeks, if pen moisture conditions allow cleaning machinery to operate.

Table 4.6: Pen cleaning details applied for each feedlot location

Parameter	Units	Value
Depth maintained above base when harvesting	mm	20
Max. number of pens cleaned per harvest day	n	5
Min. interval between pen cleaning	days	49
Max. moisture content harvested	%db	120

3.4.4.4 Controlled drainage area components

For the “standard” 10 000 SCU feedlot, it was assumed that the stocking density was 15 m²/SCU at all locations. On this basis, the following typical estimates of the components of the controlled drainage area were derived. Table 4.7 summarises the catchment area components, which are the same for each location. The MEDLI model assumes all runoff from the catchment area is directed into a holding pond via a sedimentation basin.

Pen area	= Feedlot size x Stocking density
	= 10 000 SCU x 15 m ² /SCU
	= 150 000 m ² or 15 ha
Hard area	= 1.01 x Pen area
	= 1.01 x 15 ha
	= 15.15 ha
Soft area	= 0.33 x Pen area
	= 0.33 x 15 ha
	= 4.95 ha
Total area	= Pen area + Hard area + Soft area
	= 15 ha + 15.2 ha + 5 ha
	= 35.2 ha

Table 4.7: Input values for area estimates for pen, hard and soft areas, used for all feedlot locations in MEDLI models

Feedlot Size	Pen area (ha)	Hard area (ha)	Soft area (ha)	Total area (ha)
10 000 SCU	15	15.2	5	35.2

3.4.4.5 Holding pond design and management

For the purpose of this project, the National Guidelines for Cattle Feedlots in Australia were adhered to for sizing the required holding pond for a 10 000 SCU feedlot at each location.

The holding pond was designed using SILO rainfall data for a modelling period of 100 years.

The design criteria for the holding pond is to overtop no more frequently than once every ten years. The capacity of the holding pond at each location that will comply with this design criteria is dependent on the irrigation area that is available to use the runoff captured in the holding pond. In reality, there is often an iterative design process to obtain a balance between holding pond capacity and irrigation area for each site. For simplicity, it has been assumed in this project that all locations have an irrigation area of 50 ha that can be used to irrigate pasture throughout the whole year. Grey clay was chosen as the default soil type at all locations. Tropical pasture was selected as the crop type for the Queensland locations and temperature pasture was selected for the New South Wales and Western Australia locations. All pond geometry parameters were set to values that are considered typical for a feedlot holding pond. The holding pond maximum depth was set as 4 m.

In summary, the design process, using MEDLI, was:

1. Obtain a 100-year, SILO climate file for each site. This is for the period, 1910-2010.
2. Set up a “standard” 10 000 SCU feedlot in MEDLI using data given in Table 4.3.
3. Enter manure production data for each site using data in Table 4.5..
4. Enter catchment data from Table 4.7.
5. Enter standard irrigation area data (50 ha), soil and crop type and standard irrigation scheduling rules (irrigate 0.5 ML/ha/day at 50% PAWC).
6. Enter a holding pond volume, run MEDLI and assess the overtopping frequency.
7. Repeat Step 6 until the overtopping frequency is acceptable (i.e. ten or less overtopping events in 100 years). Table 4.8 shows the holding pond capacity appropriate to each location and some performance data.

Table 4.8: Holding pond parameters at each location required to achieve an overtopping frequency of 9 events per 100 years when using a 100-year SILO climate file for each site

Location	Caroona	Comet	Dalby	Leeton	Narrogin
Design Holding Pond Capacity (ML)	81	88	59	46	97
Mean annual rainfall (mm)	600	589	632	421	522
Mean annual runoff (mm)	174	192	194	106	166
Runoff (% rainfall)	29%	33%	31%	25%	32%
Mean annual feedlot runoff (ML/yr)	60	66	67	37	57
Mean annual irrigation applied (ML/yr)	49.2	49.8	57.5	30.6	49.2
Mean annual irrigation applied (ML/ha/yr)*	0.98	0.99	1.15	0.61	0.98

* Note: the mean annual irrigation applied does not aim to match the irrigation demand. It is the amount applied as irrigation in the process of dewatering the holding pond. In most years, this volume is much less than the actual irrigation demand. The shortfall can be made up with clean, blending or shandy water.

3.4.5 Hydrology modelling using predicted climate data

Once the holding pond dimensions were specified, it was possible to define a baseline set of feedlot parameters including holding pond dimensions and all other set-up parameters related to animals, feed, waste generation and day-to-day management. These parameters were then fixed for each location.

Climate data files were then generated for a 100 year time-period ranging from 2000-2099. Methodology for generation of these files is described in the following sections of this report.

MEDLI modelling required daily input data for specific variables including daily rainfall, maximum and minimum temperatures, Class A pan evaporation and solar radiation.

The GCMs were capable of generating predicted climate datasets for the period from 2010 to 2099. Since the MEDLI modelling required input climate data spanning a 100-year period, additional SILO climate data for the period from 2000-2009 for each location were combined with the predicted climate data to generate datasets covering 100 years.

There were a total of 16 MEDLI runs at each of the five locations, comprised of:

- Historic run using SILO data from 1910-2009 used to set the holding pond dimensions at each location; and,
- Five GCMs run at each of the three RCP scenarios (2.6, 4.5, 8.5).

This enabled a comparison of MEDLI model outputs from the historical climate data and the future climate datasets to be made at each location.

MEDLI output data included summary measures of:

1. rainfall and evaporation (climate parameters);
2. runoff (hydrology);
3. overtopping frequency reported as events per 100 years as a key measure of compliance with national standards.

3.5 Accumulated heat load (AHL) modelling

3.5.1 Background

Excessive heat load (EHL) is a recognised problem in feedlot cattle particularly during summer months. EHL occurs when the combination of local environmental conditions and animal factors exceed the ability of animals to dissipate heat. EHL has the potential to cause significant production losses and adverse welfare impacts including mortality.

A great deal of research has been conducted into understanding heat load in feedlot cattle. Detailed industry information on feedlot heat load can be found in industry publications⁴ and in refereed journal articles (Gaughan et al, 2008).

3.5.2 Heat load index (HLI)

The heat load index (HLI) can be estimated as a measure of environmental heat load placed on cattle. The HLI requires input data on relative humidity, black globe temperature and wind speed.

If HLI exceeds a defined threshold based on animal and site characteristics, an animal will gain heat. For every hour that an animal is above its threshold HLI value, it will gain heat. This additional heat load accumulates over time and is reflected as an increase in body temperature. When HLI is below the threshold an animal is able to dissipate heat.

The baseline HLI applies to a standard reference animal defined as a grainfed, healthy, black, *Bos Taurus* steer with a body condition of 4+ and no access to shade. This standard reference animal will gain heat when the HLI is greater than 86 (upper threshold of HLI) and will dissipate heat when the HLI is less than 77 (lower threshold of HLI). Australian data have been used to develop a series of adjustment factors that may increase both the upper and lower HLI thresholds, conferring increased tolerance of potential hot conditions. Examples include provision of shade, altering coat colour and use of *Bos indicus* genotype cattle.

⁴ <http://www.mla.com.au/Livestock-production/Feeding-finishing-and-nutrition/Lotfeeding-and-intensive-finishing/Heat-stress>

The HLI model is a 2 part algorithm based on a black globe temperature threshold of 25°C (Gaughan et al. 2008).

$$\text{BGT} < 25^{\circ}\text{C}: \text{HLI} = 10.66 + (0.28 \times \text{RH}) + (1.3 \times \text{BGT}) - \text{WS}$$

$$\text{BGT} > 25^{\circ}\text{C}: \text{HLI} = 8.62 + (0.38 \times \text{RH}) + (1.55 \times \text{BGT}) - (0.5 \times \text{WS}) + e^{-2.4 \text{ WS}}$$

BGT= Black Globe temperature (°C)

HLI= Heat load index

RH= Relative humidity (percentage i.e. 45 not 0.45)

WS= Wind speed (metres/second)

HLI alone does not provide a sufficiently sensitive measure to determine when animals may be at risk of EHL. This is because animals may experience periods of heat accumulation during the daytime (or in the hottest parts of a day) and then dissipate that heat once the day cools off or at night when HLI falls below the lower HLI threshold.

3.5.3 Accumulated heat load (AHL)

A better measure of cumulative heat load over time is achieved using accumulated heat load units (AHLU or AHL).

Accumulated Heat Load (AHL) models body heat gain and loss from feedlot cattle based on a HLI threshold which is determined by a combination of climate, animal and management factors (Gaughan et al 2008). The AHL threshold used in the climate model evaluation was based on the reference animal, i.e. a healthy, black Angus steer, 100 days on a feedlot ration, a body condition score (BCS) of 4+ (based on the Australian 5 point BCS system; 1 lean and 5 very fat) with no access to shade.

AHLU provides a cumulative measure of heat load over time that is based on the amount of time (hours in a day for example) when HLI may be greater than the upper threshold (resulting in accumulation of heat) or less than the lower HLI threshold (resulting in loss of heat). Under conditions of prolonged heat and particularly when hot days are combined with hot nights, animals risk accumulation of heat to the point where adverse effects on production and welfare become likely.

For the reference animal the upper threshold at which the animal gains heat when $\text{HLI} \geq 86$ and the lower threshold for loss of heat is $\text{HLI} \leq 77$. Over a 24-hour period the AHL may be increasing for part or all of the time or it may be decreasing for part or all of the time. However the AHL value does not fall below zero. A zero value indicates that the animal is in thermal balance. The following equation was used to calculate the AHL in excel;

$IF (HLIACC < HLI_{Lower\ Threshold}, (HLIACC - HLI_{Lower\ Threshold})/M, IF (HLIACC > HLI_{Upper\ Threshold}, (HLIACC - HLI_{Upper\ Threshold})/M, 0)$

HLIACC = the actual HLI value at a point in time;

HLI_{Lower Threshold} = the HLI threshold below which cattle in a particular class will dissipate heat e.g. ≤ 77 for the reference animal;

HLI_{Upper Threshold} = the HLI threshold above which cattle in a particular class will gain heat e.g. ≥ 86 for the reference animal;

M = calculations of HLI per hour e.g. if every 10 minutes then M = 6, if every hour then M=1.

EHL may have serious adverse impacts if AHL rises to the point where it exceeds levels that are compatible with normal function. Once AHL exceeds 200, animals will be severely comprised and at risk of serious ill health and possible death.

In addition, prolonged or repeated exposures to AHL levels that may be greater than 50 and less than 200 may produce effects ranging from production loss to serious ill health and possible death.

The equation for calculating AHL can accumulate to very high values (>1000 on occasion). In reality values greater than about 400 are likely to be higher than is compatible with survival so maximal outputs were generally capped at 400 units or more for reporting purposes.

3.5.4 AHL modelling

AHL models were implemented using sub-daily time-step climate data as inputs and defined HLI thresholds based on assumptions about animal characteristics and key feedlot attributes such as shade.

Datasets from GCMs provided climate variable values - ambient temperature ($^{\circ}C$), relative humidity (%), solar radiation, and black globe temperature ($^{\circ}C$) - at hourly intervals for periods from 1960 to 1999 (40 years) and from 2010 to 2099 (90 years). Wind speed (m/s) could only be calculated on a daily basis. Therefore a set wind speed (from each model) was used for each hour of the day.

Hourly climate data were used to generate HLI estimates as described above. It is important to note that observed hourly climate data were not available from SILO records and historic time period data for this purpose were generated by prediction using the GCMs in the same process as the future climate datasets.

Hourly HLI values were then used in spreadsheet calculations to generate AHL estimates under each of four different heat load mitigation strategies based on modifying the upper and lower HLI thresholds which in turn influence accumulation and dissipation of heat by animals. The four heat load mitigation strategies were defined as:

- Control: the standard reference animal defined in HLI development as having a lower HLI threshold of 77 and an upper HLI threshold of 86.
- Mild mitigation: HLI lower=84 and HLI upper=89, representing the standard baseline animal with 1-2 m²/SCU shade provided in the feedlot pens.

- Moderate mitigation: HLI lower=84 and HLI upper = 93, representing an increase in HLI upper of +7 units, achievable through extra shade (3-5 m²/SCU) or by other strategies such as heat tolerant genotypes.
- Maximal mitigation: HLI lower=84 and HLI upper=96, representing maximum possible mitigation either through any combination of shade and other management strategies or by switching genotype from *Bos taurus* to purebred *Bos indicus*.

Completion of AHL estimation produced datasets containing hourly AHL estimates. Hourly AHL values were aggregated to produce a single daily maximal AHL value for every day in each time period, and for each combination of five locations, five GCMs, four scenarios and each of the four heat load mitigation strategies.

Daily AHL maxima were then aggregated to produce annual summary statistics for final reporting, using the following measures:

- Number of days per year when the daily maximal AHL exceeded defined thresholds of 50, 80, 100 and 200 units.
 - In datasets aggregated to the year level, this measure was represented as a simple count of days when AHL exceeded each threshold for each year.
 - Final summary statistics for each of the three time periods included the minimum, 25th percentile, 50th percentile (median), 75th percentile and maximum number of days per year when AHL exceeded each threshold.
 - In addition the sum of all days in each of the three time periods when AHL exceeded the defined threshold provided a single overall count of total heat load days.
- Number of heat load events per year at each AHL threshold.
 - One event is defined as all consecutive days when the daily maximal AHL was greater than a defined threshold of 50, 80, 100 and 200 AHL units. A single event could be as short as one day in duration or may be many days in duration.
 - In datasets aggregated to the year level, this measure was represented as a simple count of the number of events in each year.
 - Final summary statistics for each of the three time periods included the minimum, 25th percentile, 50th percentile (median), 75th percentile and maximum number of days per year when AHL exceeded each threshold.
 - In addition the count of all events in each of the three time periods when AHL exceeded the defined threshold provided a single overall count of total heat load events across each time period.
- Median duration in days for heat load events at each defined AHL threshold.

- This measure required multiple aggregation steps. First, all event durations in any one year were aggregated to produce a single median estimate of event duration for each year.
- Final summary statistics for each of the three time periods included the minimum, 25th percentile, 50th percentile (median), 75th percentile and maximum statistics applied to the yearly median duration estimates.

Results for heat load days, events and event duration are presented in table form.

In addition, summary plots were produced to provide simple visual summaries that can be scanned quickly for general patterns over time. Plots were based on combining the summary values from all five GCMs at the same combination of location and scenario and heat load mitigation strategy and producing a median number of heat load days across the five GCMs. Median heat load days across the five GCM outputs were estimated for each year and then these medians were plotted against time.

Each page of output displays three summary plots of median heat load days per year for each location, one for each greenhouse gas scenario (RCP2.6, RCP4.5, RCP8.5). Each plot has four lines, one for each heat load mitigation strategy (control, mild, moderate and maximal mitigation).

3.6 Water intake

An adequate, reliable supply of quality water is required for feedlot operation. While water is an essential element for cattle welfare (including survival) it is also used on feedlots for feed processing, washing cattle, trough cleaning, dust control, staff amenities, cooling, dilution of effluent in irrigation and water is lost from open storage through evaporation (Carter 2008).

A number of studies have reported on attempts to model water usage in feedlot cattle, both in Australia (Sanders et al 1994; Carter et al 2008) and elsewhere (Winchester and Morris 1956; Parker et al 2000).

The following models were applied in this project to estimate water usage in feedlots.

1. Formula described by Winchester and Morris (1956) for *Bos taurus* cattle

$$WC = DMI \times (3.413 + 0.01592 \times e^{0.17596 \times T})$$

WC = Water consumption (litres per head per day)

DMI = Dry Matter Intake (kg DM per head per day)

T = Average daily temperature (° C)

2. Formula described by Sanders et al (1994)

$$WC_{100} = 1.337 - 0.037 \times P + 0.687 \times DMI_{100} + (1.592 - 0.199 \times shading) \times \left(T \times \frac{Radn}{RH} \right)^{0.5}$$

WC_{100} = Water consumption (litres per day per 100 kg liveweight)

DMI_{100} = Dry Matter Intake per 100 kg liveweight

Shading = 0 if no shade, 1 if shade is present

T = Average daily temperature (° C)

Radn = Solar radiation (MJ/m²)

RH = Average daily Relative Humidity (%)

3. Formula described by Parker et al (2000)

$$WC = 39.2 - 0.648 \times T_{MAX} + 0.0421 \times T_{MAX}^2 - 0.0717 \times RH_{MIN}$$

WC = Water consumption (litres per head per day)

T_{MAX} = Maximum daily temperature (° C)

RH_{MIN} = Minimum daily Relative Humidity (%)

Estimates for daily values of average and maximum temperature, average and minimum relative humidity, and daily total solar radiation were derived from climate predictions performed at hourly intervals for each combination of location (Caroona, Comet, Dalby, Leeton and Narrogin), time period (2010-2099), model (CNRM-CM5, GFDL-ESM2G, HadGEM2-ES, MIROC5, MRI-CGCM3) and scenario (RCP2.6, RCP4.5, RCP8.5). These predicted climate datasets were also used for accumulated heat load modelling and are described in more detail in the previous section.

Because historic observed data were not available for all the required inputs, the same climate models were used to generate the same hourly predicted climate data for the period from 1960-1999 for each location, for use as an historic comparison dataset.

All datasets were then aggregated to daily time steps containing average daily temperature, maximum daily temperature, solar radiation, average relative humidity, and minimum relative humidity.

Observed daily rainfall data were then merged into each data file, drawn from SILO records for the historic period (1960-1999) and predicted daily rainfall data derived from climate models for the period 2010-2099 for each location, model and scenario.

Dry Matter Intake (DMI) was set at 10.3 kg DM per head per day, based on the DMI estimate used in MEDLI modelling for cattle being short fed (100 days on feed) for the domestic market.

In order to estimate DMI per 100 kg of liveweight, MEDLI parameters for the average of entry (431 kg) and exit (659 kg) liveweights for cattle in the 100 day market class were also based on the MEDLI input parameters for short-fed cattle. The average of the entry and exit weights was 545 kg. When combined with a DMI of 10.3 kg per head per day, this produced an estimate of DMI per 100 kg liveweight per day of 1.88991 kg DM per 100 kg liveweight per day, used in the Sanders et al (1994) formula for estimating water intake.

The three water consumption formulas were then implemented to calculate predicted water consumption per day for various combinations of time, location, model and scenario. All water consumption estimates were produced in the same scale (litres of water per head per day).

A series of preliminary assessments and plots were performed to inspect the estimated water intake values for each of the three methods. Our findings were very consistent with those reported by Carter (2008). Carter (2008) compared predicted water intakes using these same three methods with actual water intake usage measured over an 11-month period on a commercial Darling Downs feedlot by installing data loggers on water meters. The Sanders et al (1994) model tended to underestimate water consumption compared to actual usage and the Winchester and Morris (1956) model tended to over-estimate water consumption at higher temperatures (Carter 2008). The Parker et al (2000) model had the highest correlation with measured water usage and this model was identified as the most effective predictive model (Carter 2008).

Our preliminary findings are illustrated in two representative figures (Table 4.3 and Figure 4.4). Our findings were very consistent with the description by Carter (2008). The Sanders et al (1994) model predicted a consistently lower water consumption than the other two models and showed the least change under future climate change runs. The other two models showed generally good agreement except that on occasion in future climate runs the Winchester and Morris (1956) model produced unrealistically large daily water intake estimates (more than 200 litres per head per day). These extreme and unrealistic estimates were not seen in the Parker et al (2000) model. As a result, a decision was made to use the Parker et al (2000) model for all water intake modelling conducted in this project.

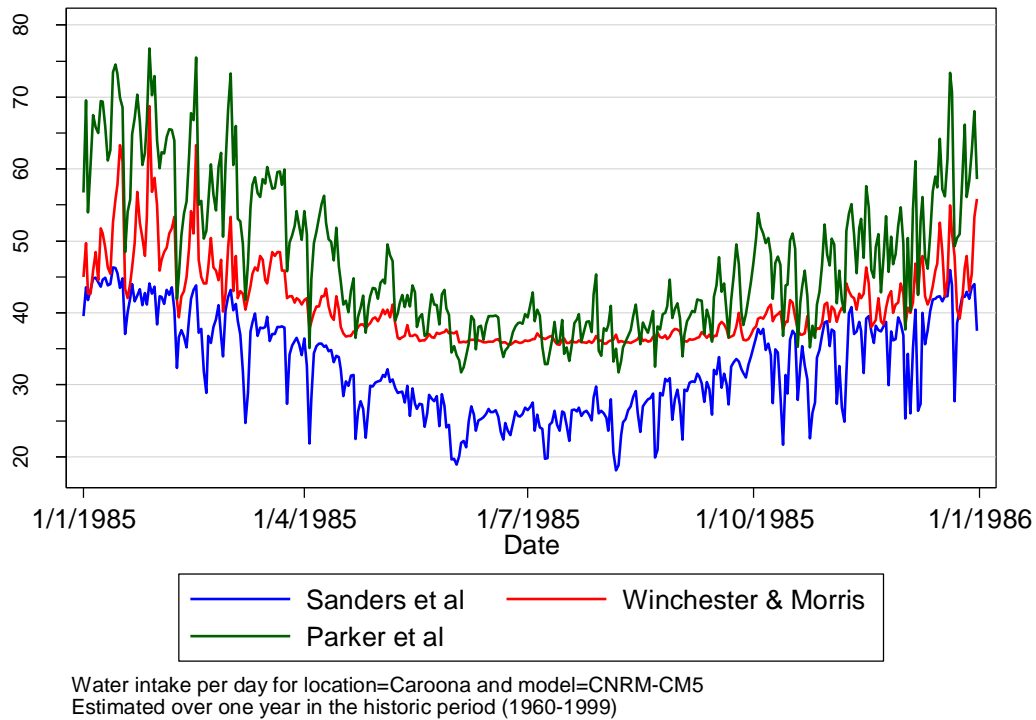


Figure 4.3: Predicted daily water intake (L/hd/day) over the course of a one year period (1985) from the middle of the historic time period. Different lines represent model outputs from the three predictive equations.

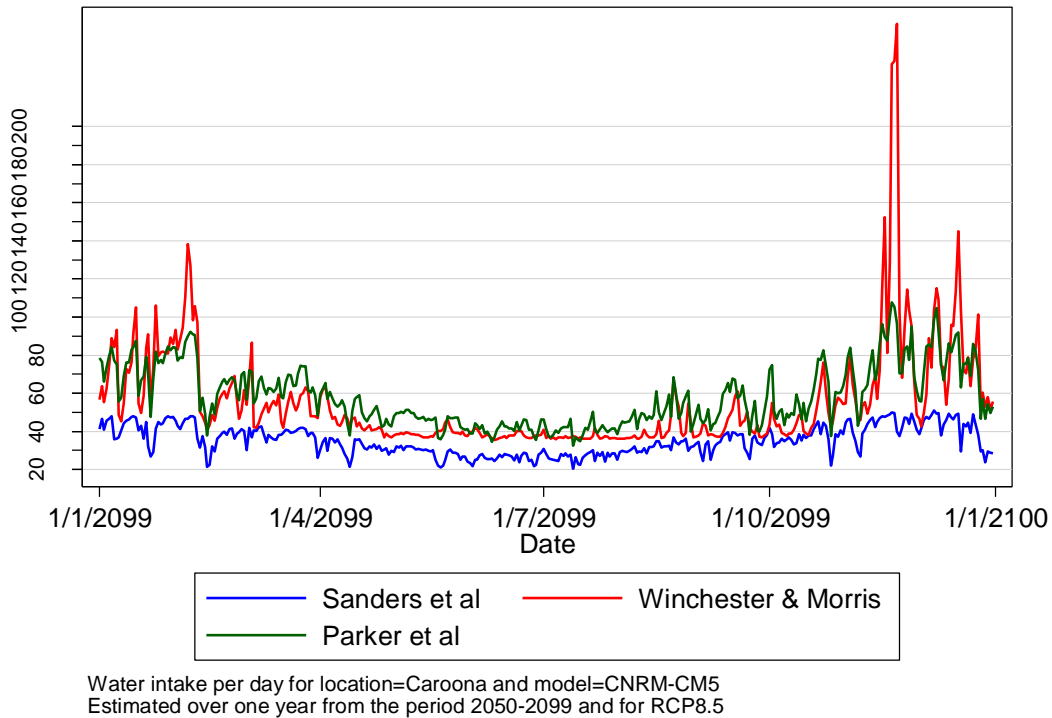


Figure 4.4: Predicted daily water intake (L/hd/day) over the course of a one year period (2099) from the end of the future climate runs. Different lines represent model outputs from the three predictive equations.

The Parker et al (2000) model was used to estimate daily water intake (L/hd/day) for the historic period (1960-1999) at each location, and for each combination of location, model and scenario for the period from 2010-2099.

Analyses were then conducted separately for three defined time periods (1960-1999, 2010-2049, and 2050-2099) as for other climate outputs in this report.

For the historic period there was only one daily estimate for each location. Box plots were used to display the median daily water intake for each month from the historic period.

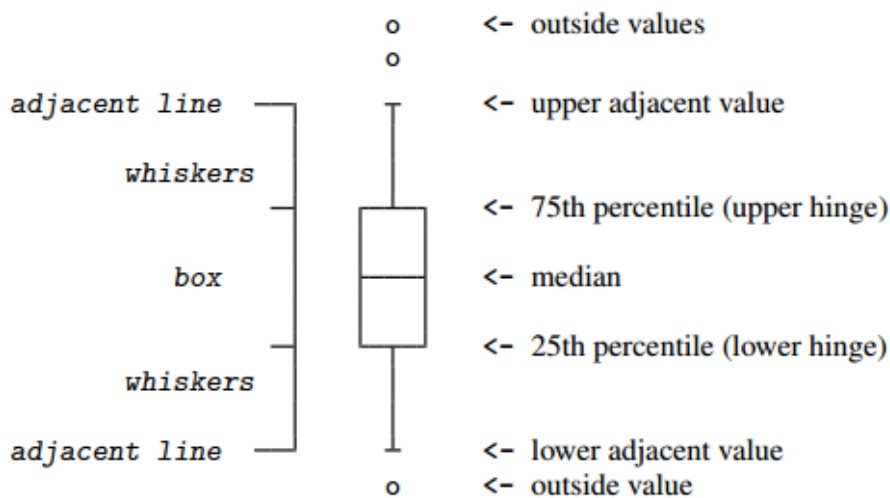


Figure 4.5: Diagrammatic representation of a box plot

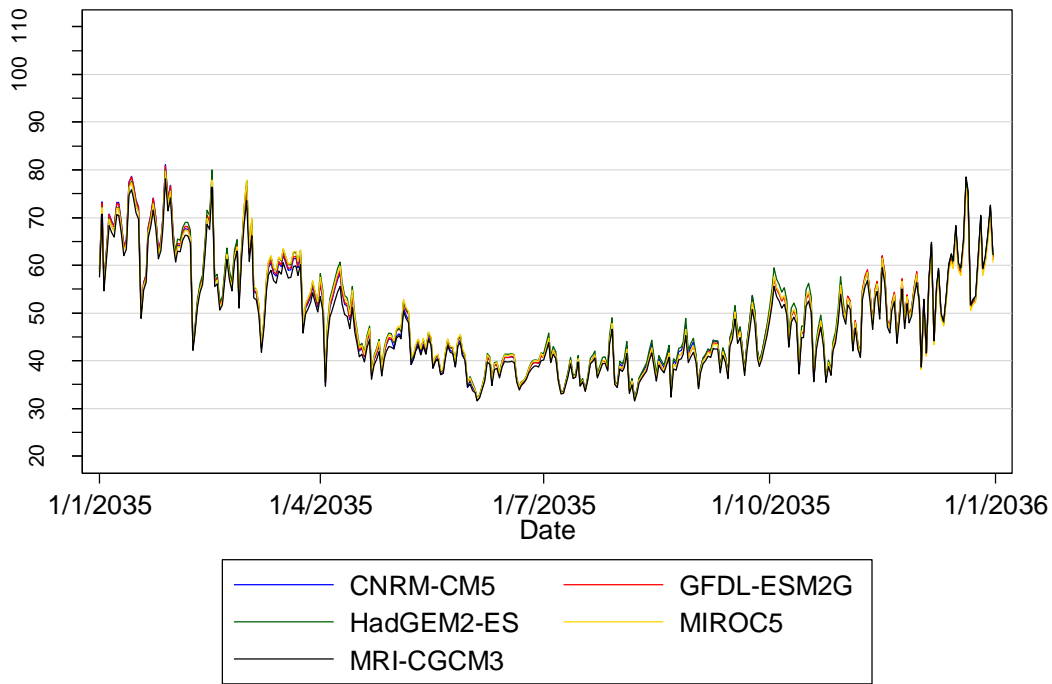
Box plots provide a very useful method of summarising data on water intake. The box covers the range from the 25th percentile to the 75th percentile of water intake and the horizontal line inside the box displays the median water intake.

Capped lines extending from the box display the range of water intake values out to limits defined by $1.5 \times \text{IQR}$. The IQR is the *inter-quartile range* and is the difference between the 25th and 75th percentiles. Values outside the capped lines are displayed as filled circles and represent more extreme water intake estimates (either very low or very high).

In future climate runs, there were challenges in determining how best to present summary data, largely because of the amount of data generated.

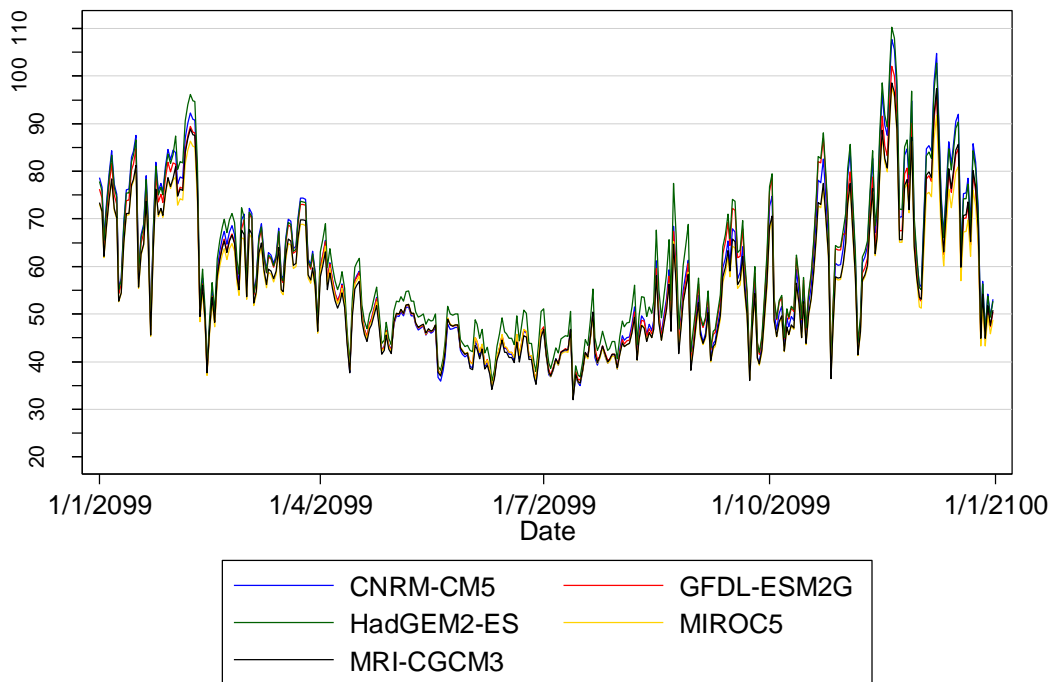
At each location and time-period combination (2010-2049 and 2050-2099), there were five models being run under each of three RCP scenarios.

Preliminary inspection of daily water intake predictions for the different models within one RCP scenario demonstrated very close agreement (see Figure 4.6 and Figure 4.7).



Water intake per day for location=Caroona, 2035, RCP2.6

Figure 4.6: Daily water intake over a one-year period (2035) at Caroona, with different lines for each of five models, all run under the same scenario (RCP2.6).



Water intake per day for location=Caroona, 2099, RCP8.5

Figure 4.7: Daily water intake over a one-year period (2099) at Caroona, with different lines for each of five models, all run under the same scenario (RCP8.5).

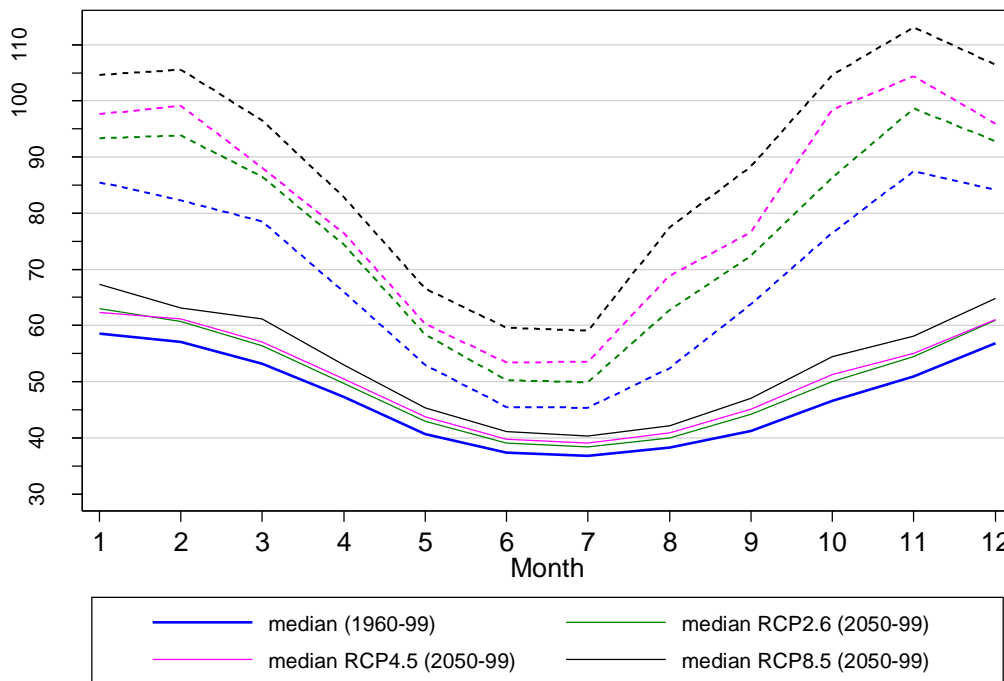
Because there was relatively little variation between models for predicted water intake at any one location and scenario, the separate daily water intake estimates for the five models were combined to produce single daily summary statistics including 25th percentile, median, 75th percentile and maximum daily water intake.

The same summary measures were produced for the historic period and this allowed direct comparison between the historic period and the two future climate periods (2010-2049 and 2050-2099). Percentage changes were then calculated by comparing the output value (for example the median daily water intake) for a future period and scenario to the same output value for the historic period from that same location. An example calculation is shown below, to calculate the % change in median daily water intake for 2010-49 and RCP2.6 when compared to the historic median daily water intake value for the same location.

$$\% \text{ change in MWI} = \frac{MWI_{2010-49, RCP2.6} - MWI_{1960-1999}}{MWI_{1960-1999}} \times 100$$

MWI= median daily water intake

In addition, summary plots were produced to show the median daily water intake for each month over the three time periods. An example plot is shown here.



Caroona, Parker et al (2000). Dashed lines show maximal values for each category

Figure 4.8: Plot showing median daily water intake for each month of the year for the period 2050-2099 at Caroona. The blue solid line shows the monthly median from the historic period for comparison.

The blue solid line is the median daily water intake estimated for the historic period. All daily water intake estimates for each month from the entire historic time period were analysed to produce a single median estimate for each month. The blue dashed line displays the single maximal daily water intake value from each month over the entire historic period.

For each of the three scenarios (2.6, 4.5, 8.5), the solid line represents the median of the daily medians. Initially, a single daily median water intake was produced for each scenario by estimating the median of the five separate model-specific estimates for each day. Then all the median daily water intake estimates from each month over the entire time period (2050-2099) were analysed to produce a single median estimate for each month.

The dashed line for any one scenario displays the single highest daily water intake estimate from any one of the underlying model estimates within that scenario and month across the entire time period.

This plot format was selected as a relatively simple option for displaying the typical (median) water intake from the historic period and from the three scenarios over a future period. In addition the dashed lines show the maximal water intake values per month from the historic period and from each scenario for the future period. These plots allow a rapid appreciation of the pattern of water intake per month and the effect of possible future climate change on water intake.

Tables of summary statistics and percentage change are also provided for more detailed presentation of water intake change over time.

3.7 Feedlot runoff

The MEDLI model generates a daily estimate of feedlot runoff (mm/day) as part of the model outputs.

Objective 2b for this project reflected the interest amongst the feedlot industry in management of water resources in the face of uncertain climate change impacts.

Water is used in feedlots for a range of purposes including cattle drinking water, feed processing, administration (staff amenities, lawns, etc.), cattle washing, sundry uses (trough cleaning, vehicle cleaning, dust control, drinking water for other stock, etc.) and irrigation. Water use includes losses through evaporation.

Effluent water that has been processed through an effluent management system may be used for irrigation purposes, either as a means of dispersing water on an intermittent basis or as a purposeful contribution to irrigation of planted crops. Effluent water is often diluted with clean water to ensure that solute concentrations are below levels that may have adverse effects on crops.

Previous studies in Australian feedlots have reported that 90% of the total water requirement in Australian feedlots is for cattle drinking water.

Effluent management systems typically incorporate storage ponds with the capacity to hold water for use either in a recycling system (where treated water may be capable of being used in the feedlot for cattle drinking or other purposes) or in irrigation systems.

Recent Australian research (B.FLT.0468; Watts et al 2012) noted that only 5% of Australian feedlots relied on surface dams for water requirements. The majority of feedlots relied on underground (bore) water (60%) or government allocations from a flow-regulated stream (26%).

As noted in another recent report (B.FLT.0348; Tucker et al 2010), effluent volumes are driven by runoff and runoff is largely driven by rainfall on the feedlot pad. Rainfall is highly variable both between feedlots and also over the course of a year within a single feedlot. Modelling in B.FLT.0348 suggests that even where irrigation use of effluent water is maximised (water is used every day if available in the effluent pond system), the average volume that can be extracted over time is around 50% of the total water entering the pond (range from 46 to 79%; Tucker et al 2010). However, there is extreme variability in the amount of water that can be extracted from effluent pond systems, largely because of variability in rainfall. Effluent pond volumes are highest in times when rainfall is high which coincides with reduced irrigation demand and conversely when irrigation demand is high (dry periods) there is likely to be reduced effluent pond water available.

The combination of effluent pond capacity being dictated mainly by compliance with pond overtopping limits rather than irrigation needs, the fact that effluent pond water is only ever likely to make a minor contribution to crop irrigation water needs on any commercial scale, and the lack of reliability of effluent water supply in times of high crop water requirements, all mean that effluent water is an inefficient contributor to crop irrigation requirements.

B.FLT.0348 concludes that sustainable yields of effluent for reuse within a feedlot may be sufficient to meet between 10-20% of the total water requirement for the feedlot and that the most useful application of this water may be for feedlot purposes such as cattle drinking water or sundry applications such as trough cleaning and cattle washing (Tucker et al 2010).

The approach to parameterising MEDLI for feedlot hydrology modelling involved setting the effluent pond volume in an iterative process to ensure that pond overtopping using historic climate data occurred at a frequency that was compliant with national guidelines. The MEDLI modelling process was not intended to allow modelling of availability of water from the effluent pond for irrigation purposes. The only measure of effluent pond water balance that was available in this modelling process was the runoff measure generated in the daily step MEDLI modelling.

An approach was developed to use runoff measures as an indication of the effect of possible climate change on effluent water balance into the future.

The hydrological cycle on feedlots can be summarised in broad input and output terms as the balance between:

- INPUTS: rainfall and the water content of manure (including faeces and urine)
- OUTPUTS: evaporation, manure harvest and runoff to the effluent management system

The major variability for water input is driven by rainfall.

When there is relatively little rain the input water will result in a rise in moisture content for the feedlot pad (without any runoff) and there will be evaporative loss occurring at some variable level each day.

When the level of rain increases it will reach a point where the feedlot pad is saturated and water starts to run off into the water management system. In addition while there may be some evaporative loss of moisture, in the face of increasing rain, the total input water will exceed evaporative losses and there will be runoff.

Runoff water can be considered as the excess of a partial balance between inputs (rain and manure) and losses before runoff (absorption into the feedlot pad, evaporation, manure harvest).

Our interest in this report is to summarise the changes in runoff pattern over time under different climate scenarios.

The change in runoff pattern provides an indication of whether feedlot runoff is increasing over time or decreasing over time (change in annual mean measures) and also whether there is a change in variability (based on assessment of the coefficient of variation). The coefficient of variation (CoV) is a standardised measure of the level of variability relative to the mean and is calculated as the standard deviation divided by the mean. When the CoV is rising it suggests that variation in the underlying data is increasing relative to the mean and conversely when CoV is declining it indicates that variation is reducing relative to the mean.

Increasing runoff provides an indication of areas or instances where there is increased flexibility in effluent management systems and where feedlots may choose to develop effluent management capacity with a view to allowing use of water for irrigation nor other purposes (recycled water for feedlot uses), rather than just developing effluent management systems for preventing environmental contamination.

Reducing runoff over time is an indication that available effluent water supplies will be expected to diminish.

If the CoV increases over time, then this would be interpreted as increasing uncertainty over possible effluent water supply from year to year.

4 Results

4.1 Summaries of future climate scenarios

4.1.1 Temperature summaries

SIL0 data were merged with predicted climate data to produce separate datasets for each combination of location, GCM model and scenario where each dataset contained daily maximum and minimum temperature values for the period running from 1 January 1900 to 31 December 2099.

Annual average maximum temperature was estimated by taking the maximum temperature value for each day and averaging all those values over each year.

An average daily temperature was estimated by the average of the daily maximum and minimum temperature values for each day. The daily average values were then averaged across each year to generate the **annual average temperature**.

For these two temperature measures, the five GCM outputs for each location and scenario combination were then combined to produce an average temperature value (average of the five model values for each year), minimum value (minimum of the five model values for each year) and a maximum value (maximum of the five model values for each year).

Plots were then produced showing these three values for each year. The area between the minimum and maximum model values was shaded since this represents the area covering the range of all model outputs. A central line showing the mean of the five model values for each year represents the likely or average pattern of temperature assuming all five models are acting as equally valid representations of future climate patterns.

Temperature anomalies for each of these two measures were based on estimating the same measure for a defined historic period (1961-1990) and then calculating the difference for each year in the predicted climate period (2010-2099) by applying the following formula:

$$T_{i(2010-2099)} - T_{k(1961-1990)}$$

where $i(2010-2099)$ = each GCM predicted annual value for the period 2010-2099, and

$k(1961-1999)$ = GCM predicted annual value for the period 1961-1999.

Where the future annual value is greater than the average from the historic period, the anomaly value is positive and where the future value is less than the average from the historic period, the anomaly is negative.

The number of days in each year when the maximum daily temperature exceeded either 35 C or 40 C was also recorded for each dataset.

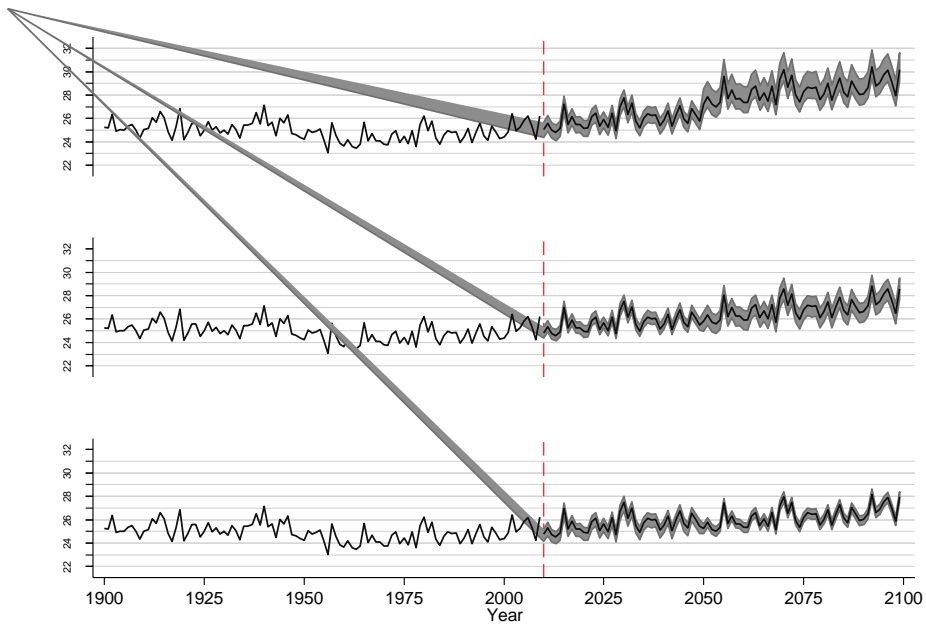
4.1.1.1 Average temperature anomaly

Table 4.1: Minimum, mean and maximum temperature anomaly based on difference between the average of five model values for each predicted climate year and the historic average for 1961-1990, reported for each location and scenario and for two different future time periods (2010-2049 and 2050-2099).

Location	RCP	Period	Min anomaly (°C)	Mean anomaly (°C)	Max anomaly (°C)
Caroona	RCP2.6	2010-2049	0.04	1.06	2.26
	RCP4.5	2010-2049	0.06	1.10	2.30
	RCP8.5	2010-2049	0.27	1.31	2.54
	RCP2.6	2050-2099	0.36	1.51	2.76
	RCP4.5	2050-2099	0.87	2.07	3.37
	RCP8.5	2050-2099	2.09	3.41	4.80
Comet	RCP2.6	2010-2049	0.04	1.14	2.14
	RCP4.5	2010-2049	0.02	1.13	2.12
	RCP8.5	2010-2049	0.22	1.33	2.34
	RCP2.6	2050-2099	0.22	1.50	2.79
	RCP4.5	2050-2099	0.76	2.08	3.42
	RCP8.5	2050-2099	2.15	3.60	5.05
Dalby	RCP2.6	2010-2049	0.29	0.96	1.97
	RCP4.5	2010-2049	0.33	1.00	2.02
	RCP8.5	2010-2049	0.46	1.14	2.17
	RCP2.6	2050-2099	0.49	1.28	2.68
	RCP4.5	2050-2099	1.02	1.82	3.27
	RCP8.5	2050-2099	2.29	3.15	4.70
Leeton	RCP2.6	2010-2049	0.09	0.96	1.71
	RCP4.5	2010-2049	0.17	1.04	1.80
	RCP8.5	2010-2049	0.28	1.16	1.92
	RCP2.6	2050-2099	0.31	1.41	3.14
	RCP4.5	2050-2099	0.90	2.06	3.88
	RCP8.5	2050-2099	2.04	3.31	5.25
Narrogin	RCP2.6	2010-2049	-0.78	0.72	1.68
	RCP4.5	2010-2049	-0.76	0.77	1.73
	RCP8.5	2010-2049	-0.71	0.82	1.78
	RCP2.6	2050-2099	-0.68	0.91	1.82
	RCP4.5	2050-2099	-0.21	1.42	2.35
	RCP8.5	2050-2099	0.62	2.35	3.34

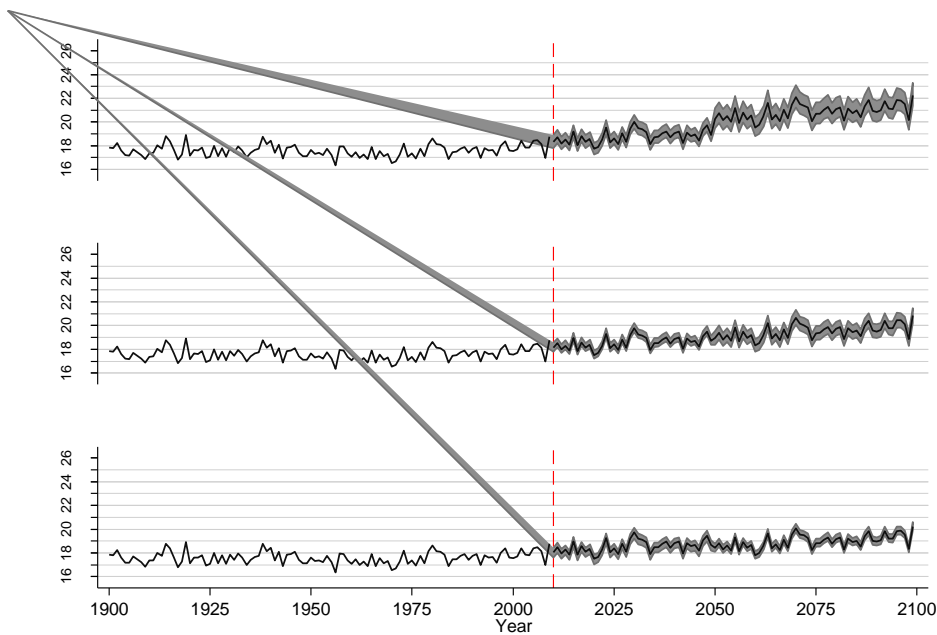
The table of numeric estimates of temperature anomalies (Table 4.1) is intended to provide a numeric summary of the change in average temperature for future climate change scenarios when compared to the average over the historic period.

4.1.1.2 Carroona



Annual ave max temp at Location= Carroona:
RCP8.5 (top), RCP4.5 (middle) & RCP2.6 (bottom) scenarios

(a)

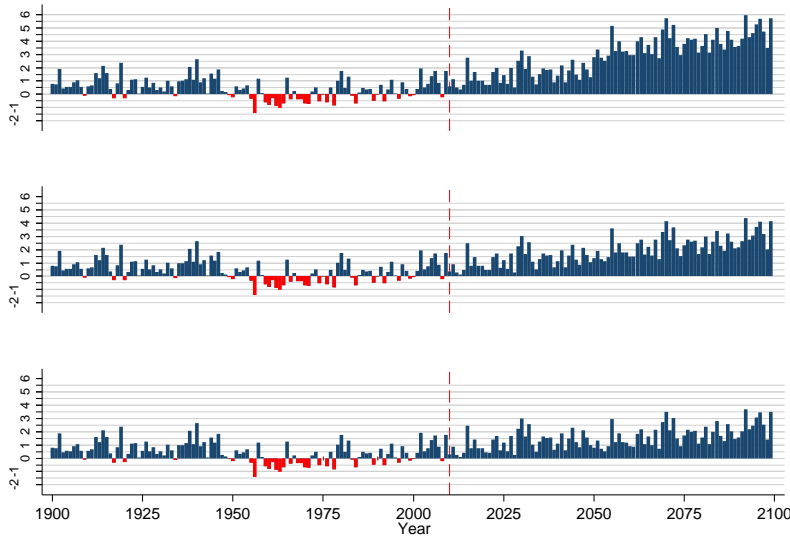


Annual average temp at Location= Carroona:
RCP8.5 (top), RCP4.5 (middle) & RCP2.6 (bottom) scenarios

(b)

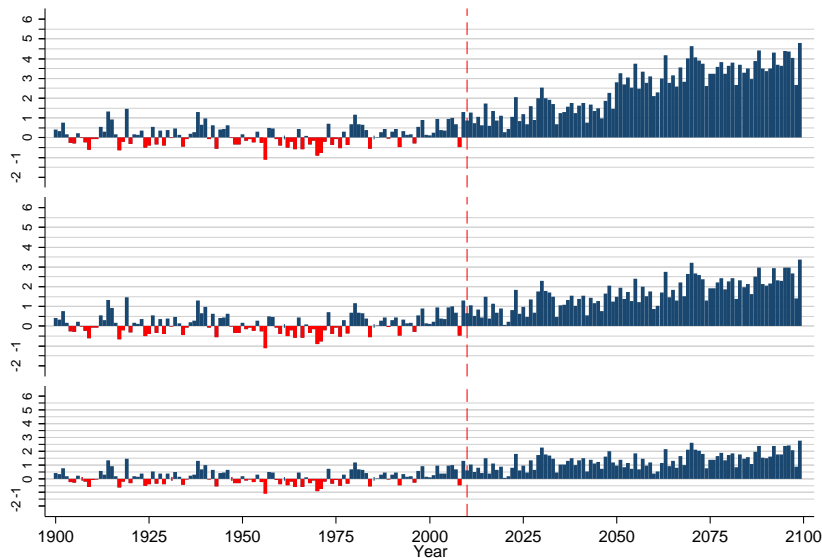
Figure 4.1: Annual average of maximum daily temperature (a) and of daily average temperature (b) from SILO data (1900-2009) and GCM predictions (2010-2099). The shaded area covers the range from minimum to maximum values of five GCMs and the dark line is the average of the five models. Separate plots are shown for each of three RCP scenarios: 8.5 (top), 4.5 (middle) and 2.6 (bottom). Location = Carroona.

The plots of annual average temperature provide a visual summary of temperature change over time under each of the three scenarios (RCP2.6, RCP4.5 and RCP8.5).



Annual max temp anomaly vs 1961-90 at Location= Carroona:
RCP8.5 (top), RCP4.5 (middle) & RCP2.6 (bottom) scenarios

(a)



Annual ave temp anomaly vs 1961-90 at Location= Carroona:
RCP8.5 (top), RCP4.5 (middle) & RCP2.6 (bottom) scenarios

(b)

Figure 4.2: Annual maximum temperature (a) and average temperature (b) anomaly based on difference between the daily value calculated from 1961-1990 and the average of five GCMs from 2010-2099. Separate plots are shown for RCP 8.5 (top), 4.5 (middle) and 2.6 (bottom) in each Figure. Blue shows an increase compared to 1961-1990 and red is a decrease. Location = Carroona.

Temperature anomaly plots provide a simple visual summary of temperature change over time, using a standard approach as is adopted by the Bureau of Meteorology⁵.

Table 4.2: Summary of the count of the number of days per year when the maximum daily temperature record was greater than 35 C at location=Caroona. Based on SILO records for the period from 1900-2009 and GCM outputs for 2010-2049 & 2050-2099 from five different models run under three RCP scenarios. Location = Caroona.

Location= Caroona	No of years		Count of days per year when max temp >35 C					
	Source	RCP	n	min	25th percentile	Median	75th percentile	max
1900-2009								
SILO data	na	110	3	13	22.5	32	59	
2010-2049								
CNRM-CM5	2.6	40	8	16	27	34	60	
GFDL-ESM2G	2.6	40	7	15.5	27.5	36	62	
HadGEM2-ES	2.6	40	8	17	31	38	61	
MIROC5	2.6	40	6	14	24	33.5	52	
MRI-CGCM3	2.6	40	5	12.5	21.5	28	50	
CNRM-CM5	4.5	40	6	14.5	25	34.5	54	
GFDL-ESM2G	4.5	40	5	16	29.5	36.5	60	
HadGEM2-ES	4.5	40	10	21	36	41.5	71	
MIROC5	4.5	40	5	13	23	32.5	51	
MRI-CGCM3	4.5	40	5	11.5	22.5	30	48	
CNRM-CM5	8.5	40	9	21	32.5	40.5	71	
GFDL-ESM2G	8.5	40	7	19	31	39.5	67	
HadGEM2-ES	8.5	40	11	25.5	41.5	48.5	75	
MIROC5	8.5	40	7	15	27	33.5	61	
MRI-CGCM3	8.5	40	7	13.5	20.5	29	50	
2050-2099								
CNRM-CM5	2.6	50	9	21	35	41	68	
GFDL-ESM2G	2.6	50	7	18	32.5	44	67	
HadGEM2-ES	2.6	50	9	24	38.5	45	78	
MIROC5	2.6	50	9	23	37.5	43	73	
MRI-CGCM3	2.6	50	8	18	32.5	41	64	
CNRM-CM5	4.5	50	9	27	41.5	50	82	
GFDL-ESM2G	4.5	50	15	31	45	58	88	
HadGEM2-ES	4.5	50	17	35	49.5	62	94	
MIROC5	4.5	50	9	20	33	42	67	
MRI-CGCM3	4.5	50	8	16	32	40	62	
CNRM-CM5	8.5	50	35	57	73	90	115	
GFDL-ESM2G	8.5	50	25	50	63.5	80	113	

⁵ <http://www.bom.gov.au/climate/change/index.shtml#tabs=Tracker&tracker=timeseries>

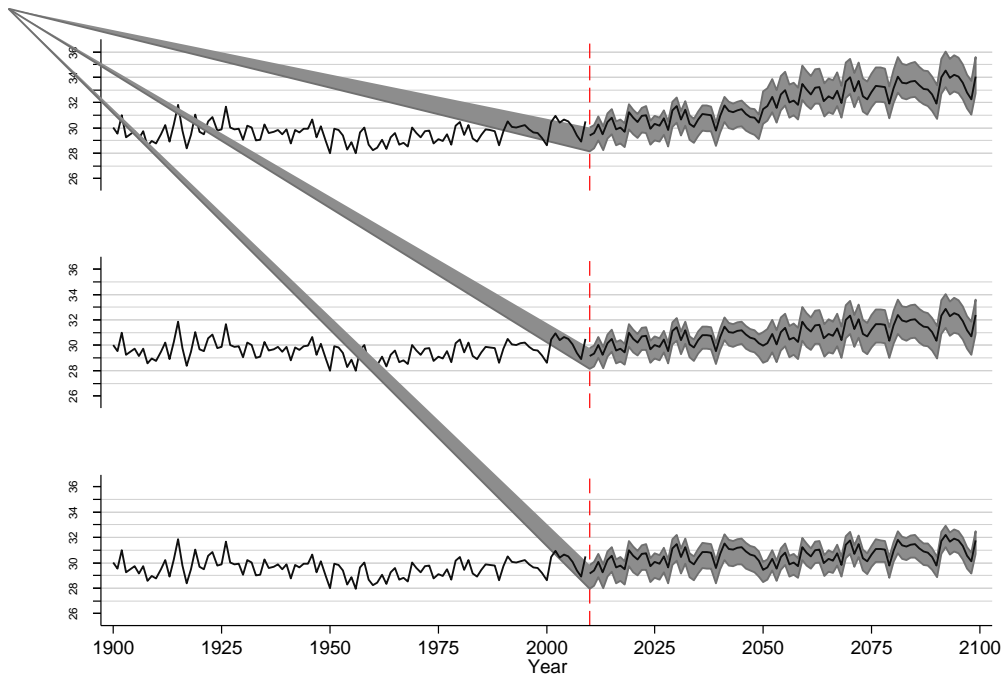
Location= Carroona	No of years		Count of days per year when max temp >35 C				
	RCP	n	min	25th percentile	Median	75th percentile	max
HadGEM2-ES	8.5	50	37	62	78.5	97	125
MIROC5	8.5	50	14	32	46	58	91
MRI-CGCM3	8.5	50	19	38	54	64	99

These tables (Table 4.2 and Table 4.3) provide a summary of the number of days when maximal temperature exceeds defined thresholds. These results provide additional detail on the possible future climate change by providing a measure of extreme days rather than measures of average change such as those provided in many of the plots of temperature change. There is a progressive increase in the number of hot days per year when considering the effect of increasing climate change (moving from RCP2.6 to RCP8.5) and when moving further into the future (2010-49 to 2050-99).

Table 4.3: Summary of the count of the number of days per year when the maximum daily temperature record was greater than 40 C at location=Caroona. Based on SILO records for the period from 1900-2009 and GCM outputs for 2010-2049 & 2050-2099 from five different models run under three RCP scenarios. Location = Caroona.

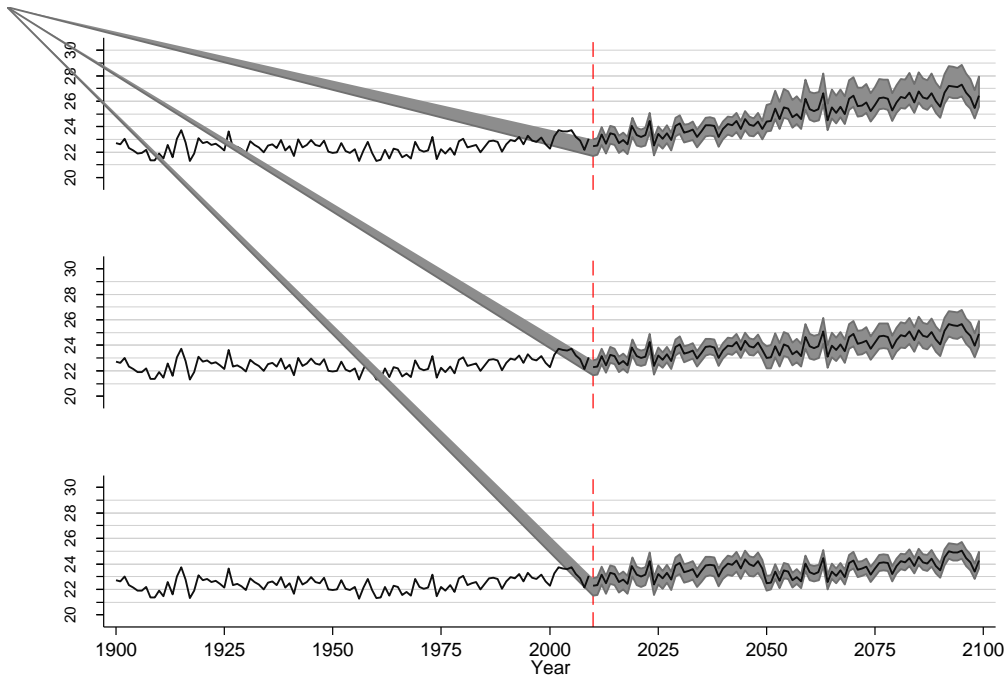
Location= Caroona		No of years	Count of days per year when max temp >40 C				
Source	RCP	n	min	25th percentile	Median	75th percentile	max
1900-2009							
SILO data	na	110	0	0	0.5	2	10
2010-2049							
CNRM-CM5	2.6	40	0	0	1	3	10
GFDL-ESM2G	2.6	40	0	0	1	2.5	9
HadGEM2-ES	2.6	40	0	0	1	3	10
MIROC5	2.6	40	0	0	1	2.5	9
MRI-CGCM3	2.6	40	0	0	0	1	6
CNRM-CM5	4.5	40	0	0	1	3	10
GFDL-ESM2G	4.5	40	0	0	2	4	8
HadGEM2-ES	4.5	40	0	0.5	2	4	12
MIROC5	4.5	40	0	0	0	2	5
MRI-CGCM3	4.5	40	0	0	0.5	2	9
CNRM-CM5	8.5	40	0	0	1.5	3.5	13
GFDL-ESM2G	8.5	40	0	0	1	3	9
HadGEM2-ES	8.5	40	0	1	3	6	15
MIROC5	8.5	40	0	0	1	2.5	9
MRI-CGCM3	8.5	40	0	0	0.5	1.5	8
2050-2099							
CNRM-CM5	2.6	50	0	0	3	5	17
GFDL-ESM2G	2.6	50	0	0	2	5	14
HadGEM2-ES	2.6	50	0	1	2.5	5	17
MIROC5	2.6	50	0	0	3	5	17
MRI-CGCM3	2.6	50	0	0	2	4	16
CNRM-CM5	4.5	50	0	1	3.5	6	18
GFDL-ESM2G	4.5	50	0	2	5.5	10	21
HadGEM2-ES	4.5	50	0	2	4	9	21
MIROC5	4.5	50	0	0	2	5	14
MRI-CGCM3	4.5	50	0	0	1	4	13
CNRM-CM5	8.5	50	2	8	16.5	26	42
GFDL-ESM2G	8.5	50	0	4	10	18	34
HadGEM2-ES	8.5	50	3	9	19	28	50
MIROC5	8.5	50	0	1	5	9	18
MRI-CGCM3	8.5	50	0	3	9	12	24

4.1.1.3 Comet



Annual ave max temp at Location= Comet:
RCP8.5 (top), RCP4.5 (middle) & RCP2.6 (bottom) scenarios

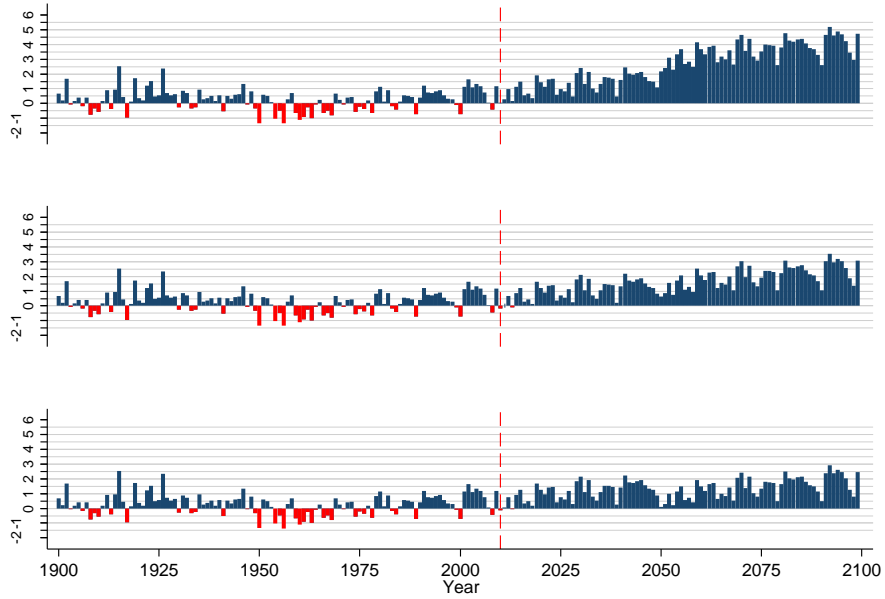
(a)



Annual average temp at Location= Comet:
RCP8.5 (top), RCP4.5 (middle) & RCP2.6 (bottom) scenarios

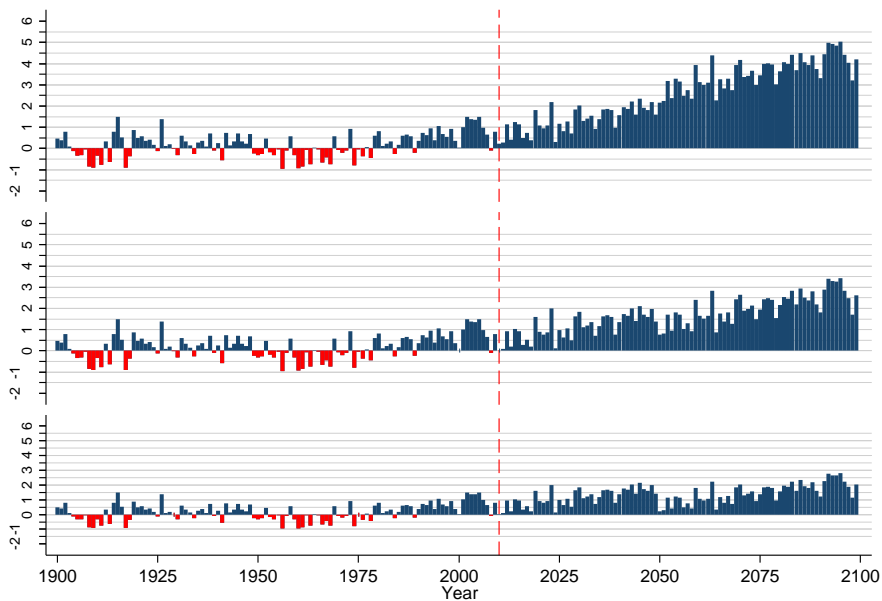
(b)

Figure 4.3: Annual average of maximum daily temperature (a) and of daily average temperature (b) from SILO data (1900-2009) and GCM predictions (2010-2099). The shaded area covers the range from minimum to maximum values of five GCMs and the dark line is the average of the five models. Separate plots are shown for each of three RCP scenarios: 8.5 (top), 4.5 (middle) and 2.6 (bottom). Location = Comet.



Annual max temp anomaly vs 1961-90 at Location= Comet:
RCP8.5 (top), RCP4.5 (middle) & RCP2.6 (bottom) scenarios

(a)



Annual ave temp anomaly vs 1961-90 at Location= Comet:
RCP8.5 (top), RCP4.5 (middle) & RCP2.6 (bottom) scenarios

(b)

Figure 4.4: Annual maximum temperature (a) and average temperature (b) anomaly based on difference between the daily value calculated from 1961-1990 and the average of five GCMs from 2010-2099. Separate plots are shown for RCP 8.5 (top), 4.5 (middle) and 2.6 (bottom) in each Figure. Blue shows an increase compared to 1961-1990 and red is a decrease. Location = Comet.

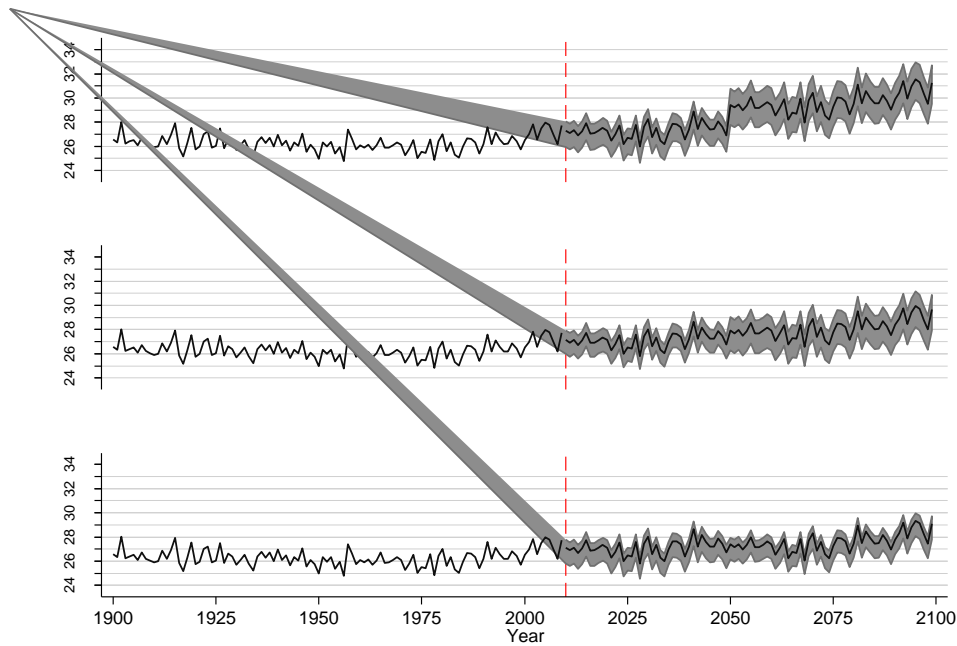
Table 4.4: Summary of the count of the number of days per year when the maximum daily temperature record was greater than 35 C. Based on SILO records for the period from 1900-2009 and GCM outputs for 2010-2049 & 2050-2099 from five different models run under three RCP scenarios. Location = Comet.

Location= Comet		No of years		Count of days per year when max temp >35 C			
Source	RCP	n	min	25th percentile	Median	75th percentile	max
1900-2009							
SILO data	na	110	6	36	48	62	115
2010-2049							
CNRM-CM5	2.6	40	22	46	58.5	72.5	107
GFDL-ESM2G	2.6	40	45	61.5	78	94.5	110
HadGEM2-ES	2.6	40	44	63.5	78.5	94	120
MIROC5	2.6	40	36	59.5	73	89	121
MRI-CGCM3	2.6	40	28	48.5	56.5	66	108
CNRM-CM5	4.5	40	19	43	50	66.5	99
GFDL-ESM2G	4.5	40	31	54.5	69.5	85	119
HadGEM2-ES	4.5	40	44	62	78.5	93	120
MIROC5	4.5	40	30	49.5	65	80.5	112
MRI-CGCM3	4.5	40	29	51	60	75	109
CNRM-CM5	8.5	40	37	60	72	88	120
GFDL-ESM2G	8.5	40	30	58.5	70.5	85.5	115
HadGEM2-ES	8.5	40	49	72.5	88	106	123
MIROC5	8.5	40	39	59	76	93	119
MRI-CGCM3	8.5	40	27	49	58	71.5	104
2050-2099							
CNRM-CM5	2.6	50	39	58	73	90	123
GFDL-ESM2G	2.6	50	20	43	55	72	106
HadGEM2-ES	2.6	50	46	66	85	105	139
MIROC5	2.6	50	52	81	94.5	114	153
MRI-CGCM3	2.6	50	38	59	70.5	83	116
CNRM-CM5	4.5	50	43	64	79.5	98	136
GFDL-ESM2G	4.5	50	50	79	96	113	149
HadGEM2-ES	4.5	50	61	92	111.5	130	170
MIROC5	4.5	50	45	67	82	99	140
MRI-CGCM3	4.5	50	33	58	66	80	114
CNRM-CM5	8.5	50	82	112	129.5	145	181
GFDL-ESM2G	8.5	50	76	108	133	147	188
HadGEM2-ES	8.5	50	107	145	163.5	180	215
MIROC5	8.5	50	62	96	115	132	171
MRI-CGCM3	8.5	50	67	93	111.5	126	159

Table 4.5: Summary of the count of the number of days per year when the maximum daily temperature record was greater than 40 C. Based on SILO records for the period from 1900-2009 and GCM outputs for 2010-2049 & 2050-2099 from five different models run under three RCP scenarios. Location = Comet.

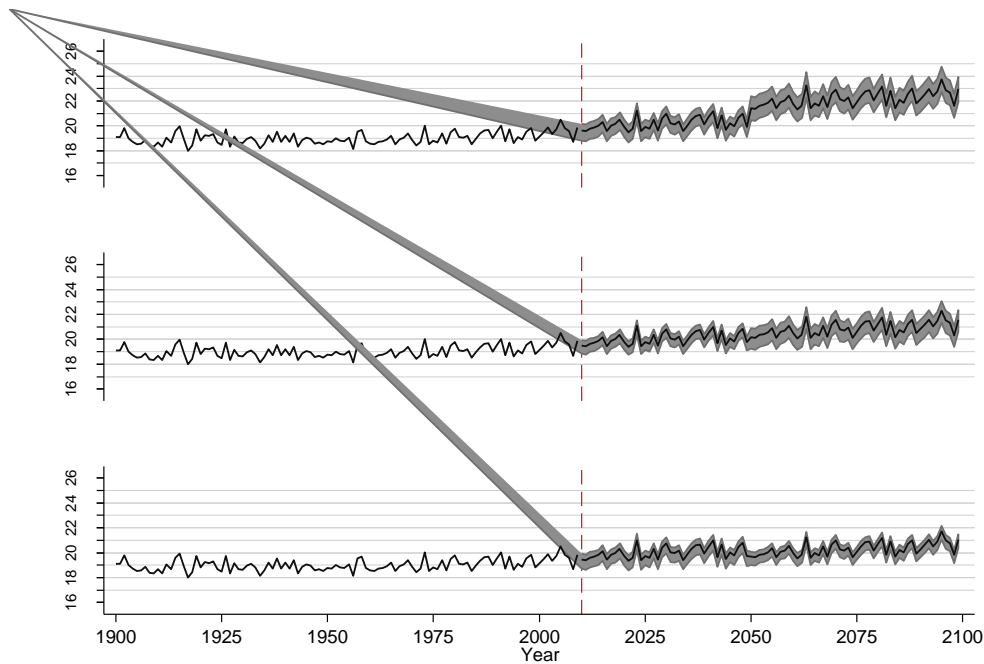
Location= Comet		No of years	Count of days per year when max temp >40 C				
Source	RCP	n	min	25th percentile	Median	75th percentile	max
1900-2009							
SILO data	na	110	0	0	1	3	14
2010-2049							
CNRM-CM5	2.6	40	0	2	4	7	17
GFDL-ESM2G	2.6	40	1	4	7	12	24
HadGEM2-ES	2.6	40	0	2	4.5	8	19
MIROC5	2.6	40	0	2	4	8.5	20
MRI-CGCM3	2.6	40	0	1	3	6.5	13
CNRM-CM5	4.5	40	0	1	3	6	15
GFDL-ESM2G	4.5	40	0	1.5	4	7	19
HadGEM2-ES	4.5	40	0	2	4.5	8	19
MIROC5	4.5	40	0	1	3	6.5	14
MRI-CGCM3	4.5	40	0	2	5	9	19
CNRM-CM5	8.5	40	0	2.5	5.5	8.5	18
GFDL-ESM2G	8.5	40	0	3	6	9	19
HadGEM2-ES	8.5	40	1	4	8	12	24
MIROC5	8.5	40	0	2	4.5	9	22
MRI-CGCM3	8.5	40	0	2	4.5	7.5	14
2050-2099							
CNRM-CM5	2.6	50	0	2	4	9	20
GFDL-ESM2G	2.6	50	0	1	2.5	6	10
HadGEM2-ES	2.6	50	0	3	7	11	24
MIROC5	2.6	50	0	4	8	14	26
MRI-CGCM3	2.6	50	0	3	6	10	18
CNRM-CM5	4.5	50	0	2	4	10	20
GFDL-ESM2G	4.5	50	2	8	15	21	32
HadGEM2-ES	4.5	50	2	9	16	21	37
MIROC5	4.5	50	0	3	5.5	12	22
MRI-CGCM3	4.5	50	0	4	9	14	25
CNRM-CM5	8.5	50	4	22	29	40	67
GFDL-ESM2G	8.5	50	4	14	21.5	28	47
HadGEM2-ES	8.5	50	10	32	42	57	92
MIROC5	8.5	50	2	10	15.5	21	42
MRI-CGCM3	8.5	50	5	15	23	30	56

4.1.1.4 Dalby



Annual ave max temp at Location= Dalby:
RCP8.5 (top), RCP4.5 (middle) & RCP2.6 (bottom) scenarios

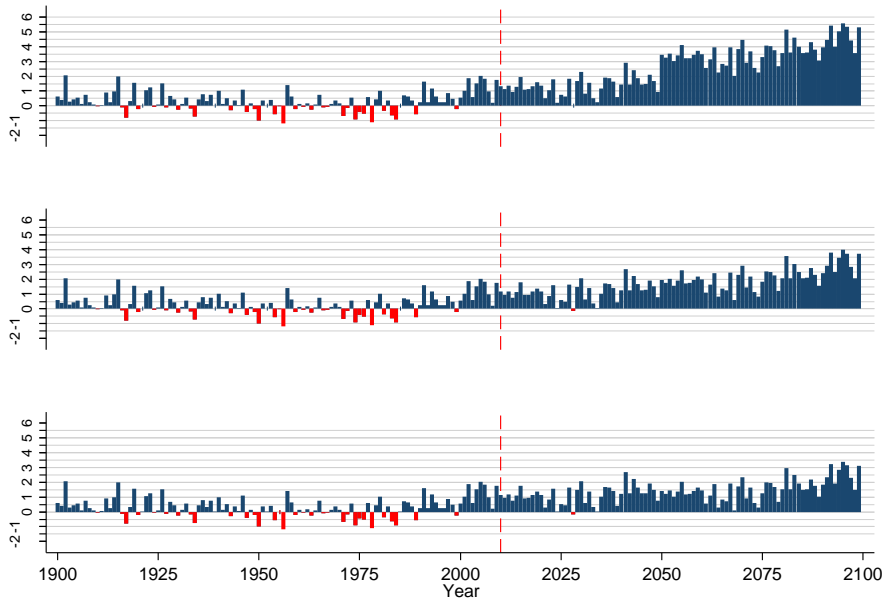
(a)



Annual average temp at Location= Dalby:
RCP8.5 (top), RCP4.5 (middle) & RCP2.6 (bottom) scenarios

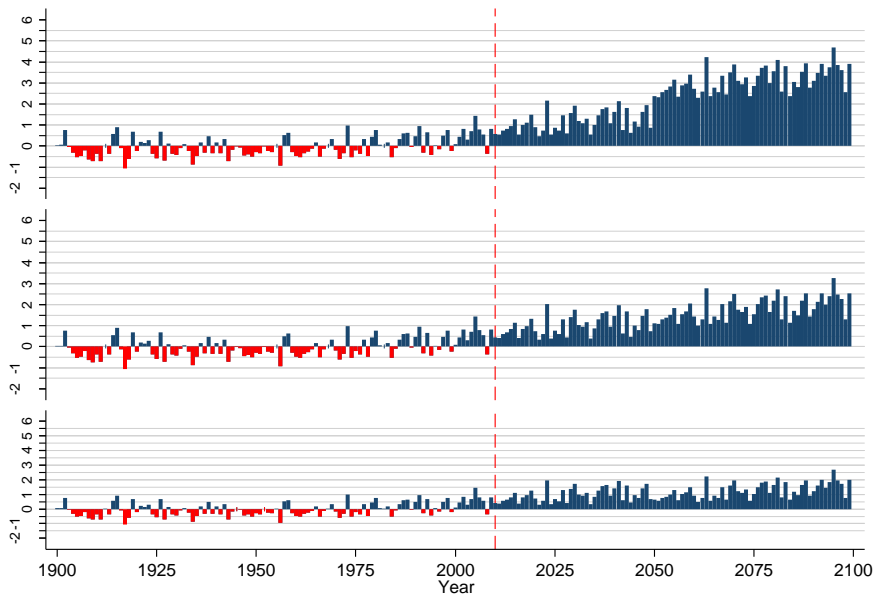
(b)

Figure 4.5: Annual average of maximum daily temperature (a) and of daily average temperature (b) from SILO data (1900-2009) and GCM predictions (2010-2099). The shaded area covers the range from minimum to maximum values of five GCMs and the dark line is the average of the five models. Separate plots are shown for each of three RCP scenarios: 8.5 (top), 4.5 (middle) and 2.6 (bottom). Location = Dalby.



Annual max temp anomaly vs 1961-90 at Location= Dalby:
RCP8.5 (top), RCP4.5 (middle) & RCP2.6 (bottom) scenarios

(a)



Annual ave temp anomaly vs 1961-90 at Location= Dalby:
RCP8.5 (top), RCP4.5 (middle) & RCP2.6 (bottom) scenarios

(b)

Figure 4.6: Annual maximum temperature (a) and average temperature (b) anomaly based on difference between the daily value calculated from 1961-1990 and the average of five GCMs from 2010-2099. Separate plots are shown for RCP 8.5 (top), 4.5 (middle) and 2.6 (bottom) in each Figure. Blue shows an increase compared to 1961-1990 and red is a decrease. Location = Dalby.

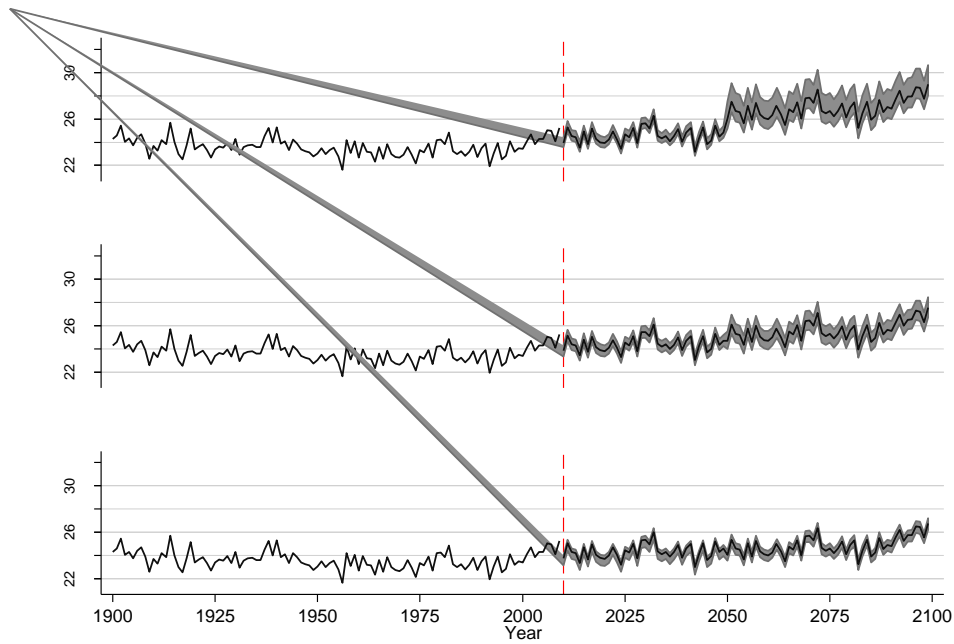
Table 4.6: Summary of the count of the number of days per year when the maximum daily temperature record was greater than 35 C. Based on SILO records for the period from 1900-2009 and GCM outputs for 2010-2049 & 2050-2099 from five different models run under three RCP scenarios. Location = Dalby.

Location= Dalby		No of years	Count of days per year when max temp >35 C				
Source	RCP	n	min	25th percentile	Median	75th percentile	max
1900-2009							
SILO data	na	110	0	9	14.5	21	41
2010-2049							
CNRM-CM5	2.6	40	6	17	23	30.5	41
GFDL-ESM2G	2.6	40	9	21.5	31.5	37.5	49
HadGEM2-ES	2.6	40	10	20.5	29.5	36	51
MIROC5	2.6	40	9	18	26	31.5	48
MRI-CGCM3	2.6	40	2	9.5	14	21	29
CNRM-CM5	4.5	40	5	13	17.5	25	33
GFDL-ESM2G	4.5	40	12	22.5	33	40	54
HadGEM2-ES	4.5	40	10	21	30.5	37	51
MIROC5	4.5	40	6	15	22	29	39
MRI-CGCM3	4.5	40	4	12	17	25	32
CNRM-CM5	8.5	40	9	21	30	36	45
GFDL-ESM2G	8.5	40	9	18	28	35	52
HadGEM2-ES	8.5	40	16	28	40	46	59
MIROC5	8.5	40	9	19	26.5	34.5	47
MRI-CGCM3	8.5	40	2	8	14	19.5	29
2050-2099							
CNRM-CM5	2.6	50	9	22	31	39	60
GFDL-ESM2G	2.6	50	9	17	26.5	34	54
HadGEM2-ES	2.6	50	11	24	34	40	65
MIROC5	2.6	50	17	28	42	47	74
MRI-CGCM3	2.6	50	5	14	21	27	51
CNRM-CM5	4.5	50	12	26	37	43	68
GFDL-ESM2G	4.5	50	20	34	46	57	81
HadGEM2-ES	4.5	50	21	38	52	63	93
MIROC5	4.5	50	10	22	32	39	64
MRI-CGCM3	4.5	50	4	16	26	30	49
CNRM-CM5	8.5	50	38	59	75	86	121
GFDL-ESM2G	8.5	50	37	53	68	81	116
HadGEM2-ES	8.5	50	52	73	89	100	141
MIROC5	8.5	50	24	40	53	62	91
MRI-CGCM3	8.5	50	14	28	42.5	50	76

Table 4.7: Summary of the count of the number of days per year when the maximum daily temperature record was greater than 40 C. Based on SILO records for the period from 1900-2009 and GCM outputs for 2010-2049 & 2050-2099 from five different models run under three RCP scenarios. Location = Dalby.

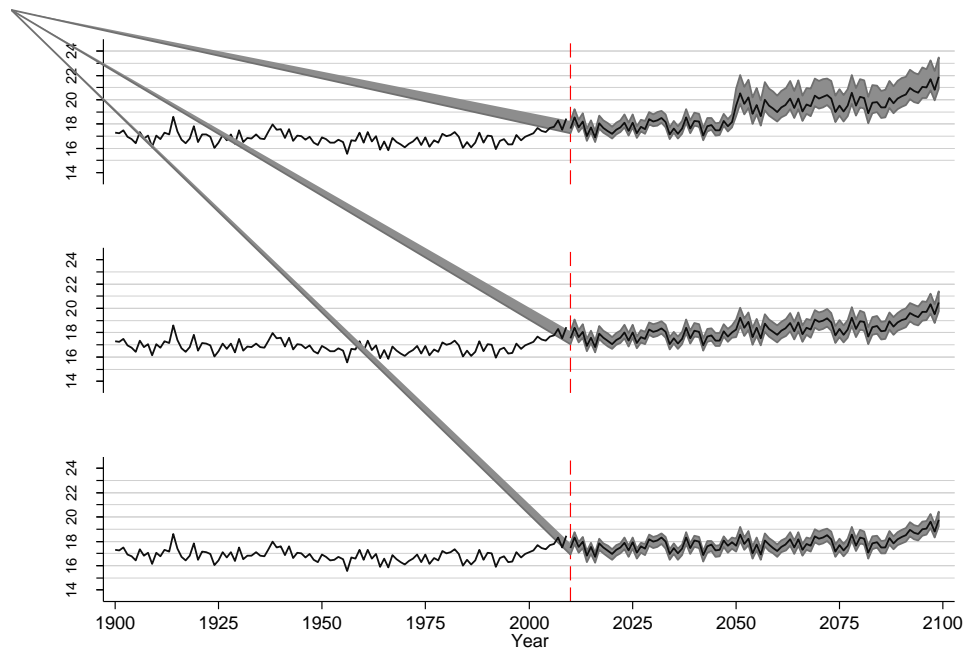
Location= Dalby		No of years	Count of days per year when max temp >40 C				
Source	RCP	n	min	25th percentile	Median	75th percentile	max
1900-2009							
SILO data	na	110	0	0	0	1	3
2010-2049							
CNRM-CM5	2.6	40	0	0	0.5	2	4
GFDL-ESM2G	2.6	40	0	0	1	3	6
HadGEM2-ES	2.6	40	0	0	1	2.5	6
MIROC5	2.6	40	0	0	1	2	4
MRI-CGCM3	2.6	40	0	0	0	1	4
CNRM-CM5	4.5	40	0	0	0	1.5	4
GFDL-ESM2G	4.5	40	0	1	1	4	9
HadGEM2-ES	4.5	40	0	0	1	3	6
MIROC5	4.5	40	0	0	0	1.5	4
MRI-CGCM3	4.5	40	0	0	0	1	4
CNRM-CM5	8.5	40	0	0	1	3	8
GFDL-ESM2G	8.5	40	0	0	1	3	9
HadGEM2-ES	8.5	40	0	0.5	2	5	10
MIROC5	8.5	40	0	0	1	2.5	5
MRI-CGCM3	8.5	40	0	0	0	1.5	6
2050-2099							
CNRM-CM5	2.6	50	0	0	1	4	10
GFDL-ESM2G	2.6	50	0	0	0.5	2	5
HadGEM2-ES	2.6	50	0	0	1	4	12
MIROC5	2.6	50	0	1	2	4	15
MRI-CGCM3	2.6	50	0	0	0	3	6
CNRM-CM5	4.5	50	0	0	1.5	4	12
GFDL-ESM2G	4.5	50	0	1	3	8	17
HadGEM2-ES	4.5	50	0	1	4	9	18
MIROC5	4.5	50	0	0	1	3	10
MRI-CGCM3	4.5	50	0	0	1	2	6
CNRM-CM5	8.5	50	1	6	12	17	34
GFDL-ESM2G	8.5	50	0	4	9	14	28
HadGEM2-ES	8.5	50	3	10	15.5	22	39
MIROC5	8.5	50	0	2	4	9	20
MRI-CGCM3	8.5	50	0	1	3	8	19

4.1.1.5 Leeton



Annual ave max temp at Location= Leeton:
RCP8.5 (top), RCP4.5 (middle) & RCP2.6 (bottom) scenarios

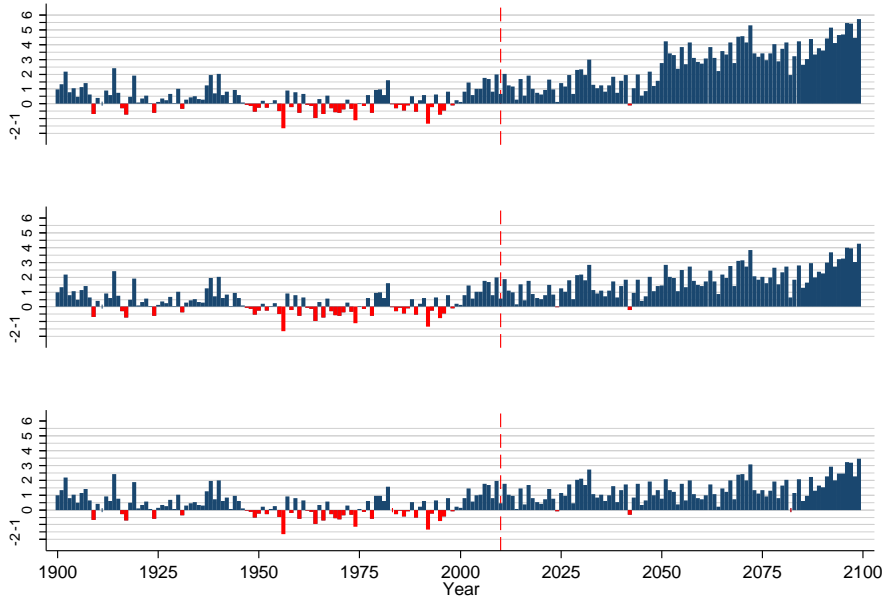
(a)



Annual average temp at Location= Leeton:
RCP8.5 (top), RCP4.5 (middle) & RCP2.6 (bottom) scenarios

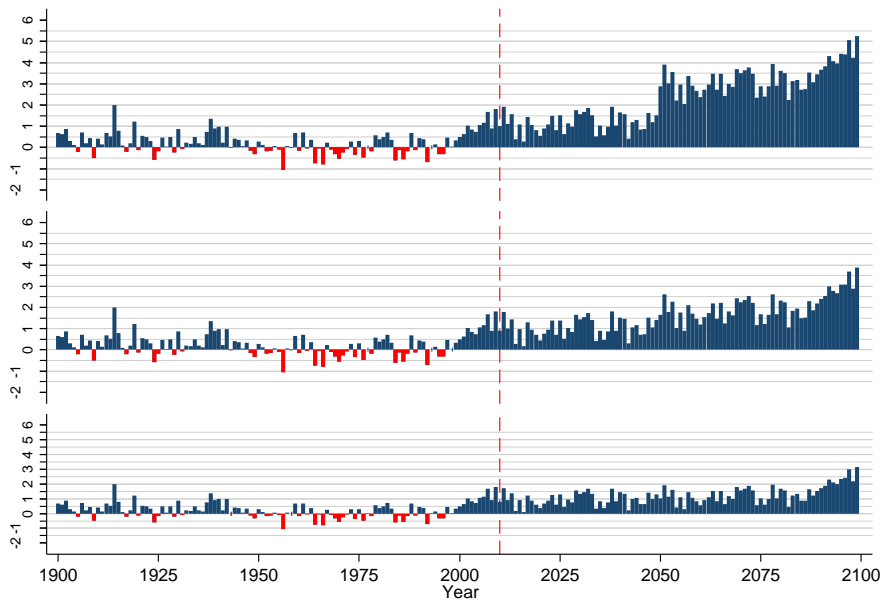
(b)

Figure 4.7: Annual average of maximum daily temperature (a) and of daily average temperature (b) from SILO data (1900-2009) and GCM predictions (2010-2099). The shaded area covers the range from minimum to maximum values of five GCMs and the dark line is the average of the five models. Separate plots are shown for each of three RCP scenarios: 8.5 (top), 4.5 (middle) and 2.6 (bottom). Location = Leeton.



Annual max temp anomaly vs 1961-90 at Location= Leeton: RCP8.5 (top), RCP4.5 (middle) & RCP2.6 (bottom) scenarios

(a)



Annual ave temp anomaly vs 1961-90 at Location= Leeton: RCP8.5 (top), RCP4.5 (middle) & RCP2.6 (bottom) scenarios

(b)

Figure 4.8: Annual maximum temperature (a) and average temperature (b) anomaly based on difference between the daily value calculated from 1961-1990 and the average of five GCMs from 2010-2099. Separate plots are shown for RCP 8.5 (top), 4.5 (middle) and 2.6 (bottom) in each Figure. Blue shows an increase compared to 1961-1990 and red is a decrease. Location = Leeton.

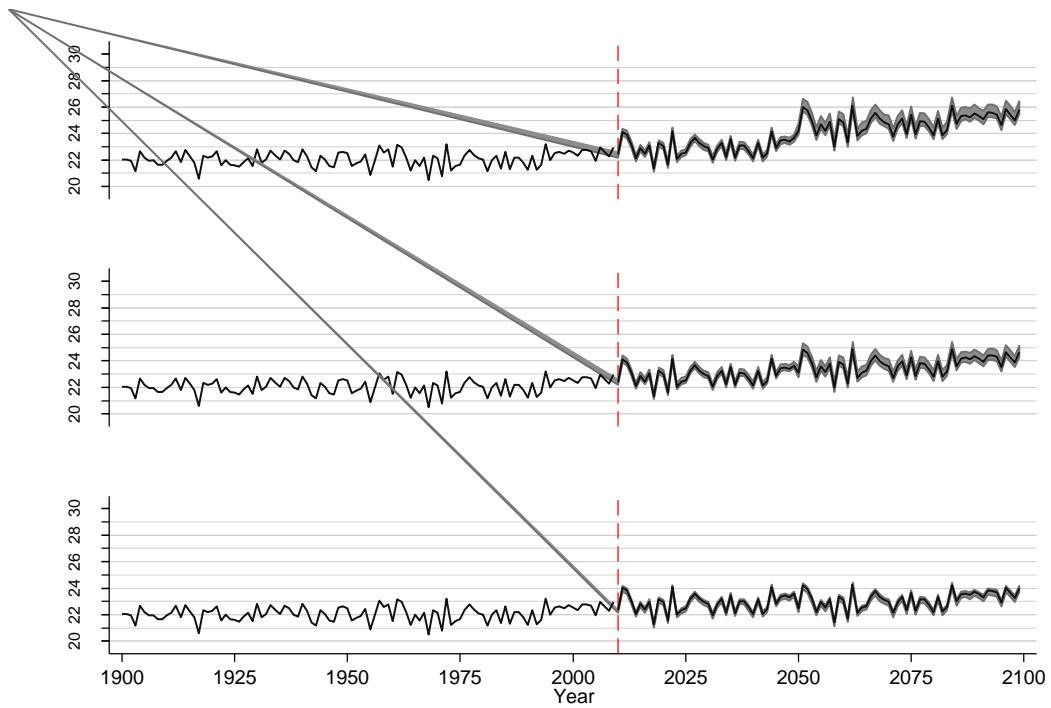
Table 4.8: Summary of the count of the number of days per year when the maximum daily temperature record was greater than 35 C. Based on SILO records for the period from 1900-2009 and GCM outputs for 2010-2049 & 2050-2099 from five different models run under three RCP scenarios. Location = Leeton.

Location= Leeton		No of years	Count of days per year when max temp >35 C				
Source	RCP	n	min	25th percentile	Median	75th percentile	max
1900-2009							
SILO data	na	110	2	19	26.5	33	54
2010-2049							
CNRM-CM5	2.6	40	8	23.5	28	41.5	55
GFDL-ESM2G	2.6	40	10	25	29.5	40.5	55
HadGEM2-ES	2.6	40	9	26	31	45.5	58
MIROC5	2.6	40	9	24.5	31	44.5	59
MRI-CGCM3	2.6	40	5	20	24.5	35	47
CNRM-CM5	4.5	40	9	24	29	40	54
GFDL-ESM2G	4.5	40	13	25	33	41.5	59
HadGEM2-ES	4.5	40	15	29.5	37	49.5	65
MIROC5	4.5	40	9	24.5	31	44	57
MRI-CGCM3	4.5	40	6	19.5	26	36.5	51
CNRM-CM5	8.5	40	11	27.5	33	47	59
GFDL-ESM2G	8.5	40	6	23	28.5	40.5	55
HadGEM2-ES	8.5	40	16	29	37.5	49	64
MIROC5	8.5	40	9	26.5	31.5	46	59
MRI-CGCM3	8.5	40	6	22	27	38.5	49
2050-2099							
CNRM-CM5	2.6	50	12	29	38	48	71
GFDL-ESM2G	2.6	50	12	27	38.5	45	69
HadGEM2-ES	2.6	50	15	33	43.5	53	79
MIROC5	2.6	50	10	29	38.5	47	67
MRI-CGCM3	2.6	50	6	23	31.5	39	59
CNRM-CM5	4.5	50	17	32	45	54	78
GFDL-ESM2G	4.5	50	21	36	51	60	90
HadGEM2-ES	4.5	50	27	41	56.5	65	93
MIROC5	4.5	50	15	32	43	53	76
MRI-CGCM3	4.5	50	6	25	35	44	63
CNRM-CM5	8.5	50	40	54	66	73	103
GFDL-ESM2G	8.5	50	33	47	61.5	72	105
HadGEM2-ES	8.5	50	50	70	80.5	94	124
MIROC5	8.5	50	25	43	56.5	65	91
MRI-CGCM3	8.5	50	23	38	48.5	59	87

Table 4.9: Summary of the count of the number of days per year when the maximum daily temperature record was greater than 40 C. Based on SILO records for the period from 1900-2009 and GCM outputs for 2010-2049 & 2050-2099 from five different models run under three RCP scenarios. Location = Leeton.

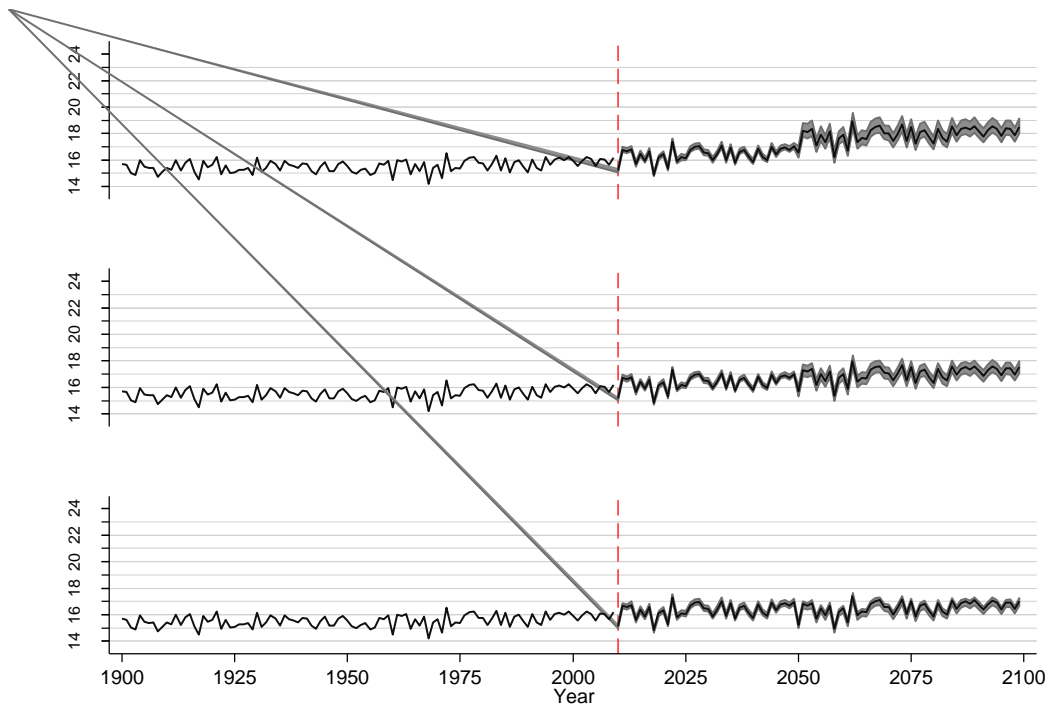
Location= Leeton		No of years	Count of days per year when max temp >40 C				
Source	RCP	n	min	25th percentile	Median	75th percentile	max
1900-2009							
SILO data	na	110	0	1	3	5	18
2010-2049							
CNRM-CM5	2.6	40	0	2	5	8.5	18
GFDL-ESM2G	2.6	40	0	2.5	4	6.5	15
HadGEM2-ES	2.6	40	0	2	4	7	16
MIROC5	2.6	40	0	2	4.5	7	18
MRI-CGCM3	2.6	40	0	1	3.5	5	12
CNRM-CM5	4.5	40	0	2	4.5	8	15
GFDL-ESM2G	4.5	40	0	2	5	8	19
HadGEM2-ES	4.5	40	0	3	6	9.5	23
MIROC5	4.5	40	0	2	4.5	7.5	18
MRI-CGCM3	4.5	40	0	1	3	5	13
CNRM-CM5	8.5	40	0	3	6	9.5	20
GFDL-ESM2G	8.5	40	0	2	4	6.5	16
HadGEM2-ES	8.5	40	0	3	6.5	11	20
MIROC5	8.5	40	0	3	5	8	19
MRI-CGCM3	8.5	40	0	2	4	6	13
2050-2099							
CNRM-CM5	2.6	50	0	3	6.5	11	30
GFDL-ESM2G	2.6	50	0	3	6	9	26
HadGEM2-ES	2.6	50	0	5	8.5	13	32
MIROC5	2.6	50	0	4	7	10	29
MRI-CGCM3	2.6	50	0	2	4.5	7	28
CNRM-CM5	4.5	50	0	4	8	13	31
GFDL-ESM2G	4.5	50	1	6	10	17	39
HadGEM2-ES	4.5	50	1	8	13.5	19	38
MIROC5	4.5	50	0	5	8.5	12	33
MRI-CGCM3	4.5	50	0	3	6	9	30
CNRM-CM5	8.5	50	2	13	19.5	29	45
GFDL-ESM2G	8.5	50	1	11	16	25	40
HadGEM2-ES	8.5	50	4	24	33	41	58
MIROC5	8.5	50	1	8	13	21	40
MRI-CGCM3	8.5	50	1	6	11	16	34

4.1.1.6 Narrogin



Annual ave max temp at Location= Narrogin:
RCP8.5 (top), RCP4.5 (middle) & RCP2.6 (bottom) scenarios

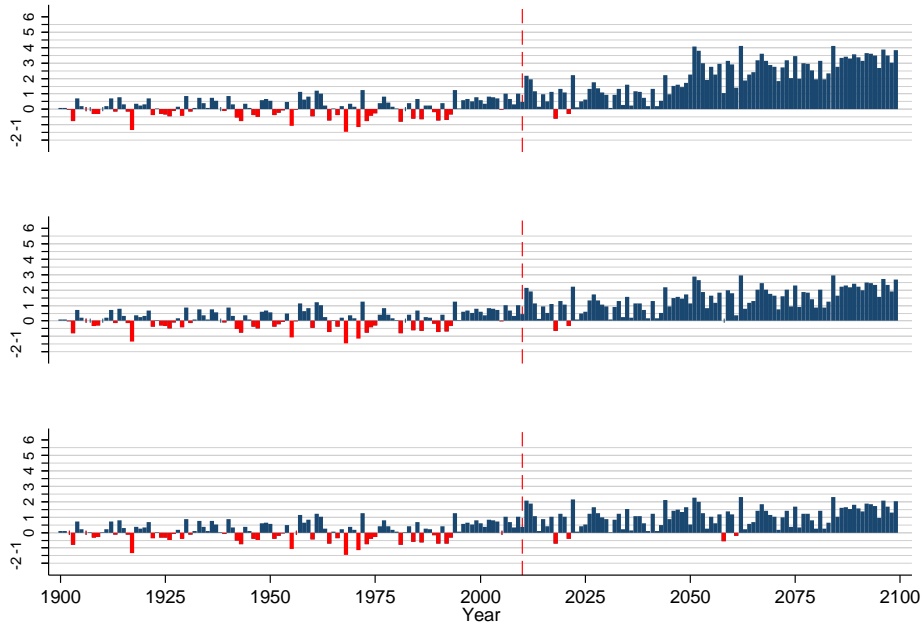
(a)



Annual average temp at Location= Narrogin:
 RCP8.5 (top), RCP4.5 (middle) & RCP2.6 (bottom) scenarios

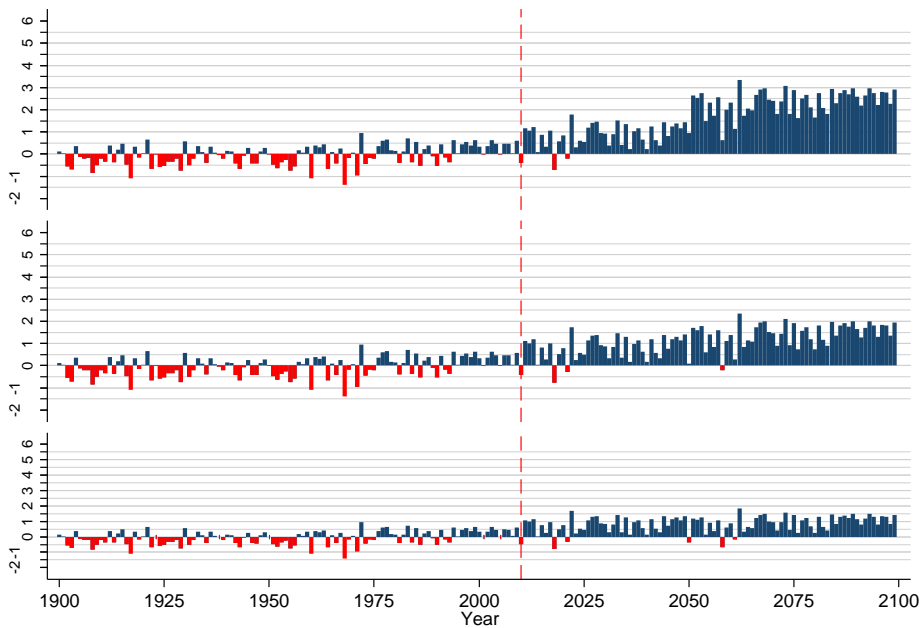
(b)

Figure 4.9: Annual average of maximum daily temperature (a) and of daily average temperature (b) from SILO data (1900-2009) and GCM predictions (2010-2099). The shaded area covers the range from minimum to maximum values of five GCMs and the dark line is the average of the five models. Separate plots are shown for each of three RCP scenarios: 8.5 (top), 4.5 (middle) and 2.6 (bottom). Location = Narrogin.



Annual max temp anomaly vs 1961-90 at Location= Narrogin:
RCP8.5 (top), RCP4.5 (middle) & RCP2.6 (bottom) scenarios

(a)



Annual ave temp anomaly vs 1961-90 at Location= Narrogin:
RCP8.5 (top), RCP4.5 (middle) & RCP2.6 (bottom) scenarios

(b)

Figure 4.10: Annual maximum temperature (a) and average temperature (b) anomaly based on difference between the daily value calculated from 1961-1990 and the average of five GCMs from 2010-2099. Separate plots are shown for RCP 8.5 (top), 4.5 (middle) and 2.6 (bottom) in each Figure. Blue shows an increase compared to 1961-1990 and red is a decrease. Location = Narrogin.

Table 4.10: Summary of the count of the number of days per year when the maximum daily temperature record was greater than 35 C. Based on SILO records for the period from 1900-2009 and GCM outputs for 2010-2049 & 2050-2099 from five different models run under three RCP scenarios. Location = Narrogin.

Location= Narrogin		No of years Count of days per year when max temp >35 C					
Source	RCP	n	min	25th percentile	Median	75th percentile	max
1900-2009							
SILO data	na	110	0	11	13.5	18	34
2010-2049							
CNRM-CM5	2.6	40	8	17	22	25	40
GFDL-ESM2G	2.6	40	9	17	20	25.5	38
HadGEM2-ES	2.6	40	9	17	23	26	41
MIROC5	2.6	40	9	15	19	25	38
MRI-CGCM3	2.6	40	8	17	22	25	40
CNRM-CM5	4.5	40	8	14.5	19	23	37
GFDL-ESM2G	4.5	40	9	16	21	25.5	38
HadGEM2-ES	4.5	40	11	18.5	23.5	28	42
MIROC5	4.5	40	12	20	23	29	43
MRI-CGCM3	4.5	40	9	16.5	21.5	25.5	40
CNRM-CM5	8.5	40	8	16	21	25	39
GFDL-ESM2G	8.5	40	10	18	22	27	40
HadGEM2-ES	8.5	40	11	19	24	28.5	41
MIROC5	8.5	40	12	19.5	23.5	29	43
MRI-CGCM3	8.5	40	8	15	19	23.5	38
2050-2099							
CNRM-CM5	2.6	50	12	18	22	28	42
GFDL-ESM2G	2.6	50	9	16	19.5	24	37
HadGEM2-ES	2.6	50	12	19	23	27	42
MIROC5	2.6	50	12	21	24.5	29	44
MRI-CGCM3	2.6	50	8	19	22	27	41
CNRM-CM5	4.5	50	12	23	26	33	47
GFDL-ESM2G	4.5	50	12	20	24	29	44
HadGEM2-ES	4.5	50	16	26	31.5	35	52
MIROC5	4.5	50	15	25	28.5	34	49
MRI-CGCM3	4.5	50	12	23	27.5	32	47
CNRM-CM5	8.5	50	20	32	37	42	61
GFDL-ESM2G	8.5	50	19	30	34.5	40	58
HadGEM2-ES	8.5	50	25	35	40	46	66
MIROC5	8.5	50	22	36	40	45	65
MRI-CGCM3	8.5	50	17	33	37	44	65

Table 4.11: Summary of the count of the number of days per year when the maximum daily temperature record was greater than 40 C. Based on SILO records for the period from 1900-2009 and GCM outputs for 2010-2049 & 2050-2099 from five different models run under three RCP scenarios. Location = Narrogin.

Location= Narrogin		No of years	Count of days per year when max temp >40 C				
Source	RCP	n	min	25th percentile	Median	75th percentile	max
1900-2009							
SILO data	na	110	0	0	0	1	7
2010-2049							
CNRM-CM5	2.6	40	0	1	2	4	11
GFDL-ESM2G	2.6	40	0	0.5	2	4	8
HadGEM2-ES	2.6	40	0	1	2	4	11
MIROC5	2.6	40	0	1	2	3	9
MRI-CGCM3	2.6	40	0	1	2.5	4	11
CNRM-CM5	4.5	40	0	0	1	2.5	8
GFDL-ESM2G	4.5	40	0	1	2	4	10
HadGEM2-ES	4.5	40	0	1	2	4	11
MIROC5	4.5	40	0	2	3	5	13
MRI-CGCM3	4.5	40	0	1	2	4	11
CNRM-CM5	8.5	40	0	1	1.5	3.5	10
GFDL-ESM2G	8.5	40	0	1	2.5	5	11
HadGEM2-ES	8.5	40	0	1	3	5	11
MIROC5	8.5	40	0	1.5	3	5	13
MRI-CGCM3	8.5	40	0	1	2	3.5	10
2050-2099							
CNRM-CM5	2.6	50	0	1	2	4	11
GFDL-ESM2G	2.6	50	0	1	2	4	10
HadGEM2-ES	2.6	50	0	2	3	5	11
MIROC5	2.6	50	0	2	3.5	6	12
MRI-CGCM3	2.6	50	0	2	3	5	11
CNRM-CM5	4.5	50	0	2	4	7	16
GFDL-ESM2G	4.5	50	0	1	3	5	11
HadGEM2-ES	4.5	50	0	3	6	9	18
MIROC5	4.5	50	0	3	4	7	16
MRI-CGCM3	4.5	50	0	2	4	7	14
CNRM-CM5	8.5	50	2	6	9	12	24
GFDL-ESM2G	8.5	50	0	4	7.5	10	21
HadGEM2-ES	8.5	50	3	7	11	15	29
MIROC5	8.5	50	3	8	10.5	14	24
MRI-CGCM3	8.5	50	3	5	9	11	18

4.1.2 Rainfall summaries

Daily rainfall records were summed to produce monthly totals and annual totals under each combination of location, model and scenario.

SILO records provided a single annual rainfall measure for each location for the historic period.

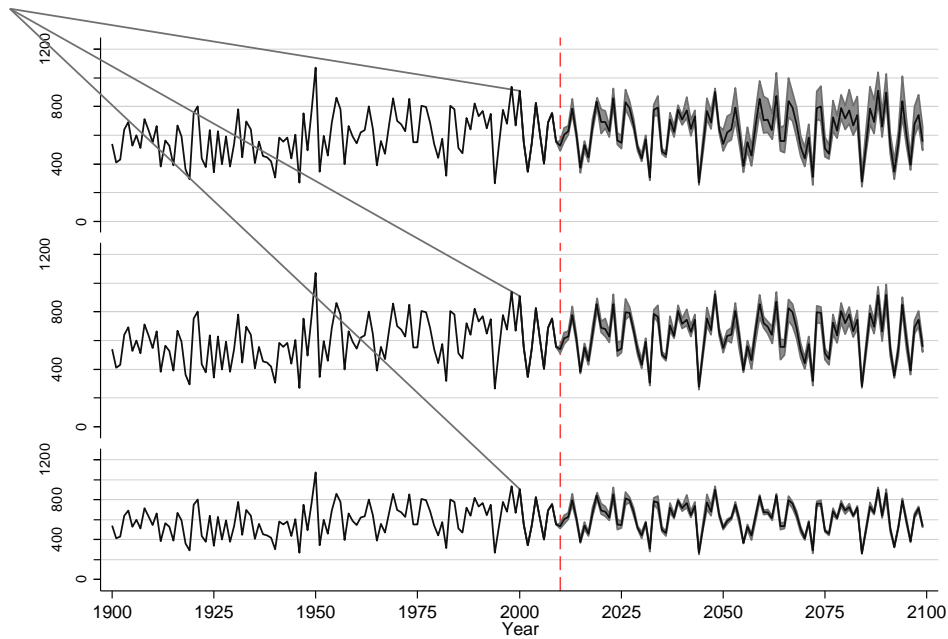
Plots of average annual rainfall were generated using SILO data for the historic period and the average of the five model estimates for each location and scenario combination. For the predicted data (2010-2099) the plots show the minimum value (minimum of the five model values for each year) and the maximum value (maximum of the five model values for each year). The area between the minimum and maximum model values was shaded since this represents the area covering the range of all model outputs. A central line showing the mean of the five model values for each year represents the likely or average pattern of annual rainfall assuming all five models are acting as equally valid representations of future climate patterns.

Rainfall anomalies for each of these two measures were based on estimating the same measure for a defined historic period (1961-1990) and then calculating the difference for each year in the predicted climate period (2010-2099) as was described for temperature summaries.

Rainfall totals for each month across the datasets (1961-1990, 2010-2049, 21050-2099) were averaged for each month and used to create plots of rainfall anomaly by month of the year in an attempt to see whether there was any evidence of particular change over time in some months of the year that may not be apparent in viewing the annual summary plots.

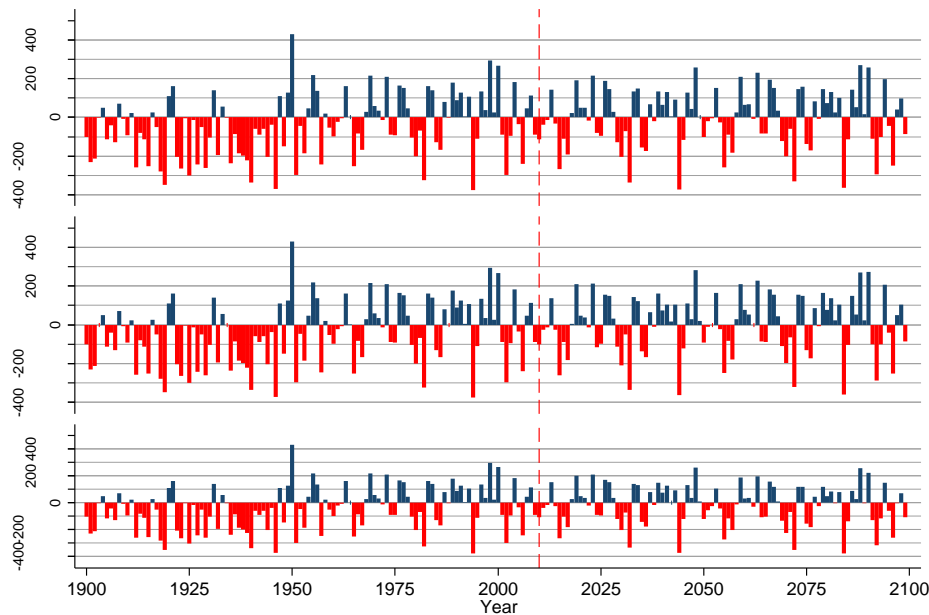
Tables of average monthly and annual rainfall were produced for each combination of location, model and scenario.

4.1.2.1 Carroona



Annual rainfall at Location= Carroona:
RCP8.5 (top), RCP4.5 (middle) & RCP2.6 (bottom) scenarios

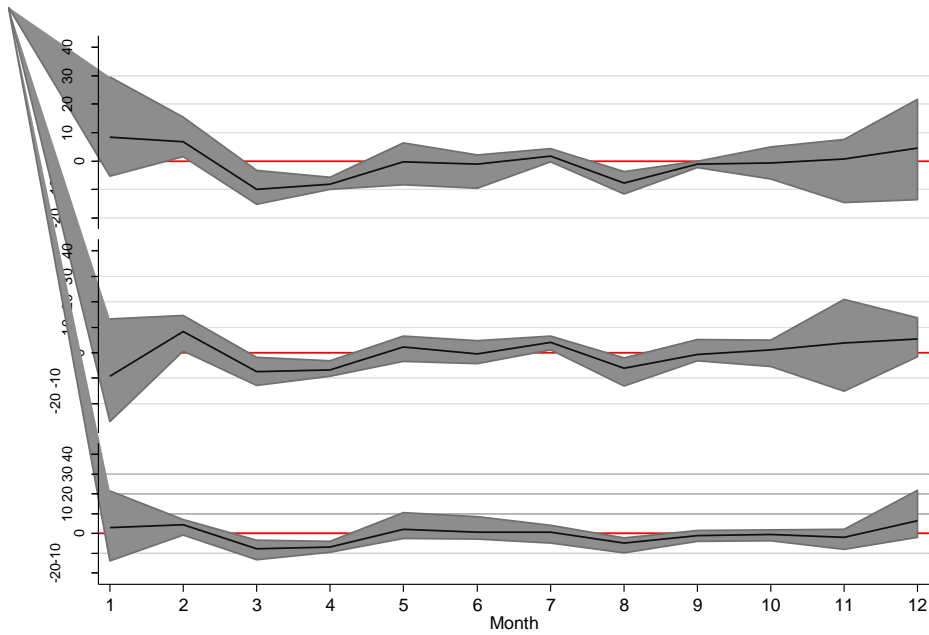
(a)



Annual rainfall anomaly vs 1961-90 at Location= Carroona:
RCP8.5 (top), RCP4.5 (middle) & RCP2.6 (bottom) scenarios

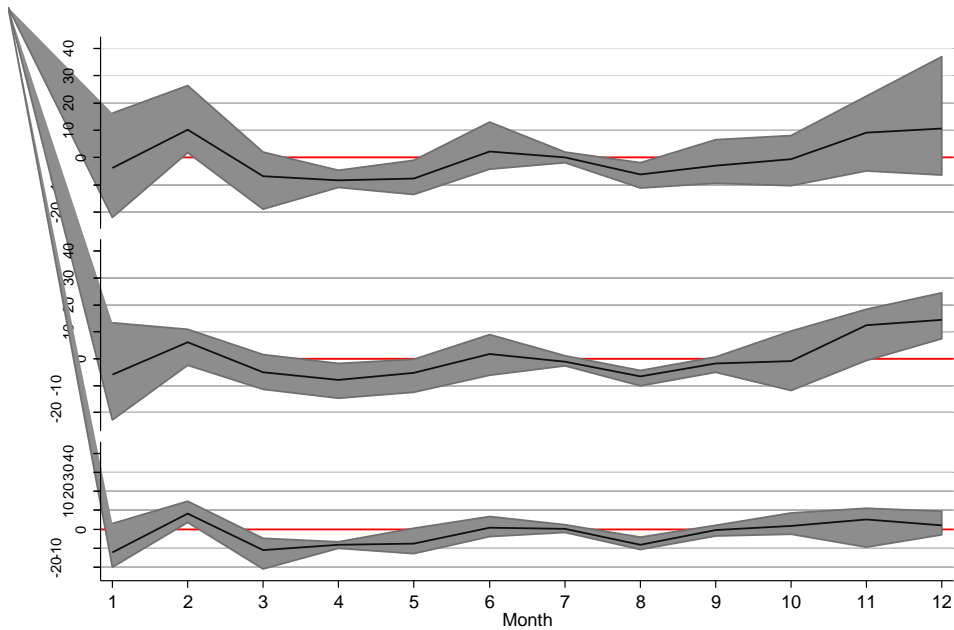
(b)

Figure 4.11: Average annual rainfall (a) and rainfall anomaly (difference between average of five GCMs and 1961-1990 average rainfall, b). Data derived from SILO records and GCM predictions (2010-2099). The shaded area to the right of 2010 in plot (a) covers the range from minimum to maximum values of five GCMs and the dark line is the average of the five models. Separate plots are shown for each of three RCP scenarios: 8.5 (top), 4.5 (middle) and 2.6 (bottom). Location = Carroona.



Monthly rainfall anomaly for 2010-2049 compared to monthly average for 1961-1990. RCP8.5 (top), RCP4.5 (middle) & RCP2.6 (bottom) scenarios

(a)



Monthly rainfall anomaly for 2050-2099 compared to monthly average for 1961-1990. At Location= Carooona: RCP8.5 (top), RCP4.5 (middle) & RCP2.6 (bottom) scenarios

(b)

Figure 4.12: Monthly rainfall anomaly based on difference between historic monthly average (1961-1990) and the monthly average of the five GCM outputs. Shaded area is the anomaly between historic and minimum or maximum value of the five GCM estimates in each month. Separate plots are shown for each of three RCP scenarios: 8.5 (top), 4.5 (middle) and 2.6 (bottom). Location = Carooona.

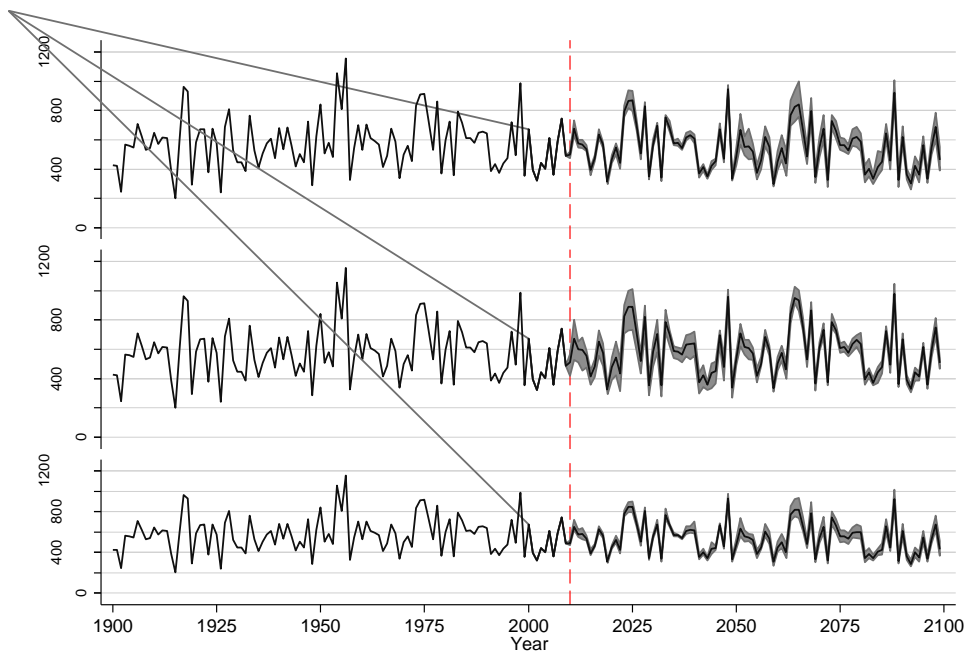
Table 4.12: Monthly and annual average rainfall (mm) based on historic SILO records and on GCM outputs for five models and three scenarios for the period 2010-2049. Location = Caroona.

	Jan	Feb	Mar	Apr	May	Jun	Jul	Aug	Sep	Oct	Nov	Dec	Year
1961-1990	95.9	56.6	50.9	42.7	49.3	34.3	39.5	43.4	41.2	59.6	60.6	68.2	642.1
1900-2009	67.9	52.6	40.9	34.7	35.9	37.8	37.7	35.5	34.4	48.1	50.8	60.7	537.0
RCP2.6													
CNRM-CM5	82.0	63.1	37.6	36.2	59.9	32.7	34.7	33.7	42.0	61.5	52.6	69.3	605.2
GFDL-ESM2G	83.3	63.7	41.4	38.8	50.0	32.4	43.6	37.8	37.1	56.0	62.6	70.7	617.3
HadGEM2-ES	109.5	60.1	47.2	38.1	46.7	31.4	41.4	40.3	39.6	57.2	55.5	76.9	643.8
MIROC5	117.6	62.3	42.0	33.2	50.8	35.1	38.2	41.2	42.7	60.3	62.4	90.0	675.5
MRI-CGCM3	102.8	55.8	47.6	33.7	49.1	42.7	42.8	39.9	39.7	60.6	60.0	66.3	641.0
RCP4.5													
CNRM-CM5	69.0	57.4	45.8	39.7	53.7	31.3	43.0	30.2	46.3	63.0	81.5	66.7	627.5
GFDL-ESM2G	82.0	65.4	38.9	35.1	52.9	30.0	40.5	36.6	38.6	54.1	70.3	75.1	619.2
HadGEM2-ES	90.0	61.9	46.1	37.9	49.1	31.5	46.0	38.2	41.7	60.9	45.5	72.6	621.3
MIROC5	109.2	71.2	49.1	34.0	45.9	37.2	45.3	41.3	38.1	60.6	64.3	81.8	677.8
MRI-CGCM3	83.4	68.8	38.1	33.6	55.9	39.0	42.8	40.1	38.1	64.4	61.0	71.7	636.7
RCP8.5													
CNRM-CM5	90.6	58.4	37.1	36.3	55.7	24.7	43.9	31.8	39.9	64.6	68.1	72.4	623.3
GFDL-ESM2G	99.3	58.1	35.6	32.9	40.9	35.5	43.8	35.9	41.0	54.3	60.6	73.0	610.8
HadGEM2-ES	96.7	60.1	47.7	34.0	52.3	33.4	39.4	39.6	39.2	62.4	45.9	54.7	605.1
MIROC5	125.5	72.1	41.0	32.7	47.0	36.0	39.1	33.3	41.0	53.2	67.8	89.9	678.6
MRI-CGCM3	109.5	68.3	43.1	37.1	49.5	36.3	39.4	37.6	38.9	59.6	64.2	73.4	656.7

Table 4.13: Monthly and annual average rainfall (mm) based on historic SILO records and on GCM outputs for five models and three scenarios for the period 2050-2099. Location = Caroonna.

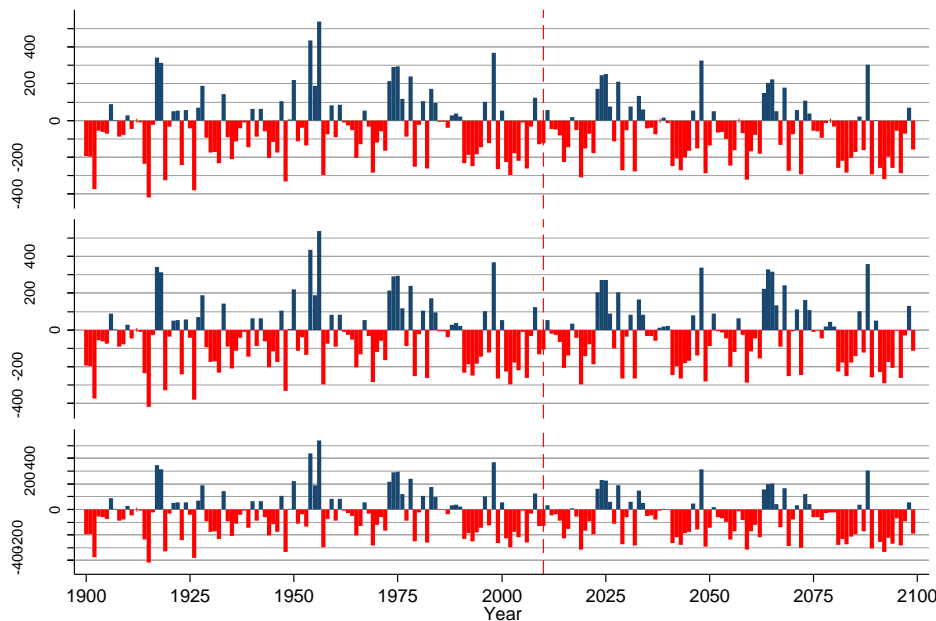
	Jan	Feb	Mar	Apr	May	Jun	Jul	Aug	Sep	Oct	Nov	Dec	Year
1961-1990	95.9	56.6	50.9	42.7	49.3	34.3	39.5	43.4	41.2	59.6	60.6	68.2	642.1
1900-2009	67.9	52.6	40.9	34.7	35.9	37.8	37.7	35.5	34.4	48.1	50.8	60.7	537.0
RCP2.6													
CNRM-CM5	81.4	60.3	39.5	35.7	49.7	30.4	39.8	32.7	42.1	68.3	70.6	68.2	618.7
GFDL-ESM2G	76.0	66.9	29.9	33.2	38.5	31.7	38.6	34.2	38.4	56.8	69.6	77.8	591.6
HadGEM2-ES	83.5	71.4	41.3	36.0	40.0	33.3	41.9	34.9	43.3	62.9	51.2	65.4	604.9
MIROC5	98.8	62.5	46.2	32.6	36.4	41.0	37.8	35.4	41.6	57.9	65.9	72.2	628.4
MRI-CGCM3	78.1	63.6	42.0	34.8	43.9	39.7	40.6	39.1	37.6	61.4	71.8	68.2	620.7
RCP4.5													
CNRM-CM5	76.0	64.6	39.4	34.1	46.0	34.1	36.9	37.0	38.4	59.8	77.0	75.6	618.9
GFDL-ESM2G	73.2	61.6	39.4	28.1	36.7	28.0	37.2	33.4	36.1	47.8	73.9	92.6	588.0
HadGEM2-ES	109.2	54.2	52.4	40.9	41.4	32.2	40.5	35.8	41.3	53.6	59.9	78.7	640.0
MIROC5	98.1	65.2	48.6	32.1	47.4	42.6	37.4	38.6	41.7	69.9	79.0	86.6	687.1
MRI-CGCM3	93.8	67.5	49.2	39.2	49.1	43.2	39.8	39.0	38.9	62.4	75.9	79.8	677.9
RCP8.5													
CNRM-CM5	74.1	58.5	32.0	38.2	48.4	30.1	37.6	35.3	35.3	59.3	64.7	61.8	575.2
GFDL-ESM2G	76.9	64.3	34.6	32.7	35.8	30.9	39.0	32.1	31.7	49.2	72.0	72.7	572.0
HadGEM2-ES	104.8	64.3	53.0	35.6	40.0	31.3	39.0	36.1	36.2	52.4	55.8	78.5	627.0
MIROC5	112.2	82.9	47.5	33.8	41.9	42.9	40.7	41.6	47.8	67.7	83.2	105.2	747.3
MRI-CGCM3	93.1	64.4	53.0	31.9	42.1	47.3	41.5	41.4	39.9	66.1	73.7	76.3	670.7

4.1.2.2 Comet



Annual rainfall at Location= Comet:
RCP8.5 (top), RCP4.5 (middle) & RCP2.6 (bottom) scenarios

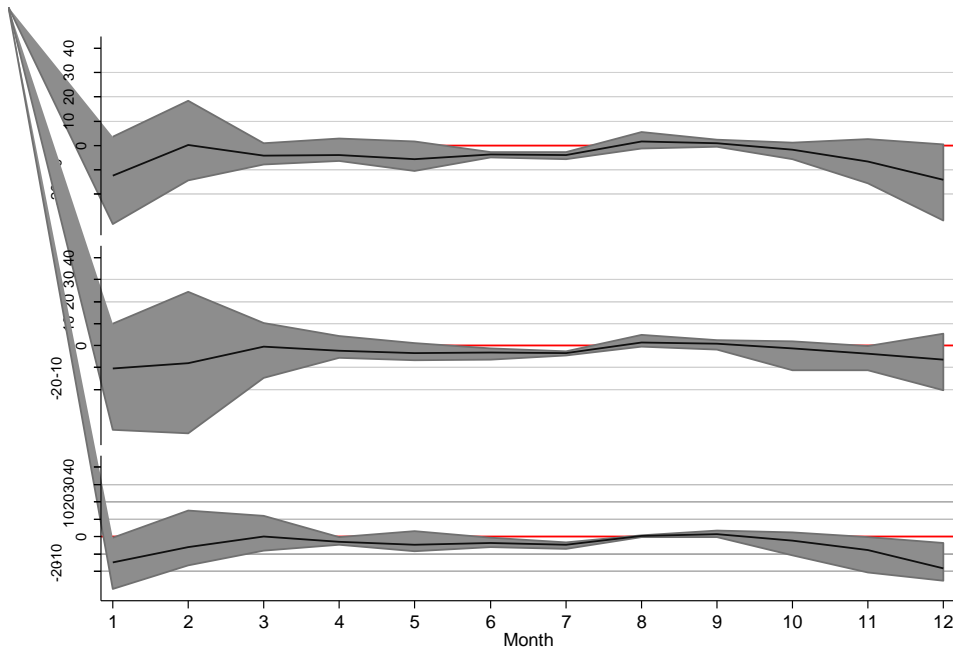
(a)



Annual rainfall anomaly vs 1961-90 at Location= Comet:
RCP8.5 (top), RCP4.5 (middle) & RCP2.6 (bottom) scenarios

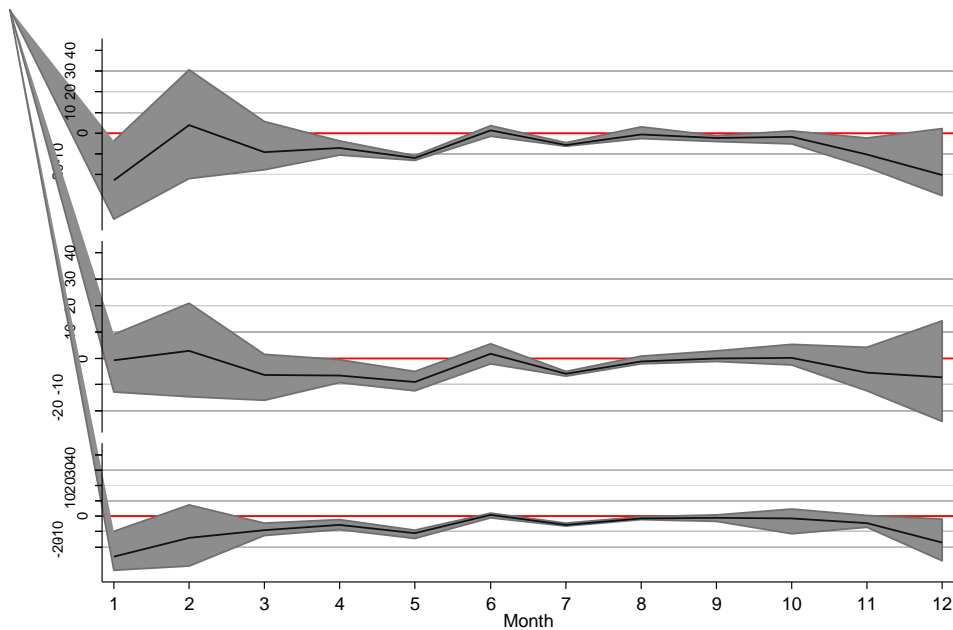
(b)

Figure 4.13: Average annual rainfall (a) and rainfall anomaly (difference between average of five GCMs and 1961-1990 average rainfall, b). Data derived from SILO records (1900-2009) and GCM predictions (2010-2099). The shaded area to the right of 2010 in plot (a) covers the range from minimum to maximum values of five GCMs and the dark line is the average of the five models. Separate plots are shown for each of three RCP scenarios: 8.5 (top), 4.5 (middle) and 2.6 (bottom). Location = Comet.



Monthly rainfall anomaly for 2010-2049 compared to monthly average for 1961-1990. RCP8.5 (top), RCP4.5 (middle) & RCP2.6 (bottom) scenarios

(a)



Monthly rainfall anomaly for 2050-2099 compared to monthly average for 1961-1990. At Location= Comet: RCP8.5 (top), RCP4.5 (middle) & RCP2.6 (bottom) scenarios

(b)

Figure 4.14: Monthly rainfall anomaly based on difference between historic monthly average (1961-1990) and the monthly average of the five GCM outputs. Shaded area is the anomaly between historic and minimum or maximum value of the five GCM estimates in each month. Separate plots are shown for each of three RCP scenarios: 8.5 (top), 4.5 (middle) and 2.6 (bottom). Location = Comet.

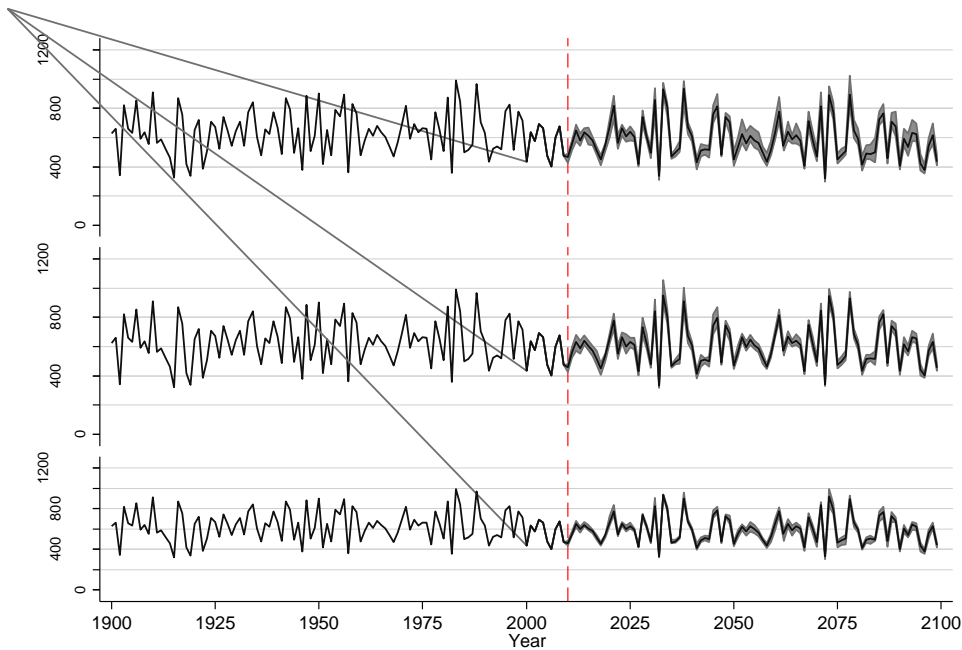
Table 4.14: Monthly and annual average rainfall (mm) based on historic SILO records and on GCM outputs for five models and three scenarios for the period 2010-2049. Location = Comet.

	Jan	Feb	Mar	Apr	May	Jun	Jul	Aug	Sep	Oct	Nov	Dec	Year
1961-1990	106.7	83.9	52.9	38.9	43.6	20.2	26.5	20.7	21.3	43.0	60.4	101.9	620.0
1900-2009	90.2	81.6	51.4	29.7	29.2	25.0	22.9	15.7	19.9	35.4	52.5	75.9	529.4
RCP2.6													
CNRM-CM5	94.0	80.4	63.2	43.1	44.7	18.3	23.6	20.1	21.7	44.8	60.1	100.8	614.7
GFDL-ESM2G	100.5	80.7	50.2	33.2	39.1	16.5	22.8	21.4	23.8	43.4	55.5	105.0	591.9
HadGEM2-ES	101.7	66.2	53.2	35.3	39.0	13.8	23.8	22.3	22.2	43.8	58.8	81.5	561.6
MIROC5	116.7	108.5	57.7	35.2	36.8	17.2	21.9	25.6	19.4	31.8	59.2	107.1	637.1
MRI-CGCM3	68.3	44.0	38.2	35.3	40.6	19.0	23.2	21.0	23.8	44.3	49.1	82.3	488.8
RCP4.5													
CNRM-CM5	80.6	82.8	64.9	38.7	46.7	19.6	22.1	20.4	23.2	43.7	39.9	98.3	581.0
GFDL-ESM2G	76.6	70.9	53.4	36.9	39.0	16.6	22.8	21.6	24.9	45.6	57.6	76.6	542.3
HadGEM2-ES	106.2	67.5	52.6	35.6	35.2	14.3	21.8	21.4	21.9	42.1	58.4	78.2	555.0
MIROC5	104.9	99.1	49.9	34.5	36.8	15.8	19.6	20.9	21.1	32.2	60.1	77.1	571.8
MRI-CGCM3	92.0	69.4	45.1	35.1	36.8	17.1	23.4	21.2	22.8	40.9	47.8	89.2	540.5
RCP8.5													
CNRM-CM5	97.5	76.9	45.0	41.8	35.1	17.3	22.8	19.3	22.6	42.2	44.8	90.0	555.0
GFDL-ESM2G	110.3	81.7	45.9	32.5	37.8	17.3	23.8	22.2	23.6	44.1	50.1	97.7	586.9
HadGEM2-ES	84.9	69.6	50.2	33.5	45.2	15.9	22.9	21.9	21.8	43.1	58.7	77.2	544.8
MIROC5	74.3	90.5	53.7	34.7	33.0	16.2	22.3	26.3	20.7	37.4	62.9	102.4	574.3
MRI-CGCM3	103.9	102.4	49.1	32.9	38.0	15.3	20.9	21.4	22.5	39.8	52.1	70.8	568.9

Table 4.15: Monthly and annual average rainfall (mm) based on historic SILO records and on GCM outputs for five models and three scenarios for the period 2050-2099. Location = Comet.

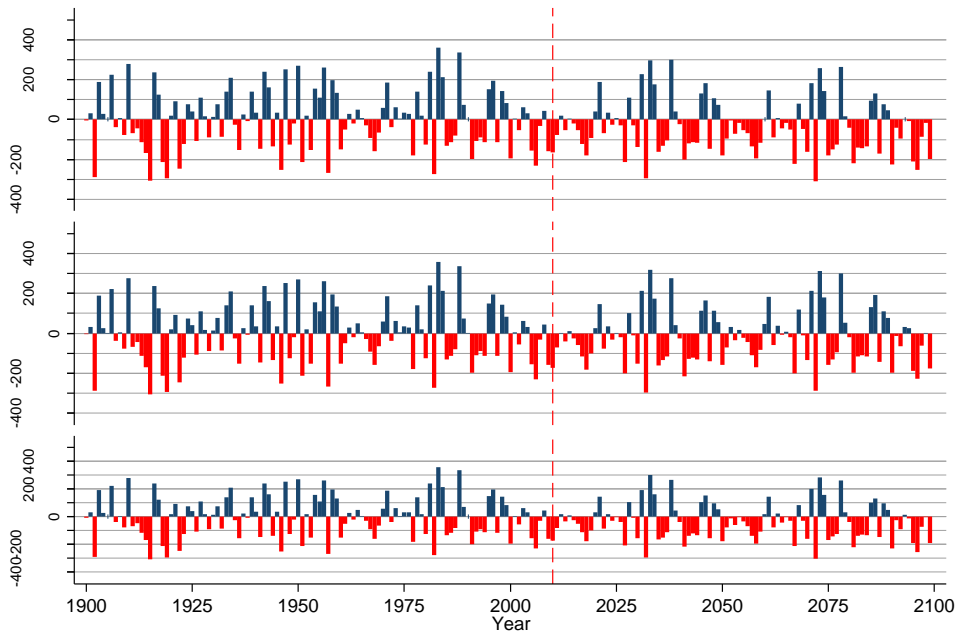
	Jan	Feb	Mar	Apr	May	Jun	Jul	Aug	Sep	Oct	Nov	Dec	Year
1961-1990	106.7	83.9	52.9	38.9	43.6	20.2	26.5	20.7	21.3	43.0	60.4	101.9	620.0
1900-2009	90.2	81.6	51.4	29.7	29.2	25.0	22.9	15.7	19.9	35.4	52.5	75.9	529.4
RCP2.6													
CNRM-CM5	71.5	63.7	48.3	36.8	34.3	22.0	20.9	18.4	20.6	47.8	56.2	100.1	540.6
GFDL-ESM2G	96.9	91.5	42.4	36.9	34.5	22.3	22.0	19.4	22.2	43.0	60.9	93.4	585.3
HadGEM2-ES	83.8	73.2	44.9	32.2	33.7	19.6	21.9	18.5	19.9	42.7	54.4	83.6	528.4
MIROC5	76.3	69.8	40.5	30.4	29.2	19.2	20.0	20.5	18.2	31.7	53.3	72.9	482.1
MRI-CGCM3	72.8	51.4	43.4	30.6	31.2	21.8	20.5	19.8	20.2	42.6	55.6	72.9	482.8
RCP4.5													
CNRM-CM5	93.8	79.0	47.1	38.3	38.7	25.7	20.3	19.8	20.5	48.3	53.3	116.0	600.9
GFDL-ESM2G	102.7	104.9	43.6	29.8	34.8	21.1	20.5	18.7	21.0	41.2	53.4	96.6	588.4
HadGEM2-ES	101.6	80.8	54.4	31.9	33.1	18.0	20.8	18.6	20.2	40.4	55.5	86.1	561.6
MIROC5	115.7	99.4	50.9	30.4	31.3	22.0	19.8	21.4	24.1	42.8	64.4	96.8	618.9
MRI-CGCM3	115.3	69.4	36.9	30.8	34.5	23.1	21.6	19.0	20.0	42.7	48.0	78.0	539.4
RCP8.5													
CNRM-CM5	65.2	62.0	38.0	35.1	32.7	23.1	20.3	18.0	17.3	44.0	43.7	80.0	479.6
GFDL-ESM2G	102.8	109.4	41.8	33.0	31.3	21.6	20.8	19.3	19.7	42.5	50.6	104.1	596.9
HadGEM2-ES	91.0	83.4	45.1	31.0	31.5	18.6	22.0	18.1	18.3	37.8	48.8	72.4	518.1
MIROC5	91.4	114.5	58.4	30.7	30.4	21.1	20.8	23.7	19.2	37.7	58.0	79.8	585.7
MRI-CGCM3	68.7	70.2	35.2	28.2	32.5	23.9	20.1	20.4	20.1	43.5	49.2	71.5	483.5

4.1.2.3 Dalby



Annual rainfall at Location= Dalby:
RCP8.5 (top), RCP4.5 (middle) & RCP2.6 (bottom) scenarios

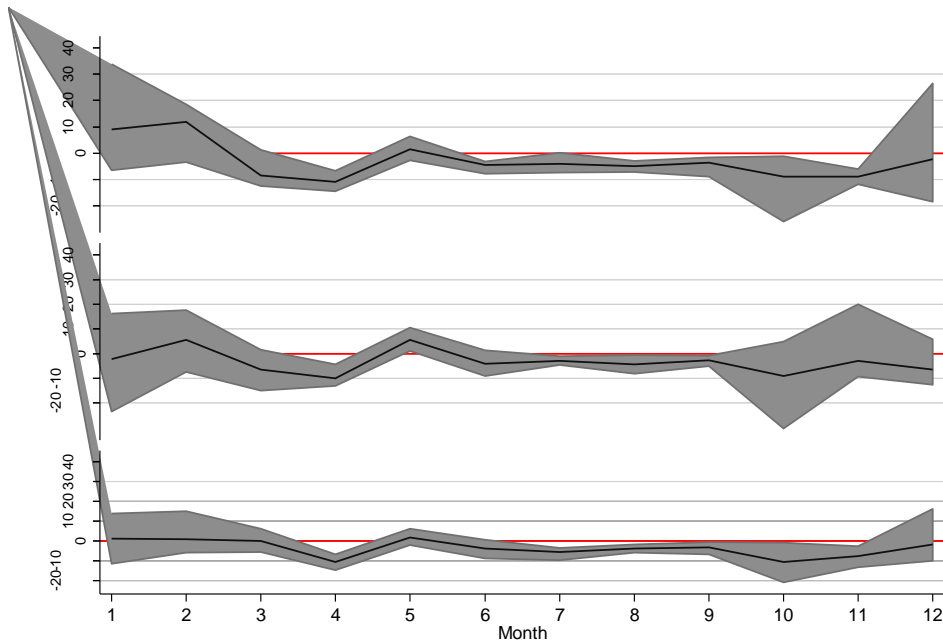
(a)



Annual rainfall anomaly vs 1961-90 at Location= Dalby:
RCP8.5 (top), RCP4.5 (middle) & RCP2.6 (bottom) scenarios

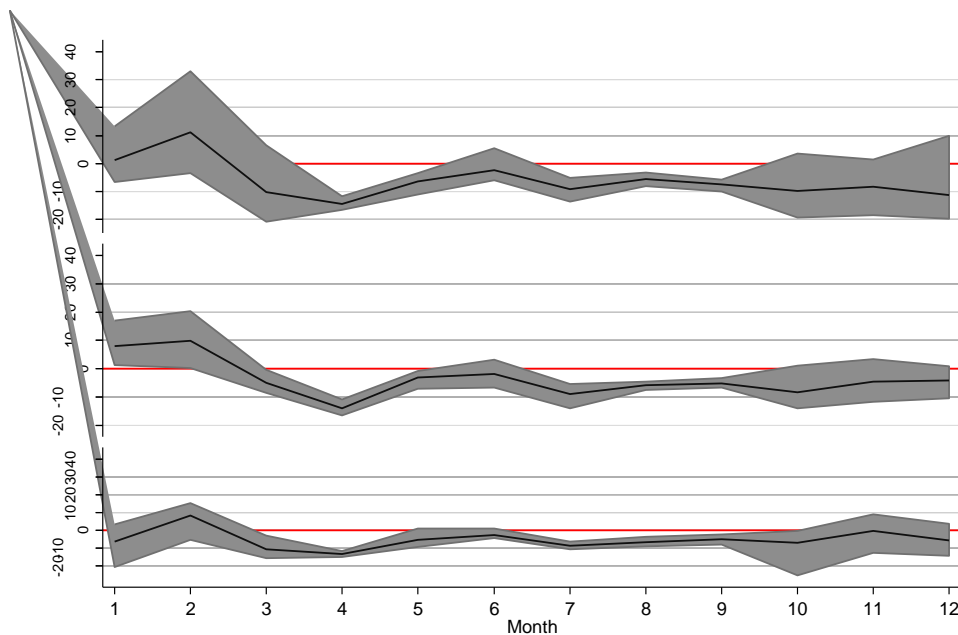
(b)

Figure 4.15: Average annual rainfall (a) and rainfall anomaly (difference between average of five GCMs and 1961-1990 average rainfall, b). Data derived from SILO records (1900-2009) and GCM predictions (2010-2099). The shaded area to the right of 2010 in plot (a) covers the range from minimum to maximum values of five GCMs and the dark line is the average of the five models. Separate plots are shown for each of three RCP scenarios: 8.5 (top), 4.5 (middle) and 2.6 (bottom). Location = Dalby.



Monthly rainfall anomaly for 2010-2049 compared to monthly average for 1961-1990. RCP8.5 (top), RCP4.5 (middle) & RCP2.6 (bottom) scenarios

(a)



Monthly rainfall anomaly for 2050-2099 compared to monthly average for 1961-1990. At Location= Dalby: RCP8.5 (top), RCP4.5 (middle) & RCP2.6 (bottom) scenarios

(b)

Figure 4.16: Monthly rainfall anomaly based on difference between historic monthly average (1961-1990) and the monthly average of the five GCM outputs. Shaded area is the anomaly between historic and minimum or maximum value of the five GCM estimates in each month. Separate plots are shown for each of three RCP scenarios: 8.5 (top), 4.5 (middle) and 2.6 (bottom). Location = Dalby.

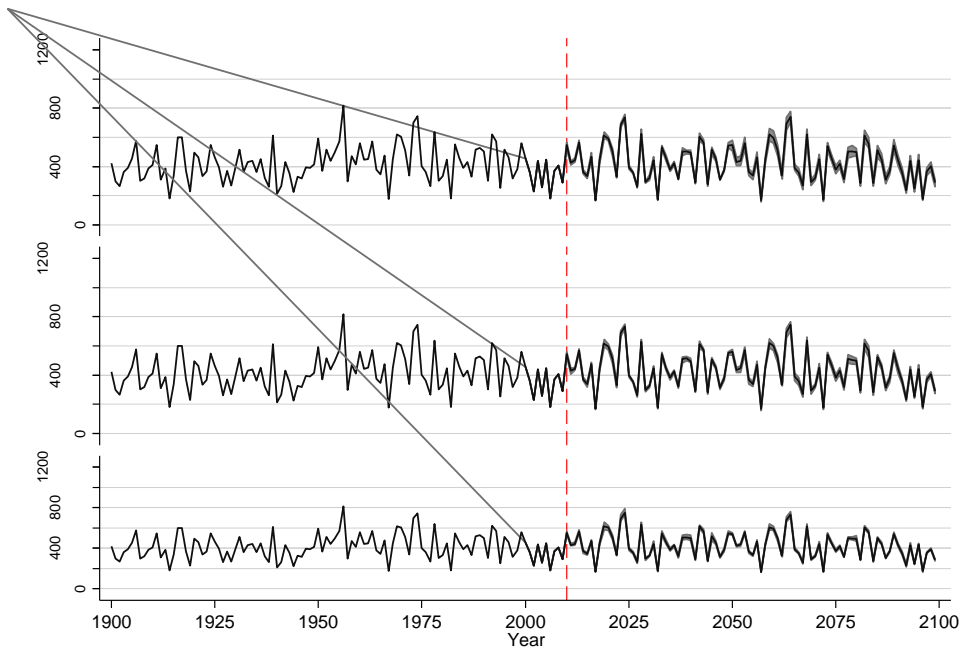
Table 4.16: Monthly and annual average rainfall (mm) based on historic SILO records and on GCM outputs for five models and three scenarios for the period 2010-2049. Location = Dalby.

	Jan	Feb	Mar	Apr	May	Jun	Jul	Aug	Sep	Oct	Nov	Dec	Year
1961-1990	73.9	67.7	53.8	45.8	40.2	31.3	39.4	31.6	33.1	61.2	75.4	94.3	647.5
1900-2009	73.1	66.6	52.9	32.6	33.8	33.4	32.4	24.7	30.1	52.3	65.7	80.9	578.3
RCP2.6													
CNRM-CM5	75.3	61.7	60.0	31.0	46.3	29.8	33.5	29.0	28.7	45.9	63.5	89.4	594.0
GFDL-ESM2G	67.9	64.8	48.1	39.0	41.6	25.7	35.7	26.5	29.2	55.8	67.5	84.2	586.0
HadGEM2-ES	87.8	69.3	53.5	36.9	38.0	22.6	34.2	27.9	32.3	51.1	72.6	84.6	610.5
MIROC5	81.8	82.8	52.0	36.2	42.4	27.5	29.7	25.6	26.4	40.2	72.6	110.5	627.5
MRI-CGCM3	62.4	64.1	56.1	32.9	41.1	31.8	35.9	29.8	31.7	60.4	62.2	93.9	602.2
RCP4.5													
CNRM-CM5	90.1	60.2	55.5	33.7	50.6	32.6	34.9	23.6	32.3	51.2	95.5	81.7	641.7
GFDL-ESM2G	58.0	67.2	41.9	34.8	44.8	23.7	36.1	26.5	29.4	55.1	66.5	85.7	569.6
HadGEM2-ES	81.7	73.0	49.4	36.4	41.4	22.4	38.3	27.3	31.4	57.4	66.7	84.5	609.8
MIROC5	78.1	85.4	52.1	41.4	45.4	28.8	37.7	31.2	28.1	31.0	66.2	100.1	625.3
MRI-CGCM3	50.3	80.4	38.8	32.8	46.5	29.3	35.6	28.2	31.2	66.1	67.1	87.3	593.5
RCP8.5													
CNRM-CM5	86.0	85.2	41.3	36.6	39.2	23.6	35.9	24.5	30.2	49.7	67.4	90.5	609.9
GFDL-ESM2G	83.1	75.9	43.9	34.7	37.5	28.2	39.6	26.9	30.6	56.5	69.4	92.9	619.1
HadGEM2-ES	67.4	64.3	41.3	31.4	46.6	27.6	32.0	28.6	30.4	60.2	63.6	75.8	569.1
MIROC5	70.5	86.1	55.2	39.0	40.0	27.9	36.2	26.4	24.2	35.3	65.7	120.9	627.3
MRI-CGCM3	107.7	86.2	44.7	32.9	45.5	26.9	32.8	26.9	31.5	60.2	66.2	79.4	640.9

Table 4.17: Monthly and annual average rainfall (mm) based on historic SILO records and on GCM outputs for five models and three scenarios for the period 2050-2099. Location = Dalby.

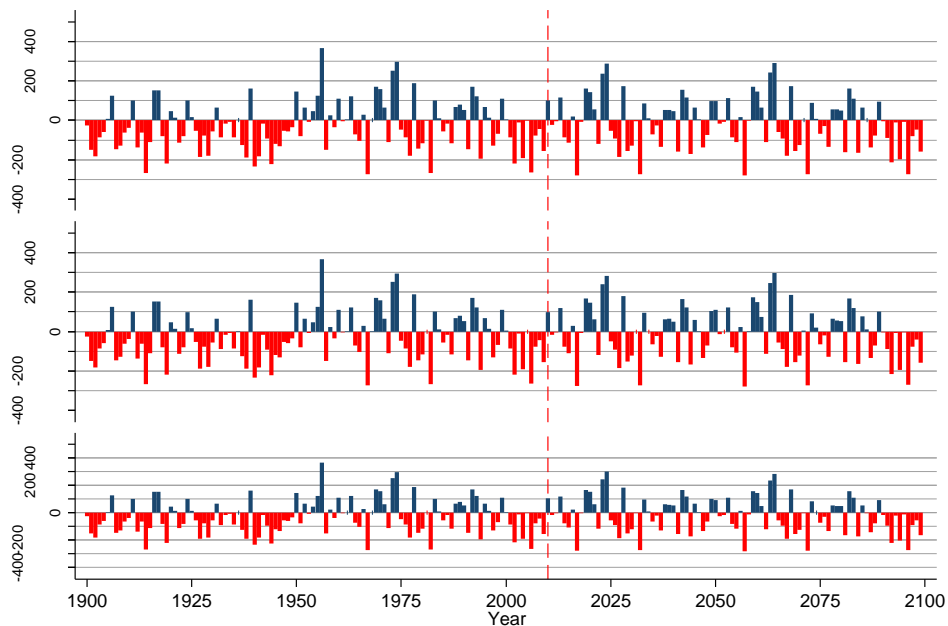
	Jan	Feb	Mar	Apr	May	Jun	Jul	Aug	Sep	Oct	Nov	Dec	Year
1961-1990	73.9	67.7	53.8	45.8	40.2	31.3	39.4	31.6	33.1	61.2	75.4	94.3	647.5
1900-2009	73.1	66.6	52.9	32.6	33.8	33.4	32.4	24.7	30.1	52.3	65.7	80.9	578.3
RCP2.6													
CNRM-CM5	77.2	62.1	50.9	33.7	41.1	26.8	28.8	22.5	30.7	57.3	83.8	82.2	597.0
GFDL-ESM2G	71.3	74.6	40.0	34.0	35.2	27.7	33.0	26.7	28.2	59.0	84.5	97.9	612.1
HadGEM2-ES	69.7	83.0	38.2	32.6	32.2	27.4	29.5	24.4	29.8	57.7	64.9	96.6	586.0
MIROC5	66.1	82.3	46.5	31.6	30.8	28.6	32.3	22.5	25.0	35.8	62.6	80.0	544.0
MRI-CGCM3	53.2	77.8	39.7	30.5	35.1	32.2	29.9	27.9	26.8	60.9	78.8	85.1	578.0
RCP4.5													
CNRM-CM5	90.9	78.6	49.0	29.3	38.0	29.8	25.4	27.1	27.3	52.2	68.2	83.8	599.7
GFDL-ESM2G	75.1	81.7	45.2	29.7	33.1	25.4	30.5	24.2	26.4	47.1	75.2	91.7	585.3
HadGEM2-ES	77.9	67.9	48.2	33.7	35.9	24.6	29.6	25.7	29.8	49.1	63.6	91.2	577.2
MIROC5	77.8	88.0	53.5	31.5	39.1	33.0	32.3	26.3	28.2	53.7	78.8	95.0	637.3
MRI-CGCM3	87.2	71.5	48.7	34.9	39.3	34.5	33.9	25.6	27.0	62.2	68.4	88.4	621.6
RCP8.5													
CNRM-CM5	71.6	64.2	33.1	32.1	36.8	26.9	25.7	24.0	24.8	51.9	67.3	74.4	532.7
GFDL-ESM2G	70.4	85.0	36.4	31.0	29.0	27.8	30.6	23.5	23.1	53.1	76.7	78.5	565.1
HadGEM2-ES	87.2	79.7	43.4	29.2	32.8	25.3	30.0	26.0	25.5	41.8	56.9	74.9	552.6
MIROC5	78.5	100.7	60.5	34.0	34.7	28.1	34.2	27.9	27.0	45.9	61.3	104.1	636.9
MRI-CGCM3	67.2	64.3	44.3	29.8	35.1	36.8	30.3	28.5	27.3	64.8	72.7	82.5	583.7

4.1.2.4 Leeton



Annual rainfall at Location= Leeton:
RCP8.5 (top), RCP4.5 (middle) & RCP2.6 (bottom) scenarios

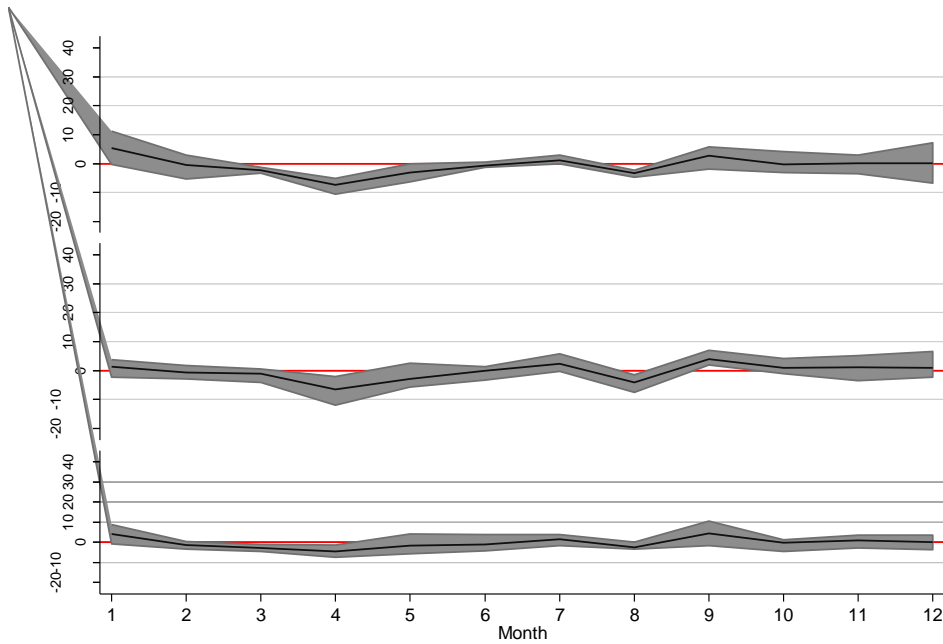
(a)



Annual rainfall anomaly vs 1961-90 at Location= Leeton:
RCP8.5 (top), RCP4.5 (middle) & RCP2.6 (bottom) scenarios

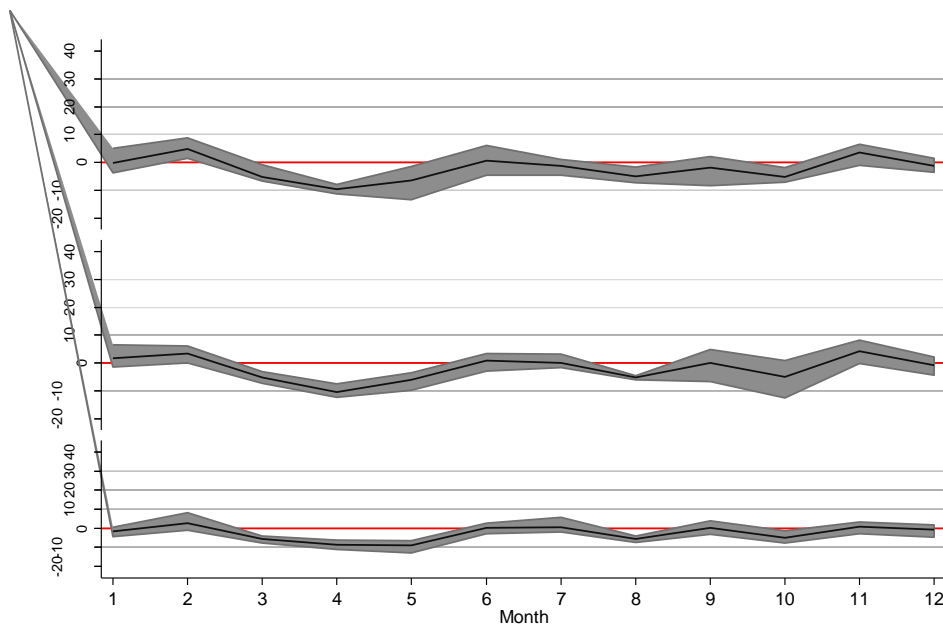
(b)

Figure 4.17: Average annual rainfall (a) and rainfall anomaly (difference between average of five GCMs and 1961-1990 average rainfall, b). Data derived from SILO records (1900-2009) and GCM predictions (2010-2099). The shaded area to the right of 2010 in plot (a) covers the range from minimum to maximum values of five GCMs and the dark line is the average of the five models. Separate plots are shown for each of three RCP scenarios: 8.5 (top), 4.5 (middle) and 2.6 (bottom). Location = Leeton.



Monthly rainfall anomaly for 2010-2049 compared to monthly average for 1961-1990. RCP8.5 (top), RCP4.5 (middle) & RCP2.6 (bottom) scenarios

(a)



Monthly rainfall anomaly for 2050-2099 compared to monthly average for 1961-1990. At Location= Leeton: RCP8.5 (top), RCP4.5 (middle) & RCP2.6 (bottom) scenarios

(b)

Figure 4.18: Monthly rainfall anomaly based on difference between historic monthly average (1961-1990) and the monthly average of the five GCM outputs. Shaded area is the anomaly between historic and minimum or maximum value of the five GCM estimates in each month. Separate plots are shown for each of three RCP scenarios: 8.5 (top), 4.5 (middle) and 2.6 (bottom). Location = Leeton.

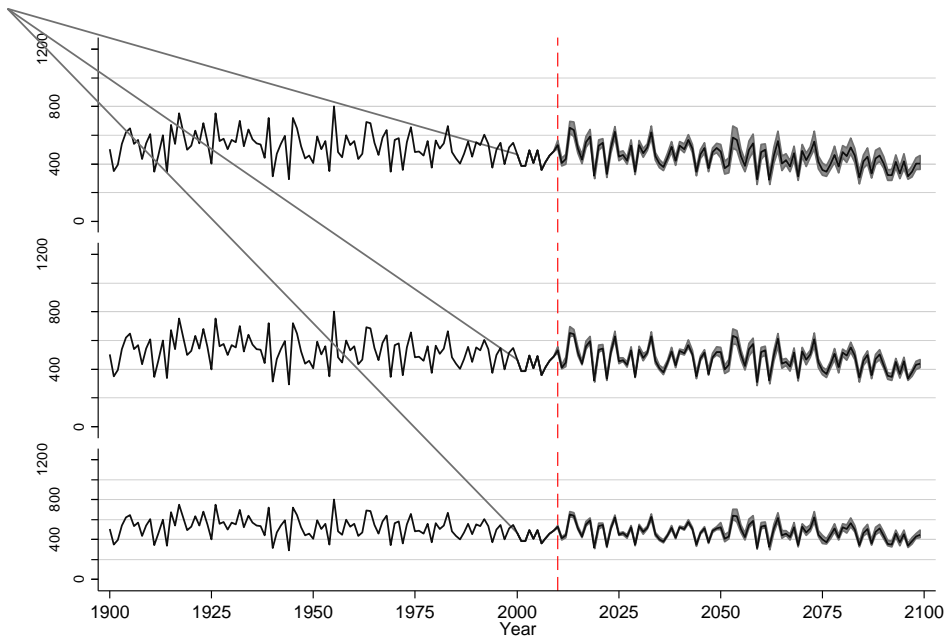
Table 4.18: Monthly and annual average rainfall (mm) based on historic SILO records and on GCM outputs for five models and three scenarios for the period 2010-2049. Location = Leeton.

	Jan	Feb	Mar	Apr	May	Jun	Jul	Aug	Sep	Oct	Nov	Dec	Year
1961-1990	34.8	30.3	34.6	42.9	46.3	33.7	37.4	43.6	38.2	44.9	28.3	33.1	448.1
1900-2009	29.5	24.2	31.2	31.0	35.3	36.0	33.6	35.2	33.1	39.2	27.3	27.4	383.1
RCP2.6													
CNRM-CM5	37.3	27.8	30.1	38.7	50.3	33.4	35.7	40.1	46.3	46.2	28.3	33.6	447.7
GFDL-ESM2G	43.7	26.9	30.7	35.6	42.2	32.1	37.7	40.9	36.7	40.4	29.0	36.8	432.4
HadGEM2-ES	34.1	29.2	32.9	39.8	41.6	29.4	38.7	43.6	40.2	45.6	25.5	33.3	433.7
MIROC5	38.2	29.8	31.9	35.6	40.5	31.5	40.9	41.1	48.8	46.3	31.3	32.4	448.1
MRI-CGCM3	41.4	30.5	33.5	41.6	49.0	37.6	41.5	40.3	41.4	45.7	31.7	29.4	463.6
RCP4.5													
CNRM-CM5	32.4	27.3	35.2	40.7	42.5	35.1	38.8	37.0	45.3	49.2	32.3	33.5	449.2
GFDL-ESM2G	35.6	29.7	30.5	36.5	43.6	33.1	37.2	42.1	40.1	43.8	33.5	39.6	445.1
HadGEM2-ES	35.3	28.6	34.0	35.5	41.7	30.5	43.2	36.1	41.9	46.3	24.8	30.8	428.6
MIROC5	38.2	30.2	34.5	31.0	40.5	34.8	42.1	40.7	42.9	46.3	26.5	34.4	442.1
MRI-CGCM3	38.6	32.0	34.0	38.5	48.8	35.1	37.4	41.3	40.9	43.9	29.6	32.0	451.9
RCP8.5													
CNRM-CM5	41.4	25.0	32.4	36.0	45.4	32.9	39.5	39.4	42.6	46.7	28.3	40.2	449.5
GFDL-ESM2G	45.9	29.5	33.1	36.6	43.2	32.8	37.8	41.2	36.3	42.9	31.3	34.8	445.3
HadGEM2-ES	34.5	28.6	33.4	35.4	41.3	32.5	40.4	40.1	39.7	49.0	24.8	26.4	425.8
MIROC5	39.3	33.1	32.0	32.3	40.0	32.9	37.3	38.9	43.9	42.9	27.6	33.3	433.4
MRI-CGCM3	39.8	32.7	31.2	37.8	46.2	34.3	37.9	41.4	42.2	41.8	30.4	31.0	446.6

Table 4.19: Monthly and annual average rainfall (mm) based on historic SILO records and on GCM outputs for five models and three scenarios for the period 2050-2099. Location = Leeton.

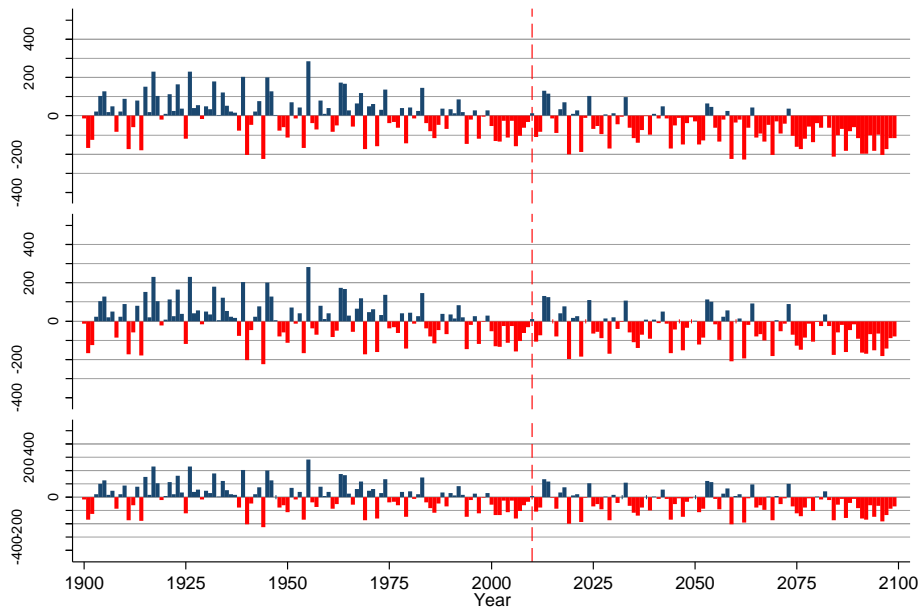
	Jan	Feb	Mar	Apr	May	Jun	Jul	Aug	Sep	Oct	Nov	Dec	Year
1961-1990	34.8	30.3	34.6	42.9	46.3	33.7	37.4	43.6	38.2	44.9	28.3	33.1	448.1
1900-2009	29.5	24.2	31.2	31.0	35.3	36.0	33.6	35.2	33.1	39.2	27.3	27.4	383.1
RCP2.6													
CNRM-CM5	32.1	30.2	30.7	34.9	39.8	34.0	36.5	36.5	42.0	43.5	30.4	33.7	424.3
GFDL-ESM2G	35.1	29.4	27.4	31.7	37.5	33.7	35.5	38.8	34.9	37.7	31.6	34.9	408.4
HadGEM2-ES	30.5	35.4	26.8	35.3	38.2	31.0	43.2	38.2	39.5	43.1	27.5	28.5	417.1
MIROC5	34.1	31.2	30.4	32.0	33.4	36.3	36.3	36.1	37.7	37.1	25.4	34.8	404.8
MRI-CGCM3	34.3	38.5	29.5	36.7	38.4	34.2	38.0	39.6	37.8	39.1	30.0	30.6	426.7
RCP4.5													
CNRM-CM5	34.5	33.0	30.6	32.1	42.7	36.3	38.3	38.6	39.7	40.6	34.6	35.2	436.2
GFDL-ESM2G	37.3	33.8	27.3	31.4	39.3	32.7	35.8	37.4	31.5	32.5	29.4	34.6	403.0
HadGEM2-ES	41.2	30.3	28.5	35.4	36.5	30.7	36.9	38.4	39.0	38.5	28.1	29.9	413.4
MIROC5	33.4	35.3	29.3	30.5	41.0	35.7	40.6	39.1	43.0	45.8	34.1	32.9	440.5
MRI-CGCM3	36.3	36.4	31.4	32.9	41.9	37.1	35.8	38.7	38.0	42.0	36.4	28.8	435.8
RCP8.5													
CNRM-CM5	31.7	31.8	27.9	31.7	44.9	32.4	32.8	38.8	39.1	41.3	30.0	31.0	413.4
GFDL-ESM2G	39.7	32.1	27.9	34.2	40.4	32.7	35.5	37.5	29.8	37.7	32.2	34.5	414.3
HadGEM2-ES	31.1	33.6	28.2	33.4	32.9	29.2	38.6	36.4	33.3	38.1	27.2	30.4	392.2
MIROC5	37.2	39.1	33.7	32.1	38.4	38.1	37.4	41.9	40.3	43.0	34.8	33.6	449.6
MRI-CGCM3	33.2	38.6	29.9	34.9	42.4	39.8	36.3	38.8	39.1	38.6	34.6	29.5	435.6

4.1.2.5 Narrogin



Annual rainfall at Location= Narrogin:
RCP8.5 (top), RCP4.5 (middle) & RCP2.6 (bottom) scenarios

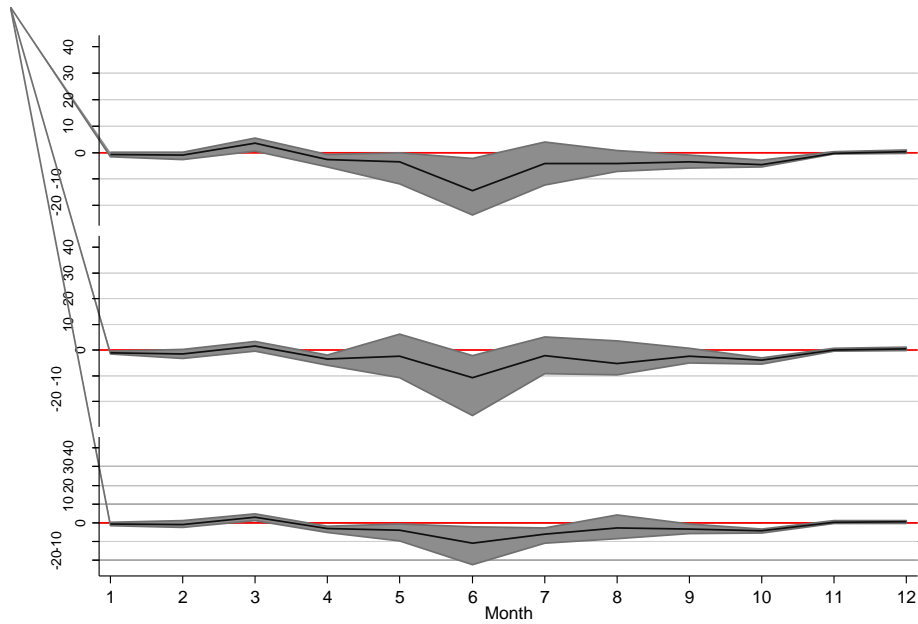
(a)



Annual rainfall anomaly vs 1961-90 at Location= Narrogin:
RCP8.5 (top), RCP4.5 (middle) & RCP2.6 (bottom) scenarios

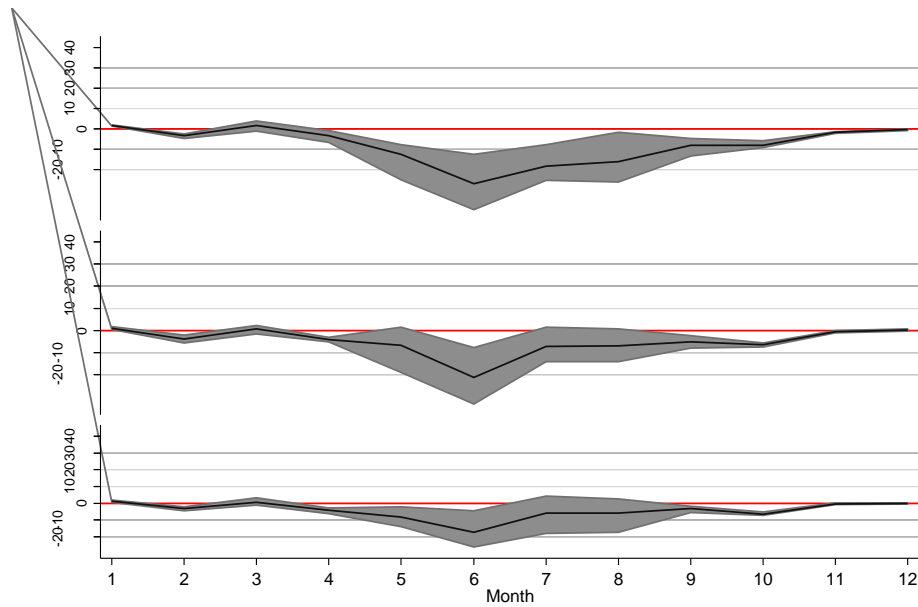
(b)

Figure 4.19: Average annual rainfall (a) and rainfall anomaly (difference between average of five GCMs and 1961-1990 average rainfall, b). Data derived from SILO records (1900-2009) and GCM predictions (2010-2099). The shaded area to the right of 2010 in plot (a) covers the range from minimum to maximum values of five GCMs and the dark line is the average of the five models. Separate plots are shown for each of three RCP scenarios: 8.5 (top), 4.5 (middle) and 2.6 (bottom). Location = Narrogin.



Monthly rainfall anomaly for 2010-2049 compared to monthly average for 1961-1990.
RCP8.5 (top), RCP4.5 (middle) & RCP2.6 (bottom) scenarios

(a)



Monthly rainfall anomaly for 2050-2099 compared to monthly average for 1961-1990.
At Location= Narrogin:
RCP8.5 (top), RCP4.5 (middle) & RCP2.6 (bottom) scenarios

(b)

Figure 4.20: Monthly rainfall anomaly based on difference between historic monthly average (1961-1990) and the monthly average of the five GCM outputs. Shaded area is the anomaly between historic and minimum or maximum value of the five GCM estimates in each month. Separate plots are shown for each of three RCP scenarios: 8.5 (top), 4.5 (middle) and 2.6 (bottom). Location = Narrogin.

Table 4.20: Monthly and annual average rainfall (mm) based on historic SILO records and on GCM outputs for five models and three scenarios for the period 2010-2049. Location = Narrogin.

	Jan	Feb	Mar	Apr	May	Jun	Jul	Aug	Sep	Oct	Nov	Dec	Year
1961-1990	15.7	19.2	15.8	35.2	64.3	97.8	89.0	66.8	45.0	34.9	22.9	12.3	518.8
1900-2009	10.6	14.7	18.4	28.0	61.4	89.0	88.0	66.3	45.0	31.6	16.9	12.4	482.4
RCP2.6													
CNRM-CM5	14.2	17.5	19.2	30.2	63.8	93.3	86.2	71.1	41.4	30.1	23.8	12.6	503.2
GFDL-ESM2G	14.8	18.1	20.7	31.1	54.8	83.2	83.3	58.3	41.5	31.4	22.9	12.7	472.5
HadGEM2-ES	15.2	18.1	17.1	33.4	59.8	95.8	81.8	67.5	44.4	31.7	22.4	12.8	499.9
MIROC5	16.1	20.4	19.0	32.7	61.4	87.2	78.0	62.9	39.2	29.4	22.9	13.5	482.4
MRI-CGCM3	15.3	16.8	17.9	33.5	61.8	75.4	85.1	60.6	41.5	31.0	24.0	12.1	474.9
RCP4.5													
CNRM-CM5	14.3	18.3	19.2	29.4	70.4	95.2	88.9	70.4	40.0	31.1	23.6	13.4	513.9
GFDL-ESM2G	14.8	19.0	18.4	32.9	53.5	84.9	86.5	57.1	43.2	31.0	22.4	12.6	476.3
HadGEM2-ES	15.3	16.3	15.4	33.1	60.1	87.2	85.0	62.8	42.6	31.8	23.1	12.8	485.4
MIROC5	14.3	19.4	18.6	30.0	58.4	95.7	79.9	57.3	41.5	29.5	22.4	12.8	479.7
MRI-CGCM3	15.0	15.9	15.9	33.2	66.9	72.4	94.2	59.6	45.8	31.7	23.2	12.1	485.7
RCP8.5													
CNRM-CM5	15.4	19.2	20.5	34.6	62.7	95.6	93.0	67.6	42.6	31.0	22.3	12.1	516.5
GFDL-ESM2G	14.8	17.9	20.7	33.1	52.5	76.1	76.9	59.9	39.2	29.5	22.3	12.6	455.1
HadGEM2-ES	14.1	16.6	16.4	29.7	63.7	88.0	79.8	64.0	44.2	32.0	23.1	12.7	484.3
MIROC5	14.7	19.3	18.4	31.2	60.8	74.3	86.4	59.6	39.8	29.4	22.3	13.2	469.3
MRI-CGCM3	15.8	18.6	21.2	33.9	64.2	83.5	88.2	62.4	42.0	30.2	22.4	12.5	494.7

Table 4.21: Monthly and annual average rainfall (mm) based on historic SILO records and on GCM outputs for five models and three scenarios for the period 2050-2099. Location = Narrogin.

	Jan	Feb	Mar	Apr	May	Jun	Jul	Aug	Sep	Oct	Nov	Dec	Year
1961-1990	15.7	19.2	15.8	35.2	64.3	97.8	89.0	66.8	45.0	34.9	22.9	12.3	518.8
1900-2009	10.6	14.7	18.4	28.0	61.4	89.0	88.0	66.3	45.0	31.6	16.9	12.4	482.4
RCP2.6													
CNRM-CM5	17.6	15.7	18.9	32.4	62.3	93.1	93.0	69.3	41.0	27.6	23.0	12.1	505.9
GFDL-ESM2G	16.2	16.4	16.7	29.7	50.3	79.2	78.4	60.6	42.8	28.3	22.0	12.0	452.6
HadGEM2-ES	17.0	14.7	15.4	32.5	55.5	84.8	79.5	65.8	43.4	29.8	22.3	12.0	472.7
MIROC5	17.0	17.0	16.8	30.7	59.0	73.8	70.9	49.3	39.5	27.7	22.5	12.5	436.9
MRI-CGCM3	17.1	16.7	14.5	29.1	52.5	71.6	93.2	59.1	42.2	29.0	22.3	11.8	459.2
RCP4.5													
CNRM-CM5	17.4	15.1	18.0	30.3	61.8	90.0	84.2	67.4	40.2	27.5	21.8	12.7	486.5
GFDL-ESM2G	16.5	16.3	17.0	30.0	45.4	67.4	74.8	57.0	38.8	28.0	21.9	12.5	425.7
HadGEM2-ES	16.5	15.2	14.1	32.1	56.2	80.1	75.9	63.2	41.0	29.3	22.3	12.0	457.9
MIROC5	16.3	17.2	17.7	31.8	65.7	80.8	90.5	58.8	37.2	28.5	22.7	13.0	480.0
MRI-CGCM3	16.2	13.4	16.3	31.1	58.2	64.6	83.6	52.7	42.7	29.2	22.5	11.9	442.5
RCP8.5													
CNRM-CM5	17.6	16.0	19.3	34.3	56.5	85.3	81.3	65.1	37.9	27.4	20.7	11.4	473.0
GFDL-ESM2G	17.1	16.3	16.8	28.5	39.1	58.1	63.7	44.7	35.6	25.9	21.5	12.0	379.4
HadGEM2-ES	17.0	14.4	14.7	32.8	54.3	75.1	69.7	57.9	40.4	29.1	21.6	12.2	439.3
MIROC5	17.3	16.7	17.3	30.8	54.8	71.2	65.0	40.7	31.8	25.6	21.2	12.2	404.8
MRI-CGCM3	17.4	16.3	19.7	32.4	54.0	64.5	73.9	44.2	38.9	26.6	21.5	11.5	420.9

4.2 Feedlot hydrology modelling

MEDLI modelling outputs were generated for a number of output measures including rainfall, evaporation, runoff, and the number of holding pond overtopping events.

MEDLI outputs for rainfall, evaporation and runoff were analysed to generate simple summary statistics (mean, 10th percentile, 90th percentile and maximum values for a 24 hour period) to allow comparisons between predicted climate scenarios and historic values for each location.

Additional summary statistics were generated for rainfall based on the number of days in each 100 year period when rainfall fell in each of a number of defined intervals to provide an indication of the range of possible daily rainfall values.

Finally, the number of pond overtopping events is reported as a rate of events per 100 years. These data were then analysed using negative binomial modelling, a widely used statistical method applied to count data modelling the occurrence of relatively rare events.

4.2.1 Pond overtopping rate

Pond overtopping rates were estimated as events per 100 years.

Table 4.22: Pond overtopping frequency at each location, reported as events per 100 years, for the SILO dataset serving as an historic control and for each combination of GCM and scenario.

Source	Period	Scenario	Caroona	Comet	Dalby	Leeton	Narrogin
			Overtopping events per 100 years				
SILO (1910-2009)	1910-2009	Historic control	9	9	9	9	9
CNRM-CM5	2000-2099	RCP2.6	4	9	4	0	0
GFDL-ESM2G	2000-2099	RCP2.6	4	6	4	0	0
HadGEM2-ES	2000-2099	RCP2.6	10	3	8	0	0
MIROC5	2000-2099	RCP2.6	10	3	9	0	0
MRI-CGCM3	2000-2099	RCP2.6	9	3	5	2	0
CNRM-CM5	2000-2099	RCP4.5	8	9	10	0	1
GFDL-ESM2G	2000-2099	RCP4.5	4	7	6	0	0
HadGEM2-ES	2000-2099	RCP4.5	11	6	5	0	0
MIROC5	2000-2099	RCP4.5	14	7	12	0	0
MRI-CGCM3	2000-2099	RCP4.5	7	4	7	0	0
CNRM-CM5	2000-2099	RCP8.5	22	5	5	0	1
GFDL-ESM2G	2000-2099	RCP8.5	17	6	7	0	0
HadGEM2-ES	2000-2099	RCP8.5	32	5	5	0	0
MIROC5	2000-2099	RCP8.5	43	5	17	0	0
MRI-CGCM3	2000-2099	RCP8.5	39	3	8	1	0

Data from Table 4.22 were analysed using negative binomial modelling for count events in order to allow comparisons between scenarios and locations. Data from separate GCMs at one combination of location and scenario were treated as replicates for modelling purposes. A mean event rate (overtopping events per 100 years) was estimated for each location and scenario (average of the five GCM values for that location and scenario). 95% confidence intervals were generated for each from the data. 95% confidence intervals were not generated for the historic runs because these overtopping events were the result of pond volume manipulation until the MEDLI model returned an overtopping frequency of 9 events per 100 years. These are displayed in Figure 4.21.

An attempt was made to statistically compare event rates at each location between the scenarios (including the historic event rate).

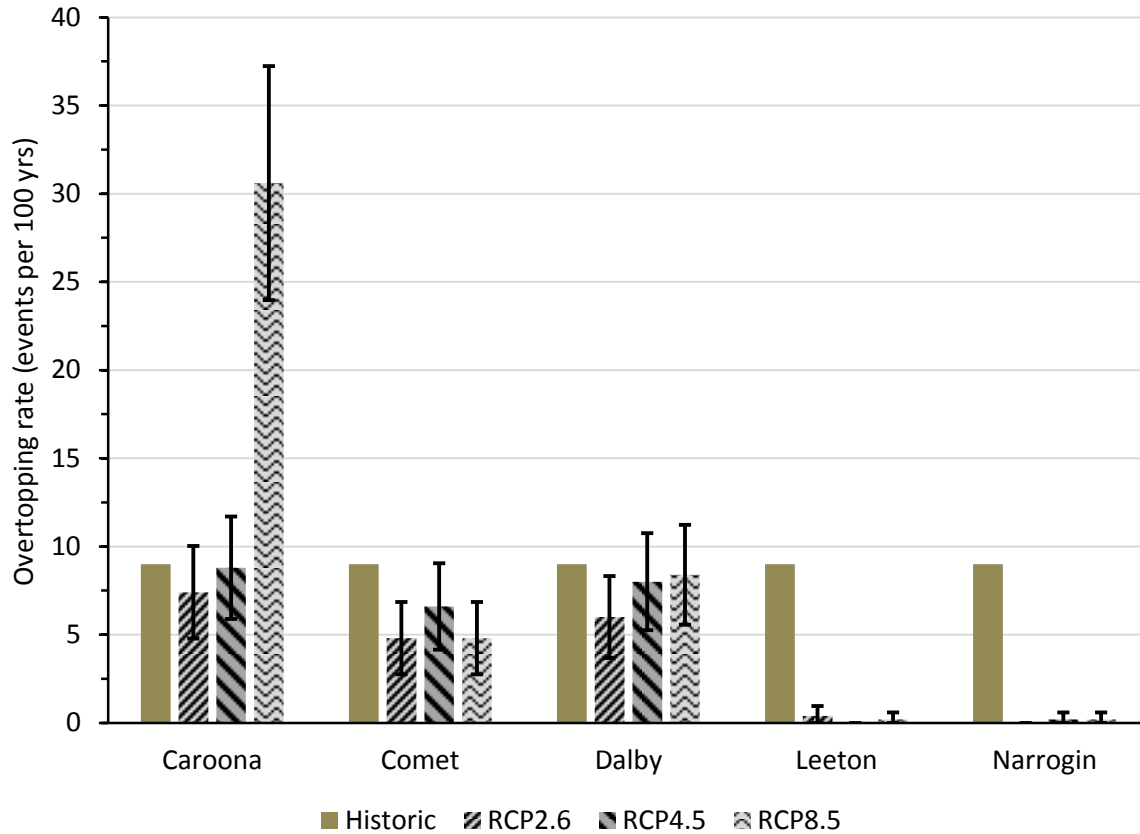


Figure 4.21: Plot of mean overtopping rate (events per 100 years) for each location and scenario (historic, RCP2.6, RCP4.5 and RCP8.5). Bars represent 95% confidence intervals either side of the mean.

For Comet and Dalby, there was no difference in event rate between any comparison involving the historic event rate and any of the three scenario event rates ($p > 0.05$). These findings suggested that predicted changes in future climate under any of the three scenarios were not associated with any increase in pond overtopping rates.

At Caroona, there was no difference in overtopping rates between the historic estimate (9 events per 100 years) and estimates for both RCP2.6 and RCP4.5 ($P > 0.05$). The mean overtopping rate for RCP8.5 of 31 events per 100 years, was significantly higher than any of the other three rate estimates for Caroona ($p < 0.05$).

In contrast both Leeton and Narrogin showed a reduction in overtopping events from the historic runs to the future scenarios. Because the future scenario estimates were very close to zero and in several cases were equal to zero, the model outputs produced unstable standard errors and it was not possible to derive valid p -values from comparing the historic event to future scenario specific event rates.

The practical implications of these findings are that at all locations and under all except one scenario, there was no evidence to suggest that current approaches to managing runoff will be inadequate in the future. The exception to this was at Caroona under the most severe climate

change scenario (RCP8.5). In this situation, models suggested that there was a relatively large increase in overtopping frequency.

4.2.2 Rainfall

The datasets used in the MEDLI feedlot hydrology modelling were arranged in a slightly different way compared to the datasets used to derive summaries of future climate scenarios in Section 4.1.

In the MEDLI hydrology modelling the historic dataset is derived from SILO data for each location covering a 100 year period from 1910-2009.

All predicted climate data summaries from the MEDLI modelling data are derived from a combined dataset covering a 100 year period from 2000-2099 and comprising 10 years of SILO records (2000-2009) and 90 years of predicted climate runs from each GCM and scenario combination. This was done because modelling of pond overtopping rates was designed to be based on 100-year datasets in order to generate overtopping rates in units of events per 100 years.

4.2.2.1 Caroona

Table 4.23: Summary statistics for rainfall at Caroona derived from MEDLI modelling datasets. GCM ave / SILO is the ratio of the average across all GCM outputs for that scenario to the SILO mean value.

Climate data	Scenario	Mean annual rainfall	10 th percentile annual rainfall	90 th percentile annual rainfall	Maximum 24 hr rainfall event
		(mm)	(mm)	(mm)	(mm)
SILO (1910-2009)	Historic	597	377	810	109
CNRM-CM5	RCP2.6	613	401	793	99
GFDL-ESM2G	RCP2.6	605	398	789	104
HadGEM2-ES	RCP2.6	622	401	807	112
MIROC5	RCP2.6	646	414	854	120
MRI-CGCM3	RCP2.6	629	401	826	106
<i>GCM ave / SILO</i>		<i>1.04</i>	<i>1.07</i>	<i>1.00</i>	<i>0.99</i>
CNRM-CM5	RCP4.5	622	401	824	101
GFDL-ESM2G	RCP4.5	604	401	787	106
HadGEM2-ES	RCP4.5	630	401	832	124
MIROC5	RCP4.5	677	422	892	111
MRI-CGCM3	RCP4.5	655	416	863	101
<i>GCM ave / SILO</i>		<i>1.07</i>	<i>1.08</i>	<i>1.04</i>	<i>1.00</i>
CNRM-CM5	RCP8.5	599	396	783	93
GFDL-ESM2G	RCP8.5	592	382	770	101
HadGEM2-ES	RCP8.5	617	401	824	119
MIROC5	RCP8.5	707	455	928	129
MRI-CGCM3	RCP8.5	660	410	863	112
<i>GCM ave / SILO</i>		<i>1.06</i>	<i>1.08</i>	<i>1.03</i>	<i>1.02</i>

This table shows that there was a very slight increase over time in the mean annual rainfall when calculated over a 100-year period. The RCP2.6 average annual rainfall was 1.04-fold higher (4% increase) than the historic mean annual rainfall.

Table 4.24: Count of the number of days when daily rainfall (mm) fell within each 100-year interval at Caroona. GCM ave / SILO is the ratio of the average across all GCM outputs for that scenario to the SILO value.

Source	Intervals of daily rainfall (mm)								
	0	1-25	26-50	51-75	76-100	101-125	126-150	151-175	176+
Count of the number of days when daily rainfall records fell within each interval									
SILO 1910-2009	28,378	7,709	370	53	14	1	0	0	0
RCP2.6									
CNRM-CM5	28,572	7,512	359	60	22	0	0	0	0
GFDL-ESM2G	28,585	7,506	357	58	18	1	0	0	0
HadGEM2-ES	28,545	7,517	374	66	19	4	0	0	0
MIROC5	28,479	7,545	396	74	22	9	0	0	0
MRI-CGCM3	28,511	7,542	381	69	20	2	0	0	0
<i>GCM ave / SILO</i>	<i>1.01</i>	<i>0.98</i>	<i>1.01</i>	<i>1.23</i>	<i>1.44</i>	<i>3.20</i>	-	-	-
RCP4.5									
CNRM-CM5	28,525	7,530	391	59	19	1	0	0	0
GFDL-ESM2G	28,608	7,486	357	53	19	2	0	0	0
HadGEM2-ES	28,536	7,512	383	71	18	5	0	0	0
MIROC5	28,403	7,561	448	80	25	8	0	0	0
MRI-CGCM3	28,525	7,530	391	59	19	1	0	0	0
<i>GCM ave / SILO</i>	<i>1.00</i>	<i>0.98</i>	<i>1.06</i>	<i>1.22</i>	<i>1.43</i>	<i>3.40</i>	-	-	-
RCP8.5									
CNRM-CM5	28,621	7,479	348	58	19	0	0	0	0
GFDL-ESM2G	28,633	7,479	334	58	20	1	0	0	0
HadGEM2-ES	28,583	7,483	365	71	18	5	0	0	0
MIROC5	28,397	7,537	461	87	26	14	3	0	0
MRI-CGCM3	28,493	7,508	414	83	20	7	0	0	0
<i>GCM ave / SILO</i>	<i>1.01</i>	<i>0.97</i>	<i>1.04</i>	<i>1.35</i>	<i>1.47</i>	<i>5.40</i>	-	-	-

Tables of summary statistics based on counts when rainfall exceeded daily thresholds (

Table 4.24) are intended to provide a summary of occurrence of more extreme rainfall events. Tables and plots of average rainfall do not provide any indication of the occurrence of more extreme rainfall events and overtopping may occur in response to extreme rainfall within a relatively short period of time. This table clearly shows that there is a progressive rise in occurrence of extreme rainfall events. For example, there was a 1.47 fold increase (47% increase) in the number of days per 100-years when 76-100 mm of rain fell in a single day (comparing RCP8.5 to historic records).

4.2.2.2 Comet

Table 4.25: Summary statistics for rainfall at Comet derived from MEDLI modelling datasets. GCM ave / SILO is the ratio of the average across all GCM outputs for that scenario to the SILO mean value.

Climate data	Scenario	Mean annual rainfall (mm)	10 percentile annual rainfall (mm)	90 percentile annual rainfall (mm)	Maximum 24 hr rainfall event (mm)
SILO (1910-2009)	Historic	588	587	768	173
CNRM-CM5	RCP2.6	553	349	811	125
GFDL-ESM2G	RCP2.6	560	354	784	119
HadGEM2-ES	RCP2.6	536	340	776	109
MIROC5	RCP2.6	520	321	742	131
MRI-CGCM3	RCP2.6	508	314	732	110
<i>GCM ave / SILO</i>		<i>0.91</i>	<i>0.57</i>	<i>1.00</i>	<i>0.69</i>
CNRM-CM5	RCP4.5	597	376	871	124
GFDL-ESM2G	RCP4.5	581	363	843	136
HadGEM2-ES	RCP4.5	556	355	790	108
MIROC5	RCP4.5	615	395	890	132
MRI-CGCM3	RCP4.5	515	320	731	123
<i>GCM ave / SILO</i>		<i>0.97</i>	<i>0.62</i>	<i>1.07</i>	<i>0.72</i>
CNRM-CM5	RCP8.5	512	321	743	111
GFDL-ESM2G	RCP8.5	583	363	835	131
HadGEM2-ES	RCP8.5	527	331	760	109
MIROC5	RCP8.5	573	363	817	134
MRI-CGCM3	RCP8.5	520	321	741	135
<i>GCM ave / SILO</i>		<i>0.92</i>	<i>0.58</i>	<i>1.01</i>	<i>0.72</i>

There was a small but noticeable decline in 100-average rainfall that did not appear to vary between RCP scenarios. On average the mean rainfall for the RCP2.6 models represented a 0.91-fold reduction (reduction of 9%) compared to the historic mean annual rainfall determined from the 1910-2009 period.

Table 4.26: Count of the number of days when daily rainfall (mm) fell within each interval at Comet. GCM ave / SILO is the ratio of the average across all GCM outputs for that scenario to the SILO value.

Source	Intervals of daily rainfall (mm)								
	0	1-25	26-50	51-75	76-100	101-125	126-150	151-175	176+
Count of the number of days when daily rainfall records fell within each interval									
SILO 1910-2009	29,799	6,218	392	83	23	7	2	1	0
RCP2.6									
CNRM-CM5	29,700	6,375	362	58	25	5	0	0	0
GFDL-ESM2G	29,664	6,406	368	58	22	7	0	0	0
HadGEM2-ES	29,715	6,374	356	52	25	3	0	0	0
MIROC5	29,788	6,332	331	48	20	5	1	0	0
MRI-CGCM3	29,797	6,344	312	51	20	1	0	0	0
<i>GCM ave / SILO</i>	<i>1.00</i>	<i>1.02</i>	<i>0.88</i>	<i>0.64</i>	<i>0.97</i>	<i>0.60</i>	<i>0.10</i>	<i>0.00</i>	<i>-</i>
RCP4.5									
CNRM-CM5	29,623	6,380	410	74	27	11	0	0	0
GFDL-ESM2G	29,632	6,401	395	65	20	10	2	0	0
HadGEM2-ES	29,696	6,362	381	56	25	5	0	0	0
MIROC5	29,616	6,360	434	76	23	12	4	0	0
MRI-CGCM3	29,774	6,354	319	55	20	3	0	0	0
<i>GCM ave / SILO</i>	<i>1.00</i>	<i>1.02</i>	<i>0.99</i>	<i>0.79</i>	<i>1.00</i>	<i>1.17</i>	<i>0.60</i>	<i>0.00</i>	<i>-</i>
RCP8.5									
CNRM-CM5	29,771	6,362	319	51	17	5	0	0	0
GFDL-ESM2G	29,634	6,400	392	65	21	10	3	0	0
HadGEM2-ES	29,759	6,351	338	49	27	1	0	0	0
MIROC5	29,668	6,369	388	67	22	6	5	0	0
MRI-CGCM3	29,740	6,382	331	49	17	5	1	0	0
<i>GCM ave / SILO</i>	<i>1.00</i>	<i>1.02</i>	<i>0.90</i>	<i>0.68</i>	<i>0.90</i>	<i>0.77</i>	<i>0.90</i>	<i>0.00</i>	<i>-</i>

There appeared to be a slight increase in heavy rainfall days in the RCP4.5 scenario but a more noticeable decline in heavy rainfall days in the other two scenarios when compared to the historic 100-year period.

4.2.2.3 Dalby

Table 4.27: Summary statistics for rainfall at Dalby derived from MEDLI modelling datasets. GCM ave / SILO is the ratio of the average across all GCM outputs for that scenario to the SILO mean value.

Climate data	Scenario	Mean annual rainfall	10 percentile annual rainfall	90 percentile annual rainfall	Maximum 24 hr rainfall event
		(mm)	(mm)	(mm)	(mm)
SILO (1910-2009)	Historic	650	653	819	118
CNRM-CM5	RCP2.6	592	451	770	109
GFDL-ESM2G	RCP2.6	597	436	787	118
HadGEM2-ES	RCP2.6	594	433	796	132
MIROC5	RCP2.6	579	417	787	134
MRI-CGCM3	RCP2.6	586	418	759	124
<i>GCM ave / SILO</i>		<i>0.91</i>	<i>0.66</i>	<i>0.95</i>	<i>1.05</i>
CNRM-CM5	RCP4.5	613	446	825	129
GFDL-ESM2G	RCP4.5	577	418	757	130
HadGEM2-ES	RCP4.5	589	425	797	118
MIROC5	RCP4.5	625	461	840	138
MRI-CGCM3	RCP4.5	605	444	787	130
<i>GCM ave / SILO</i>		<i>0.93</i>	<i>0.67</i>	<i>0.98</i>	<i>1.09</i>
CNRM-CM5	RCP8.5	567	408	742	138
GFDL-ESM2G	RCP8.5	587	421	770	135
HadGEM2-ES	RCP8.5	560	408	749	127
MIROC5	RCP8.5	626	451	828	140
MRI-CGCM3	RCP8.5	605	436	797	140
<i>GCM ave / SILO</i>		<i>0.91</i>	<i>0.65</i>	<i>0.95</i>	<i>1.15</i>

Annual rainfall measures estimated over 100-years of records showed a small decline for future scenarios when compared to the historic mean. The overall effect of the RCP2.6 scenario was a 0.91-fold decline (9% reduction) in mean annual rainfall.

Table 4.28: Count of the number of days when daily rainfall (mm) fell within each interval at Dalby. GCM ave / SILO is the ratio of the average across all GCM outputs for that scenario to the SILO value.

Source	Intervals of daily rainfall (mm)								
	0	1-25	26-50	51-75	76-100	101-125	126-150	151-175	176+
Count of the number of days when daily rainfall records fell within each interval									
SILO 1910-2009	29,069	6,899	466	62	22	7	0	0	0
RCP2.6									
CNRM-CM5	29,349	6,679	421	48	22	6	0	0	0
GFDL-ESM2G	29,348	6,687	414	44	25	7	0	0	0
HadGEM2-ES	29,385	6,648	415	47	20	9	1	0	0
MIROC5	29,450	6,604	399	37	22	11	2	0	0
MRI-CGCM3	29,366	6,689	397	44	21	8	0	0	0
<i>GCM ave / SILO</i>	<i>1.01</i>	<i>0.97</i>	<i>0.88</i>	<i>0.71</i>	<i>1.00</i>	<i>1.17</i>	-	-	-
RCP4.5									
CNRM-CM5	29,336	6,660	442	53	23	10	1	0	0
GFDL-ESM2G	29,431	6,632	388	43	22	8	1	0	0
HadGEM2-ES	29,410	6,630	410	48	21	6	0	0	0
MIROC5	29,279	6,699	458	51	22	15	1	0	0
MRI-CGCM3	29,342	6,682	419	49	24	8	1	0	0
<i>GCM ave / SILO</i>	<i>1.01</i>	<i>0.97</i>	<i>0.91</i>	<i>0.79</i>	<i>1.02</i>	<i>1.34</i>	-	-	-
RCP8.5									
CNRM-CM5	29,447	6,644	363	42	21	7	1	0	0
GFDL-ESM2G	29,404	6,651	394	43	23	9	1	0	0
HadGEM2-ES	29,441	6,659	353	46	16	9	1	0	0
MIROC5	29,326	6,647	451	62	21	13	5	0	0
MRI-CGCM3	29,337	6,682	423	55	19	8	1	0	0
<i>GCM ave / SILO</i>	<i>1.01</i>	<i>0.96</i>	<i>0.85</i>	<i>0.80</i>	<i>0.91</i>	<i>1.31</i>	-	-	-

Even though the mean annual rainfall was predicted to have declined slightly in all three RCP scenarios, the occurrence of individual heavy rainfall days is shown to increase. There was a 1.17-fold (17% increase) increase in the number of days per 100-years when 101-125 mm of rain was recorded for the RCP2.6 scenario when compared to the historic 100-year period. The number of heavy rainfall days is still small, considering that these counts represent the total number of days over a 100-year period.

4.2.2.4 Leeton

Table 4.29: Summary statistics for rainfall at Leeton derived from MEDLI modelling datasets. GCM ave / SILO is the ratio of the average across all GCM outputs for that scenario to the SILO mean value.

Climate data	Scenario	Mean annual rainfall (mm)	10 percentile annual rainfall (mm)	90 percentile annual rainfall (mm)	Maximum 24 hr rainfall event (mm)
SILO (1910-2009)	Historic	419	256	597	81
CNRM-CM5	RCP2.6	420	257	600	82
GFDL-ESM2G	RCP2.6	426	257	615	81
HadGEM2-ES	RCP2.6	416	252	602	91
MIROC5	RCP2.6	416	248	586	81
MRI-CGCM3	RCP2.6	433	257	619	99
<i>GCM ave / SILO</i>		<i>1.01</i>	<i>0.99</i>	<i>1.01</i>	<i>1.07</i>
CNRM-CM5	RCP4.5	432	262	622	84
GFDL-ESM2G	RCP4.5	414	257	594	87
HadGEM2-ES	RCP4.5	412	250	589	81
MIROC5	RCP4.5	431	261	609	90
MRI-CGCM3	RCP4.5	433	261	623	93
<i>GCM ave / SILO</i>		<i>1.01</i>	<i>1.01</i>	<i>1.02</i>	<i>1.07</i>
CNRM-CM5	RCP8.5	421	257	597	81
GFDL-ESM2G	RCP8.5	420	257	600	82
HadGEM2-ES	RCP8.5	401	240	568	86
MIROC5	RCP8.5	433	262	611	100
MRI-CGCM3	RCP8.5	431	260	615	99
<i>GCM ave / SILO</i>		<i>1.01</i>	<i>1.00</i>	<i>1.00</i>	<i>1.11</i>

There was no change in the mean annual rainfall over any of the scenarios when calculated on a 100-year period.

Table 4.30: Count of the number of days when daily rainfall (mm) fell within each interval at Leeton. GCM ave / SILO is the ratio of the average across all GCM outputs for that scenario to the SILO value.

Source	Intervals of daily rainfall (mm)								
	0	1-25	26-50	51-75	76-100	101-125	126-150	151-175	176+
Count of the number of days when daily rainfall records fell within each interval									
SILO 1910-2009	29,361	6,938	205	20	1	1	0	0	0
RCP2.6									
CNRM-CM5	29,730	6,564	214	15	2	0	0	0	0
GFDL-ESM2G	29,759	6,534	212	16	4	1	0	0	0
HadGEM2-ES	29,724	6,574	205	19	3	4	0	0	0
MIROC5	29,746	6,553	209	15	2	9	0	0	0
MRI-CGCM3	29,703	6,573	228	18	3	2	0	0	0
<i>GCM ave / SILO</i>	<i>1.01</i>	<i>0.95</i>	<i>1.04</i>	<i>0.83</i>	<i>2.80</i>	<i>3.20</i>	-	-	-
RCP4.5									
CNRM-CM5	29,662	6,613	230	18	2	1	0	0	0
GFDL-ESM2G	29,765	6,535	208	15	2	2	0	0	0
HadGEM2-ES	29,747	6,558	200	17	3	5	0	0	0
MIROC5	29,670	6,610	227	15	3	8	0	0	0
MRI-CGCM3	29,707	6,563	234	17	4	1	0	0	0
<i>GCM ave / SILO</i>	<i>1.01</i>	<i>0.95</i>	<i>1.07</i>	<i>0.82</i>	<i>2.80</i>	<i>3.40</i>	-	-	-
RCP8.5									
CNRM-CM5	29,718	6,577	213	15	2	0	0	0	0
GFDL-ESM2G	29,759	6,534	212	16	4	1	0	0	0
HadGEM2-ES	29,781	6,541	185	16	2	5	0	0	0
MIROC5	29,693	6,575	237	16	4	14	3	0	0
MRI-CGCM3	29,702	6,573	232	14	4	7	0	0	0
<i>GCM ave / SILO</i>	<i>1.01</i>	<i>0.95</i>	<i>1.05</i>	<i>0.77</i>	<i>3.20</i>	<i>5.40</i>	-	-	-

There was an increase in the number of heavy rainfall days but the actual number of heavy rainfall days is still relatively small, considering that these counts represent the total number of days over a 100-year period.

4.2.2.5 Narrogin

Table 4.31: Summary statistics for rainfall at Narrogin derived from MEDLI modelling datasets. GCM ave / SILO is the ratio of the average across all GCM outputs for that scenario to the SILO mean value.

Climate data	Scenario	Mean annual rainfall	10 percentile annual rainfall	90 percentile annual rainfall	Maximum 24 hr rainfall event
		(mm)	(mm)	(mm)	(mm)
SILO (1910-2009)	Historic	524	374	672	138
CNRM-CM5	RCP2.6	459	345	571	137
GFDL-ESM2G	RCP2.6	498	377	614	138
HadGEM2-ES	RCP2.6	480	360	596	138
MIROC5	RCP2.6	455	341	573	138
MRI-CGCM3	RCP2.6	433	257	619	99
<i>GCM ave / SILO</i>		<i>0.89</i>	<i>0.90</i>	<i>0.88</i>	<i>0.94</i>
CNRM-CM5	RCP4.5	492	371	616	138
GFDL-ESM2G	RCP4.5	447	333	556	137
HadGEM2-ES	RCP4.5	467	350	569	138
MIROC5	RCP4.5	475	359	599	134
MRI-CGCM3	RCP4.5	475	359	599	139
<i>GCM ave / SILO</i>		<i>0.90</i>	<i>0.95</i>	<i>0.87</i>	<i>0.99</i>
CNRM-CM5	RCP8.5	487	361	609	138
GFDL-ESM2G	RCP8.5	415	300	506	139
HadGEM2-ES	RCP8.5	457	340	560	139
MIROC5	RCP8.5	434	320	532	138
MRI-CGCM3	RCP8.5	452	334	564	138
<i>GCM ave / SILO</i>		<i>0.86</i>	<i>0.89</i>	<i>0.82</i>	<i>1.00</i>

There was a substantial decline in mean annual rainfall for each of the climate change scenarios when compared to the historic 100-year mean annual rainfall.

Table 4.32: Count of the number of days when daily rainfall (mm) fell within each interval at Narrogin. GCM ave / SILO is the ratio of the average across all GCM outputs for that scenario to the SILO value.

Source	Intervals of daily rainfall (mm)								
	0	1-25	26-50	51-75	76-100	101-125	126-150	151-175	176+
Count of the number of days when daily rainfall records fell within each interval									
SILO 1910-2009	27,107	9,212	190	10	4	0	2	0	0
RCP2.6									
CNRM-CM5	27,590	8,768	149	12	4	0	2	0	0
GFDL-ESM2G	27,764	8,631	116	8	4	0	2	0	0
HadGEM2-ES	27,686	8,691	133	9	4	0	2	0	0
MIROC5	27,757	8,631	121	11	2	1	2	0	0
MRI-CGCM3	29,703	6,573	228	18	3	0	0	0	0
<i>GCM ave / SILO</i>	<i>1.04</i>	<i>0.90</i>	<i>0.79</i>	<i>1.16</i>	<i>0.85</i>	-	<i>0.80</i>	-	-
RCP4.5									
CNRM-CM5	27,635	8,723	149	12	4	0	2	0	0
GFDL-ESM2G	27,807	8,595	109	9	3	0	2	0	0
HadGEM2-ES	27,742	8,654	115	8	4	0	2	0	0
MIROC5	27,682	8,697	127	13	4	0	2	0	0
MRI-CGCM3	27,762	8,645	106	6	4	0	2	0	0
<i>GCM ave / SILO</i>	<i>1.02</i>	<i>0.94</i>	<i>0.64</i>	<i>0.96</i>	<i>0.95</i>	-	<i>1.00</i>	-	-
RCP8.5									
CNRM-CM5	27,642	8,726	138	13	4	0	2	0	0
GFDL-ESM2G	27,951	8,471	91	7	3	0	2	0	0
HadGEM2-ES	27,776	8,627	110	7	3	0	2	0	0
MIROC5	27,924	8,484	101	11	3	0	2	0	0
MRI-CGCM3	27,778	8,614	118	10	3	0	2	0	0
<i>GCM ave / SILO</i>	<i>1.03</i>	<i>0.93</i>	<i>0.59</i>	<i>0.96</i>	<i>0.80</i>	-	<i>1.00</i>	-	-

There was a decline in the number of heavy rainfall days for each of the climate change scenarios when compared to the historic 100-year period.

4.2.3 Evaporation

4.2.3.1 Carroona

Table 4.33: Summary statistics for evaporation (mm per year for annual summaries and mm per day for maximum daily evaporation) at Carroona, derived from MEDLI modelling datasets. GCM ave / SILO is the ratio of the average across all GCM outputs for that scenario to the SILO mean value.

Climate data	Scenario	Mean annual evaporation (mm)	10 percentile annual evaporation (mm)	90 percentile annual evaporation (mm)	Maximum 24 hr evaporation (mm)
SILO (1910-2009)	Historic	1824	1647	1993	16
CNRM-CM5	RCP2.6	1851	1755	1960	11
GFDL-ESM2G	RCP2.6	1847	1757	1962	11
HadGEM2-ES	RCP2.6	1840	1746	1945	11
MIROC5	RCP2.6	1835	1741	1945	11
MRI-CGCM3	RCP2.6	1837	1743	1949	11
<i>GCM ave / SILO</i>		<i>1.01</i>	<i>1.06</i>	<i>0.98</i>	<i>0.69</i>
CNRM-CM5	RCP4.5	1840	1749	1955	11
GFDL-ESM2G	RCP4.5	1855	1757	1979	11
HadGEM2-ES	RCP4.5	1848	1755	1954	10
MIROC5	RCP4.5	1809	1715	1909	10
MRI-CGCM3	RCP4.5	1820	1725	1922	11
<i>GCM ave / SILO</i>		<i>1.01</i>	<i>1.06</i>	<i>0.98</i>	<i>0.66</i>
CNRM-CM5	RCP8.5	1896	1793	2034	11
GFDL-ESM2G	RCP8.5	1877	1782	2007	11
HadGEM2-ES	RCP8.5	1879	1783	2003	11
MIROC5	RCP8.5	1815	1723	1914	10
MRI-CGCM3	RCP8.5	1841	1746	1954	11
<i>GCM ave / SILO</i>		<i>1.02</i>	<i>1.07</i>	<i>0.99</i>	<i>0.68</i>

Evaporation statistics are provided as a summary of possible future climate change effects. The evidence for Carroona suggests that future scenarios might be associated with a decline in annual measures of evaporation when compared to the historic 100-year period.

4.2.3.2 Comet

Table 4.34: Summary statistics for evaporation (mm per year for annual summaries and mm per day for maximum daily evaporation) at Comet, derived from MEDLI modelling datasets. GCM ave / SILO is the ratio of the average across all GCM outputs for that scenario to the SILO mean value.

Climate data	Scenario	Mean annual evaporation (mm)	10 percentile annual evaporation (mm)	90 percentile annual evaporation (mm)	Maximum 24 hr evaporation (mm)
SILO (1910-2009)	Historic	2097	2118	2261	15
CNRM-CM5	RCP2.6	2131	2023	2230	11
GFDL-ESM2G	RCP2.6	2128	2029	2223	11
HadGEM2-ES	RCP2.6	2154	2043	2249	10
MIROC5	RCP2.6	2177	2058	2284	11
MRI-CGCM3	RCP2.6	2143	2029	2242	11
<i>GCM ave / SILO</i>		<i>1.02</i>	<i>0.96</i>	<i>0.99</i>	<i>0.72</i>
CNRM-CM5	RCP4.5	2110	2001	2207	10
GFDL-ESM2G	RCP4.5	2151	2036	2255	11
HadGEM2-ES	RCP4.5	2170	2058	2276	11
MIROC5	RCP4.5	2134	2026	2232	10
MRI-CGCM3	RCP4.5	2137	2025	2233	11
<i>GCM ave / SILO</i>		<i>1.02</i>	<i>0.96</i>	<i>0.99</i>	<i>0.71</i>
CNRM-CM5	RCP8.5	2177	2065	2303	11
GFDL-ESM2G	RCP8.5	2170	2058	2276	11
HadGEM2-ES	RCP8.5	2200	2058	2319	11
MIROC5	RCP8.5	2153	2039	2250	11
MRI-CGCM3	RCP8.5	2164	2058	2275	11
<i>GCM ave / SILO</i>		<i>1.04</i>	<i>0.97</i>	<i>1.01</i>	<i>0.73</i>

There was relatively little change in summary measures of evaporation for Comet though the maximal 24-hour evaporation estimates appeared to be reduced.

4.2.3.3 Dalby

Table 4.35: Summary statistics for evaporation (mm per year for annual summaries and mm per day for maximum daily evaporation) at Dalby, derived from MEDLI modelling datasets. GCM ave / SILO is the ratio of the average across all GCM outputs for that scenario to the SILO mean value.

Climate data	Scenario	Mean annual evaporation	10 percentile annual evaporation	90 percentile annual evaporation	Maximum 24 hr evaporation
		(mm)	(mm)	(mm)	(mm)
SILO (1910-2009)	Historic	1992	1990	2110	18
CNRM-CM5	RCP2.6	1962	1863	2061	11
GFDL-ESM2G	RCP2.6	1963	1871	2058	10
HadGEM2-ES	RCP2.6	1980	1888	2078	11
MIROC5	RCP2.6	1976	1875	2084	10
MRI-CGCM3	RCP2.6	1965	1866	2069	11
<i>GCM ave / SILO</i>		<i>0.99</i>	<i>0.94</i>	<i>0.98</i>	<i>0.59</i>
CNRM-CM5	RCP4.5	1950	1851	2054	10
GFDL-ESM2G	RCP4.5	1990	1889	2100	11
HadGEM2-ES	RCP4.5	1986	1884	2094	10
MIROC5	RCP4.5	1943	1852	2035	10
MRI-CGCM3	RCP4.5	1957	1862	2052	11
<i>GCM ave / SILO</i>		<i>0.99</i>	<i>0.94</i>	<i>0.98</i>	<i>0.58</i>
CNRM-CM5	RCP8.5	2016	1891	2148	11
GFDL-ESM2G	RCP8.5	1995	1869	2127	11
HadGEM2-ES	RCP8.5	2025	1908	2153	11
MIROC5	RCP8.5	1953	1862	2045	10
MRI-CGCM3	RCP8.5	1975	1864	2085	11
<i>GCM ave / SILO</i>		<i>1.00</i>	<i>0.94</i>	<i>1.00</i>	<i>0.60</i>

There was relatively little change in summary measures of evaporation for Dalby though the maximal 24-hour evaporation estimates appeared to be reduced.

4.2.3.4 Leeton

Table 4.36: Summary statistics for evaporation (mm per year for annual summaries and mm per day for maximum daily evaporation) at Leeton, derived from MEDLI modelling datasets. GCM ave / SILO is the ratio of the average across all GCM outputs for that scenario to the SILO mean value.

Climate data	Scenario	Mean annual evaporation	10 percentile annual evaporation	90 percentile annual evaporation	Maximum 24 hr evaporation
		(mm)	(mm)	(mm)	(mm)
SILO (1910-2009)	Historic	1772	1619	1924	19
CNRM-CM5	RCP2.6	1807	1702	1936	11
GFDL-ESM2G	RCP2.6	1790	1679	1903	11
HadGEM2-ES	RCP2.6	1803	1692	1912	11
MIROC5	RCP2.6	1794	1685	1909	11
MRI-CGCM3	RCP2.6	1768	1656	1882	11
<i>GCM ave / SILO</i>		<i>1.01</i>	<i>1.04</i>	<i>0.99</i>	<i>0.58</i>
CNRM-CM5	RCP4.5	1785	1678	1902	11
GFDL-ESM2G	RCP4.5	1796	1689	1925	11
HadGEM2-ES	RCP4.5	1821	1719	1944	11
MIROC5	RCP4.5	1785	1672	1892	11
MRI-CGCM3	RCP4.5	1766	1654	1878	11
<i>GCM ave / SILO</i>		<i>1.01</i>	<i>1.04</i>	<i>0.99</i>	<i>0.58</i>
CNRM-CM5	RCP8.5	1818	1707	1951	11
GFDL-ESM2G	RCP8.5	1807	1702	1936	11
HadGEM2-ES	RCP8.5	1851	1733	1993	11
MIROC5	RCP8.5	1798	1691	1915	11
MRI-CGCM3	RCP8.5	1785	1683	1903	11
<i>GCM ave / SILO</i>		<i>1.02</i>	<i>1.05</i>	<i>1.01</i>	<i>0.58</i>

There was relatively little change in summary measures of evaporation for Leeton though the maximal 24-hour evaporation estimates appeared to be reduced.

4.2.3.5 Narrogin

Table 4.37: Summary statistics for evaporation (mm per year for annual summaries and mm per day for maximum daily evaporation) at Narrogin, derived from MEDLI modelling datasets. GCM ave / SILO is the ratio of the average across all GCM outputs for that scenario to the SILO mean value.

Climate data	Scenario	Mean annual evaporation (mm)	10 percentile annual evaporation (mm)	90 percentile annual evaporation (mm)	Maximum 24 hr evaporation (mm)
SILO (1910-2009)	Historic	1539	1450	1656	15
CNRM-CM5	RCP2.6	1753	1676	1818	11
GFDL-ESM2G	RCP2.6	1737	1811	1774	11
HadGEM2-ES	RCP2.6	1739	1659	1803	11
MIROC5	RCP2.6	1742	1668	1806	11
MRI-CGCM3	RCP2.6	1768	1656	1882	11
<i>GCM ave / SILO</i>		<i>1.14</i>	<i>1.17</i>	<i>1.10</i>	<i>0.73</i>
CNRM-CM5	RCP4.5	1745	1665	1815	10
GFDL-ESM2G	RCP4.5	1759	1685	1827	11
HadGEM2-ES	RCP4.5	1756	1679	1826	11
MIROC5	RCP4.5	1750	1669	1814	10
MRI-CGCM3	RCP4.5	1750	1669	1814	11
<i>GCM ave / SILO</i>		<i>1.14</i>	<i>1.15</i>	<i>1.10</i>	<i>0.71</i>
CNRM-CM5	RCP8.5	1761	1674	1848	11
GFDL-ESM2G	RCP8.5	1778	1699	1862	11
HadGEM2-ES	RCP8.5	1773	1688	1855	11
MIROC5	RCP8.5	1777	1700	1857	11
MRI-CGCM3	RCP8.5	1751	1670	1830	11
<i>GCM ave / SILO</i>		<i>1.15</i>	<i>1.16</i>	<i>1.12</i>	<i>0.73</i>

There was an increase in summary measures of evaporation for Narrogin though the maximal 24-hour evaporation estimates appeared to be reduced.

4.2.4 Runoff

The following tables provide summary statistics for the daily MEDLI outputs for feedlot runoff. These summary statistics are based on the 100-year intervals used in MEDLI modelling. A more detailed summary of runoff measures is provided in Section 4.5 which uses runoff measures as an indication of effluent water balance.

4.2.4.1 Caroona

Table 4.38: Summary statistics for evaporation (mm per year for annual summaries and mm per day for maximum daily evaporation) at Caroona, derived from MEDLI modelling datasets

Climate data	Scenario	Mean annual runoff	10 percentile annual runoff	90 percentile annual runoff	Maximum 24 hr runoff
		(mm)	(mm)	(mm)	(mm)
SILO (1910-2009)	Historic	173	72	301	81
CNRM-CM5	RCP2.6	182	95	299	77
GFDL-ESM2G	RCP2.6	177	96	298	82
HadGEM2-ES	RCP2.6	187	97	309	90
MIROC5	RCP2.6	200	106	318	98
MRI-CGCM3	RCP2.6	190	103	310	88
CNRM-CM5	RCP4.5	186	101	299	79
GFDL-ESM2G	RCP4.5	176	98	292	83
HadGEM2-ES	RCP4.5	192	101	317	101
MIROC5	RCP4.5	217	111	352	91
MRI-CGCM3	RCP4.5	206	111	330	79
CNRM-CM5	RCP8.5	173	91	293	72
GFDL-ESM2G	RCP8.5	170	90	285	81
HadGEM2-ES	RCP8.5	186	92	311	97
MIROC5	RCP8.5	237	114	398	110
MRI-CGCM3	RCP8.5	207	107	328	91

4.2.4.2 Comet

Table 4.39: Summary statistics for evaporation (mm per year for annual summaries and mm per day for maximum daily evaporation) at Comet, derived from MEDLI modelling datasets

Climate data	Scenario	Mean annual evaporation	10 percentile annual evaporation	90 percentile annual evaporation	Maximum 24 hr evaporation
		(mm)	(mm)	(mm)	(mm)
SILO (1910-2009)	Historic	193	180	293	143
CNRM-CM5	RCP2.6	173	68	307	110
GFDL-ESM2G	RCP2.6	175	67	295	102
HadGEM2-ES	RCP2.6	161	67	309	90
MIROC5	RCP2.6	154	63	263	112
MRI-CGCM3	RCP2.6	147	57	270	95
CNRM-CM5	RCP4.5	198	80	375	109
GFDL-ESM2G	RCP4.5	188	81	308	117
HadGEM2-ES	RCP4.5	172	73	323	444
MIROC5	RCP4.5	208	95	328	117
MRI-CGCM3	RCP4.5	153	57	281	98
CNRM-CM5	RCP8.5	151	56	300	96
GFDL-ESM2G	RCP8.5	191	80	310	116
HadGEM2-ES	RCP8.5	157	65	291	90
MIROC5	RCP8.5	183	81	290	118
MRI-CGCM3	RCP8.5	154	63	266	116

4.2.4.3 Dalby

Table 4.40: Summary statistics for evaporation (mm per year for annual summaries and mm per day for maximum daily evaporation) at Dalby, derived from MEDLI modelling datasets

Climate data	Scenario	Mean annual evaporation	10 percentile annual evaporation	90 percentile annual evaporation	Maximum 24 hr evaporation
		(mm)	(mm)	(mm)	(mm)
SILO (1910-2009)	Historic	197	192	268	94
CNRM-CM5	RCP2.6	180	95	265	90
GFDL-ESM2G	RCP2.6	182	102	270	91
HadGEM2-ES	RCP2.6	181	101	266	104
MIROC5	RCP2.6	177	91	262	106
MRI-CGCM3	RCP2.6	176	98	258	96
CNRM-CM5	RCP4.5	193	109	292	104
GFDL-ESM2G	RCP4.5	172	92	258	102
HadGEM2-ES	RCP4.5	178	99	284	91
MIROC5	RCP4.5	202	112	323	110
MRI-CGCM3	RCP4.5	187	108	275	102
CNRM-CM5	RCP8.5	166	88	263	110
GFDL-ESM2G	RCP8.5	178	101	277	107
HadGEM2-ES	RCP8.5	163	88	258	99
MIROC5	RCP8.5	205	111	309	113
MRI-CGCM3	RCP8.5	186	101	271	112

4.2.4.4 Leeton

Table 4.41: Summary statistics for evaporation (mm per year for annual summaries and mm per day for maximum daily evaporation) at Leeton, derived from MEDLI modelling datasets

Climate data	Scenario	Mean annual evaporation	10 percentile annual evaporation	90 percentile annual evaporation	Maximum 24 hr evaporation
		(mm)	(mm)	(mm)	(mm)
SILO (1910-2009)	Historic	106	49	181	57
CNRM-CM5	RCP2.6	100	45	170	59
GFDL-ESM2G	RCP2.6	103	49	173	57
HadGEM2-ES	RCP2.6	98	43	174	67
MIROC5	RCP2.6	98	46	170	57
MRI-CGCM3	RCP2.6	108	49	185	74
CNRM-CM5	RCP4.5	106	51	174	61
GFDL-ESM2G	RCP4.5	97	45	168	63
HadGEM2-ES	RCP4.5	96	43	169	57
MIROC5	RCP4.5	105	50	172	66
MRI-CGCM3	RCP4.5	107	53	177	69
CNRM-CM5	RCP8.5	100	48	169	58
GFDL-ESM2G	RCP8.5	100	45	170	59
HadGEM2-ES	RCP8.5	90	39	159	62
MIROC5	RCP8.5	106	49	182	75
MRI-CGCM3	RCP8.5	106	52	178	74

4.2.4.5 Narrogin

Table 4.42: Summary statistics for evaporation (mm per year for annual summaries and mm per day for maximum daily evaporation) at Narrogin, derived from MEDLI modelling datasets

Climate data	Scenario	Mean annual evaporation	10 percentile annual evaporation	90 percentile annual evaporation	Maximum 24 hr evaporation
		(mm)	(mm)	(mm)	(mm)
SILO (1910-2009)	Historic	167	99	257	109
CNRM-CM5	RCP2.6	106	59	163	108
GFDL-ESM2G	RCP2.6	129	127	122	109
HadGEM2-ES	RCP2.6	117	62	180	109
MIROC5	RCP2.6	105	57	171	109
MRI-CGCM3	RCP2.6	107	49	182	74
CNRM-CM5	RCP4.5	125	73	192	109
GFDL-ESM2G	RCP4.5	100	55	163	108
HadGEM2-ES	RCP4.5	110	60	172	109
MIROC5	RCP4.5	116	63	180	105
MRI-CGCM3	RCP4.5	116	63	180	110
CNRM-CM5	RCP8.5	121	67	195	109
GFDL-ESM2G	RCP8.5	85	41	146	110
HadGEM2-ES	RCP8.5	103	56	166	110
MIROC5	RCP8.5	95	48	154	109
MRI-CGCM3	RCP8.5	103	54	173	109

4.3 Accumulated heat load (AHL) modelling outputs

4.3.1 Plots of median heat load days per year

Plots of median heat load days per year provide a relatively simple, visual overview of the broad patterns of expected changes in heat load for each of the time periods.

No mitigation strategies were applied to the historic time period (1960-1999) and this part of the plot shows a single line representing heat load patterns in the past for comparative purposes.

A vertical dotted line is displayed on each plot at 2010 to signify the beginning of the predicted future climate datasets. Different lines are displayed for each of the four mitigation strategies.

The black line (representing no mitigation) provides a representation of the expected pattern of change over time in heat load days under each of the RCP scenarios at each location.

The coloured lines representing progressively more protective mitigation strategies provide a representation of the level of reduction in heat load days that can be achieved under differing levels of mitigation.

There is a minor issue with overlap of lines resulting in obscuring the pattern for some lines. Lines are plotted in order of increasing mitigation strategy so that if lines for maximal and moderate mitigation are identical, the maximal line (blue) will lie over the top of the moderate line (green) and the moderate line may not be apparent on the plot.

A number of general points can be made from scanning all the plots in the following pages:

- At every location the general pattern is for the number of heat load days to rise over time and most noticeably in the period after 2050.
- At every location, the general pattern is for the rise in heat load days to be progressively larger as the RCP scenarios move from mild (RCP2.6) to moderate (RCP4.5) to high (RCP8.5).
- There is considerable variation between locations with two locations (Dalby and Narrogin) showing noticeably less increase in heat load days than the other three locations. Comet shows the largest rise in heat load days over time.
- Finally, mitigation strategies progressively reduce the number of heat load days in all locations and under all RCP scenarios. In some cases mild or moderate mitigation strategies are sufficient to reduce the median number of heat load days to zero. In other cases (Comet and Leeton), moderate or even maximal mitigation strategies appear to be required to reduce the median number of heat load days but even under these interventions the median number of heat load days may still exceed zero for some locations.

4.3.1.1 Caroona, RCP2.6

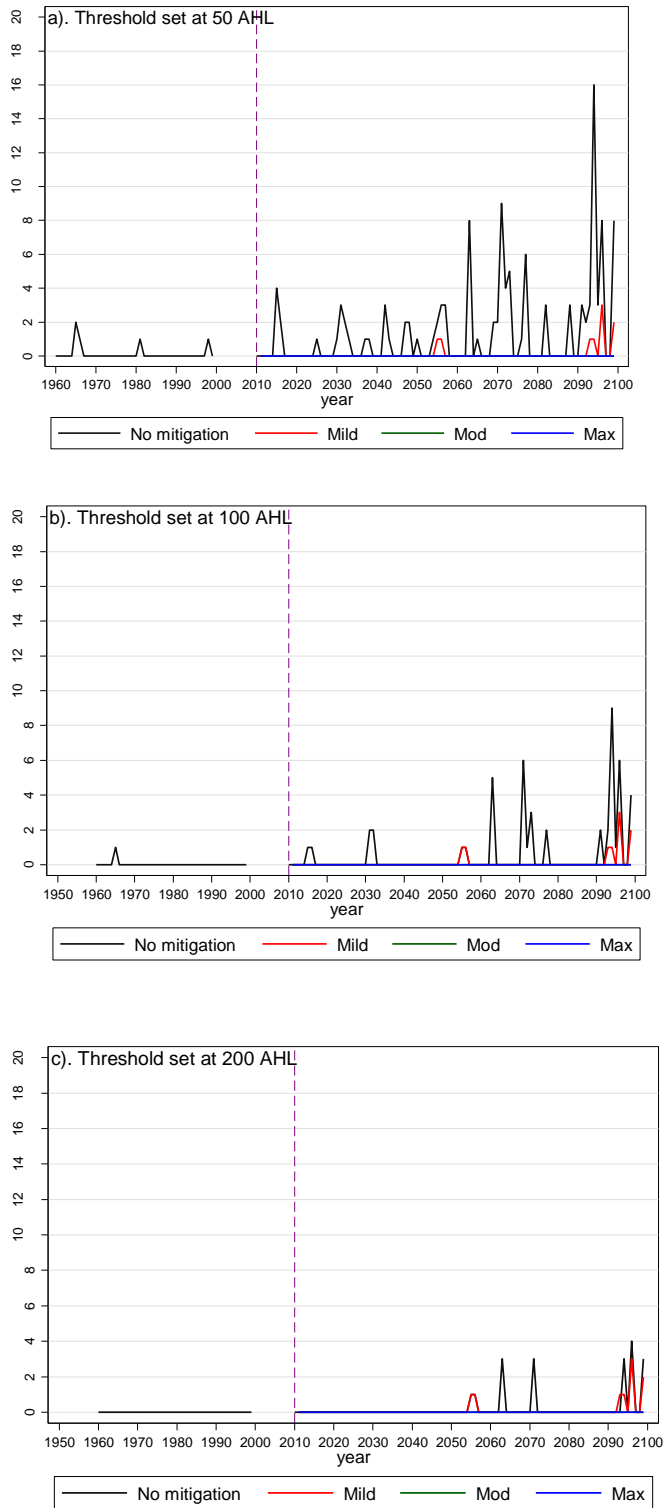


Figure 4.22: Number of days per year when AHL > threshold, showing historic (1960-99) and future runs (2010-2099), under each of four mitigation strategies. Location= Caroona, scenario=RCP2.6. Y-scale maximum=20.

4.3.1.2 Caroona, RCP4.5

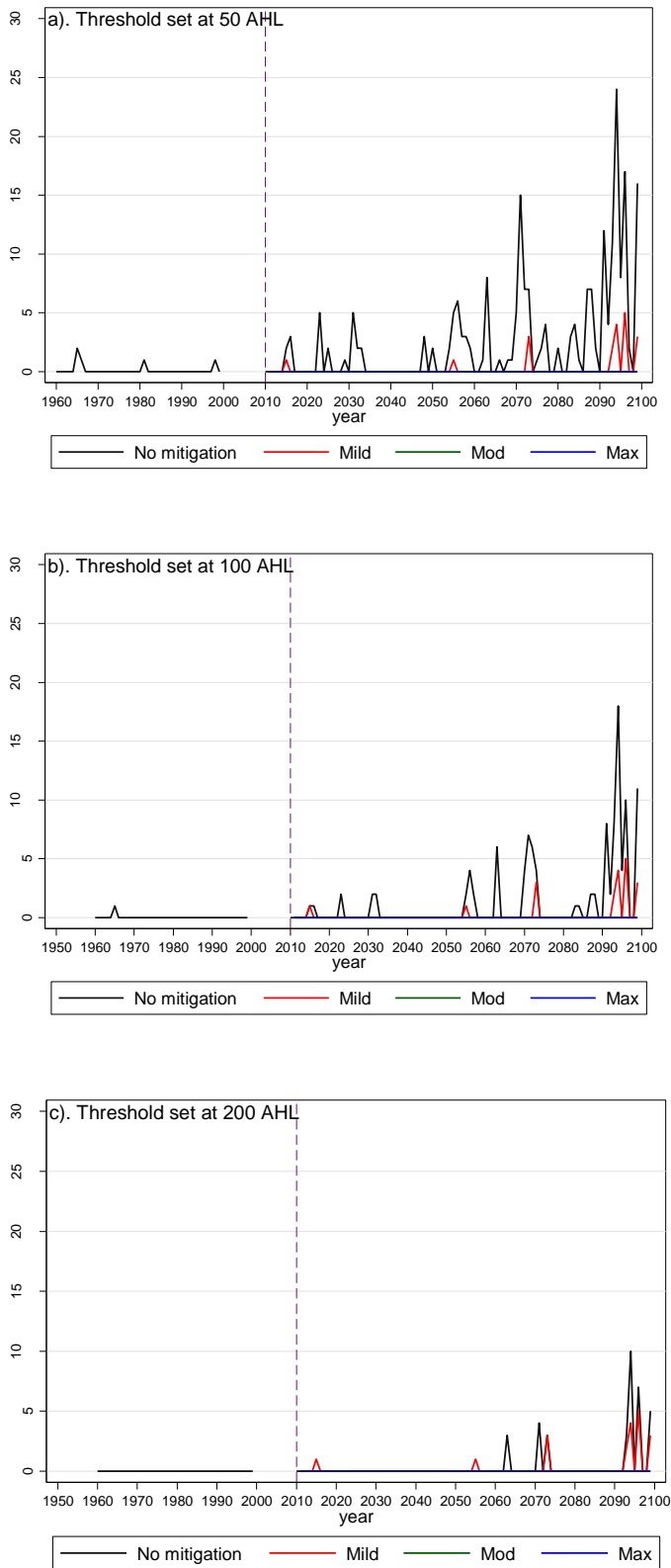


Figure 4.23: Number of days per year when AHL > threshold, showing historic (1960-99) and future runs (2010-2099), under each of four mitigation strategies. Location= Caroona, scenario=RCP4.5. Y-scale maximum=30.

4.3.1.3 Caroona, RCP8.5

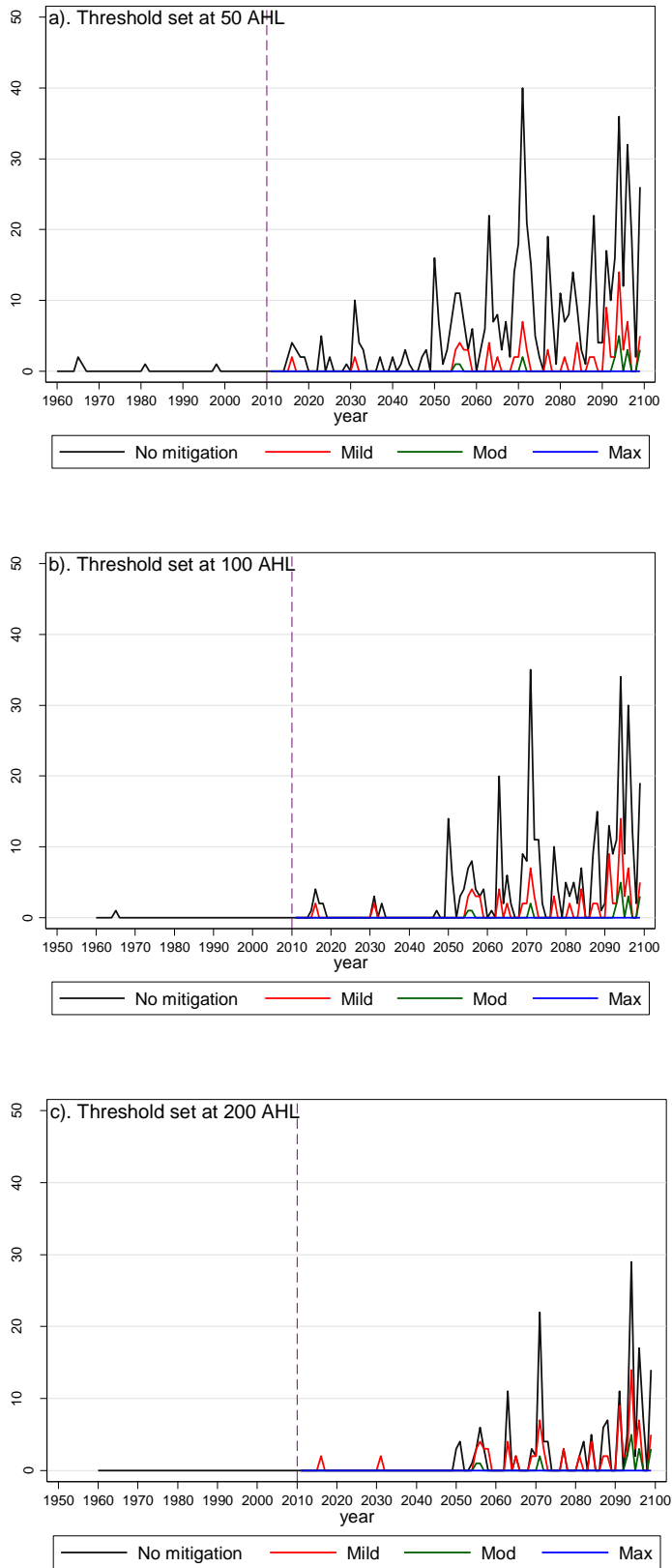


Figure 4.24: Number of days per year when AHL > threshold, showing historic (1960-99) and future runs (2010-2099), under each of four mitigation strategies. Location= Caroona, scenario=RCP8.5. Y-scale maximum=50.

4.3.1.4 Comet, RCP2.6

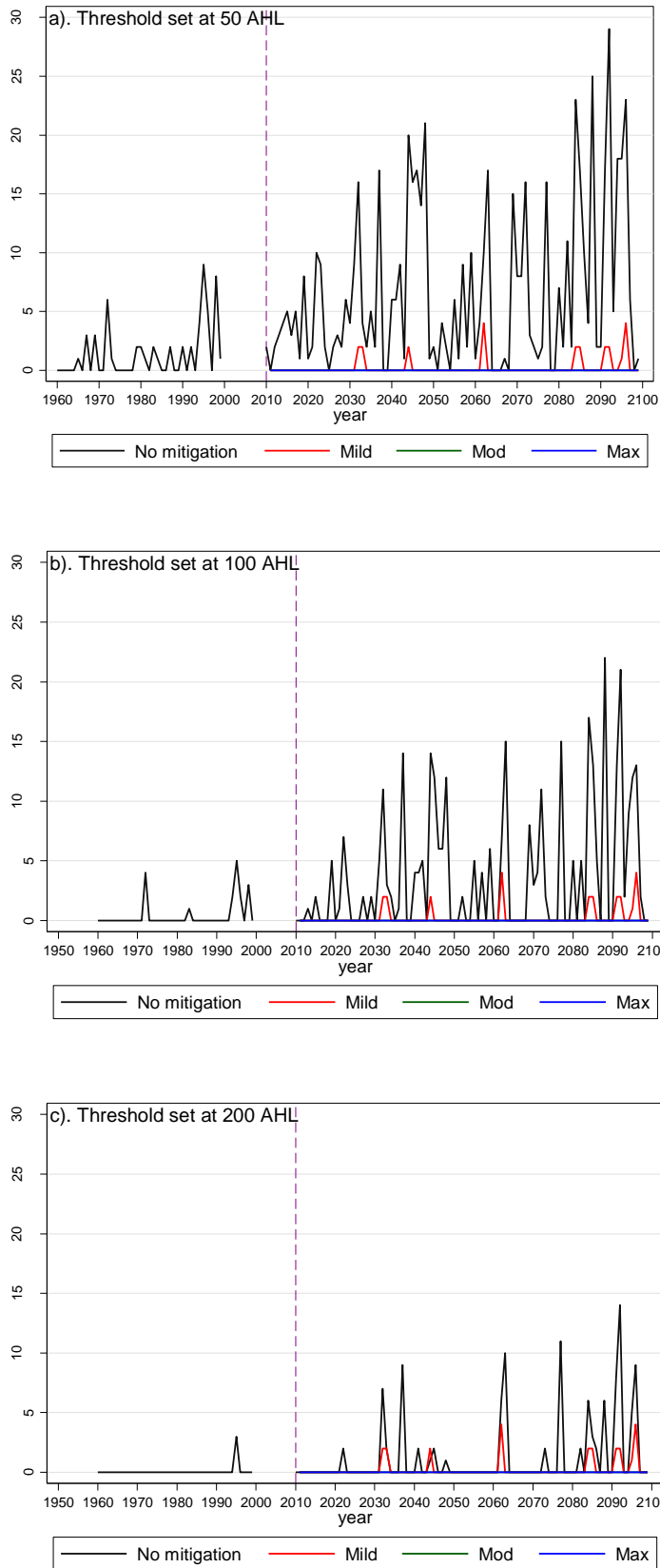


Figure 4.25: Number of days per year when AHL > threshold, showing historic (1960-99) and future runs (2010-2099), under each of four mitigation strategies. Location= Comet, scenario=RCP2.6. Y-scale maximum=30.

4.3.1.5 Comet, RCP4.5

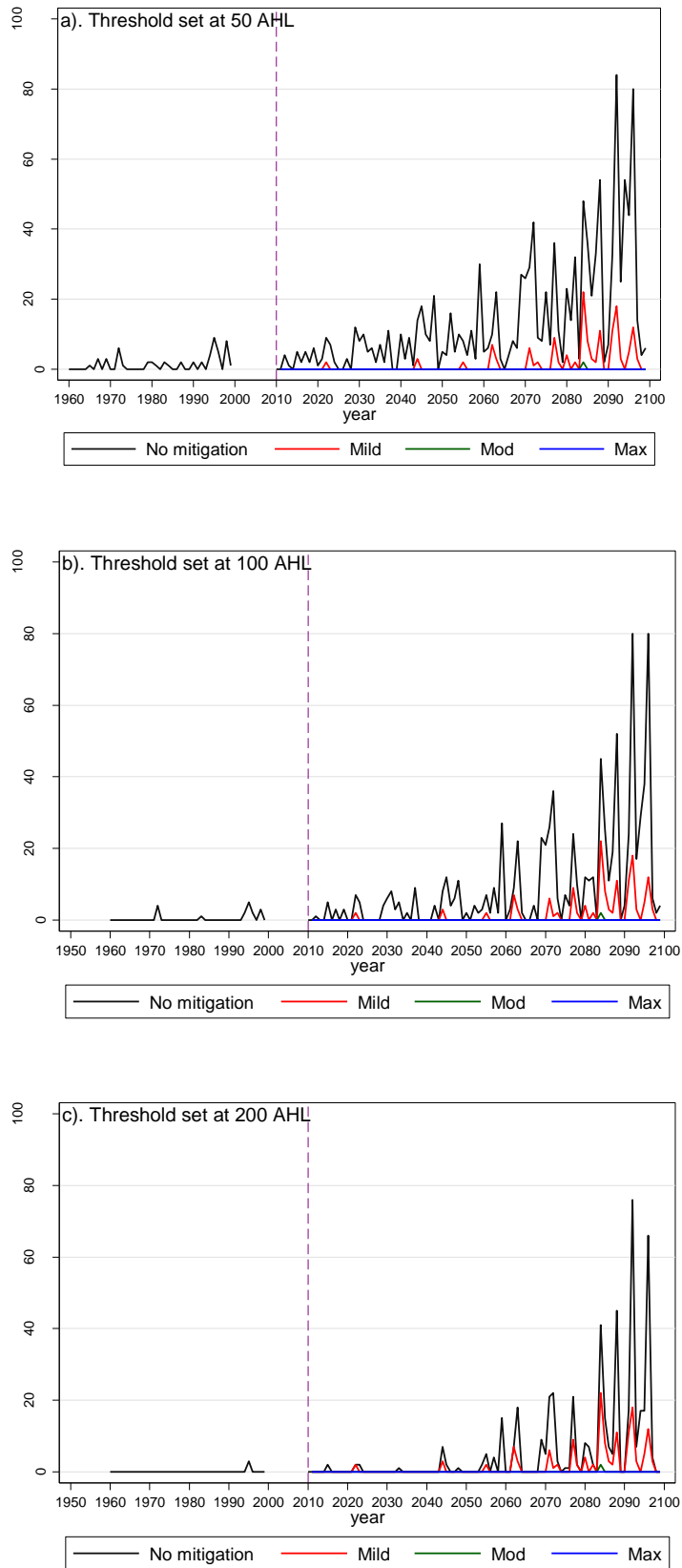


Figure 4.26: Number of days per year when AHL > threshold, showing historic (1960-99) and future runs (2010-2099), under each of four mitigation strategies. Location= Comet, scenario=RCP4.5. Y-scale maximum=100.

4.3.1.6 Comet, RCP8.5

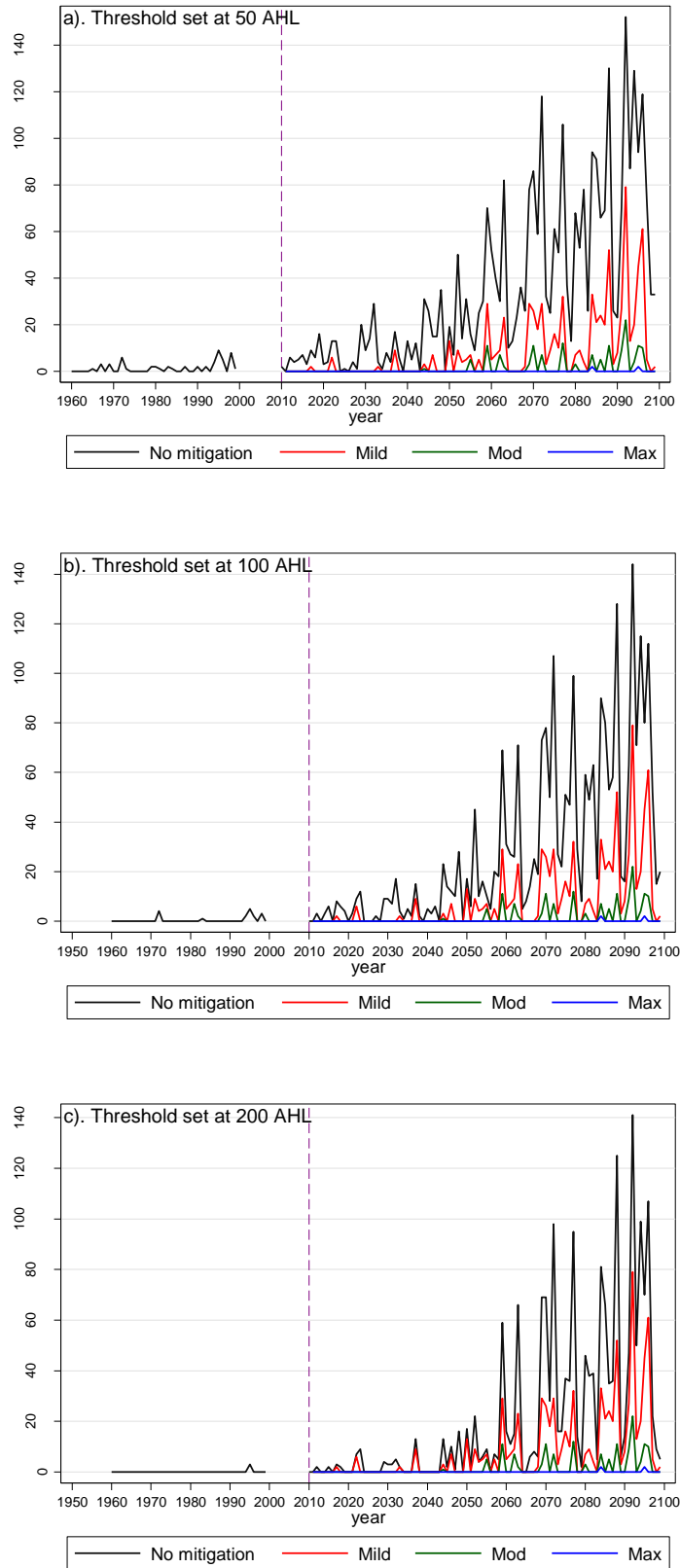


Figure 4.27: Number of days per year when AHL > threshold, showing historic (1960-99) and future runs (2010-2099), under each of four mitigation strategies. Location= Comet, scenario=RCP8.5. Y-scale maximum=140.

4.3.1.7 Dalby, RCP2.6

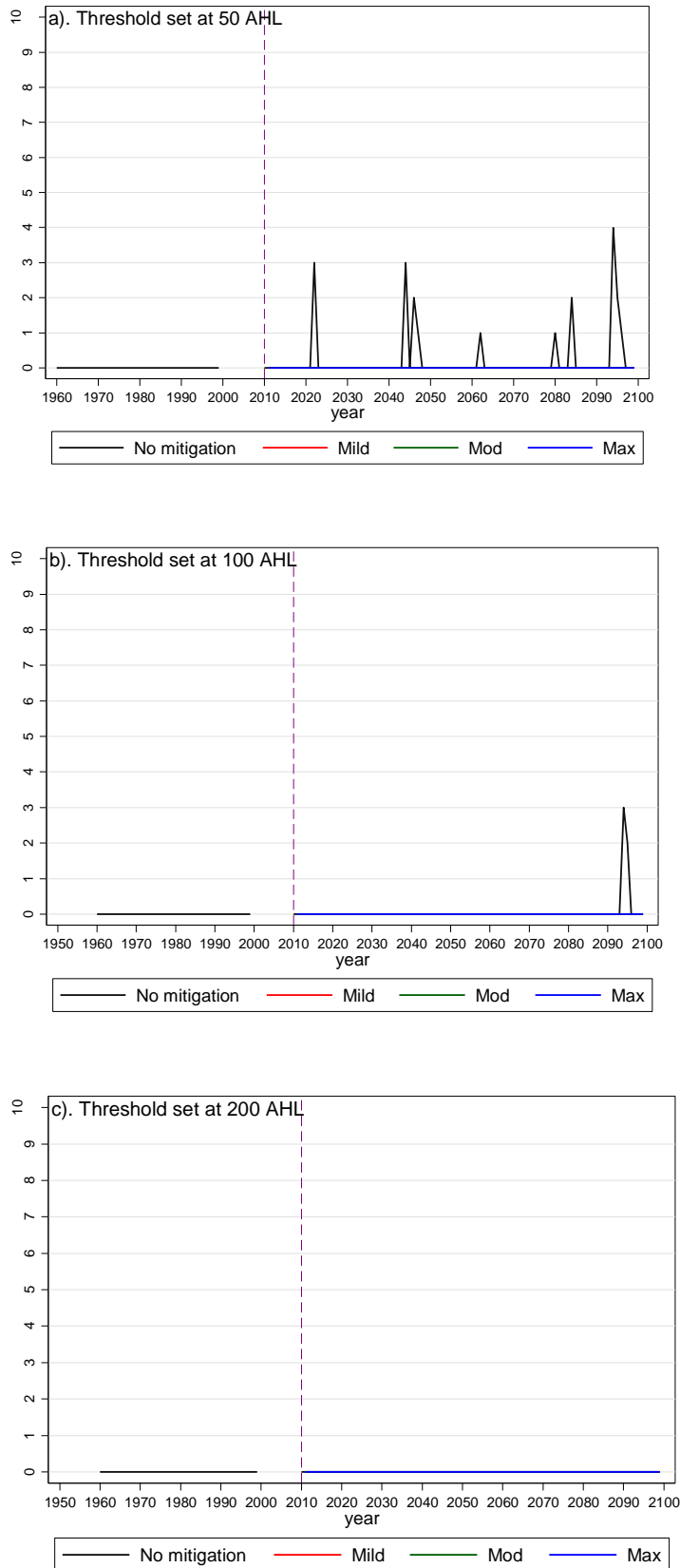


Figure 4.28: Number of days per year when AHL > threshold, showing historic (1960-99) and future runs (2010-2099), under each of four mitigation strategies. Location= Dalby, scenario=RCP2.6. Y-scale maximum=10.

4.3.1.8 Dalby, RCP4.5

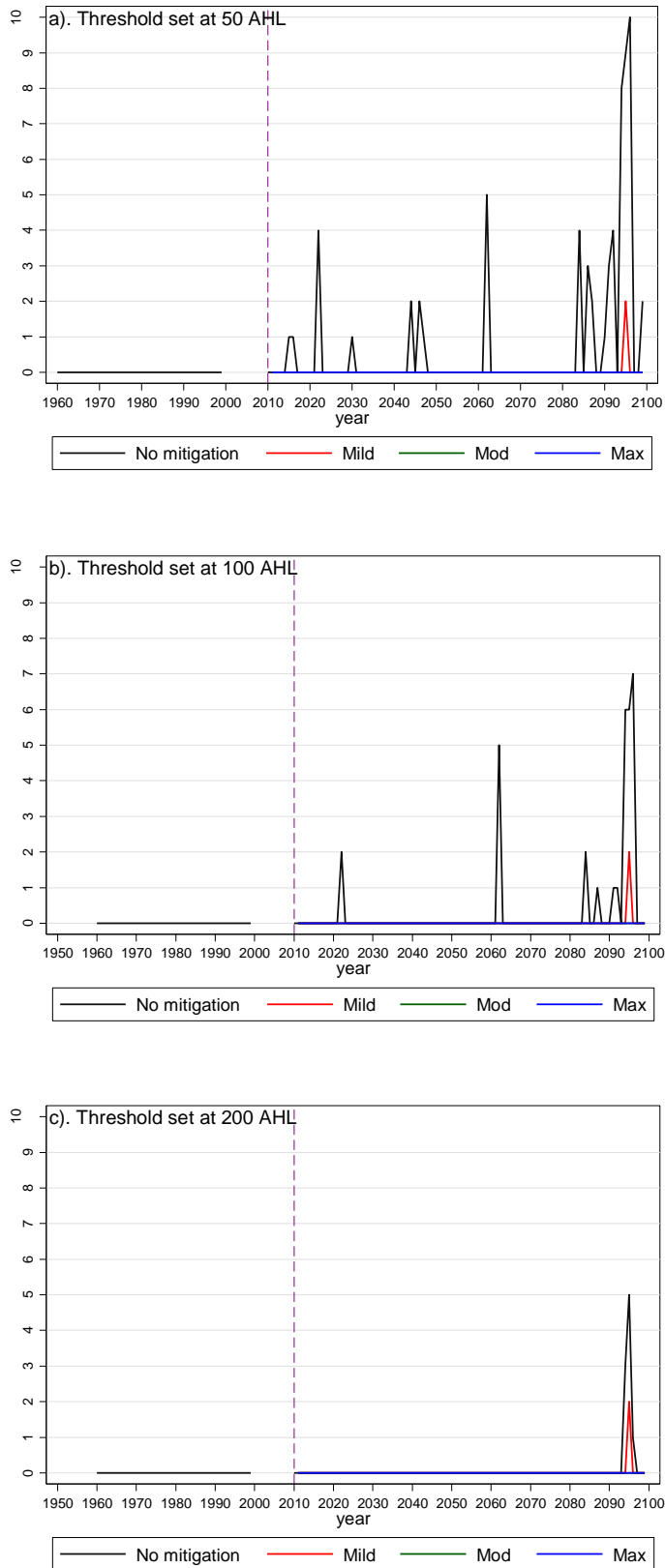


Figure 4.29: Number of days per year when AHL > threshold, showing historic (1960-99) and future runs (2010-2099), under each of four mitigation strategies. Location= Dalby, scenario=RCP4.5. Y-scale maximum=10.

4.3.1.9 Dalby, RCP8.5

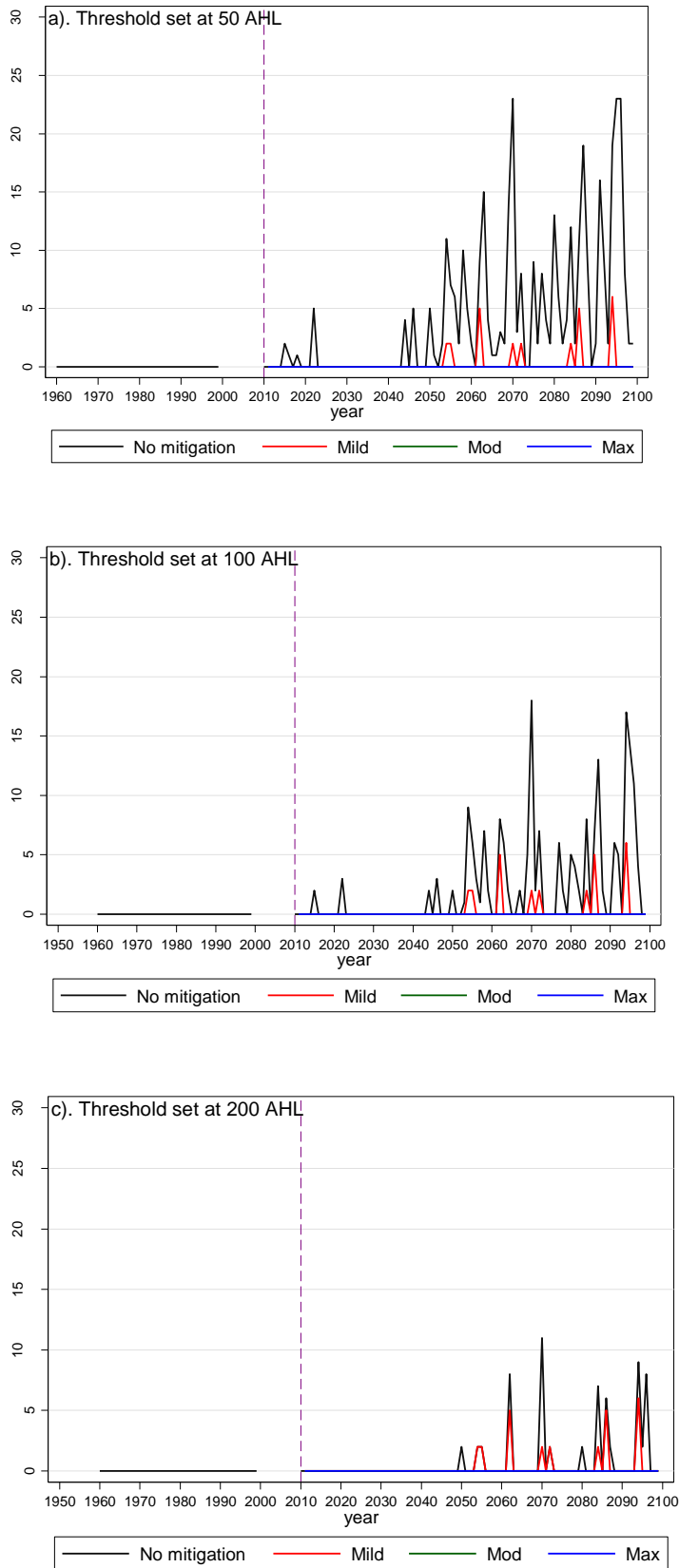


Figure 4.30: Number of days per year when AHL > threshold, showing historic (1960-99) and future runs (2010-2099), under each of four mitigation strategies. Location= Dalby, scenario=RCP8.5. Y-scale maximum=30.

4.3.1.10 Leeton, RCP2.6

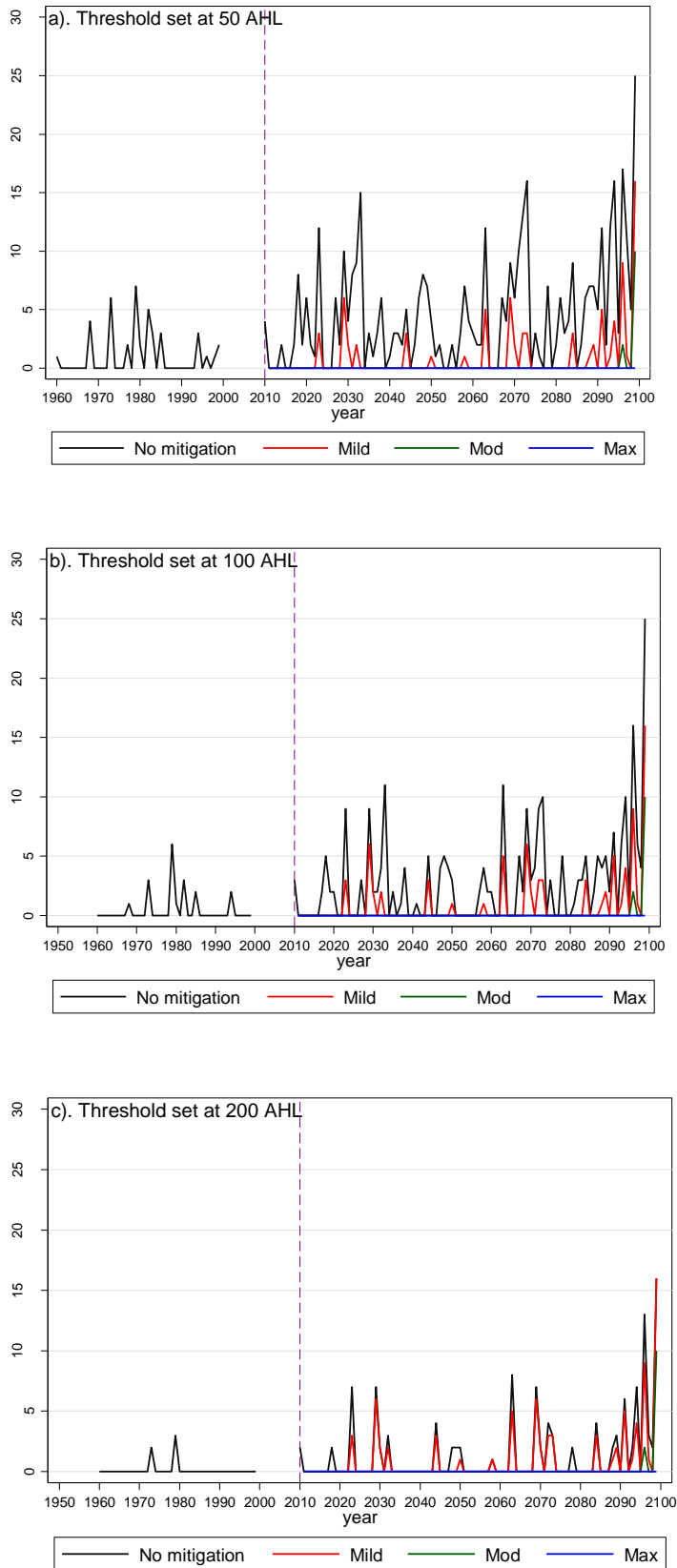


Figure 4.31: Number of days per year when AHL > threshold, showing historic (1960-99) and future runs (2010-2099), under each of four mitigation strategies. Location= Leeton, scenario=RCP2.6. Y-scale maximum=30.

4.3.1.11 Leeton, RCP4.5

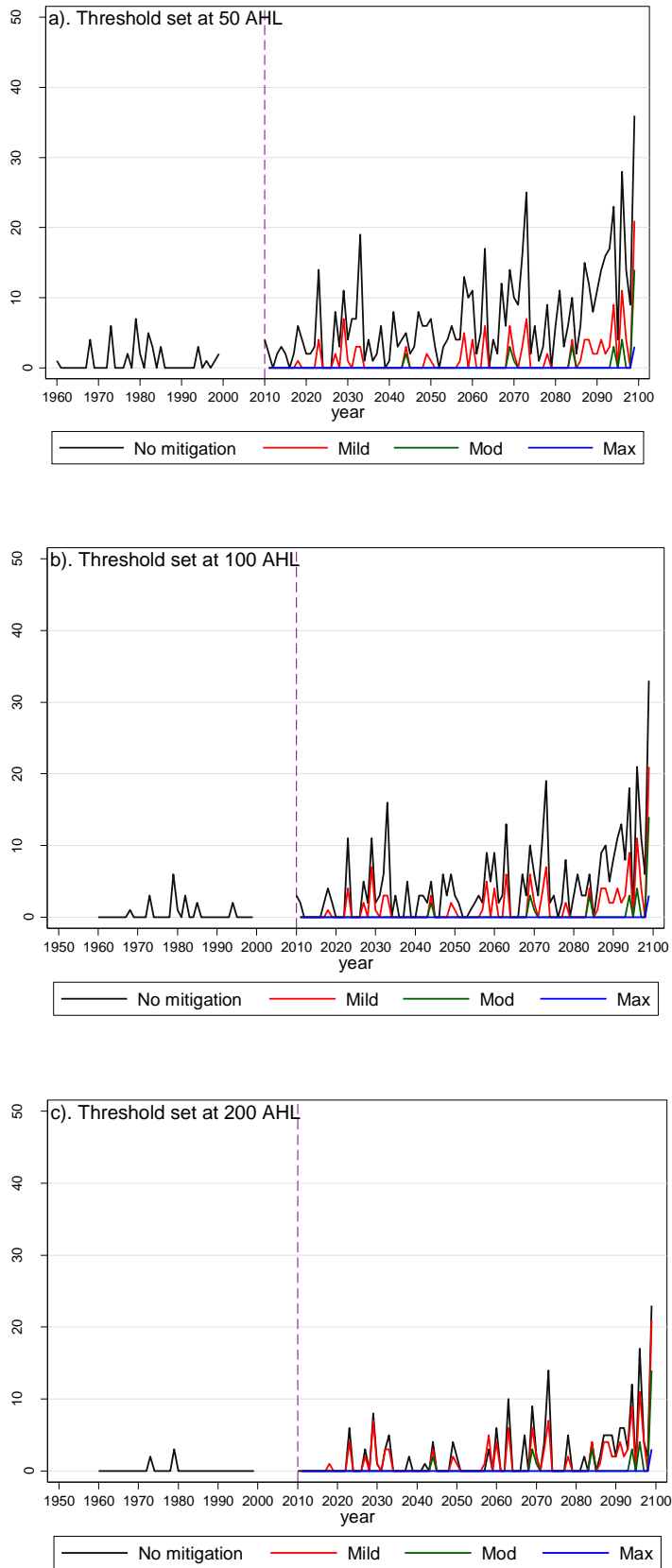


Figure 4.32: Number of days per year when AHL > threshold, showing historic (1960-99) and future runs (2010-2099), under each of four mitigation strategies. Location= Leeton, scenario=RCP4.5. Y-scale maximum=50.

4.3.1.12 Leeton, RCP8.5

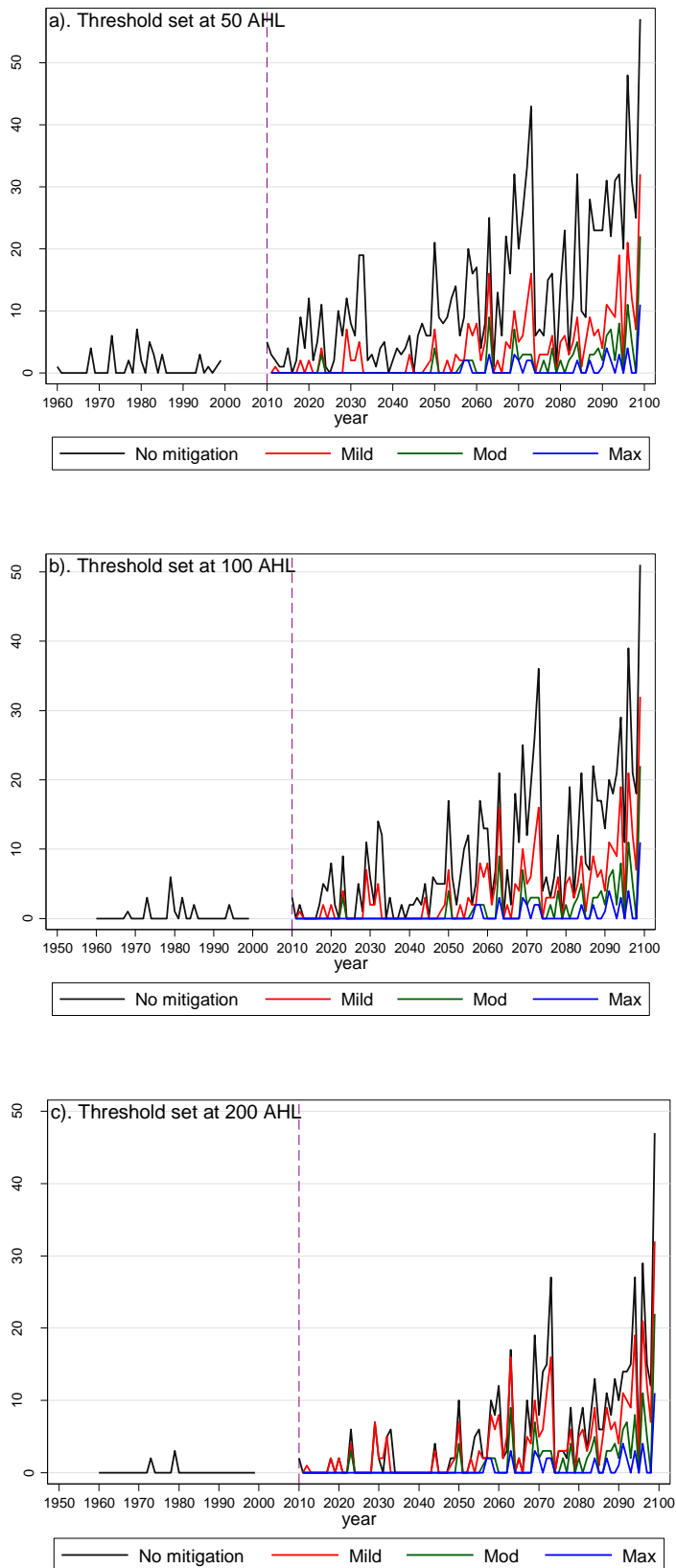


Figure 4.33: Number of days per year when AHL > threshold, showing historic (1960-99) and future runs (2010-2099), under each of four mitigation strategies. Location= Leeton, scenario=RCP8.5. Y-scale maximum=50.

4.3.1.13 Narrogin, RCP2.6

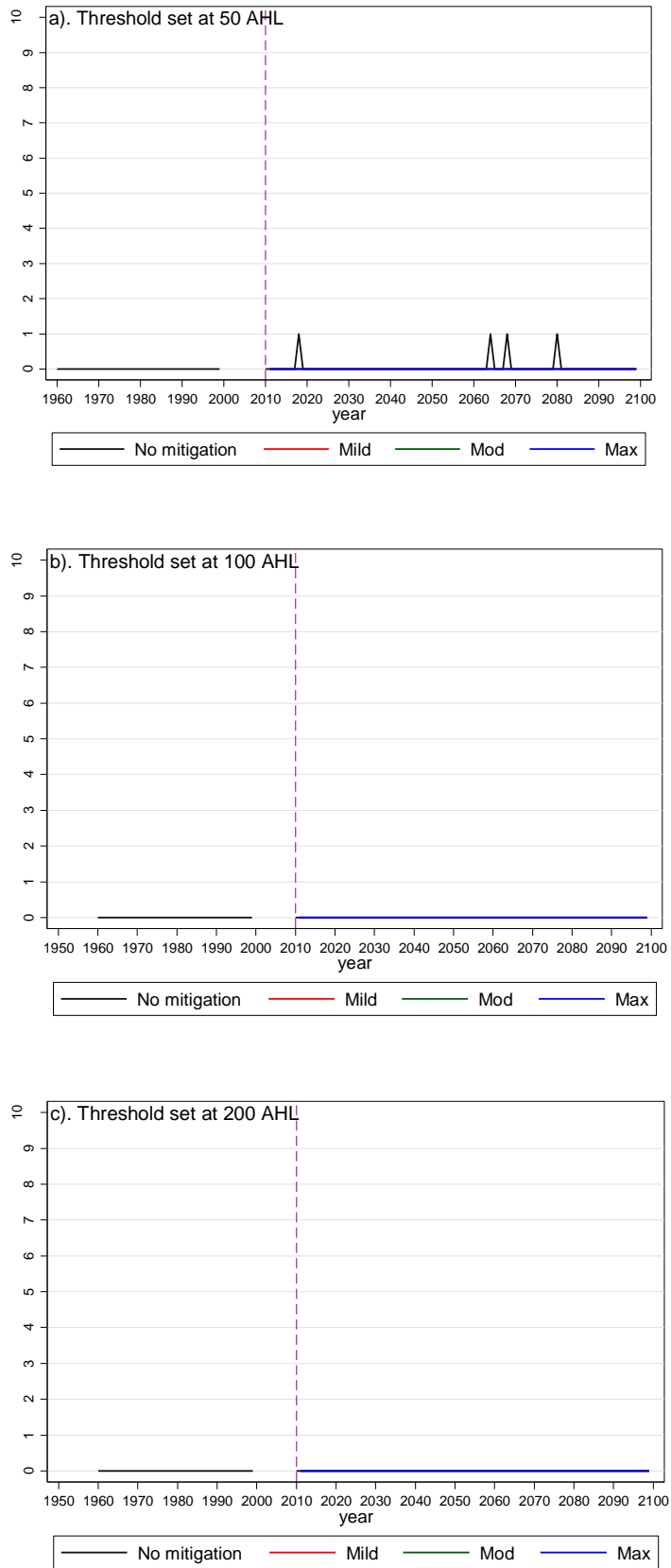


Figure 4.34: Number of days per year when AHL > threshold, showing historic (1960-99) and future runs (2010-2099), under each of four mitigation strategies. Location= Narrogin, scenario=RCP2.6. Y-scale maximum=10.

4.3.1.14 Narrogin, RCP4.5

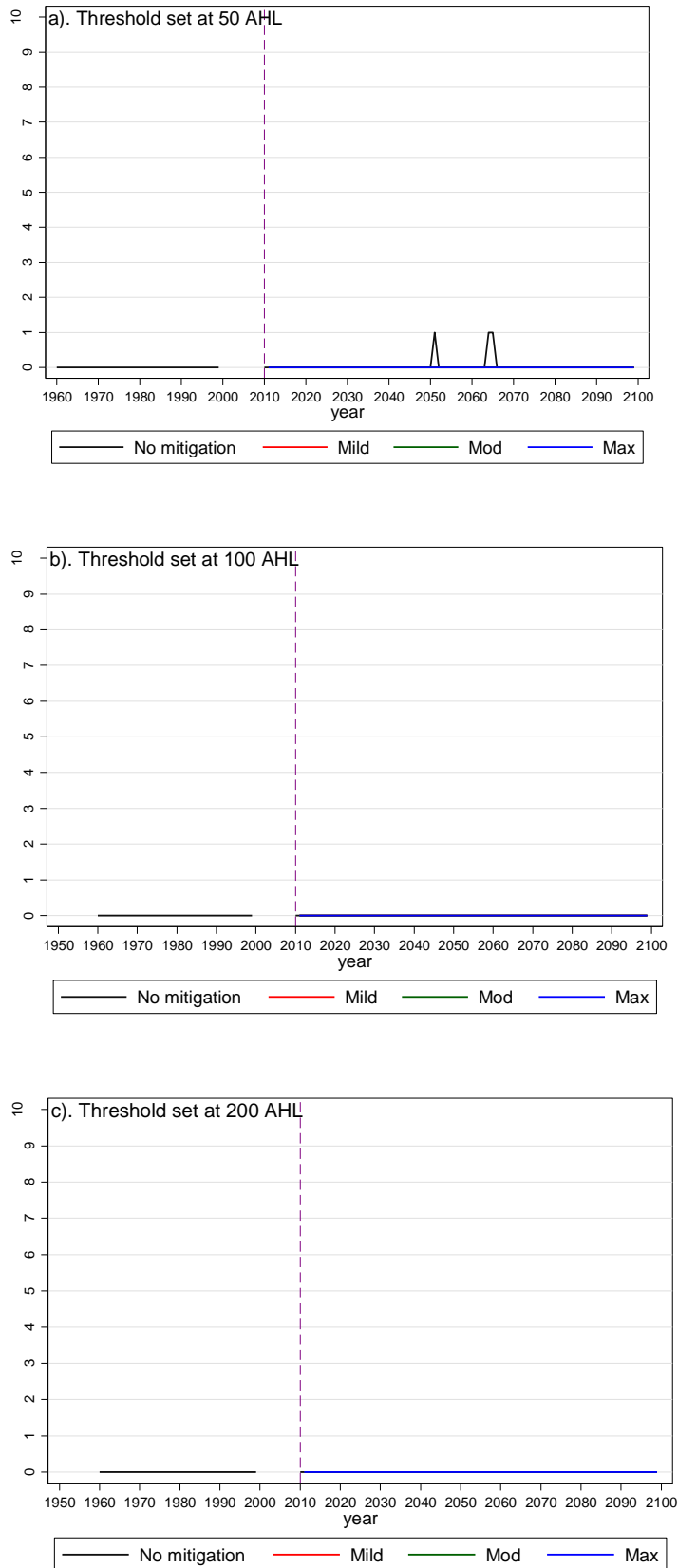


Figure 4.35: Number of days per year when AHL > threshold, showing historic (1960-99) and future runs (2010-2099), under each of four mitigation strategies. Location= Narrogin, scenario=RCP4.5. Y-scale maximum=10.

4.3.1.15 Narrogin, RCP8.5

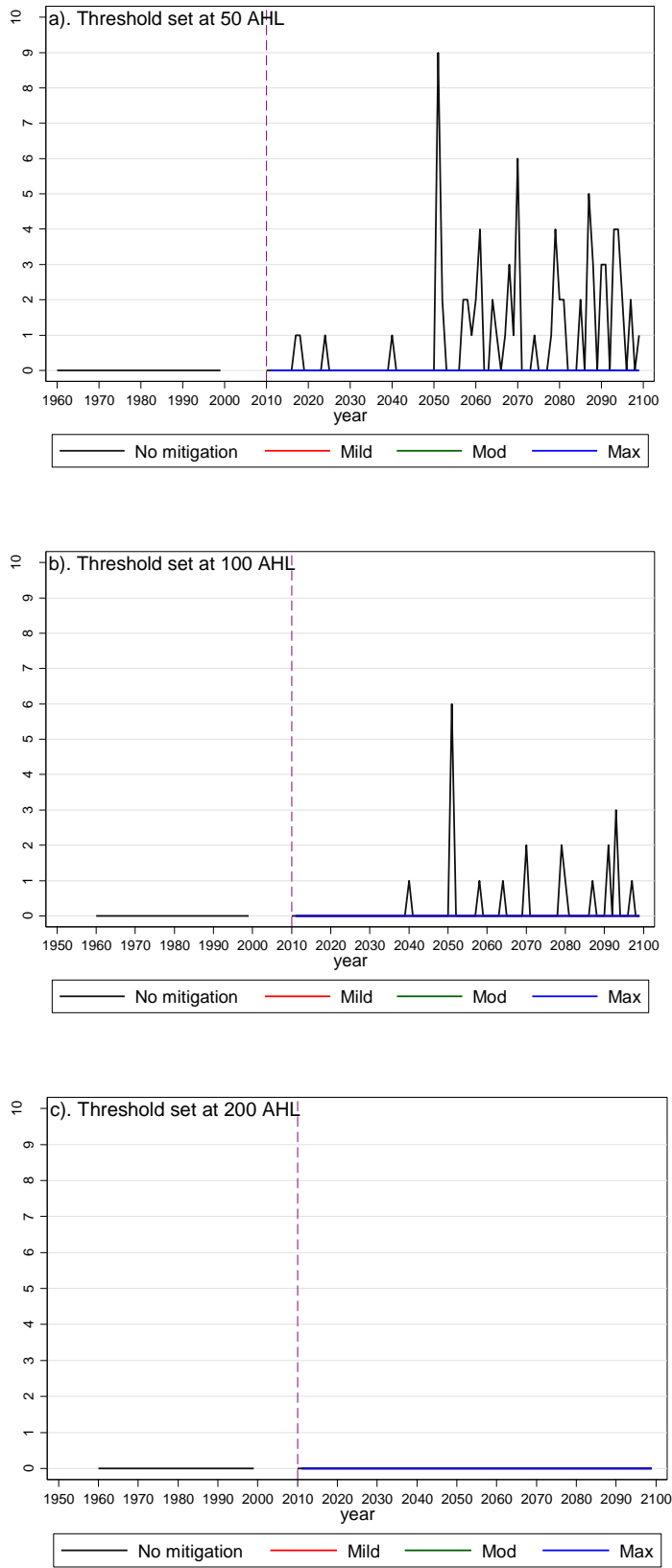


Figure 4.36: Number of days per year when AHL > threshold, showing historic (1960-99) and future runs (2010-2099), under each of four mitigation strategies. Location= Narrogin, scenario=RCP8.5. Y-scale maximum=10.

4.3.2 Tables of summary statistics for heat load days per year

Summary statistics were produced for the number of days per year when AHL was greater than 100 AHLU including minimum days, 25th percentile, median (50th percentile), 75th percentile and maximum number of days. Summaries were produced under four mitigation options (no mitigation, mild mitigation, moderate mitigation and maximal mitigation). These summaries provide an excellent overview of the effect of various climate change scenarios on heat load in different locations and the possible benefits of mitigation.

Summary statistics are produced for each combination of location, GCM and RCP scenario.

Within each location, GCM and RCP scenario, results are presented for the historic period (1960-1999) and for two future time periods (2010-2049 and 2050-2099). Future time periods are divided into two components because there was an increasing level of change over time for most runs (comparing 2050-2099 to 2010-2049).

In addition, separate tables of results are provided for each of the four mitigation strategies to provide summary statistics under no intervention and under progressively more intensive mitigation.

To limit space, results are provided only for AHL>100 and only for summary statistics based on the number of days per year when AHL>100.

Additional output for other AHL thresholds (50 AHLU and 200 AHLU) and for other output measures (number of events per year and median event duration) are provided in the Appendices.

A number of general points can be made from scanning the tables in the following pages.

The median estimates for heat load days over each time period that are presented in the tables in the following pages are not directly comparable to the median line plots displayed in the previous section.

The plots involved generation of a median number of heat load days across the five GCMs for each year within each combination of location and RCP. The tables provide a median number of heat load days that is produced from all years of data within one GCM and RCP and at each location.

The tables provide slightly different information to the plots and in particular provide a more detailed representation of the variation between GCMs and of the range of possible outcomes within one GCM row.

The range of possible outcomes within one GCM row is of particular interest since it indicates that even when the median number of heat load days in a time period may be zero or a relatively low number, the 75th percentile and maximal values for the same row may be very high. These situations reflect increased year to year variability in the future and represent risk of intermittent high heat load events occurring against a background of relatively low general risk.

There is general agreement with the patterns displayed in the plots in the previous section.

At every location the general pattern is for the number of heat load days to rise over time and most noticeably in the period after 2050.

At every location, the general pattern is for the rise in heat load days to be progressively larger as the RCP scenarios move from mild (RCP2.6) to moderate (RCP4.5) to high (RCP8.5).

There is considerable variation between locations with two locations (Dalby and Narrogin) showing noticeably less increase in heat load days than the other three locations. Comet shows the largest rise in heat load days over time.

Finally, mitigation strategies progressively reduce the number of heat load days in all locations and under all RCP scenarios. In some cases mild or moderate mitigation strategies are sufficient to reduce the median number of heat load days to zero. In other cases (Comet and Leeton), moderate or even maximal mitigation strategies appear to be required to reduce the median number of heat load days but even under these interventions the median number of heat load days may still exceed zero for some locations.

Table 4.43: Summary of number of days per 10 years when AHL >100 for each location and RCP, averaged across all five models, and reported for the historic time period and for two future time periods with no mitigation and with mild, moderate and maximal mitigation strategies implemented. RCP8.5, no CNRM-CM5 refers to an average across four models with all data from one model (CNRM-CM5) removed.

Location	1960-99					2050-2099				
	Mitigation strategies					Mitigation strategies				
	None	Mild	Mod	Max		None	Mild	Mod	Max	
Number of days per 10 years when AHL>100, across all models										
Caroona										
RCP2.6	0.8	6.7	0.7	0.2	0.2	28.8	7.3	1	0.3	
RCP4.5	0.8	7.1	1.1	0.4	0.2	54.8	13.7	2.6	0.4	
RCP8.5	0.8	101.7	37.8	14.5	3.2	682.6	354.5	195.6	89.3	
RCP8.5, no CNRM-CM5		4.7	1.1	0.1	0.1	71.9	19.7	5.2	0.5	
Comet										
RCP2.6	15.2	82.8	13.4	3	0	129.2	24.8	5.6	0.1	
RCP4.5	15.2	64.5	11.6	2.3	0	339.6	82.9	15.9	1.4	
RCP8.5	15.2	596.6	247.6	94.9	23.1	2166.9	1212.4	764.3	370.1	
RCP8.5, no CNRM-CM5		45.4	9.3	2.1	0.1	470.5	146.8	51.2	5.3	
Dalby										
RCP2.6	0.6	2	0	0	0	8.4	1.8	0.2	0	
RCP4.5	0.6	2.1	0.4	0	0	60.2	15.1	3.2	0.2	
RCP8.5	0.6	1.4	34	9.3	1.9	684.3	338.1	174.3	66.4	
RCP8.5, no CNRM-CM5		2.9	0.4	0	0	41.4	10	3.5	0.4	
Leeton										
RCP2.6	13.2	46.7	14.1	2.3	0.1	96.7	35.2	8.6	1.2	
RCP4.5	13.2	64.6	18.6	3.5	0.8	175.3	71.1	20.8	5.6	
RCP8.5	13.2	183	84.5	42.7	17.6	826.5	468.6	269.8	135.2	
RCP8.5, no CNRM-CM5		29.7	9	1.9	0.1	182.7	85.4	37.3	12.2	
Narrogin										
RCP2.6	0.2	0.8	0.2	0	0	1.4	0.2	0	0	
RCP4.5	0.2	1	0.2	0	0	2.4	0.4	0.1	0	
RCP8.5	0.2	19	6.6	1.8	0	100.3	44.3	18.1	7	
RCP8.5, no CNRM-CM5		0.6	0.1	0	0	4.2	0.7	0.2	0.1	

Table 4.43 provides a single summary table showing a single measure of heat load represented by the number of days per 10 year period when AHL > 100 units. This measure is directly comparable across the different time periods (1960-1999, 2010-2049 and 2050-2099). It is produced by averaging the results for all five models within each location and RCP combination. The measure is provided under four heat load mitigation strategies as defined in the methodology (Section 3.5), including no mitigation, mild mitigation, moderate mitigation and maximal mitigation.

The following tables provide detailed results for each location and RCP and model.

4.3.2.1 Carroona, RCP2.6

Table 4.44: Summary statistics for count of the number of days per year when AHL>100. Location=Carroona, RCP2.6, time periods= 1960-1999, 2010-2049, 2050-2099. No mitigation implemented.

mit=none Model	AHL threshold	Count of years (n)	Summary of per-annum counts of days when AHL > threshold					
			min	p25	median	p75	max	all yrs
1960-1999								
CNRM-CM5	100	40	0	0	0	0	1	2
GFDL-ESM2G	100	40	0	0	0	0	0	0
HadGEM2-ES	100	40	0	0	0	0	3	4
MIROC5	100	40	0	0	0	0	0	0
MRI-CGCM3	100	40	0	0	0	0	1	2
Days per 10 yrs, all models								0.8
2010-2049								
CNRM-CM5	100	40	0	0	0	1	6	31
GFDL-ESM2G	100	40	0	0	0	0	6	14
HadGEM2-ES	100	40	0	0	0	0	3	10
MIROC5	100	40	0	0	0	0	2	6
MRI-CGCM3	100	40	0	0	0	0	3	6
Days per 10 yrs, all models								6.7
2050-2099								
CNRM-CM5	100	50	0	0	0	4	11	108
GFDL-ESM2G	100	50	0	0	0	0	4	22
HadGEM2-ES	100	50	0	0	0	1	10	65
MIROC5	100	50	0	0	0	0	8	31
MRI-CGCM3	100	50	0	0	0	2	10	62
Days per 10 yrs, all models								28.8

Table 4.45: Summary statistics for count of the number of days per year when AHL>100.
Location=Caroona, RCP2.6, time periods= 2010-2049, 2050-2099. Mild mitigation implemented.

mit=mild Model	AHL threshold	Count of years (n)	Summary of per-annum counts of days when AHL > threshold					
			min	p25	median	p75	max	all yrs
2010-2049								
CNRM-CM5	100	40	0	0	0	0	2	4
GFDL-ESM2G	100	40	0	0	0	0	0	0
HadGEM2-ES	100	40	0	0	0	0	1	2
MIROC5	100	40	0	0	0	0	0	0
MRI-CGCM3	100	40	0	0	0	0	1	1
Days per 10 yrs, all models								0.7
2050-2099								
CNRM-CM5	100	50	0	0	0	0	7	32
GFDL-ESM2G	100	50	0	0	0	0	2	7
HadGEM2-ES	100	50	0	0	0	0	4	17
MIROC5	100	50	0	0	0	0	4	8
MRI-CGCM3	100	50	0	0	0	0	4	9
Days per 10 yrs, all models								7.3

Table 4.46: Summary statistics for count of the number of days per year when AHL>100. Location=Caroona, RCP2.6, time periods= 2010-2049, 2050-2099. Moderate mitigation implemented.

mit=mod Model	AHL threshold	Count of years (n)	Summary of per-annum counts of days when AHL > threshold					
			min	p25	median	p75	max	all yrs
2010-2049								
CNRM-CM5	100	40	0	0	0	0	0	0
GFDL-ESM2G	100	40	0	0	0	0	0	0
HadGEM2-ES	100	40	0	0	0	0	1	2
MIROC5	100	40	0	0	0	0	0	0
MRI-CGCM3	100	40	0	0	0	0	0	0
Days per 10 yrs, all models								0.2
2050-2099								
CNRM-CM5	100	50	0	0	0	0	2	2
GFDL-ESM2G	100	50	0	0	0	0	1	2
HadGEM2-ES	100	50	0	0	0	0	2	4
MIROC5	100	50	0	0	0	0	0	0
MRI-CGCM3	100	50	0	0	0	0	2	2
Days per 10 yrs, all models								1

Table 4.47: Summary statistics for count of the number of days per year when AHL>100. Location=Caroona, RCP2.6, time periods= 2010-2049, 2050-2099. Maximal mitigation implemented.

mit=max Model	AHL threshold	Count of years (n)	Summary of per-annum counts of days when AHL > threshold					
			min	p25	median	p75	max	all yrs
2010-2049								
CNRM-CM5	100	40	0	0	0	0	0	0
GFDL-ESM2G	100	40	0	0	0	0	0	0
HadGEM2-ES	100	40	0	0	0	0	1	2
MIROC5	100	40	0	0	0	0	0	0
MRI-CGCM3	100	40	0	0	0	0	0	0
Days per 10 yrs, all models								0.2
2050-2099								
CNRM-CM5	100	50	0	0	0	0	0	0
GFDL-ESM2G	100	50	0	0	0	0	1	1
HadGEM2-ES	100	50	0	0	0	0	1	2
MIROC5	100	50	0	0	0	0	0	0
MRI-CGCM3	100	50	0	0	0	0	0	0
Days per 10 yrs, all models								0.3

4.3.2.2 Carooona, RCP4.5

Table 4.48: Summary statistics for count of the number of days per year when AHL>100. Location=Carooona, RCP4.5, time periods= 1960-1999, 2010-2049, 2050-2099. No mitigation implemented.

mit=none Model	AHL threshold	Count of years (n)	Summary of per-annum counts of days when AHL > threshold					
			min	p25	median	p75	max	all yrs
1960-1999								
CNRM-CM5	100	40	0	0	0	0	1	2
GFDL-ESM2G	100	40	0	0	0	0	0	0
HadGEM2-ES	100	40	0	0	0	0	3	4
MIROC5	100	40	0	0	0	0	0	0
MRI-CGCM3	100	40	0	0	0	0	1	2
Days per 10 yrs, all models								0.8
2010-2049								
CNRM-CM5	100	40	0	0	0	0.5	8	28
GFDL-ESM2G	100	40	0	0	0	0	4	10
HadGEM2-ES	100	40	0	0	0	1	7	27
MIROC5	100	40	0	0	0	0	1	2
MRI-CGCM3	100	40	0	0	0	0	2	4
Days per 10 yrs, all models								7.1
2050-2099								
CNRM-CM5	100	50	0	0	2.5	6	25	202
GFDL-ESM2G	100	50	0	0	0	3	18	125
HadGEM2-ES	100	50	0	0	1	4	21	138
MIROC5	100	50	0	0	0	0	6	26
MRI-CGCM3	100	50	0	0	0	0	14	57
Days per 10 yrs, all models								54.8

Table 4.49: Summary statistics for count of the number of days per year when AHL>100.
Location=Caroona, RCP4.5, time periods= 2010-2049, 2050-2099. Mild mitigation implemented.

mit=mild Model	AHL threshold	Count of years (n)	Summary of per-annum counts of days when AHL > threshold					
			min	p25	median	p75	max	all yrs
2010-2049								
CNRM-CM5	100	40	0	0	0	0	2	6
GFDL-ESM2G	100	40	0	0	0	0	0	0
HadGEM2-ES	100	40	0	0	0	0	2	4
MIROC5	100	40	0	0	0	0	1	1
MRI-CGCM3	100	40	0	0	0	0	0	0
Days per 10 yrs, all models								1.1
2050-2099								
CNRM-CM5	100	50	0	0	0	2	11	70
GFDL-ESM2G	100	50	0	0	0	0	9	22
HadGEM2-ES	100	50	0	0	0	0	9	28
MIROC5	100	50	0	0	0	0	2	3
MRI-CGCM3	100	50	0	0	0	0	4	14
Days per 10 yrs, all models								13.7

Table 4.50: Summary statistics for count of the number of days per year when AHL>100. Location=Caroona, RCP4.5, time periods= 2010-2049, 2050-2099. Moderate mitigation implemented.

mit=mod Model	AHL threshold	Count of years (n)	Summary of per-annum counts of days when AHL > threshold					
			min	p25	median	p75	max	all yrs
2010-2049								
CNRM-CM5	100	40	0	0	0	0	2	2
GFDL-ESM2G	100	40	0	0	0	0	0	0
HadGEM2-ES	100	40	0	0	0	0	1	2
MIROC5	100	40	0	0	0	0	0	0
MRI-CGCM3	100	40	0	0	0	0	0	0
Days per 10 yrs, all models								0.4
2050-2099								
CNRM-CM5	100	50	0	0	0	0	6	16
GFDL-ESM2G	100	50	0	0	0	0	0	0
HadGEM2-ES	100	50	0	0	0	0	3	10
MIROC5	100	50	0	0	0	0	0	0
MRI-CGCM3	100	50	0	0	0	0	0	0
Days per 10 yrs, all models								2.6

Table 4.51: Summary statistics for count of the number of days per year when AHL>100. Location=Caroona, RCP4.5, time periods= 2010-2049, 2050-2099. Maximal mitigation implemented.

mit=max Model	AHL threshold	Count of years (n)	Summary of per-annum counts of days when AHL > threshold					
			min	p25	median	p75	max	all yrs
2010-2049								
CNRM-CM5	100	40	0	0	0	0	0	0
GFDL-ESM2G	100	40	0	0	0	0	0	0
HadGEM2-ES	100	40	0	0	0	0	1	2
MIROC5	100	40	0	0	0	0	0	0
MRI-CGCM3	100	40	0	0	0	0	0	0
Days per 10 yrs, all models								0.2
2050-2099								
CNRM-CM5	100	50	0	0	0	0	0	0
GFDL-ESM2G	100	50	0	0	0	0	0	0
HadGEM2-ES	100	50	0	0	0	0	2	4
MIROC5	100	50	0	0	0	0	0	0
MRI-CGCM3	100	50	0	0	0	0	0	0
Days per 10 yrs, all models								0.4

4.3.2.3 Caroona, RCP8.5

Table 4.52: Summary statistics for count of the number of days per year when AHL>100. Location=Caroona, RCP8.5, time periods= 1960-1999, 2010-2049, 2050-2099. No mitigation implemented.

mit=none Model	AHL threshold	Count of years (n)	Summary of per-annum counts of days when AHL > threshold					
			min	p25	median	p75	max	all yrs
1960-1999								
CNRM-CM5	100	40	0	0	0	0	1	2
GFDL-ESM2G	100	40	0	0	0	0	0	0
HadGEM2-ES	100	40	0	0	0	0	3	4
MIROC5	100	40	0	0	0	0	0	0
MRI-CGCM3	100	40	0	0	0	0	1	2
Days per 10 yrs, all models								0.8
2010-2049								
CNRM-CM5	100	40	0	11	20.5	35	71	942
GFDL-ESM2G	100	40	0	0	0	0	7	15
HadGEM2-ES	100	40	0	0	0	1.5	9	44
MIROC5	100	40	0	0	0	0	2	6
MRI-CGCM3	100	40	0	0	0	0	2	10
Days per 10 yrs, all models								101.7
2050-2099								
CNRM-CM5	100	50	37	82	108	134	171	5388
GFDL-ESM2G	100	50	0	0	4	9	35	342
HadGEM2-ES	100	50	0	4	10.5	20	63	686
MIROC5	100	50	0	0	0	3	24	135
MRI-CGCM3	100	50	0	0	3.5	7	30	275
Days per 10 yrs, all models								682.6
Without CNRM-CM5								
2010-2049	Days per 10 yrs							4.7
2050-2099	Days per 10 yrs							71.9

Table 4.53: Summary statistics for count of the number of days per year when AHL>100. Location=Caroona, RCP8.5, time periods= 2010-2049, 2050-2099. Mild mitigation implemented.

mit=mild Model	AHL threshold	Count of years (n)	Summary of per-annum counts of days when AHL > threshold					
			min	p25	median	p75	max	all yrs
2010-2049								
CNRM-CM5	100	40	0	2	7	13.5	44	360
GFDL-ESM2G	100	40	0	0	0	0	5	7
HadGEM2-ES	100	40	0	0	0	0	4	9
MIROC5	100	40	0	0	0	0	2	2
MRI-CGCM3	100	40	0	0	0	0	0	0
Days per 10 yrs, all models								37.8
2050-2099								
CNRM-CM5	100	50	19	36	62	82	135	3151
GFDL-ESM2G	100	50	0	0	0	3	14	80
HadGEM2-ES	100	50	0	0	2	5	28	226
MIROC5	100	50	0	0	0	0	12	38
MRI-CGCM3	100	50	0	0	0	1	9	50
Days per 10 yrs, all models								354.5
Without CNRM-CM5								
2010-2049	Days per 10 yrs							1.1
2050-2099	Days per 10 yrs							19.7

Table 4.54: Summary statistics for count of the number of days per year when AHL>100. Location=Caroona, RCP8.5, time periods= 2010-2049, 2050-2099. Moderate mitigation implemented.

mit=mod Model	AHL threshold	Count of years (n)	Summary of per-annum counts of days when AHL > threshold					
			min	p25	median	p75	max	all yrs
2010-2049								
CNRM-CM5	100	40	0	0	2	5	24	143
GFDL-ESM2G	100	40	0	0	0	0	0	0
HadGEM2-ES	100	40	0	0	0	0	1	2
MIROC5	100	40	0	0	0	0	0	0
MRI-CGCM3	100	40	0	0	0	0	0	0
Days per 10 yrs, all models								14.5
2050-2099								
CNRM-CM5	100	50	3	17	35	50	103	1852
GFDL-ESM2G	100	50	0	0	0	0	5	14
HadGEM2-ES	100	50	0	0	0	2	14	82
MIROC5	100	50	0	0	0	0	2	4
MRI-CGCM3	100	50	0	0	0	0	3	4
Days per 10 yrs, all models								195.6
Without CNRM-CM5								
2010-2049	Days per 10 yrs							0.1
2050-2099	Days per 10 yrs							5.2

Table 4.55: Summary statistics for count of the number of days per year when AHL>100. Location=Caroona, RCP8.5, time periods= 2010-2049, 2050-2099. Maximal mitigation implemented.

mit=max Model	AHL threshold	Count of years (n)	Summary of per-annum counts of days when AHL > threshold					
			min	p25	median	p75	max	all yrs
2010-2049								
CNRM-CM5	100	40	0	0	0	1	5	30
GFDL-ESM2G	100	40	0	0	0	0	0	0
HadGEM2-ES	100	40	0	0	0	0	1	2
MIROC5	100	40	0	0	0	0	0	0
MRI-CGCM3	100	40	0	0	0	0	0	0
Days per 10 yrs, all models								3.2
2050-2099								
CNRM-CM5	100	50	0	7	15.5	25	57	883
GFDL-ESM2G	100	50	0	0	0	0	0	0
HadGEM2-ES	100	50	0	0	0	0	2	10
MIROC5	100	50	0	0	0	0	0	0
MRI-CGCM3	100	50	0	0	0	0	0	0
Days per 10 yrs, all models								89.3
Without CNRM-CM5								
2010-2049	Days per 10 yrs							0.1
2050-2099	Days per 10 yrs							0.5

4.3.2.4 Comet, RCP2.6

Table 4.56: Summary statistics for count of the number of days per year when AHL>100. Location=Comet, RCP2.6, time periods= 1960-1999, 2010-2049, 2050-2099. No mitigation implemented.

mit=none Model	AHL threshold	Count of years (n)	Summary of per-annum counts of days when AHL > threshold					
			min	p25	median	p75	max	all yrs
1960-1999								
CNRM-CM5	100	40	0	0	0	0	7	21
GFDL-ESM2G	100	40	0	0	0	0	4	18
HadGEM2-ES	100	40	0	0	0	1	6	34
MIROC5	100	40	0	0	0	0	5	11
MRI-CGCM3	100	40	0	0	0	1.5	12	68
Days per 10 yrs, all models								15.2
2010-2049								
CNRM-CM5	100	40	0	0	2	4.5	15	137
GFDL-ESM2G	100	40	0	0	4.5	14	38	348
HadGEM2-ES	100	40	0	2	5	8	25	246
MIROC5	100	40	0	0	0	1	25	83
MRI-CGCM3	100	40	0	0	0	0	6	14
Days per 10 yrs, all models								82.8
2050-2099								
CNRM-CM5	100	50	0	0	3	12	61	411
GFDL-ESM2G	100	50	0	0	0	4	22	168
HadGEM2-ES	100	50	0	3	6	13	34	432
MIROC5	100	50	0	0	0	8	23	195
MRI-CGCM3	100	50	0	0	0	2	17	86
Days per 10 yrs, all models								129.2

Table 4.57: Summary statistics for count of the number of days per year when AHL>100. Location= Comet, RCP2.6, time periods= 2010-2049, 2050-2099. Mild mitigation implemented.

mit=mild Model	AHL threshold	Count of years (n)	Summary of per-annum counts of days when AHL > threshold					
			min	p25	median	p75	max	all yrs
2010-2049								
CNRM-CM5	100	40	0	0	0	0	2	8
GFDL-ESM2G	100	40	0	0	0	2	13	55
HadGEM2-ES	100	40	0	0	1	2	10	65
MIROC5	100	40	0	0	0	0	6	6
MRI-CGCM3	100	40	0	0	0	0	0	0
Days per 10 yrs, all models								13.4
2050-2099								
CNRM-CM5	100	50	0	0	0	2	18	91
GFDL-ESM2G	100	50	0	0	0	0	5	18
HadGEM2-ES	100	50	0	0	1	2	12	106
MIROC5	100	50	0	0	0	0	6	27
MRI-CGCM3	100	50	0	0	0	0	4	6
Days per 10 yrs, all models								24.8

Table 4.58: Summary statistics for count of the number of days per year when AHL>100. Location= Comet, RCP2.6, time periods= 2010-2049, 2050-2099. Moderate mitigation implemented.

mit=mod Model	AHL threshold	Count of years (n)	Summary of per-annum counts of days when AHL > threshold					
			min	p25	median	p75	max	all yrs
2010-2049								
CNRM-CM5	100	40	0	0	0	0	0	0
GFDL-ESM2G	100	40	0	0	0	0	3	5
HadGEM2-ES	100	40	0	0	0	0	5	25
MIROC5	100	40	0	0	0	0	0	0
MRI-CGCM3	100	40	0	0	0	0	0	0
Days per 10 yrs, all models								3
2050-2099								
CNRM-CM5	100	50	0	0	0	0	5	5
GFDL-ESM2G	100	50	0	0	0	0	0	0
HadGEM2-ES	100	50	0	0	0	1	7	45
MIROC5	100	50	0	0	0	0	3	6
MRI-CGCM3	100	50	0	0	0	0	0	0
Days per 10 yrs, all models								5.6

Table 4.59: Summary statistics for count of the number of days per year when AHL>100. Location= Comet, RCP2.6, time periods= 2010-2049, 2050-2099. Maximal mitigation implemented.

mit=max Model	AHL threshold	Count of years (n)	Summary of per-annum counts of days when AHL > threshold					
			min	p25	median	p75	max	all yrs
2010-2049								
CNRM-CM5	100	40	0	0	0	0	0	0
GFDL-ESM2G	100	40	0	0	0	0	0	0
HadGEM2-ES	100	40	0	0	0	0	0	0
MIROC5	100	40	0	0	0	0	0	0
MRI-CGCM3	100	40	0	0	0	0	0	0
Days per 10 yrs, all models								0
2050-2099								
CNRM-CM5	100	50	0	0	0	0	0	0
GFDL-ESM2G	100	50	0	0	0	0	0	0
HadGEM2-ES	100	50	0	0	0	0	1	1
MIROC5	100	50	0	0	0	0	0	0
MRI-CGCM3	100	50	0	0	0	0	0	0
Days per 10 yrs, all models								0.1

4.3.2.5 Comet, RCP4.5

Table 4.60: Summary statistics for count of the number of days per year when AHL>100. Location= Comet, RCP4.5, time periods= 1960-1999, 2010-2049, 2050-2099. No mitigation implemented.

mit=none Model	AHL threshold	Count of years (n)	Summary of per-annum counts of days when AHL > threshold					
			min	p25	median	p75	max	all yrs
1960-1999								
CNRM-CM5	100	40	0	0	0	0	7	21
GFDL-ESM2G	100	40	0	0	0	0	4	18
HadGEM2-ES	100	40	0	0	0	1	6	34
MIROC5	100	40	0	0	0	0	5	11
MRI-CGCM3	100	40	0	0	0	1.5	12	68
Days per 10 yrs, all models								15.2
2010-2049								
CNRM-CM5	100	40	0	0	1	5.5	13	125
GFDL-ESM2G	100	40	0	0	2	7	28	182
HadGEM2-ES	100	40	0	2	5	10	25	272
MIROC5	100	40	0	0	0	0	10	38
MRI-CGCM3	100	40	0	0	0	0	6	28
Days per 10 yrs, all models								64.5
2050-2099								
CNRM-CM5	100	50	0	4	10	27	80	887
GFDL-ESM2G	100	50	0	3	11.5	29	87	903
HadGEM2-ES	100	50	1	6	15.5	35	84	1135
MIROC5	100	50	0	0	2	7	42	275
MRI-CGCM3	100	50	0	0	0	7	30	196
Days per 10 yrs, all models								339.6

Table 4.61: Summary statistics for count of the number of days per year when AHL>100. Location= Comet, RCP4.5, time periods= 2010-2049, 2050-2099. Mild mitigation implemented.

mit=mild Model	AHL threshold	Count of years (n)	Summary of per-annum counts of days when AHL > threshold					
			min	p25	median	p75	max	all yrs
2010-2049								
CNRM-CM5	100	40	0	0	0	0	3	11
GFDL-ESM2G	100	40	0	0	0	0	5	22
HadGEM2-ES	100	40	0	0	1	2	11	78
MIROC5	100	40	0	0	0	0	3	5
MRI-CGCM3	100	40	0	0	0	0	0	0
Days per 10 yrs, all models								11.6
2050-2099								
CNRM-CM5	100	50	0	0	0	4	22	160
GFDL-ESM2G	100	50	0	0	2	7	32	238
HadGEM2-ES	100	50	0	2	5	10	39	373
MIROC5	100	50	0	0	0	0	8	30
MRI-CGCM3	100	50	0	0	0	0	7	28
Days per 10 yrs, all models								82.9

Table 4.62: Summary statistics for count of the number of days per year when AHL>100. Location= Comet, RCP4.5, time periods= 2010-2049, 2050-2099. Moderate mitigation implemented.

mit=mod Model	AHL threshold	Count of years (n)	Summary of per-annum counts of days when AHL > threshold					
			min	p25	median	p75	max	all yrs
2010-2049								
CNRM-CM5	100	40	0	0	0	0	0	0
GFDL-ESM2G	100	40	0	0	0	0	2	4
HadGEM2-ES	100	40	0	0	0	0	6	19
MIROC5	100	40	0	0	0	0	0	0
MRI-CGCM3	100	40	0	0	0	0	0	0
Days per 10 yrs, all models								2.3
2050-2099								
CNRM-CM5	100	50	0	0	0	0	10	26
GFDL-ESM2G	100	50	0	0	0	0	13	21
HadGEM2-ES	100	50	0	0	1	3	15	108
MIROC5	100	50	0	0	0	0	2	2
MRI-CGCM3	100	50	0	0	0	0	2	2
Days per 10 yrs, all models								15.9

Table 4.63: Summary statistics for count of the number of days per year when AHL>100. Location= Comet, RCP4.5, time periods= 2010-2049, 2050-2099. Maximal mitigation implemented.

mit=max Model	AHL threshold	Count of years (n)	Summary of per-annum counts of days when AHL > threshold					
			min	p25	median	p75	max	all yrs
2010-2049								
CNRM-CM5	100	40	0	0	0	0	0	0
GFDL-ESM2G	100	40	0	0	0	0	0	0
HadGEM2-ES	100	40	0	0	0	0	0	0
MIROC5	100	40	0	0	0	0	0	0
MRI-CGCM3	100	40	0	0	0	0	0	0
Days per 10 yrs, all models								0
2050-2099								
CNRM-CM5	100	50	0	0	0	0	0	0
GFDL-ESM2G	100	50	0	0	0	0	0	0
HadGEM2-ES	100	50	0	0	0	0	3	14
MIROC5	100	50	0	0	0	0	0	0
MRI-CGCM3	100	50	0	0	0	0	0	0
Days per 10 yrs, all models								1.4

4.3.2.6 Comet, RCP8.5

Table 4.64: Summary statistics for count of the number of days per year when AHL>100. Location= Comet, RCP8.5, time periods= 1960-1999, 2010-2049, 2050-2099. No mitigation implemented.

mit=none Model	AHL threshold	Count of years (n)	Summary of per-annum counts of days when AHL > threshold					
			min	p25	median	p75	max	all yrs
1960-1999								
CNRM-CM5	100	40	0	0	0	0	7	21
GFDL-ESM2G	100	40	0	0	0	0	4	18
HadGEM2-ES	100	40	0	0	0	1	6	34
MIROC5	100	40	0	0	0	0	5	11
MRI-CGCM3	100	40	0	0	0	1.5	12	68
Days per 10 yrs, all models								15.2
2010-2049								
CNRM-CM5	100	40	59	100.5	133	161.5	185	5240
GFDL-ESM2G	100	40	0	0	5	8.5	31	268
HadGEM2-ES	100	40	0	2.5	5	10.5	28	312
MIROC5	100	40	0	0	0	5	19	120
MRI-CGCM3	100	40	0	0	0	0	7	26
Days per 10 yrs, all models								596.6
2050-2099								
CNRM-CM5	100	50	192	225	243	265	307	12259
GFDL-ESM2G	100	50	4	17	38	71	144	2332
HadGEM2-ES	100	50	23	60	93.5	118	192	4687
MIROC5	100	50	0	4	11	34	103	1103
MRI-CGCM3	100	50	0	8	15.5	39	103	1288
Days per 10 yrs, all models								2166.9
Without CNRM-CM5								
2010-2049	Days per 10 yrs							45.4
2050-2099	Days per 10 yrs							470.5

Table 4.65: Summary statistics for count of the number of days per year when AHL>100. Location= Comet, RCP8.5, time periods= 2010-2049, 2050-2099. Mild mitigation implemented.

mit=mild Model	AHL threshold	Count of years (n)	Summary of per-annum counts of days when AHL > threshold					
			min	p25	median	p75	max	all yrs
2010-2049								
CNRM-CM5	100	40	14	34	48.5	83	120	2328
GFDL-ESM2G	100	40	0	0	0	0	10	39
HadGEM2-ES	100	40	0	0	1	2.5	11	85
MIROC5	100	40	0	0	0	0	9	24
MRI-CGCM3	100	40	0	0	0	0	0	0
Days per 10 yrs, all models								247.6
2050-2099								
CNRM-CM5	100	50	90	166	186.5	205	247	9189
GFDL-ESM2G	100	50	0	0	7.5	23	79	696
HadGEM2-ES	100	50	4	13	29	44	113	1660
MIROC5	100	50	0	0	2	7	39	260
MRI-CGCM3	100	50	0	0	0	12	55	319
Days per 10 yrs, all models								1212.4
Without CNRM-CM5								
2010-2049	Days per 10 yrs							9.3
2050-2099	Days per 10 yrs							146.8

Table 4.66: Summary statistics for count of the number of days per year when AHL>100. Location= Comet, RCP8.5, time periods= 2010-2049, 2050-2099. Moderate mitigation implemented.

mit=mod	AHL threshold	Count of years (n)	Summary of per-annum counts of days when AHL > threshold					
			min	p25	median	p75	max	all yrs
2010-2049								
CNRM-CM5	100	40	0	10.5	15.5	37	61	915
GFDL-ESM2G	100	40	0	0	0	0	0	0
HadGEM2-ES	100	40	0	0	0	1	8	32
MIROC5	100	40	0	0	0	0	2	2
MRI-CGCM3	100	40	0	0	0	0	0	0
Days per 10 yrs, all models								94.9
2050-2099								
CNRM-CM5	100	50	49	97	137.5	161	206	6619
GFDL-ESM2G	100	50	0	0	0	3	22	141
HadGEM2-ES	100	50	0	4	9	18	76	819
MIROC5	100	50	0	0	0	0	7	33
MRI-CGCM3	100	50	0	0	0	0	18	31
Days per 10 yrs, all models								764.3
Without CNRM-CM5								
2010-2049	Days per 10 yrs							2.1
2050-2099	Days per 10 yrs							51.2

Table 4.67: Summary statistics for count of the number of days per year when AHL>100. Location= Comet, RCP8.5, time periods= 2010-2049, 2050-2099. Maximal mitigation implemented.

mit=max Model	AHL threshold	Count of years (n)	Summary of per-annum counts of days when AHL > threshold					
			min	p25	median	p75	max	all yrs
2010-2049								
CNRM-CM5	100	40	0	0	2.5	9.5	27	230
GFDL-ESM2G	100	40	0	0	0	0	0	0
HadGEM2-ES	100	40	0	0	0	0	1	1
MIROC5	100	40	0	0	0	0	0	0
MRI-CGCM3	100	40	0	0	0	0	0	0
Days per 10 yrs, all models								23.1
2050-2099								
CNRM-CM5	100	50	12	41	67.5	95	145	3596
GFDL-ESM2G	100	50	0	0	0	0	0	0
HadGEM2-ES	100	50	0	0	1	3	10	101
MIROC5	100	50	0	0	0	0	2	2
MRI-CGCM3	100	50	0	0	0	0	2	2
Days per 10 yrs, all models								370.1
Without CNRM-CM5								
2010-2049	Days per 10 yrs							0.1
2050-2099	Days per 10 yrs							5.3

4.3.2.7 Dalby, RCP2.6

Table 4.68: Summary statistics for count of the number of days per year when AHL>100. Location=Dalby, RCP2.6, time periods= 1960-1999, 2010-2049, 2050-2099. No mitigation implemented.

mit=none Model	AHL threshold	Count of years (n)	Summary of per-annum counts of days when AHL > threshold					
			min	p25	median	p75	max	all yrs
1960-1999								
CNRM-CM5	100	40	0	0	0	0	0	0
GFDL-ESM2G	100	40	0	0	0	0	0	0
HadGEM2-ES	100	40	0	0	0	0	1	1
MIROC5	100	40	0	0	0	0	0	0
MRI-CGCM3	100	40	0	0	0	0	3	5
Days per 10 yrs, all models								0.6
2010-2049								
CNRM-CM5	100	40	0	0	0	0	2	4
GFDL-ESM2G	100	40	0	0	0	0	2	8
HadGEM2-ES	100	40	0	0	0	0	3	8
MIROC5	100	40	0	0	0	0	0	0
MRI-CGCM3	100	40	0	0	0	0	0	0
Days per 10 yrs, all models								2
2050-2099								
CNRM-CM5	100	50	0	0	0	0	9	40
GFDL-ESM2G	100	50	0	0	0	0	3	5
HadGEM2-ES	100	50	0	0	0	1	5	26
MIROC5	100	50	0	0	0	0	5	13
MRI-CGCM3	100	50	0	0	0	0	0	0
Days per 10 yrs, all models								8.4

Table 4.69: Summary statistics for count of the number of days per year when AHL>100. Location= Dalby, RCP2.6, time periods= 2010-2049, 2050-2099. Mild mitigation implemented.

mit=mild	AHL threshold	Count of years (n)	Summary of per-annum counts of days when AHL > threshold					
			min	p25	median	p75	max	all yrs
Model								
2010-2049								
CNRM-CM5	100	40	0	0	0	0	0	0
GFDL-ESM2G	100	40	0	0	0	0	0	0
HadGEM2-ES	100	40	0	0	0	0	0	0
MIROC5	100	40	0	0	0	0	0	0
MRI-CGCM3	100	40	0	0	0	0	0	0
Days per 10 yrs, all models								0
2050-2099								
CNRM-CM5	100	50	0	0	0	0	5	10
GFDL-ESM2G	100	50	0	0	0	0	0	0
HadGEM2-ES	100	50	0	0	0	0	3	6
MIROC5	100	50	0	0	0	0	2	2
MRI-CGCM3	100	50	0	0	0	0	0	0
Days per 10 yrs, all models								1.8

Table 4.70: Summary statistics for count of the number of days per year when AHL>100. Location= Dalby, RCP2.6, time periods= 2010-2049, 2050-2099. Moderate mitigation implemented.

mit=mod	AHL threshold	Count of years (n)	Summary of per-annum counts of days when AHL > threshold					
			min	p25	median	p75	max	all yrs
Model		(n)	min	p25	median	p75	max	all yrs
2010-2049								
CNRM-CM5	100	40	0	0	0	0	0	0
GFDL-ESM2G	100	40	0	0	0	0	0	0
HadGEM2-ES	100	40	0	0	0	0	0	0
MIROC5	100	40	0	0	0	0	0	0
MRI-CGCM3	100	40	0	0	0	0	0	0
Days per 10 yrs, all models								0
2050-2099								
CNRM-CM5	100	50	0	0	0	0	2	2
GFDL-ESM2G	100	50	0	0	0	0	0	0
HadGEM2-ES	100	50	0	0	0	0	0	0
MIROC5	100	50	0	0	0	0	0	0
MRI-CGCM3	100	50	0	0	0	0	0	0
Days per 10 yrs, all models								0.2

Table 4.71: Summary statistics for count of the number of days per year when AHL>100. Location= Dalby, RCP2.6, time periods= 2010-2049, 2050-2099. Maximal mitigation implemented.

mit=max Model	AHL threshold	Count of years (n)	Summary of per-annum counts of days when AHL > threshold					
			min	p25	median	p75	max	all yrs
2010-2049								
CNRM-CM5	100	40	0	0	0	0	0	0
GFDL-ESM2G	100	40	0	0	0	0	0	0
HadGEM2-ES	100	40	0	0	0	0	0	0
MIROC5	100	40	0	0	0	0	0	0
MRI-CGCM3	100	40	0	0	0	0	0	0
Days per 10 yrs, all models								0
2050-2099								
CNRM-CM5	100	50	0	0	0	0	0	0
GFDL-ESM2G	100	50	0	0	0	0	0	0
HadGEM2-ES	100	50	0	0	0	0	0	0
MIROC5	100	50	0	0	0	0	0	0
MRI-CGCM3	100	50	0	0	0	0	0	0
Days per 10 yrs, all models								0

4.3.2.8 Dalby, RCP4.5

Table 4.72: Summary statistics for count of the number of days per year when AHL>100. Location= Dalby, RCP4.5, time periods= 1960-1999, 2010-2049, 2050-2099. No mitigation implemented.

mit=none Model	AHL threshold	Count of years (n)	Summary of per-annum counts of days when AHL > threshold					
			min	p25	median	p75	max	all yrs
1960-1999								
CNRM-CM5	100	40	0	0	0	0	0	0
GFDL-ESM2G	100	40	0	0	0	0	0	0
HadGEM2-ES	100	40	0	0	0	0	1	1
MIROC5	100	40	0	0	0	0	0	0
MRI-CGCM3	100	40	0	0	0	0	3	5
Days per 10 yrs, all models								0.6
2010-2049								
CNRM-CM5	100	40	0	0	0	0	2	4
GFDL-ESM2G	100	40	0	0	0	0	2	2
HadGEM2-ES	100	40	0	0	0	0	3	10
MIROC5	100	40	0	0	0	0	3	5
MRI-CGCM3	100	40	0	0	0	0	0	0
Days per 10 yrs, all models								2.1
2050-2099								
CNRM-CM5	100	50	0	0	0	0	103	414
GFDL-ESM2G	100	50	0	0	0	2	9	65
HadGEM2-ES	100	50	0	0	1	3	7	102
MIROC5	100	50	0	0	0	0	5	12
MRI-CGCM3	100	50	0	0	0	0	4	9
Days per 10 yrs, all models								60.2

Table 4.73: Summary statistics for count of the number of days per year when AHL>100. Location= Dalby, RCP4.5, time periods= 2010-2049, 2050-2099. Mild mitigation implemented.

mit=mild Model	AHL threshold	Count of years (n)	Summary of per-annum counts of days when AHL > threshold					
			min	p25	median	p75	max	all yrs
2010-2049								
CNRM-CM5	100	40	0	0	0	0	0	0
GFDL-ESM2G	100	40	0	0	0	0	0	0
HadGEM2-ES	100	40	0	0	0	0	2	4
MIROC5	100	40	0	0	0	0	0	0
MRI-CGCM3	100	40	0	0	0	0	0	0
Days per 10 yrs, all models								0.4
2050-2099								
CNRM-CM5	100	50	0	0	0	0	55	116
GFDL-ESM2G	100	50	0	0	0	0	2	12
HadGEM2-ES	100	50	0	0	0	0	5	23
MIROC5	100	50	0	0	0	0	0	0
MRI-CGCM3	100	50	0	0	0	0	0	0
Days per 10 yrs, all models								15.1

Table 4.74: Summary statistics for count of the number of days per year when AHL>100. Location= Dalby, RCP4.5, time periods= 2010-2049, 2050-2099. Moderate mitigation implemented.

mit=mod Model	AHL threshold	Count of years (n)	Summary of per-annum counts of days when AHL > threshold					
			min	p25	median	p75	max	all yrs
2010-2049								
CNRM-CM5	100	40	0	0	0	0	0	0
GFDL-ESM2G	100	40	0	0	0	0	0	0
HadGEM2-ES	100	40	0	0	0	0	0	0
MIROC5	100	40	0	0	0	0	0	0
MRI-CGCM3	100	40	0	0	0	0	0	0
Days per 10 yrs, all models								0
2050-2099								
CNRM-CM5	100	50	0	0	0	0	18	25
GFDL-ESM2G	100	50	0	0	0	0	0	0
HadGEM2-ES	100	50	0	0	0	0	4	7
MIROC5	100	50	0	0	0	0	0	0
MRI-CGCM3	100	50	0	0	0	0	0	0
Days per 10 yrs, all models								3.2

Table 4.75: Summary statistics for count of the number of days per year when AHL>100. Location= Dalby, RCP4.5, time periods= 2010-2049, 2050-2099. Maximal mitigation implemented.

mit=max Model	AHL threshold	Count of years (n)	Summary of per-annum counts of days when AHL > threshold					
			min	p25	median	p75	max	all yrs
2010-2049								
CNRM-CM5	100	40	0	0	0	0	0	0
GFDL-ESM2G	100	40	0	0	0	0	0	0
HadGEM2-ES	100	40	0	0	0	0	0	0
MIROC5	100	40	0	0	0	0	0	0
MRI-CGCM3	100	40	0	0	0	0	0	0
Days per 10 yrs, all models								0
2050-2099								
CNRM-CM5	100	50	0	0	0	0	2	2
GFDL-ESM2G	100	50	0	0	0	0	0	0
HadGEM2-ES	100	50	0	0	0	0	0	0
MIROC5	100	50	0	0	0	0	0	0
MRI-CGCM3	100	50	0	0	0	0	0	0
Days per 10 yrs, all models								0.2

4.3.2.9 Dalby, RCP8.5

Table 4.76: Summary statistics for count of the number of days per year when AHL>100. Location= Dalby, RCP8.5, time periods= 1960-1999, 2010-2049, 2050-2099. No mitigation implemented.

mit=none Model	AHL threshold	Count of years (n)	Summary of per-annum counts of days when AHL > threshold					
			min	p25	median	p75	max	all yrs
1960-1999								
CNRM-CM5	100	40	0	0	0	0	0	0
GFDL-ESM2G	100	40	0	0	0	0	0	0
HadGEM2-ES	100	40	0	0	0	0	1	1
MIROC5	100	40	0	0	0	0	0	0
MRI-CGCM3	100	40	0	0	0	0	3	5
Days per 10 yrs, all models								0.6
2010-2049								
CNRM-CM5	100	40	3	15	23.5	33	58	1002
GFDL-ESM2G	100	40	0	0	0	0	4	10
HadGEM2-ES	100	40	0	0	0	1	4	30
MIROC5	100	40	0	0	0	0	3	5
MRI-CGCM3	100	40	0	0	0	0	2	2
Days per 10 yrs, all models								104.9
2050-2099								
CNRM-CM5	100	50	53	100	119.5	142	184	6015
GFDL-ESM2G	100	50	0	0	2	6	18	178
HadGEM2-ES	100	50	0	3	8.5	13	51	519
MIROC5	100	50	0	0	0	2	14	93
MRI-CGCM3	100	50	0	0	0	0	7	38
Days per 10 yrs, all models								684.3
Without CNRM-CM5								
2010-2049	Days per 10 yrs							2.9
2050-2099	Days per 10 yrs							41.4

Table 4.77: Summary statistics for count of the number of days per year when AHL>100. Location= Dalby, RCP8.5, time periods= 2010-2049, 2050-2099. Mild mitigation implemented.

mit=mild		Count of years (n)	Summary of per-annum counts of days when AHL > threshold					
Model	AHL threshold		min	p25	median	p75	max	all yrs
2010-2049								
CNRM-CM5	100	40	0	2.5	7.5	11.5	30	334
GFDL-ESM2G	100	40	0	0	0	0	0	0
HadGEM2-ES	100	40	0	0	0	0	2	6
MIROC5	100	40	0	0	0	0	0	0
MRI-CGCM3	100	40	0	0	0	0	0	0
Days per 10 yrs, all models								34
2050-2099								
CNRM-CM5	100	50	16	45	62	79	120	3182
GFDL-ESM2G	100	50	0	0	0	0	5	26
HadGEM2-ES	100	50	0	0	2	4	12	159
MIROC5	100	50	0	0	0	0	6	11
MRI-CGCM3	100	50	0	0	0	0	3	3
Days per 10 yrs, all models								338.1
Without CNRM-CM5								
2010-2049	Days per 10 yrs							0.4
2050-2099	Days per 10 yrs							10.0

Table 4.78: Summary statistics for count of the number of days per year when AHL>100. Location= Dalby, RCP8.5, time periods= 2010-2049, 2050-2099. Moderate mitigation implemented.

mit=mod		Count of years (n)	Summary of per-annum counts of days when AHL > threshold					
Model	AHL threshold		min	p25	median	p75	max	all yrs
2010-2049								
CNRM-CM5	100	40	0	0	2	3.5	10	93
GFDL-ESM2G	100	40	0	0	0	0	0	0
HadGEM2-ES	100	40	0	0	0	0	0	0
MIROC5	100	40	0	0	0	0	0	0
MRI-CGCM3	100	40	0	0	0	0	0	0
Days per 10 yrs, all models								9.3
2050-2099								
CNRM-CM5	100	50	6	20	32	43	80	1673
GFDL-ESM2G	100	50	0	0	0	0	0	0
HadGEM2-ES	100	50	0	0	1	2	9	70
MIROC5	100	50	0	0	0	0	0	0
MRI-CGCM3	100	50	0	0	0	0	0	0
Days per 10 yrs, all models								174.3
Without CNRM-CM5								
2010-2049	Days per 10 yrs							0.0
2050-2099	Days per 10 yrs							3.5

Table 4.79: Summary statistics for count of the number of days per year when AHL>100. Location= Dalby, RCP8.5, time periods= 2010-2049, 2050-2099. Maximal mitigation implemented.

mit=max Model	AHL threshold	Count of years (n)	Summary of per-annum counts of days when AHL > threshold					
			min	p25	median	p75	max	all yrs
2010-2049								
CNRM-CM5	100	40	0	0	0	0	6	19
GFDL-ESM2G	100	40	0	0	0	0	0	0
HadGEM2-ES	100	40	0	0	0	0	0	0
MIROC5	100	40	0	0	0	0	0	0
MRI-CGCM3	100	40	0	0	0	0	0	0
Days per 10 yrs, all models								1.9
2050-2099								
CNRM-CM5	100	50	0	5	11.5	17	46	657
GFDL-ESM2G	100	50	0	0	0	0	0	0
HadGEM2-ES	100	50	0	0	0	0	3	7
MIROC5	100	50	0	0	0	0	0	0
MRI-CGCM3	100	50	0	0	0	0	0	0
Days per 10 yrs, all models								66.4
Without CNRM-CM5								
2010-2049	Days per 10 yrs							0.0
2050-2099	Days per 10 yrs							0.4

4.3.2.10 Leeton, RCP2.6

Table 4.80: Summary statistics for count of the number of days per year when AHL>100. Location=Leeton, RCP2.6, time periods= 1960-1999, 2010-2049, 2050-2099. No mitigation implemented.

mit=none Model	AHL threshold	Count of years (n)	Summary of per-annum counts of days when AHL > threshold					
			min	p25	median	p75	max	all yrs
1960-1999								
CNRM-CM5	100	40	0	0	0	0	5	13
GFDL-ESM2G	100	40	0	0	0	0	6	23
HadGEM2-ES	100	40	0	0	0	1	7	33
MIROC5	100	40	0	0	0	0	5	16
MRI-CGCM3	100	40	0	0	0	2	8	47
Days per 10 yrs, all models								13.2
2010-2049								
CNRM-CM5	100	40	0	0	2	3.5	10	105
GFDL-ESM2G	100	40	0	0	0	2	9	63
HadGEM2-ES	100	40	0	0	2	5.5	17	130
MIROC5	100	40	0	0	0	2	16	68
MRI-CGCM3	100	40	0	0	2	3	11	101
Days per 10 yrs, all models								46.7
2050-2099								
CNRM-CM5	100	50	0	0	2.5	6	28	197
GFDL-ESM2G	100	50	0	0	2	4	17	127
HadGEM2-ES	100	50	0	1	5	10	30	342
MIROC5	100	50	0	0	0	3	20	99
MRI-CGCM3	100	50	0	0	2	6	25	202
Days per 10 yrs, all models								96.7

Table 4.81: Summary statistics for count of the number of days per year when AHL>100. Location= Leeton, RCP2.6, time periods= 2010-2049, 2050-2099. Mild mitigation implemented.

mit=mild Model	AHL threshold	Count of years (n)	Summary of per-annum counts of days when AHL > threshold					
			min	p25	median	p75	max	all yrs
2010-2049								
CNRM-CM5	100	40	0	0	0	0.5	8	39
GFDL-ESM2G	100	40	0	0	0	0	5	16
HadGEM2-ES	100	40	0	0	0	1	7	37
MIROC5	100	40	0	0	0	0	7	20
MRI-CGCM3	100	40	0	0	0	0.5	6	29
Days per 10 yrs, all models								14.1
2050-2099								
CNRM-CM5	100	50	0	0	0	3	16	82
GFDL-ESM2G	100	50	0	0	0	0	12	37
HadGEM2-ES	100	50	0	0	1	5	19	135
MIROC5	100	50	0	0	0	0	12	31
MRI-CGCM3	100	50	0	0	0	2	16	67
Days per 10 yrs, all models								35.2

Table 4.82: Summary statistics for count of the number of days per year when AHL>100. Location= Leeton, RCP2.6, time periods= 2010-2049, 2050-2099. Moderate mitigation implemented.

mit=mod Model	AHL threshold	Count of years (n)	Summary of per-annum counts of days when AHL > threshold					
			min	p25	median	p75	max	all yrs
2010-2049								
CNRM-CM5	100	40	0	0	0	0	3	5
GFDL-ESM2G	100	40	0	0	0	0	3	6
HadGEM2-ES	100	40	0	0	0	0	4	5
MIROC5	100	40	0	0	0	0	0	0
MRI-CGCM3	100	40	0	0	0	0	4	7
Days per 10 yrs, all models								2.3
2050-2099								
CNRM-CM5	100	50	0	0	0	0	11	20
GFDL-ESM2G	100	50	0	0	0	0	2	2
HadGEM2-ES	100	50	0	0	0	1	13	42
MIROC5	100	50	0	0	0	0	0	0
MRI-CGCM3	100	50	0	0	0	0	10	22
Days per 10 yrs, all models								8.6

Table 4.83: Summary statistics for count of the number of days per year when AHL>100. Location= Leeton, RCP2.6, time periods= 2010-2049, 2050-2099. Maximal mitigation implemented.

mit=max Model	AHL threshold	Count of years (n)	Summary of per-annum counts of days when AHL > threshold					
			min	p25	median	p75	max	all yrs
2010-2049								
CNRM-CM5	100	40	0	0	0	0	0	0
GFDL-ESM2G	100	40	0	0	0	0	0	0
HadGEM2-ES	100	40	0	0	0	0	0	0
MIROC5	100	40	0	0	0	0	0	0
MRI-CGCM3	100	40	0	0	0	0	1	1
Days per 10 yrs, all models								0.1
2050-2099								
CNRM-CM5	100	50	0	0	0	0	0	0
GFDL-ESM2G	100	50	0	0	0	0	0	0
HadGEM2-ES	100	50	0	0	0	0	5	11
MIROC5	100	50	0	0	0	0	0	0
MRI-CGCM3	100	50	0	0	0	0	1	1
Days per 10 yrs, all models								1.2

4.3.2.11 Leeton, RCP4.5

Table 4.84: Summary statistics for count of the number of days per year when AHL>100. Location= Leeton, RCP4.5, time periods= 1960-1999, 2010-2049, 2050-2099. No mitigation implemented.

mit=none Model	AHL threshold	Count of years (n)	Summary of per-annum counts of days when AHL > threshold					all yrs
			min	p25	median	p75	max	
1960-1999								
CNRM-CM5	100	40	0	0	0	0	5	13
GFDL-ESM2G	100	40	0	0	0	0	6	23
HadGEM2-ES	100	40	0	0	0	1	7	33
MIROC5	100	40	0	0	0	0	5	16
MRI-CGCM3	100	40	0	0	0	2	8	47
Days per 10 yrs, all models								13.2
2010-2049								
CNRM-CM5	100	40	0	0	2	4.5	15	113
GFDL-ESM2G	100	40	0	0	2	3.5	16	110
HadGEM2-ES	100	40	0	2	4	10	32	243
MIROC5	100	40	0	0	0	2	16	72
MRI-CGCM3	100	40	0	0	2	4	12	108
Days per 10 yrs, all models								64.6
2050-2099								
CNRM-CM5	100	50	0	2	5	10	33	327
GFDL-ESM2G	100	50	0	0	5	8	33	315
HadGEM2-ES	100	50	0	4	11.5	18	42	644
MIROC5	100	50	0	0	2	5	25	207
MRI-CGCM3	100	50	0	2	3.5	7	25	260
Days per 10 yrs, all models								175.3

Table 4.85: Summary statistics for count of the number of days per year when AHL>100. Location= Leeton, RCP4.5, time periods= 2010-2049, 2050-2099. Mild mitigation implemented.

mit=mild Model	AHL threshold	Count of years (n)	Summary of per-annum counts of days when AHL > threshold					
			min	p25	median	p75	max	all yrs
2010-2049								
CNRM-CM5	100	40	0	0	0	0	7	30
GFDL-ESM2G	100	40	0	0	0	0	5	26
HadGEM2-ES	100	40	0	0	1	4	12	92
MIROC5	100	40	0	0	0	0	3	14
MRI-CGCM3	100	40	0	0	0	0	8	24
Days per 10 yrs, all models								18.6
2050-2099								
CNRM-CM5	100	50	0	0	0	4	22	114
GFDL-ESM2G	100	50	0	0	1	3	21	118
HadGEM2-ES	100	50	0	1	4.5	9	24	306
MIROC5	100	50	0	0	0	2	15	81
MRI-CGCM3	100	50	0	0	0	2	16	92
Days per 10 yrs, all models								71.1

Table 4.86: Summary statistics for count of the number of days per year when AHL>100. Location= Leeton, RCP4.5, time periods= 2010-2049, 2050-2099. Moderate mitigation implemented.

mit=mod Model	AHL threshold	Count of years (n)	Summary of per-annum counts of days when AHL > threshold					
			min	p25	median	p75	max	all yrs
2010-2049								
CNRM-CM5	100	40	0	0	0	0	3	6
GFDL-ESM2G	100	40	0	0	0	0	3	7
HadGEM2-ES	100	40	0	0	0	0	6	14
MIROC5	100	40	0	0	0	0	2	2
MRI-CGCM3	100	40	0	0	0	0	6	6
Days per 10 yrs, all models								3.5
2050-2099								
CNRM-CM5	100	50	0	0	0	0	14	30
GFDL-ESM2G	100	50	0	0	0	0	14	32
HadGEM2-ES	100	50	0	0	1	3	17	106
MIROC5	100	50	0	0	0	0	5	14
MRI-CGCM3	100	50	0	0	0	0	9	26
Days per 10 yrs, all models								20.8

Table 4.87: Summary statistics for count of the number of days per year when AHL>100. Location= Leeton, RCP4.5, time periods= 2010-2049, 2050-2099. Maximal mitigation implemented.

mit=max Model	AHL threshold	Count of years (n)	Summary of per-annum counts of days when AHL > threshold					
			min	p25	median	p75	max	all yrs
2010-2049								
CNRM-CM5	100	40	0	0	0	0	2	2
GFDL-ESM2G	100	40	0	0	0	0	1	1
HadGEM2-ES	100	40	0	0	0	0	2	2
MIROC5	100	40	0	0	0	0	0	0
MRI-CGCM3	100	40	0	0	0	0	3	3
Days per 10 yrs, all models								0.8
2050-2099								
CNRM-CM5	100	50	0	0	0	0	6	8
GFDL-ESM2G	100	50	0	0	0	0	3	8
HadGEM2-ES	100	50	0	0	0	1	10	33
MIROC5	100	50	0	0	0	0	3	7
MRI-CGCM3	100	50	0	0	0	0	0	0
Days per 10 yrs, all models								5.6

4.3.2.12 Leeton, RCP8.5

Table 4.88: Summary statistics for count of the number of days per year when AHL>100. Location= Leeton, RCP8.5, time periods= 1960-1999, 2010-2049, 2050-2099. No mitigation implemented.

mit=none Model	AHL threshold	Count of years (n)	Summary of per-annum counts of days when AHL > threshold					
			min	p25	median	p75	max	all yrs
1960-1999								
CNRM-CM5	100	40	0	0	0	0	5	13
GFDL-ESM2G	100	40	0	0	0	0	6	23
HadGEM2-ES	100	40	0	0	0	1	7	33
MIROC5	100	40	0	0	0	0	5	16
MRI-CGCM3	100	40	0	0	0	2	8	47
Days per 10 yrs, all models								13.2
2010-2049								
CNRM-CM5	100	40	5	19.5	29	47.5	76	1355
GFDL-ESM2G	100	40	0	0	0	2	8	57
HadGEM2-ES	100	40	0	1	4.5	9.5	26	242
MIROC5	100	40	0	0	0	2	11	72
MRI-CGCM3	100	40	0	0	2	5	14	104
Days per 10 yrs, all models								183
2050-2099								
CNRM-CM5	100	50	41	68	91	109	162	4612
GFDL-ESM2G	100	50	0	4	11.5	19	51	644
HadGEM2-ES	100	50	4	21	34.5	49	90	1902
MIROC5	100	50	0	2	7.5	15	33	496
MRI-CGCM3	100	50	0	6	11	17	41	611
Days per 10 yrs, all models								826.5
Without CNRM-CM5								
2010-2049	Days per 10 yrs							29.7
2050-2099	Days per 10 yrs							182.7

Table 4.89: Summary statistics for count of the number of days per year when AHL>100. Location= Leeton, RCP8.5, time periods= 2010-2049, 2050-2099. Mild mitigation implemented.

mit=mild Model	AHL threshold	Count of years (n)	Summary of per-annum counts of days when AHL > threshold					
			min	p25	median	p75	max	all yrs
2010-2049								
CNRM-CM5	100	40	0	10	15	25	50	701
GFDL-ESM2G	100	40	0	0	0	0	4	18
HadGEM2-ES	100	40	0	0	0.5	3	12	75
MIROC5	100	40	0	0	0	0	5	16
MRI-CGCM3	100	40	0	0	0	2	7	35
Days per 10 yrs, all models								84.5
2050-2099								
CNRM-CM5	100	50	15	38	61	77	114	2978
GFDL-ESM2G	100	50	0	2	5	8	32	272
HadGEM2-ES	100	50	2	9	17.5	27	53	986
MIROC5	100	50	0	0	2.5	6	21	203
MRI-CGCM3	100	50	0	0	3	6	30	247
Days per 10 yrs, all models								468.6
Without CNRM-CM5								
2010-2049	Days per 10 yrs							9.0
2050-2099	Days per 10 yrs							85.4

Table 4.90: Summary statistics for count of the number of days per year when AHL>100. Location= Leeton, RCP8.5, time periods= 2010-2049, 2050-2099. Moderate mitigation implemented.

mit=mod Model	AHL threshold	Count of years (n)	Summary of per-annum counts of days when AHL > threshold					
			min	p25	median	p75	max	all yrs
2010-2049								
CNRM-CM5	100	40	0	5	7.5	15.5	36	397
GFDL-ESM2G	100	40	0	0	0	0	3	3
HadGEM2-ES	100	40	0	0	0	0	6	21
MIROC5	100	40	0	0	0	0	0	0
MRI-CGCM3	100	40	0	0	0	0	3	6
Days per 10 yrs, all models								42.7
2050-2099								
CNRM-CM5	100	50	6	22	40	52	88	1952
GFDL-ESM2G	100	50	0	0	0	2	22	94
HadGEM2-ES	100	50	0	3	9	13	36	493
MIROC5	100	50	0	0	0	2	14	79
MRI-CGCM3	100	50	0	0	0	2	15	80
Days per 10 yrs, all models								269.8
Without CNRM-CM5								
2010-2049	Days per 10 yrs							1.9
2050-2099	Days per 10 yrs							37.3

Table 4.91: Summary statistics for count of the number of days per year when AHL>100. Location= Leeton, RCP8.5, time periods= 2010-2049, 2050-2099. Maximal mitigation implemented.

mit=max Model	AHL threshold	Count of years (n)	Summary of per-annum counts of days when AHL > threshold					
			min	p25	median	p75	max	all yrs
2010-2049								
CNRM-CM5	100	40	0	0.5	3	7	18	174
GFDL-ESM2G	100	40	0	0	0	0	0	0
HadGEM2-ES	100	40	0	0	0	0	2	2
MIROC5	100	40	0	0	0	0	0	0
MRI-CGCM3	100	40	0	0	0	0	0	0
Days per 10 yrs, all models								17.6
2050-2099								
CNRM-CM5	100	50	0	12	20.5	28	57	1108
GFDL-ESM2G	100	50	0	0	0	0	11	34
HadGEM2-ES	100	50	0	0	2	4	22	173
MIROC5	100	50	0	0	0	0	2	13
MRI-CGCM3	100	50	0	0	0	0	8	24
Days per 10 yrs, all models								135.2
Without CNRM-CM5								
2010-2049	Days per 10 yrs							0.1
2050-2099	Days per 10 yrs							12.2

4.3.2.13 Narrogin, RCP2.6

Table 4.92: Summary statistics for count of the number of days per year when AHL>100. Location=Narrogin, RCP2.6, time periods= 1960-1999, 2010-2049, 2050-2099. No mitigation implemented.

mit=none Model	AHL threshold	Count of years (n)	Summary of per-annum counts of days when AHL > threshold					
			min	p25	median	p75	max	all yrs
1960-1999								
CNRM-CM5	100	40	0	0	0	0	0	0
GFDL-ESM2G	100	40	0	0	0	0	0	0
HadGEM2-ES	100	40	0	0	0	0	1	2
MIROC5	100	40	0	0	0	0	0	0
MRI-CGCM3	100	40	0	0	0	0	0	0
Days per 10 yrs, all models								0.2
2010-2049								
CNRM-CM5	100	40	0	0	0	0	0	0
GFDL-ESM2G	100	40	0	0	0	0	1	1
HadGEM2-ES	100	40	0	0	0	0	2	3
MIROC5	100	40	0	0	0	0	1	1
MRI-CGCM3	100	40	0	0	0	0	2	3
Days per 10 yrs, all models								0.8
2050-2099								
CNRM-CM5	100	50	0	0	0	0	2	2
GFDL-ESM2G	100	50	0	0	0	0	1	1
HadGEM2-ES	100	50	0	0	0	0	2	5
MIROC5	100	50	0	0	0	0	1	2
MRI-CGCM3	100	50	0	0	0	0	2	4
Days per 10 yrs, all models								1.4

Table 4.93: Summary statistics for count of the number of days per year when AHL>100. Location= Narrogin, RCP2.6, time periods= 2010-2049, 2050-2099. Mild mitigation implemented.

mit=mild Model	AHL threshold	Count of years (n)	Summary of per-annum counts of days when AHL > threshold					
			min	p25	median	p75	max	all yrs
2010-2049								
CNRM-CM5	100	40	0	0	0	0	0	0
GFDL-ESM2G	100	40	0	0	0	0	0	0
HadGEM2-ES	100	40	0	0	0	0	1	2
MIROC5	100	40	0	0	0	0	0	0
MRI-CGCM3	100	40	0	0	0	0	0	0
Days per 10 yrs, all models								0.2
2050-2099								
CNRM-CM5	100	50	0	0	0	0	0	0
GFDL-ESM2G	100	50	0	0	0	0	0	0
HadGEM2-ES	100	50	0	0	0	0	1	2
MIROC5	100	50	0	0	0	0	0	0
MRI-CGCM3	100	50	0	0	0	0	0	0
Days per 10 yrs, all models								0.2

Table 4.94: Summary statistics for count of the number of days per year when AHL>100. Location= Narrogin, RCP2.6, time periods= 2010-2049, 2050-2099. Moderate mitigation implemented.

mit=mod Model	AHL threshold	Count of years (n)	Summary of per-annum counts of days when AHL > threshold					
			min	p25	median	p75	max	all yrs
2010-2049								
CNRM-CM5	100	40	0	0	0	0	0	0
GFDL-ESM2G	100	40	0	0	0	0	0	0
HadGEM2-ES	100	40	0	0	0	0	0	0
MIROC5	100	40	0	0	0	0	0	0
MRI-CGCM3	100	40	0	0	0	0	0	0
Days per 10 yrs, all models								0
2050-2099								
CNRM-CM5	100	50	0	0	0	0	0	0
GFDL-ESM2G	100	50	0	0	0	0	0	0
HadGEM2-ES	100	50	0	0	0	0	0	0
MIROC5	100	50	0	0	0	0	0	0
MRI-CGCM3	100	50	0	0	0	0	0	0
Days per 10 yrs, all models								0

Table 4.95: Summary statistics for count of the number of days per year when AHL>100. Location=Narrogen, RCP2.6, time periods= 2010-2049, 2050-2099. Maximal mitigation implemented.

mit=max Model	AHL threshold	Count of years (n)	Summary of per-annum counts of days when AHL > threshold					
			min	p25	median	p75	max	all yrs
2010-2049								
CNRM-CM5	100	40	0	0	0	0	0	0
GFDL-ESM2G	100	40	0	0	0	0	0	0
HadGEM2-ES	100	40	0	0	0	0	0	0
MIROC5	100	40	0	0	0	0	0	0
MRI-CGCM3	100	40	0	0	0	0	0	0
Days per 10 yrs, all models								0
2050-2099								
CNRM-CM5	100	50	0	0	0	0	0	0
GFDL-ESM2G	100	50	0	0	0	0	0	0
HadGEM2-ES	100	50	0	0	0	0	0	0
MIROC5	100	50	0	0	0	0	0	0
MRI-CGCM3	100	50	0	0	0	0	0	0
Days per 10 yrs, all models								0

4.3.2.14 Narrogin, RCP4.5

Table 4.96: Summary statistics for count of the number of days per year when AHL>100. Location= Narrogin, RCP4.5, time periods= 1960-1999, 2010-2049, 2050-2099. No mitigation implemented.

mit=none Model	AHL threshold	Count of years (n)	Summary of per-annum counts of days when AHL > threshold					
			min	p25	median	p75	max	all yrs
1960-1999								
CNRM-CM5	100	40	0	0	0	0	0	0
GFDL-ESM2G	100	40	0	0	0	0	0	0
HadGEM2-ES	100	40	0	0	0	0	1	2
MIROC5	100	40	0	0	0	0	0	0
MRI-CGCM3	100	40	0	0	0	0	0	0
Days per 10 yrs, all models								0.2
2010-2049								
CNRM-CM5	100	40	0	0	0	0	0	0
GFDL-ESM2G	100	40	0	0	0	0	1	1
HadGEM2-ES	100	40	0	0	0	0	2	4
MIROC5	100	40	0	0	0	0	1	2
MRI-CGCM3	100	40	0	0	0	0	2	3
Days per 10 yrs, all models								1
2050-2099								
CNRM-CM5	100	50	0	0	0	0	3	6
GFDL-ESM2G	100	50	0	0	0	0	1	1
HadGEM2-ES	100	50	0	0	0	0	2	9
MIROC5	100	50	0	0	0	0	1	2
MRI-CGCM3	100	50	0	0	0	0	2	6
Days per 10 yrs, all models								2.4

Table 4.97: Summary statistics for count of the number of days per year when AHL>100. Location= Narrogin, RCP4.5, time periods= 2010-2049, 2050-2099. Mild mitigation implemented.

mit=mild Model	AHL threshold	Count of years (n)	Summary of per-annum counts of days when AHL > threshold					
			min	p25	median	p75	max	all yrs
2010-2049								
CNRM-CM5	100	40	0	0	0	0	0	0
GFDL-ESM2G	100	40	0	0	0	0	0	0
HadGEM2-ES	100	40	0	0	0	0	1	2
MIROC5	100	40	0	0	0	0	0	0
MRI-CGCM3	100	40	0	0	0	0	0	0
Days per 10 yrs, all models								0.2
2050-2099								
CNRM-CM5	100	50	0	0	0	0	0	0
GFDL-ESM2G	100	50	0	0	0	0	0	0
HadGEM2-ES	100	50	0	0	0	0	2	3
MIROC5	100	50	0	0	0	0	0	0
MRI-CGCM3	100	50	0	0	0	0	1	1
Days per 10 yrs, all models								0.4

Table 4.98: Summary statistics for count of the number of days per year when AHL>100. Location= Narrogin, RCP4.5, time periods= 2010-2049, 2050-2099. Moderate mitigation implemented.

mit=mod Model	AHL threshold	Count of years (n)	Summary of per-annum counts of days when AHL > threshold					
			min	p25	median	p75	max	all yrs
2010-2049								
CNRM-CM5	100	40	0	0	0	0	0	0
GFDL-ESM2G	100	40	0	0	0	0	0	0
HadGEM2-ES	100	40	0	0	0	0	0	0
MIROC5	100	40	0	0	0	0	0	0
MRI-CGCM3	100	40	0	0	0	0	0	0
Days per 10 yrs, all models								0
2050-2099								
CNRM-CM5	100	50	0	0	0	0	0	0
GFDL-ESM2G	100	50	0	0	0	0	0	0
HadGEM2-ES	100	50	0	0	0	0	1	1
MIROC5	100	50	0	0	0	0	0	0
MRI-CGCM3	100	50	0	0	0	0	0	0
Days per 10 yrs, all models								0.1

Table 4.99: Summary statistics for count of the number of days per year when AHL>100. Location= Narrogin, RCP4.5, time periods= 2010-2049, 2050-2099. Maximal mitigation implemented.

mit=max Model	AHL threshold	Count of years (n)	Summary of per-annum counts of days when AHL > threshold					
			min	p25	median	p75	max	all yrs
2010-2049								
CNRM-CM5	100	40	0	0	0	0	0	0
GFDL-ESM2G	100	40	0	0	0	0	0	0
HadGEM2-ES	100	40	0	0	0	0	0	0
MIROC5	100	40	0	0	0	0	0	0
MRI-CGCM3	100	40	0	0	0	0	0	0
Days per 10 yrs, all models								0
2050-2099								
CNRM-CM5	100	50	0	0	0	0	0	0
GFDL-ESM2G	100	50	0	0	0	0	0	0
HadGEM2-ES	100	50	0	0	0	0	0	0
MIROC5	100	50	0	0	0	0	0	0
MRI-CGCM3	100	50	0	0	0	0	0	0
Days per 10 yrs, all models								0

4.3.2.15 Narrogin, RCP8.5

Table 4.100: Summary statistics for count of the number of days per year when AHL>100. Location= Narrogin, RCP8.5, time periods= 1960-1999, 2010-2049, 2050-2099. No mitigation implemented.

mit=none Model	AHL threshold	Count of years (n)	Summary of per-annum counts of days when AHL > threshold					
			min	p25	median	p75	max	all yrs
1960-1999								
CNRM-CM5	100	40	0	0	0	0	0	0
GFDL-ESM2G	100	40	0	0	0	0	0	0
HadGEM2-ES	100	40	0	0	0	0	1	2
MIROC5	100	40	0	0	0	0	0	0
MRI-CGCM3	100	40	0	0	0	0	0	0
Days per 10 yrs, all models								0.2
2010-2049								
CNRM-CM5	100	40	0	2	3	6	19	181
GFDL-ESM2G	100	40	0	0	0	0	1	2
HadGEM2-ES	100	40	0	0	0	0	2	4
MIROC5	100	40	0	0	0	0	1	1
MRI-CGCM3	100	40	0	0	0	0	2	2
Days per 10 yrs, all models								19
2050-2099								
CNRM-CM5	100	50	4	13	16	23	45	920
GFDL-ESM2G	100	50	0	0	0	0	3	5
HadGEM2-ES	100	50	0	0	0	2	10	48
MIROC5	100	50	0	0	0	0	2	4
MRI-CGCM3	100	50	0	0	0	0	6	26
Days per 10 yrs, all models								100.3
Without CNRM-CM5								
2010-2049	Days per 10 yrs							0.6
2050-2099	Days per 10 yrs							4.2

Table 4.101: Summary statistics for count of the number of days per year when AHL>100.
Location= Narrogin, RCP8.5, time periods= 2010-2049, 2050-2099. Mild mitigation implemented.

mit=mild Model	AHL threshold	Count of years (n)	Summary of per-annum counts of days when AHL > threshold					
			min	p25	median	p75	max	all yrs
2010-2049								
CNRM-CM5	100	40	0	0	1	2	11	64
GFDL-ESM2G	100	40	0	0	0	0	0	0
HadGEM2-ES	100	40	0	0	0	0	1	2
MIROC5	100	40	0	0	0	0	0	0
MRI-CGCM3	100	40	0	0	0	0	0	0
Days per 10 yrs, all models								6.6
2050-2099								
CNRM-CM5	100	50	0	5	7.5	13	22	429
GFDL-ESM2G	100	50	0	0	0	0	1	1
HadGEM2-ES	100	50	0	0	0	0	2	8
MIROC5	100	50	0	0	0	0	1	2
MRI-CGCM3	100	50	0	0	0	0	2	3
Days per 10 yrs, all models								44.3
Without CNRM-CM5								
2010-2049	Days per 10 yrs							0.1
2050-2099	Days per 10 yrs							0.7

Table 4.102: Summary statistics for count of the number of days per year when AHL>100. Location= Narrogin, RCP8.5, time periods= 2010-2049, 2050-2099. Moderate mitigation implemented.

mit=mod Model	AHL threshold	Count of years (n)	Summary of per-annum counts of days when AHL > threshold					
			min	p25	median	p75	max	all yrs
2010-2049								
CNRM-CM5	100	40	0	0	0	0.5	3	18
GFDL-ESM2G	100	40	0	0	0	0	0	0
HadGEM2-ES	100	40	0	0	0	0	0	0
MIROC5	100	40	0	0	0	0	0	0
MRI-CGCM3	100	40	0	0	0	0	0	0
Days per 10 yrs, all models								1.8
2050-2099								
CNRM-CM5	100	50	0	1	2	6	16	178
GFDL-ESM2G	100	50	0	0	0	0	0	0
HadGEM2-ES	100	50	0	0	0	0	2	3
MIROC5	100	50	0	0	0	0	0	0
MRI-CGCM3	100	50	0	0	0	0	0	0
Days per 10 yrs, all models								18.1
Without CNRM-CM5								
2010-2049	Days per 10 yrs							0.0
2050-2099	Days per 10 yrs							0.2

Table 4.103: Summary statistics for count of the number of days per year when AHL>100. Location= Narrogin, RCP8.5, time periods= 2010-2049, 2050-2099. Maximal mitigation implemented.

mit=max Model	AHL threshold	Count of years (n)	Summary of per-annum counts of days when AHL > threshold					
			min	p25	median	p75	max	all yrs
2010-2049								
CNRM-CM5	100	40	0	0	0	0	0	0
GFDL-ESM2G	100	40	0	0	0	0	0	0
HadGEM2-ES	100	40	0	0	0	0	0	0
MIROC5	100	40	0	0	0	0	0	0
MRI-CGCM3	100	40	0	0	0	0	0	0
Days per 10 yrs, all models								0
2050-2099								
CNRM-CM5	100	50	0	0	0	2	10	69
GFDL-ESM2G	100	50	0	0	0	0	0	0
HadGEM2-ES	100	50	0	0	0	0	1	1
MIROC5	100	50	0	0	0	0	0	0
MRI-CGCM3	100	50	0	0	0	0	0	0
Days per 10 yrs, all models								7
Without CNRM-CM5								
2010-2049	Days per 10 yrs							0.0
2050-2099	Days per 10 yrs							0.1

4.4 Daily water intake

Water intake estimates were estimated for a single representative beast using input parameters from the MEDLI model parameterisation for short fed animals. All water intake estimates were generated in units of *litres/head/day*.

Water intake summaries are provided in graphical and tabular form using median daily water intake (L/hd/day) as the measure. Tables and plots of summary measures for water intake have also been generated using units of mega-litres per 1,000 head per year (ML/'000head/yr) to provide a measure that can be compared to industry recommendations for feedlot management.

4.4.1 Caroona

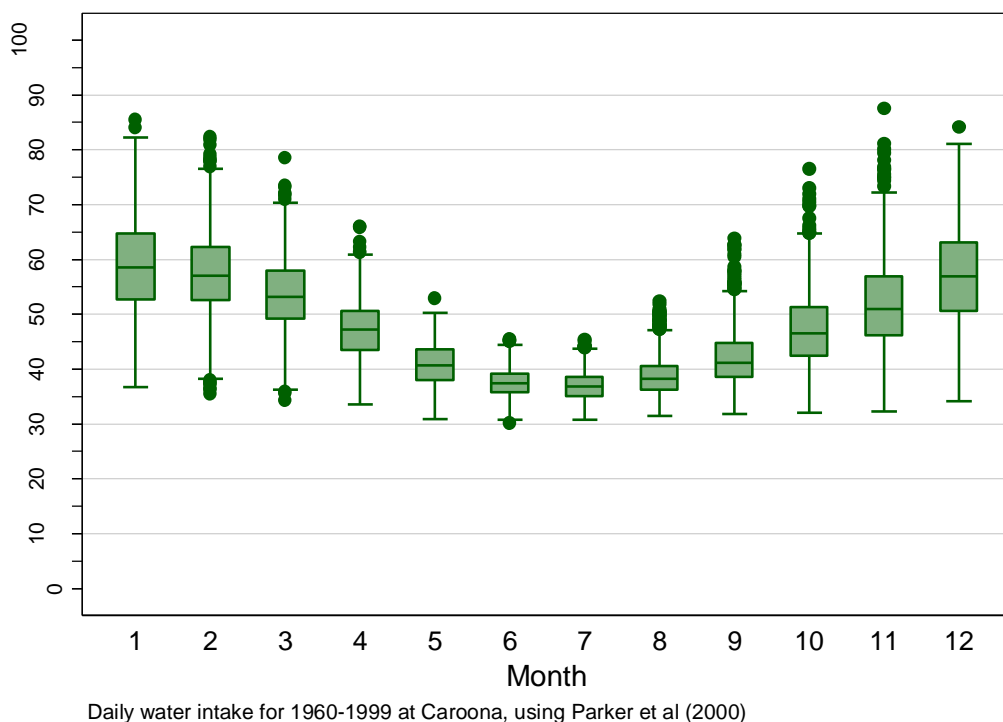
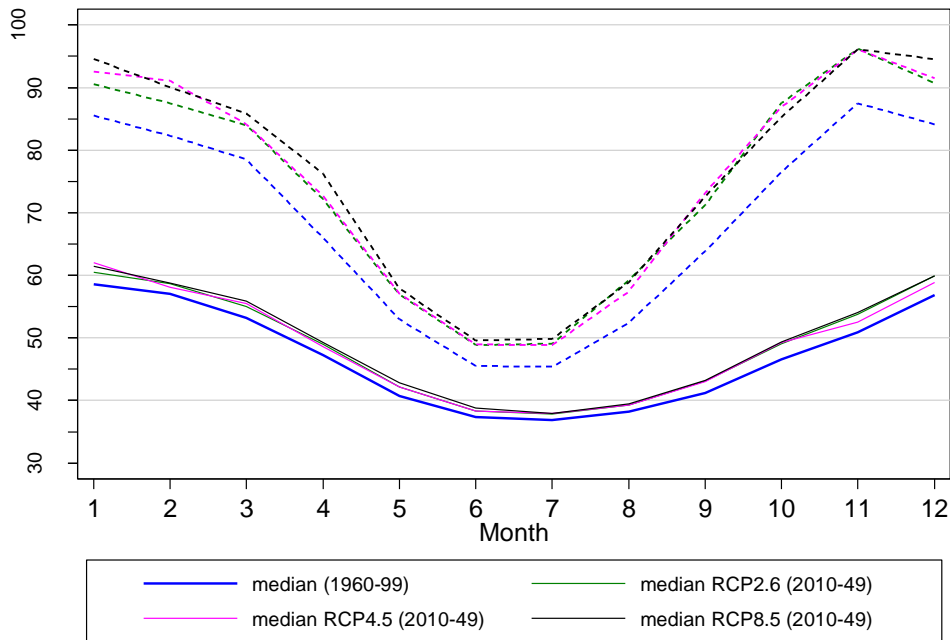


Figure 4.37: Box plot showing median water usage (L/hd/day) at Caroona by month from daily predictions over the period 1960-1999.

At each location, daily estimates of water intake from the historic period (1960-1999) were summarised using box-plots showing the median daily water intake, inter-quartile range and full range of values for each month of the year. This provides an excellent overall summary of the pattern of water intake over the course of a year.

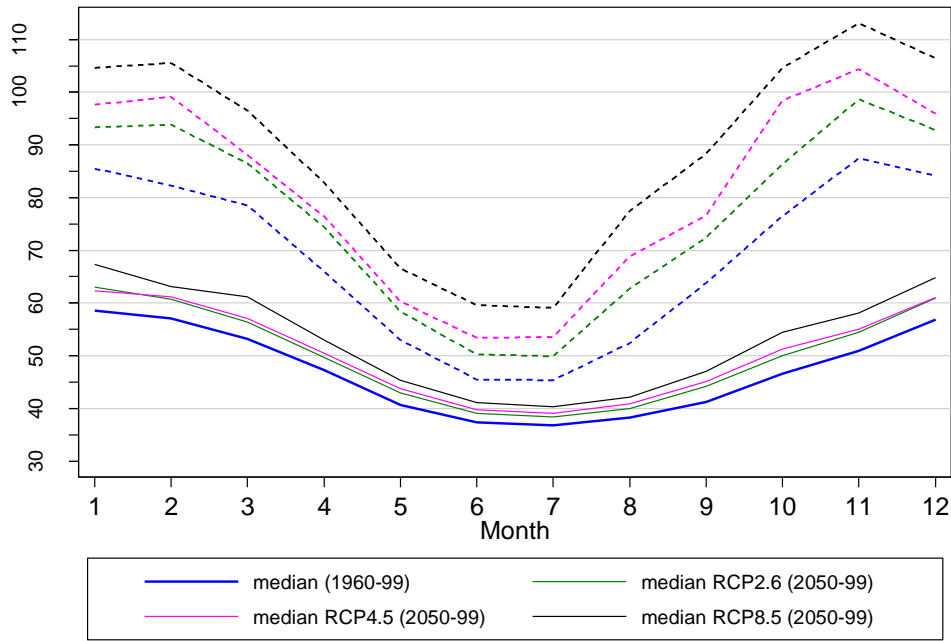
The general pattern is consistent with other reports on water intake in cattle. There is a peak in water intake through the summer months and a decline in autumn to a nadir in the winter, followed by a rise again in the spring. There is a wide range in daily water intake, from a low of around 30 L/hd/day in the winter to a high approaching 90 L/hd./day. A more realistic estimate of the normal range in upper and lower water usage values is likely to be obtained from the 25th and 75th percentile estimates. These estimates represent thresholds that include the lower and upper 25% of

predictions and therefore are not susceptible to unusual or extreme, isolated predictions. These estimates range from around 30 to 80 L/hd/day.



Caroona, Parker et al (2000). Dashed lines show maximal values for each category

Figure 4.38: Predicted median daily water intake by month of year at Caroona for the period from 2010-2049 (solid lines). The solid blue line is the median predicted water intake from the historic period (1960-1999), provided for comparative purposes. Dashed lines shows the maximum daily water intake for each month.



Caroona, Parker et al (2000). Dashed lines show maximal values for each category

Figure 4.39: Predicted median daily water intake by month of year at Caroona for the period from 2050-2099 (solid lines). The solid blue line is the median predicted water intake from the historic period (1960-1999), provided for comparative purposes. Dashed lines shows the maximum daily water intake for each month.

Table 4.104: Summary statistics for daily water intake (L/hd/day) by month of year for Caroona for the historic period (1960-1999) and for each of three scenarios in 2010-2049. Summary statistics for the future period are derived from all five model outputs within each scenario. % changes are based on comparison to the same statistics from the historic period.

Source	Measure	Month											
		1	2	3	4	5	6	7	8	9	10	11	12
1960-1999 (historic)	Min	37	36	34	34	31	30	31	31	32	32	32	34
	25th percentile	53	53	49	44	38	36	35	36	38	42	46	51
	Median	59	57	53	47	41	37	37	38	41	47	51	57
	75th percentile	65	62	58	51	44	39	39	41	45	51	57	63
	Max	86	82	79	66	53	45	45	52	64	77	87	84
2010-2049 & RCP2.6	Median	61	59	55	49	42	38	38	39	43	49	54	60
	% change	3%	3%	3%	4%	4%	2%	3%	3%	5%	5%	6%	5%
	25th percentile	54	54	51	45	39	36	36	37	40	44	48	53
	% change	3%	2%	3%	3%	3%	2%	2%	2%	4%	4%	5%	4%
	75th percentile	67	64	60	53	45	40	40	42	47	54	61	67
	% change	4%	3%	4%	4%	4%	3%	3%	4%	5%	6%	6%	6%
	Max	89	85	82	70	56	48	48	56	70	84	95	90
% change	4%	4%	5%	5%	6%	5%	5%	6%	9%	9%	8%	7%	
2010-2049 & RCP4.5	Median	62	58	55	49	42	38	38	39	43	49	53	59
	% change	6%	2%	4%	3%	4%	2%	3%	3%	4%	6%	3%	4%
	25th percentile	56	53	51	45	39	36	36	37	40	44	47	52
	% change	5%	2%	4%	3%	3%	2%	2%	2%	3%	5%	3%	3%
	75th percentile	69	63	61	52	45	40	40	42	47	55	59	65
	% change	6%	2%	5%	3%	4%	3%	4%	3%	5%	7%	4%	4%
	Max	92	84	83	69	56	48	48	56	69	84	91	88
% change	7%	2%	6%	4%	6%	5%	6%	6%	9%	10%	5%	5%	
2010-2049 & RCP8.5	Median	61	59	56	49	43	39	38	39	43	49	54	60
	% change	5%	3%	5%	4%	5%	4%	3%	3%	5%	6%	6%	5%
	25th percentile	55	54	51	45	40	37	36	37	40	44	49	53
	% change	4%	3%	5%	4%	4%	3%	2%	2%	4%	5%	5%	4%
	75th percentile	68	64	61	53	46	41	40	42	47	55	61	67
	% change	5%	3%	5%	5%	6%	5%	4%	4%	6%	7%	7%	6%
	Max	91	86	84	70	58	49	48	56	70	85	96	90
% change	6%	4%	7%	6%	9%	8%	6%	7%	10%	11%	9%	7%	

The findings show a mild increase in daily water intake from the historic period to the 2010-2049 period (3-11% increase over historic values). The rise in daily water intake is highest in the RCP8.5 scenario. There is a relatively larger increase in maximal intake values compared to the increased in the median intake. This is consistent with a higher frequency of climate events that induce short term increases in water intake while the overall impact on routine water impact (as expressed by median water intake) is less substantive.

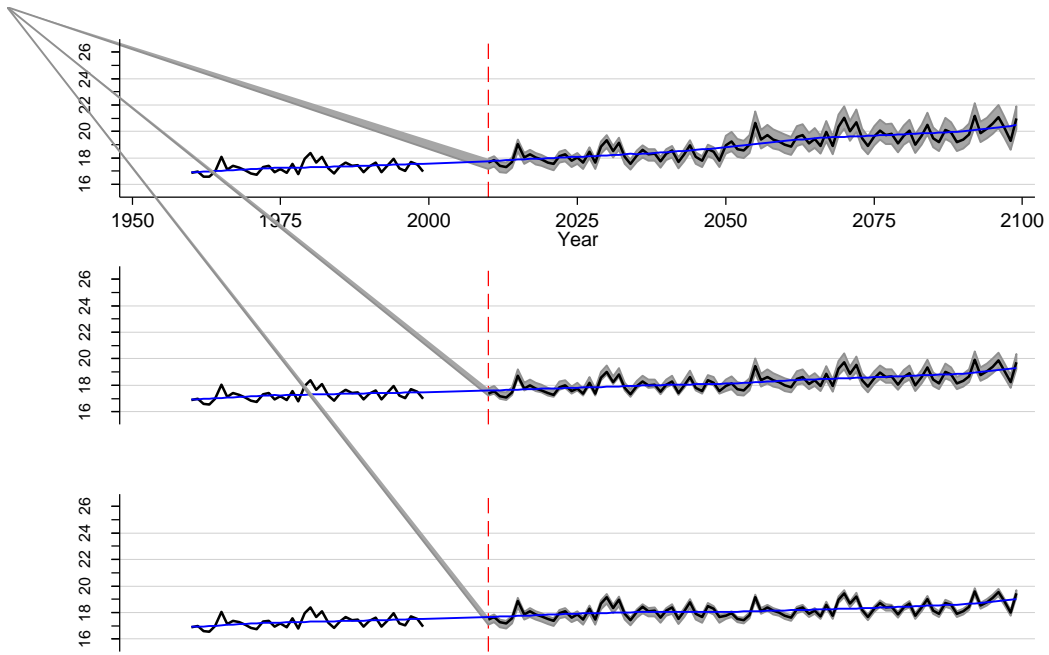
Table 4.105: Summary statistics for daily water intake (L/hd/day) by month of year for Carroona for the historic period (1960-1999) and for each of three scenarios in 2050-2099. Summary statistics for the future period are derived from all five model outputs within each scenario. % changes are based on comparison to the same statistics from the historic period. perc=percentile.

Source	Measure	Month											
		1	2	3	4	5	6	7	8	9	10	11	12
1960-1999 (historic)	Min	37	36	34	34	31	30	31	31	32	32	32	34
	25th perc	53	53	49	44	38	36	35	36	38	42	46	51
	Median	59	57	53	47	41	37	37	38	41	47	51	57
	75th perc	65	62	58	51	44	39	39	41	45	51	57	63
	Max	86	82	79	66	53	45	45	52	64	77	87	84
2050-99 & RCP2.6	Median	63	61	56	50	43	39	38	40	44	50	54	61
	% change	8%	6%	6%	5%	6%	5%	4%	5%	7%	7%	7%	7%
	25th perc	56	56	52	45	40	37	36	38	40	45	49	54
	% change	7%	6%	5%	4%	5%	4%	3%	4%	5%	6%	5%	6%
	75th perc	70	67	62	54	46	41	41	43	49	56	61	67
	% change	9%	7%	6%	6%	6%	6%	5%	6%	9%	9%	8%	7%
	Max	93	93	85	71	57	49	49	60	71	85	95	91
% change	9%	13%	8%	7%	8%	8%	7%	15%	11%	11%	9%	9%	
2050-99 & RCP4.5	Median	62	61	57	50	44	40	39	41	45	51	55	61
	% change	6%	7%	7%	7%	7%	7%	6%	7%	9%	10%	8%	7%
	25th perc	56	56	52	46	41	37	37	38	41	46	49	54
	% change	6%	6%	7%	6%	6%	5%	4%	6%	7%	8%	6%	7%
	75th perc	70	67	62	55	47	42	41	44	50	58	62	68
	% change	8%	8%	8%	8%	9%	8%	7%	9%	12%	12%	9%	7%
	Max	92	94	86	73	59	51	50	63	74	89	97	92
% change	7%	14%	10%	10%	11%	12%	11%	21%	16%	16%	11%	9%	
2050-99 & RCP8.5	Median	67	63	61	53	45	41	40	42	47	54	58	65
	% change	15%	11%	15%	12%	11%	10%	9%	10%	14%	17%	14%	14%
	25th perc	60	58	56	48	42	38	38	39	43	48	51	57
	% change	13%	9%	13%	11%	10%	8%	7%	9%	11%	14%	11%	12%
	75th perc	76	69	67	58	49	44	43	46	53	62	66	72
	% change	17%	11%	16%	14%	13%	12%	11%	13%	18%	21%	16%	14%
	Max	101	98	94	78	62	54	53	67	80	98	105	99
% change	18%	19%	20%	18%	18%	18%	18%	29%	26%	28%	20%	17%	

The findings show a moderate to substantive increase in daily water intake from the historic period to the 2050-2099 period (4-29% increase over historic values). The rise in daily water intake is highest in the RCP8.5 scenario. There is a relatively larger increase in maximal intake values compared to the increase in the median intake. This is consistent with a higher frequency of climate events that induce short term increases in water intake while the overall impact on routine water intake (as expressed by median water intake) is less substantive.

Table 4.106: summary statistics for water intake at Caroona expressed as ML per thousand head per year, based on aggregating daily water intake estimates to produce an annual estimate.

Year	Model	Scenario	min	p25	median	p75	max
(ML / '000 head / year)							
1960-1999	None	None	16.6	16.9	17.2	17.5	18.4
2010-2049	Combined	RCP2.6	17.1	17.5	17.9	18.3	19.1
			<i>% change from historic</i>	3%	4%	4%	4%
	Combined	RCP4.5	17.2	17.6	17.9	18.3	19.1
			<i>% change from historic</i>	4%	4%	4%	4%
	Combined	RCP8.5	17.3	17.7	18.0	18.4	19.3
			<i>% change from historic</i>	4%	4%	4%	5%
2050-2099	Combined	RCP2.6	17.4	17.9	18.3	18.7	19.6
			<i>% change from historic</i>	5%	6%	6%	7%
	Combined	RCP4.5	17.7	18.2	18.6	19.0	20.0
			<i>% change from historic</i>	7%	8%	8%	9%
	Combined	RCP8.5	18.5	19.1	19.6	20.0	21.1
			<i>% change from historic</i>	12%	13%	14%	15%



Annual water intake at Carroona:
RCP8.5 (top), RCP4.5 (middle) & RCP2.6 (bottom) scenarios

Figure 4.40: Plot of annual water intake (ML/1000 head/year) at Carroona by year for each of three scenarios over two periods (1960-1999 and 2010-2099). Water intake for 2010-2099 shows the range from minimum to maximum annual values across the five models (shaded area) and the median (black line). The blue line shows a smoothed long-term average.

4.4.2 Comet

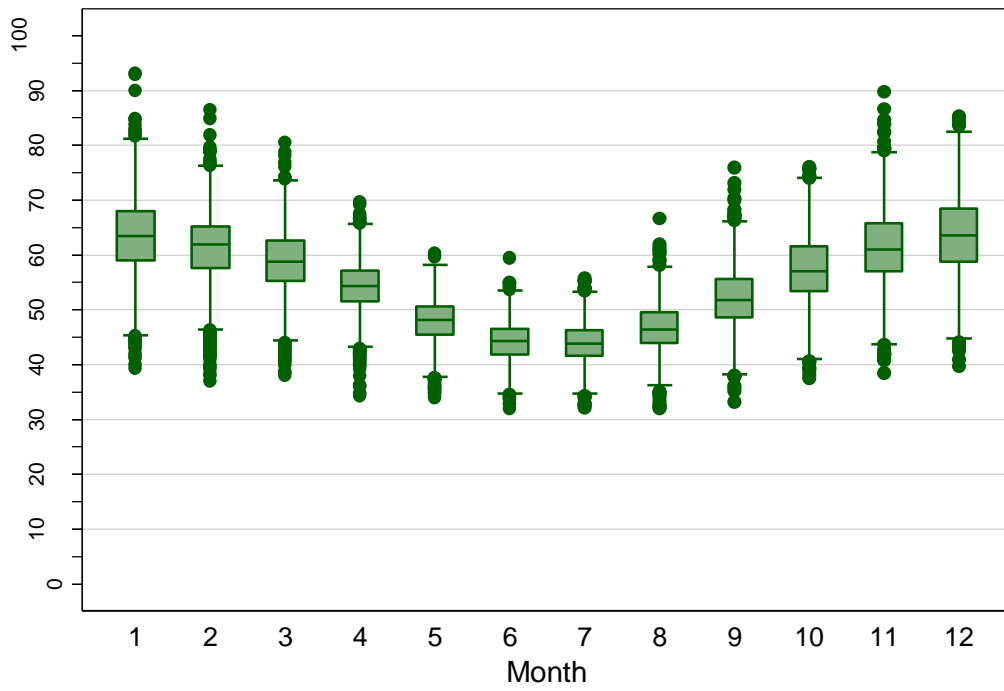
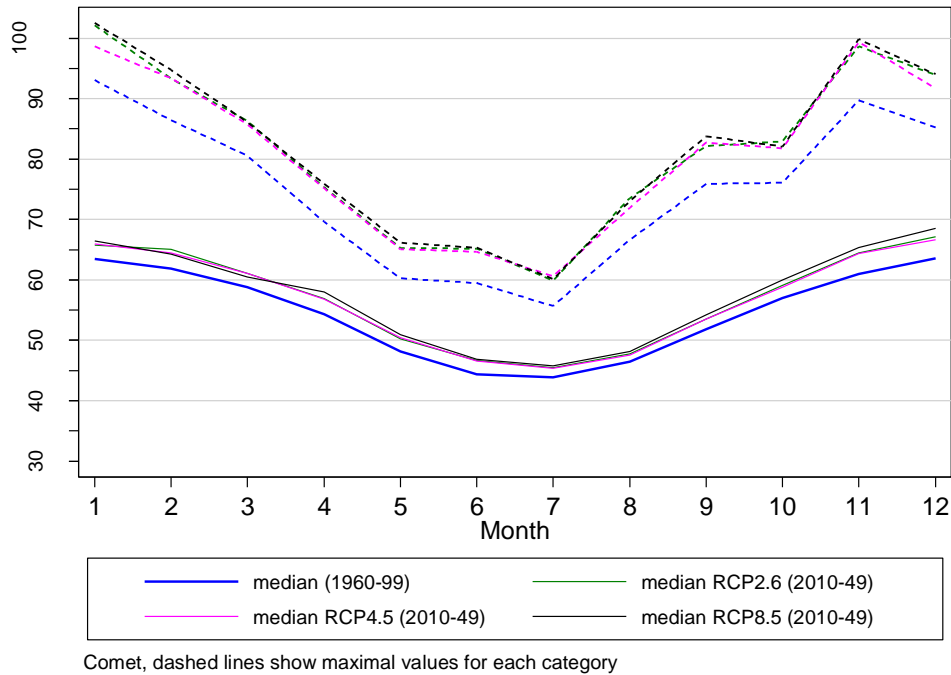
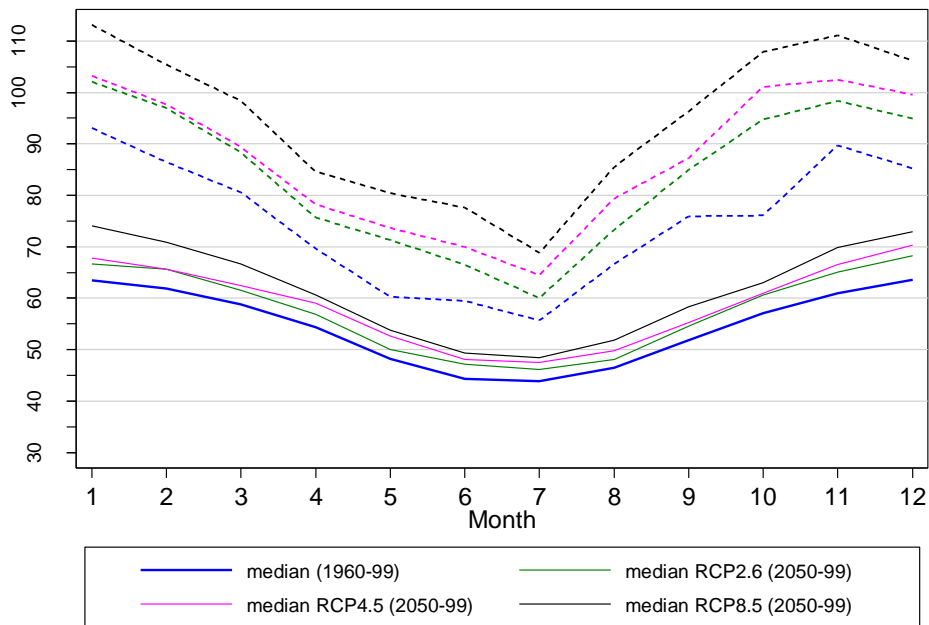


Figure 4.41: Box plot showing median water usage (L/hd/day) at Comet by month from daily predictions over the period 1960-1999.



Comet, dashed lines show maximal values for each category

Figure 4.42: Predicted median daily water intake by month of year at Comet for the period from 2010-2049 (solid lines). The solid blue line is the median predicted water intake from the historic period (1960-1999), provided for comparative purposes. Dashed lines shows the maximum daily water intake for each month.



Comet, dashed lines show maximal values for each category

Figure 4.43: Predicted median daily water intake by month of year at Comet for the period from 2050-2099 (solid lines). The solid blue line is the median predicted water intake from the historic period (1960-1999), provided for comparative purposes. Dashed lines shows the maximum daily water intake for each month.

Table 4.107: Summary statistics for daily water intake (L/hd/day) by month of year for Comet for the historic period (1960-1999) and for each of three scenarios in 2010-2049. Summary statistics for the future period are derived from all five model outputs within each scenario. % changes are based on comparison to the same statistics from the historic period. perc = percentile.

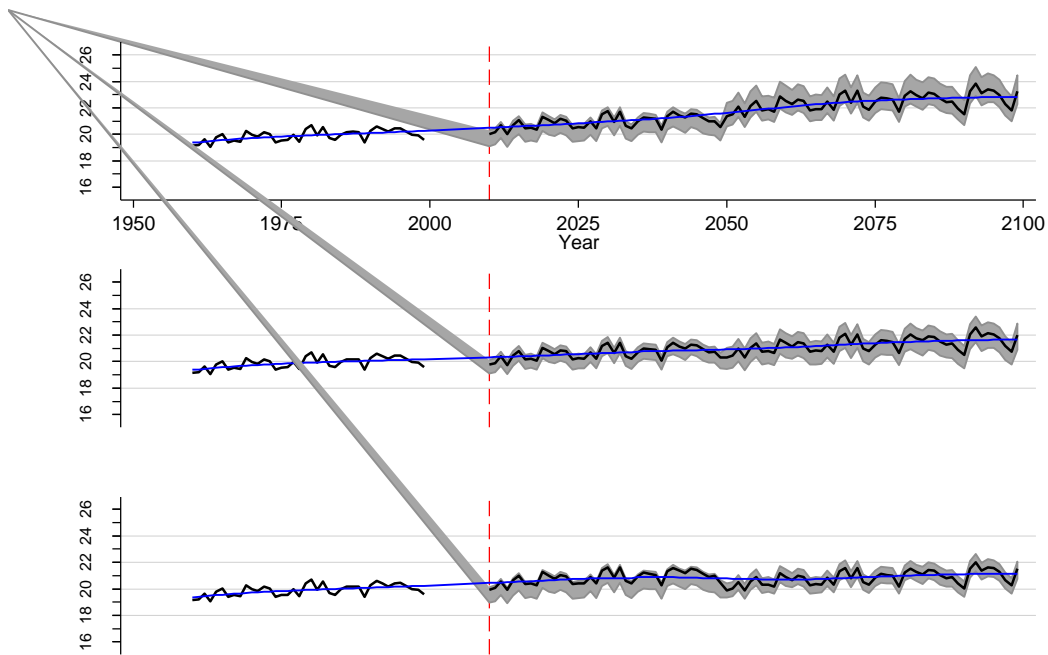
Source	Measure	Month											
		1	2	3	4	5	6	7	8	9	10	11	12
1960-1999 (historic)	Min	39	37	38	34	34	32	32	32	33	37	38	40
	25th perc	59	58	55	51	45	42	41	44	49	53	57	59
	Median	63	62	59	54	48	44	44	46	52	57	61	64
	75th perc	68	65	63	57	51	46	46	50	56	62	66	68
	Max	93	86	81	70	60	59	56	67	76	76	90	85
2010-2049 & RCP2.6	Median	66	65	61	57	50	47	45	48	53	59	64	67
	% change	4%	5%	4%	5%	4%	5%	4%	3%	3%	4%	6%	6%
	25th perc	61	60	57	54	47	44	43	45	50	55	60	62
	% change	3%	5%	4%	4%	4%	5%	3%	3%	3%	3%	6%	5%
	75th perc	71	69	65	60	53	49	48	51	58	64	70	73
	% change	4%	5%	4%	5%	5%	6%	4%	3%	3%	4%	6%	6%
	Max	98	92	85	74	64	64	59	70	79	80	96	91
% change	5%	6%	5%	6%	6%	8%	5%	5%	5%	5%	7%	7%	
2010-2049 & RCP4.5	Median	66	64	61	57	50	47	45	48	53	59	64	67
	% change	4%	4%	4%	5%	5%	5%	4%	2%	3%	3%	6%	5%
	25th perc	61	60	57	54	47	44	43	45	50	55	60	61
	% change	4%	4%	4%	4%	4%	4%	3%	2%	3%	3%	5%	4%
	75th perc	71	68	65	60	53	49	48	51	58	64	70	72
	% change	4%	4%	4%	5%	5%	6%	4%	3%	3%	3%	6%	5%
	Max	98	91	85	74	64	64	59	69	80	79	96	90
% change	5%	5%	5%	6%	6%	8%	5%	4%	5%	4%	7%	6%	
2010-2049 & RCP8.5	Median	66	64	61	58	51	47	46	48	54	60	65	69
	% change	5%	4%	3%	7%	6%	6%	4%	4%	5%	5%	7%	8%
	25th perc	61	60	57	55	48	44	43	45	51	56	61	63
	% change	4%	4%	3%	6%	5%	5%	4%	3%	4%	5%	7%	7%
	75th perc	71	68	65	61	54	49	49	52	58	65	71	74
	% change	5%	4%	3%	7%	6%	6%	5%	4%	5%	6%	8%	8%
	Max	99	91	84	76	65	65	59	70	81	81	98	93
% change	6%	5%	4%	9%	8%	9%	6%	6%	7%	6%	9%	9%	

Table 4.108: Summary statistics for daily water intake (L/hd/day) by month of year for Comet for the historic period (1960-1999) and for each of three scenarios in 2050-2099. Summary statistics for the future period are derived from all five model outputs within each scenario. % changes are based on comparison to the same statistics from the historic period. perc= percentile.

Source	Measure	Month											
		1	2	3	4	5	6	7	8	9	10	11	12
1960-1999 (historic)	Min	39	37	38	34	34	32	32	32	33	37	38	40
	25th perc	59	58	55	51	45	42	41	44	49	53	57	59
	Median	63	62	59	54	48	44	44	46	52	57	61	64
	75th perc	68	65	63	57	51	46	46	50	56	62	66	68
	Max	93	86	81	70	60	59	56	67	76	76	90	85
2050-99 & RCP2.6	Median	67	66	62	57	50	47	46	48	55	61	65	68
	% change	5%	6%	5%	5%	4%	6%	5%	3%	5%	6%	7%	7%
	25th perc	62	61	58	54	47	44	43	45	51	57	61	63
	% change	5%	5%	5%	4%	4%	5%	5%	3%	5%	6%	6%	7%
	75th perc	72	70	65	60	53	50	49	51	59	66	71	74
	% change	5%	7%	4%	5%	4%	7%	6%	3%	6%	7%	7%	8%
	Max	99	93	85	73	68	65	60	70	81	92	97	94
% change	6%	7%	5%	5%	12%	10%	7%	5%	6%	21%	8%	10%	
2050-99 & RCP4.5	Median	68	66	62	59	53	48	47	50	55	61	67	70
	% change	7%	6%	6%	9%	9%	8%	8%	7%	7%	7%	9%	11%
	25th perc	63	60	59	56	49	45	44	47	51	57	62	65
	% change	7%	5%	6%	8%	9%	7%	7%	6%	6%	6%	9%	10%
	75th perc	73	70	66	62	56	51	50	53	60	66	72	76
	% change	7%	7%	6%	9%	10%	10%	9%	8%	7%	8%	10%	11%
	Max	101	93	86	77	72	67	62	73	82	93	100	97
% change	9%	7%	7%	10%	20%	13%	12%	10%	8%	22%	11%	14%	
2050-99 & RCP8.5	Median	74	71	67	61	54	49	48	52	58	63	70	73
	% change	17%	14%	13%	12%	12%	11%	11%	12%	13%	10%	15%	15%
	25th perc	68	65	63	57	50	46	45	48	54	59	65	67
	% change	16%	13%	13%	11%	11%	9%	9%	10%	11%	10%	14%	14%
	75th perc	80	75	71	64	57	53	52	56	63	69	76	79
	% change	18%	16%	13%	12%	13%	13%	12%	13%	14%	11%	16%	15%
	Max	112	101	93	80	75	70	64	78	89	97	106	101
% change	21%	17%	16%	14%	24%	18%	15%	17%	17%	28%	19%	19%	

Table 4.109: summary statistics for water intake at Comet expressed as ML per thousand head per year, based on aggregating daily water intake estimates to produce an annual estimate.

Year	Model	Scenario	min	p25	median	p75	max
(ML / '000 head / year)							
1960-1999	None	None	19.1	19.5	20.0	20.2	20.7
2010-2049	Combined	RCP2.6	19.7	20.2	20.7	20.9	21.4
<i>% change from historic</i>			3%	3%	4%	4%	3%
	Combined	RCP4.5	19.7	20.1	20.6	20.9	21.4
<i>% change from historic</i>			3%	3%	3%	3%	3%
	Combined	RCP8.5	19.9	20.3	20.8	21.1	21.6
<i>% change from historic</i>			4%	4%	4%	4%	4%
2050-2099	Combined	RCP2.6	19.9	20.4	20.9	21.3	22.1
<i>% change from historic</i>			4%	4%	5%	5%	7%
	Combined	RCP4.5	20.2	20.8	21.3	21.7	22.5
<i>% change from historic</i>			6%	6%	7%	8%	9%
	Combined	RCP8.5	21.3	21.9	22.5	23.0	23.8
<i>% change from historic</i>			12%	12%	13%	14%	15%



Annual water intake at Comet:
RCP8.5 (top), RCP4.5 (middle) & RCP2.6 (bottom) scenarios

Figure 4.44: Plot of annual water intake (ML/1000 head/year) at Comet by year for each of three scenarios over two periods (1960-1999 and 2010-2099). Water intake for 2010-2099 shows the range from minimum to maximum annual values across the five models (shaded area) and the median (black line). The blue line shows a smoothed long-term average.

4.4.3 Dalby

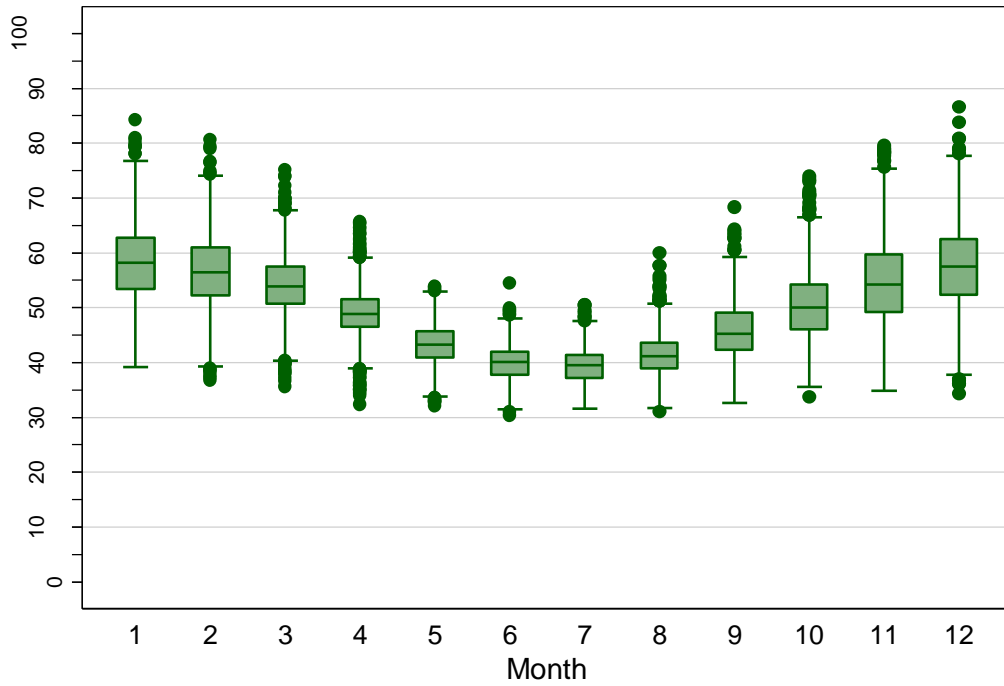


Figure 4.45: Box plot showing median water usage (L/hd/day) at Dalby by month from daily predictions over the period 1960-1999.

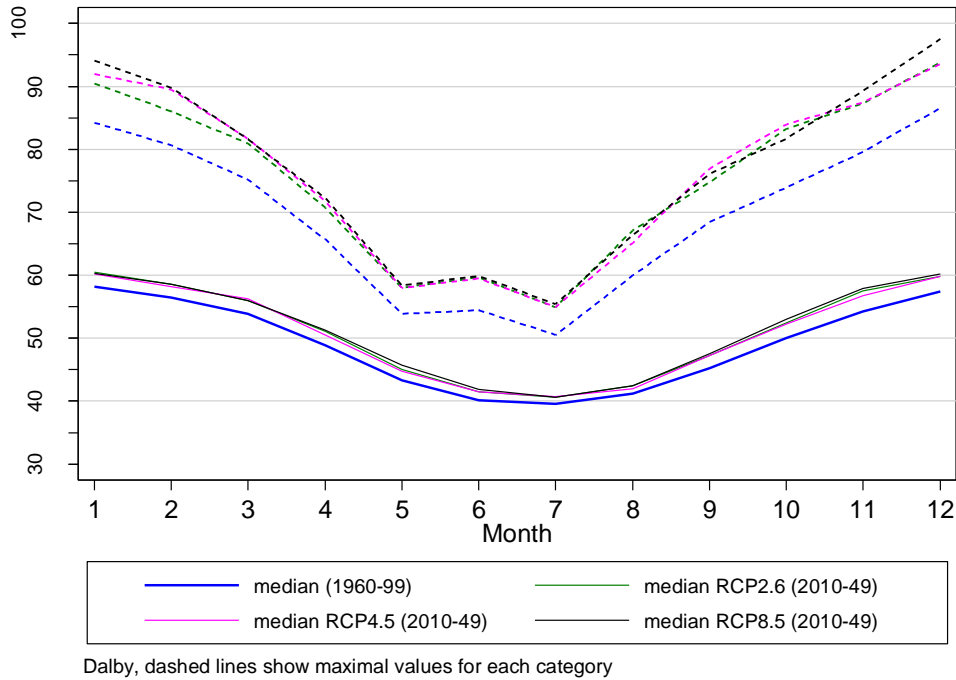


Figure 4.46: Predicted median daily water intake by month of year at Dalby for the period from 2010-2049 (solid lines). The solid blue line is the median predicted water intake from the historic period (1960-1999), provided for comparative purposes. Dashed lines shows the maximum daily water intake for each month.

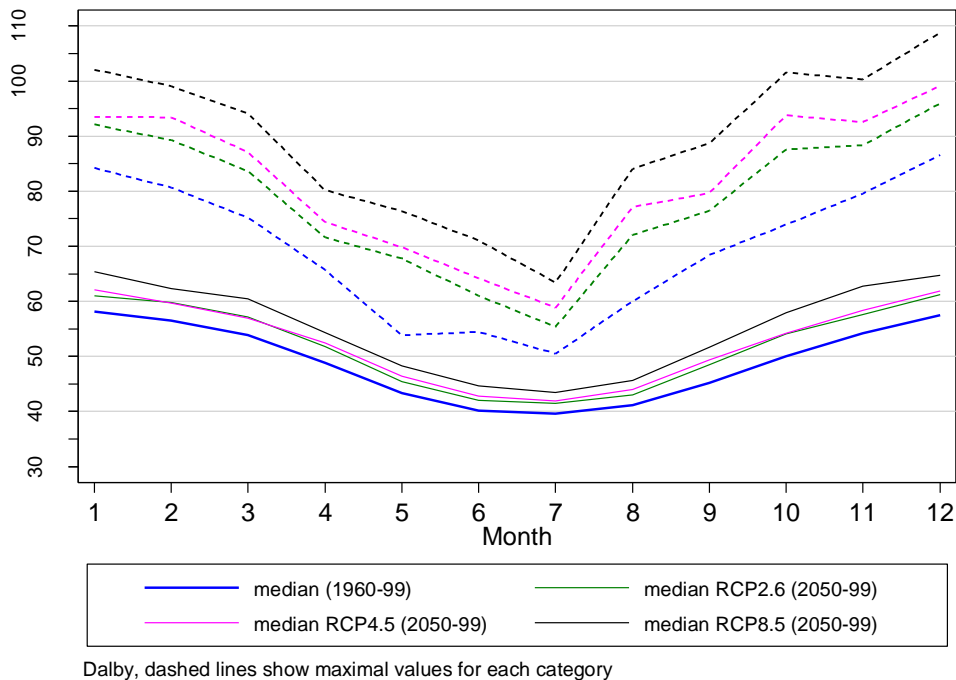


Figure 4.47: Predicted median daily water intake by month of year at Dalby for the period from 2050-2099 (solid lines). The solid blue line is the median predicted water intake from the historic period (1960-1999), provided for comparative purposes. Dashed lines shows the maximum daily water intake for each month.

Table 4.110: Summary statistics for daily water intake (L/hd/day) by month of year for Dalby for the historic period (1960-1999) and for each of three scenarios in 2010-2049. Summary statistics for the future period are derived from all five model outputs within each scenario. % changes are based on comparison to the same statistics from the historic period. perc = percentile.

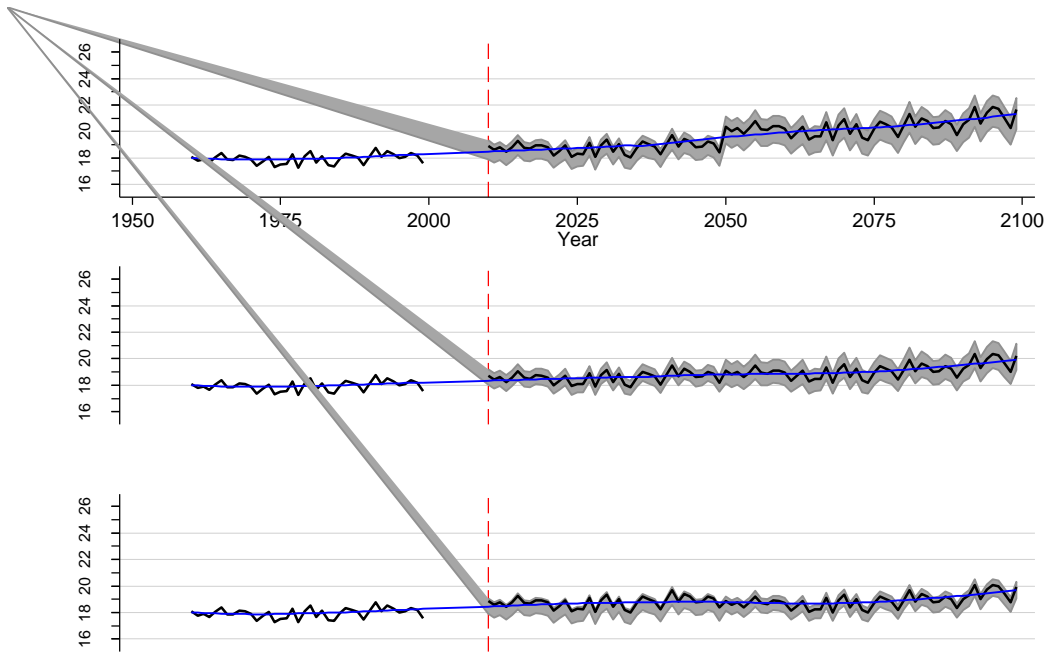
Source	Measure	Month											
		1	2	3	4	5	6	7	8	9	10	11	12
1960-1999 (historic)	Min	39	37	36	32	32	30	32	31	33	34	35	34
	25th perc	53	52	51	46	41	38	37	39	42	46	49	52
	Median	58	56	54	49	43	40	40	41	45	50	54	57
	75th perc	63	61	58	52	46	42	41	44	49	54	60	62
	Max	84	81	75	66	54	54	51	60	68	74	80	87
2010-2049 & RCP2.6	Median	60	59	56	51	45	41	41	42	47	52	58	60
	% change	4%	4%	4%	4%	4%	3%	3%	3%	5%	5%	6%	4%
	25th perc	55	54	52	48	42	39	38	40	44	48	52	54
	% change	4%	3%	4%	4%	3%	3%	2%	3%	4%	4%	5%	4%
	75th perc	65	63	60	54	48	44	43	45	52	57	64	65
	% change	4%	4%	4%	5%	5%	4%	3%	4%	5%	6%	6%	5%
	Max	89	85	79	70	57	58	53	64	74	79	86	91
% change	5%	5%	5%	6%	6%	6%	4%	6%	8%	7%	8%	6%	
2010-2049 & RCP4.5	Median	60	58	56	50	45	41	41	42	47	52	57	60
	% change	4%	3%	4%	3%	3%	3%	3%	2%	5%	5%	5%	4%
	25th perc	55	54	53	48	42	39	38	39	44	48	51	54
	% change	3%	3%	4%	3%	3%	3%	2%	2%	4%	4%	4%	4%
	75th perc	65	63	60	53	47	44	43	45	52	57	63	65
	% change	4%	3%	5%	4%	4%	4%	3%	2%	5%	5%	5%	4%
	Max	88	84	80	69	57	58	53	62	74	79	85	91
% change	5%	4%	6%	5%	5%	6%	5%	4%	8%	7%	6%	6%	
2010-2049 & RCP8.5	Median	60	59	56	51	46	42	41	42	48	53	58	60
	% change	4%	4%	4%	5%	6%	4%	3%	3%	5%	6%	7%	5%
	25th perc	55	54	52	49	43	39	38	40	44	48	52	55
	% change	3%	3%	4%	5%	5%	3%	2%	3%	4%	5%	6%	4%
	75th perc	65	63	60	54	49	44	43	45	52	58	64	66
	% change	4%	4%	4%	5%	6%	5%	3%	4%	6%	7%	7%	5%
	Max	89	85	79	70	58	59	53	64	74	80	87	92
% change	5%	5%	5%	7%	8%	8%	5%	6%	9%	9%	9%	6%	

Table 4.111: Summary statistics for daily water intake (L/hd/day) by month of year for Dalby for the historic period (1960-1999) and for each of three scenarios in 2050-2099. Summary statistics for the future period are derived from all five model outputs within each scenario. % changes are based on comparison to the same statistics from the historic period. perc = percentile.

Source	Measure	Month											
		1	2	3	4	5	6	7	8	9	10	11	12
1960-1999 (historic)	Min	39	37	36	32	32	30	32	31	33	34	35	34
	25th perc	53	52	51	46	41	38	37	39	42	46	49	52
	Median	58	56	54	49	43	40	40	41	45	50	54	57
	75th perc	63	61	58	52	46	42	41	44	49	54	60	62
	Max	84	81	75	66	54	54	51	60	68	74	80	87
2050-99 & RCP2.6	Median	61	60	57	52	45	42	41	43	48	54	58	61
	% change	5%	6%	6%	6%	5%	5%	5%	4%	7%	8%	6%	7%
	25th perc	56	55	54	49	43	39	39	40	45	49	52	56
	% change	5%	5%	6%	5%	4%	4%	4%	4%	6%	7%	6%	6%
	75th perc	66	65	61	55	48	44	44	46	53	59	64	67
	% change	5%	7%	6%	7%	5%	6%	6%	5%	8%	10%	7%	7%
	Max	89	88	83	71	65	59	54	68	75	85	86	94
% change	6%	9%	10%	8%	21%	8%	7%	14%	9%	15%	8%	8%	
2050-99 & RCP4.5	Median	62	60	57	52	46	43	42	44	49	54	58	62
	% change	7%	6%	6%	7%	7%	7%	6%	7%	9%	8%	8%	8%
	25th perc	57	55	53	50	43	40	39	41	45	49	53	56
	% change	7%	5%	5%	7%	6%	5%	5%	6%	7%	7%	7%	7%
	75th perc	67	65	61	56	49	45	44	47	54	60	65	68
	% change	7%	7%	6%	8%	8%	8%	7%	8%	11%	10%	8%	8%
	Max	91	88	83	72	67	61	55	72	77	86	88	95
% change	9%	9%	10%	10%	25%	11%	9%	20%	13%	16%	10%	10%	
2050-99 & RCP8.5	Median	65	62	60	54	48	45	43	46	52	58	63	65
	% change	12%	10%	12%	11%	12%	11%	10%	11%	14%	16%	16%	13%
	25th perc	60	57	56	51	45	41	40	42	47	52	56	58
	% change	12%	9%	11%	10%	10%	9%	8%	9%	12%	13%	14%	12%
	75th perc	71	68	65	58	52	48	46	49	57	64	70	71
	% change	14%	12%	13%	12%	13%	13%	11%	13%	17%	18%	17%	14%
	Max	98	93	89	76	72	65	58	77	83	94	96	101
% change	16%	15%	19%	15%	33%	20%	16%	28%	21%	27%	21%	16%	

Table 4.112: summary statistics for water intake at Dalby expressed as ML per thousand head per year, based on aggregating daily water intake estimates to produce an annual estimate.

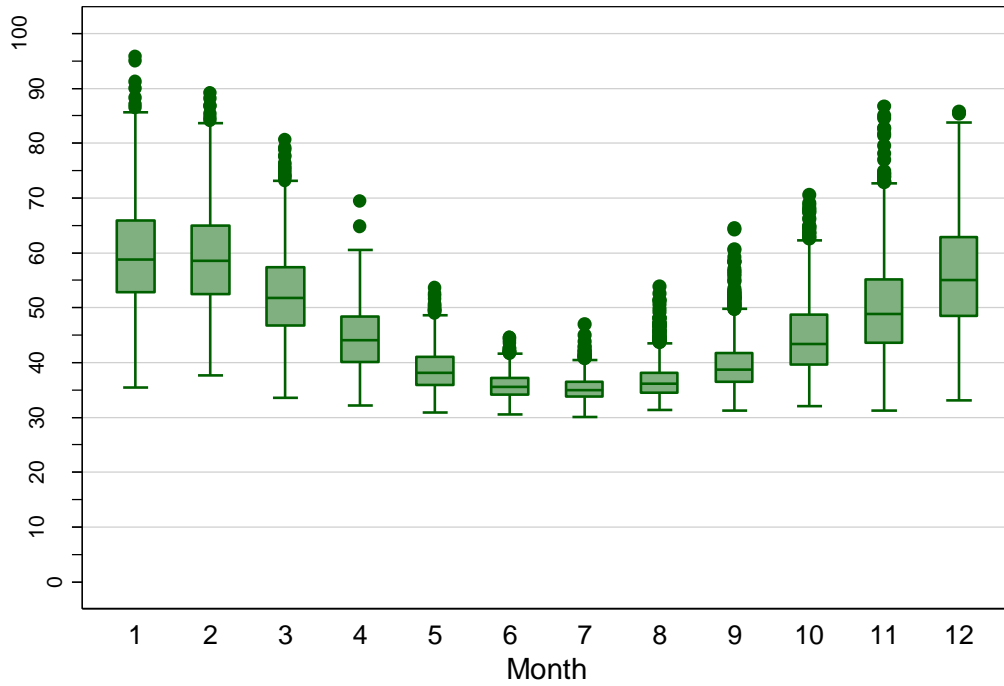
Year	Model	Scenario	min	p25	median	p75	max
(ML / '000 head / year)							
1960-1999	None	None	17.3	17.6	18.0	18.2	18.8
2010-2049	Combined	RCP2.6	17.8	18.2	18.6	18.8	19.5
<i>% change from historic</i>			3%	3%	3%	4%	4%
	Combined	RCP4.5	17.9	18.2	18.6	18.8	19.5
<i>% change from historic</i>			3%	3%	3%	4%	4%
	Combined	RCP8.5	17.9	18.3	18.7	18.9	19.6
<i>% change from historic</i>			4%	4%	4%	4%	4%
2050-2099	Combined	RCP2.6	18.0	18.5	18.8	19.2	20.1
<i>% change from historic</i>			4%	5%	5%	6%	7%
	Combined	RCP4.5	18.3	18.9	19.2	19.5	20.5
<i>% change from historic</i>			6%	7%	6%	8%	9%
	Combined	RCP8.5	19.2	19.9	20.2	20.6	21.7
<i>% change from historic</i>			11%	13%	12%	13%	15%



Annual water intake at Dalby:
RCP8.5 (top), RCP4.5 (middle) & RCP2.6 (bottom) scenarios

Figure 4.48: Plot of annual water intake (ML/1000 head/year) at Dalby by year for each of three scenarios over two periods (1960-1999 and 2010-2099). Water intake for 2010-2099 shows the range from minimum to maximum annual values across the five models (shaded area) and the median (black line). The blue line shows a smoothed long-term average.

4.4.4 Leeton



Daily water intake for 1960-1999 at Leeton, using methods in Parker et al (2000)

Figure 4.49: Box plot showing median water usage (L/hd/day) at Leeton by month from daily predictions over the period 1960-1999.

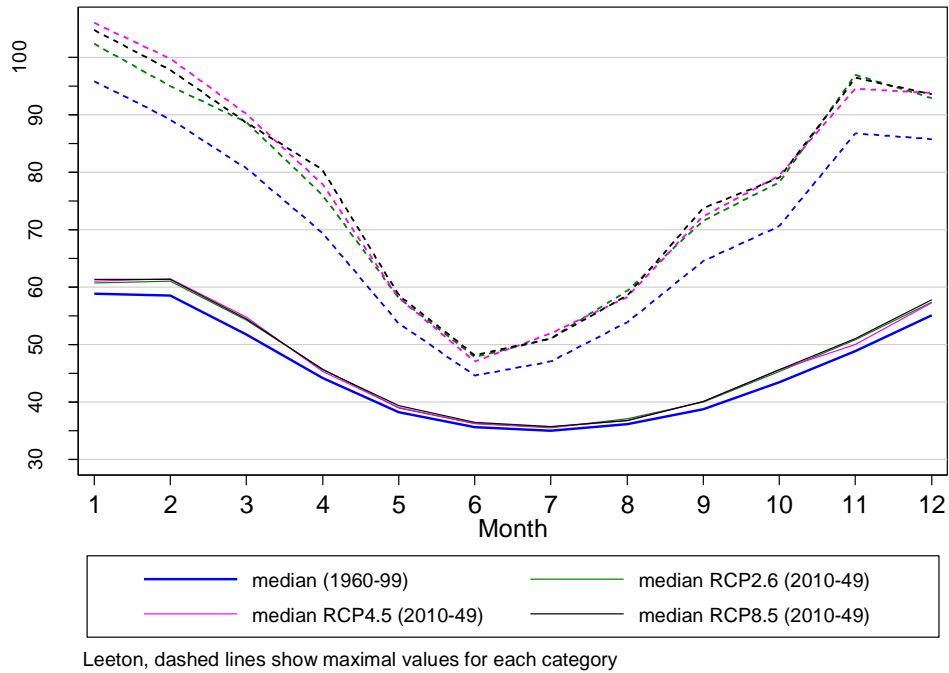


Figure 4.50: Predicted median daily water intake by month of year at Leeton for the period from 2010-2049 (solid lines). The solid blue line is the median predicted water intake from the historic period (1960-1999), provided for comparative purposes. Dashed lines shows the maximum daily water intake for each month.

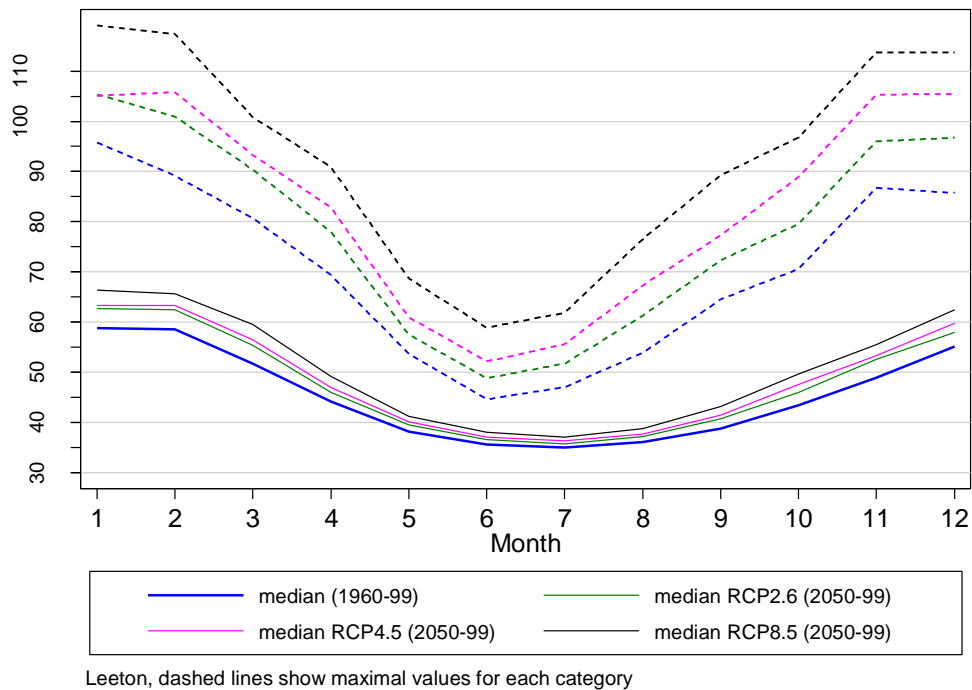


Figure 4.51: Predicted median daily water intake by month of year at Carroona for the period from 2050-2099 (solid lines). The solid blue line is the median predicted water intake from the historic period (1960-1999), provided for comparative purposes. Dashed lines shows the maximum daily water intake for each month.

Table 4.113: Summary statistics for daily water intake (L/hd/day) by month of year for Leeton for the historic period (1960-1999) and for each of three scenarios in 2010-2049. Summary statistics for the future period are derived from all five model outputs within each scenario. % changes are based on comparison to the same statistics from the historic period. perc = percentile.

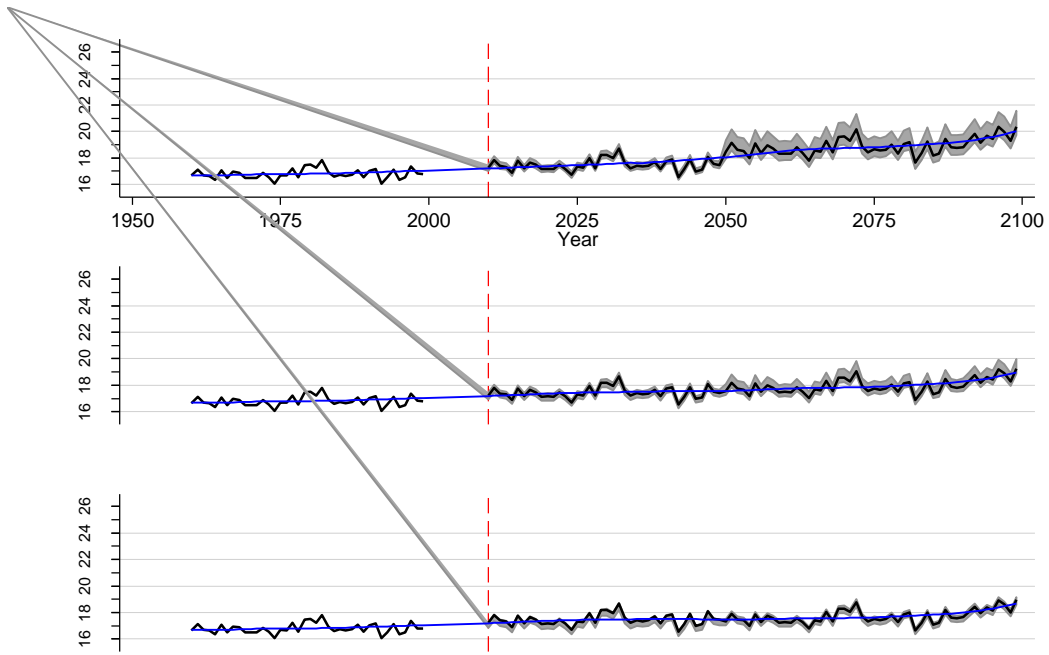
Source	Measure	Month											
		1	2	3	4	5	6	7	8	9	10	11	12
1960-1999 (historic)	Min	35	38	34	32	31	31	30	31	31	32	31	33
	25th perc	53	53	47	40	36	34	34	35	36	40	44	48
	Median	59	59	52	44	38	36	35	36	39	43	49	55
	75th perc	66	65	57	48	41	37	36	38	42	49	55	63
	Max	96	89	81	69	54	45	47	54	64	71	87	86
2010-2049 & RCP2.6	Median	61	61	54	46	39	36	36	37	40	45	51	57
	% change	3%	4%	5%	4%	2%	2%	1%	3%	3%	4%	4%	4%
	25th perc	54	54	49	41	36	35	34	35	37	41	45	50
	% change	3%	4%	4%	3%	1%	1%	1%	2%	2%	3%	3%	3%
	75th perc	68	68	60	51	42	38	37	39	43	51	58	66
	% change	4%	5%	5%	5%	3%	3%	2%	3%	4%	5%	5%	5%
	Max	100	94	86	74	57	47	49	58	70	76	93	91
% change	5%	6%	7%	7%	5%	5%	5%	8%	8%	8%	7%	6%	
2010-2049 & RCP4.5	Median	61	61	55	45	39	36	36	37	40	46	50	57
	% change	4%	5%	6%	3%	2%	2%	2%	2%	3%	5%	2%	4%
	25th perc	55	55	49	41	36	35	34	35	37	41	44	50
	% change	3%	4%	5%	2%	2%	1%	1%	1%	2%	4%	2%	3%
	75th perc	69	69	61	50	42	38	37	39	44	52	57	66
	% change	4%	6%	6%	3%	3%	2%	3%	2%	4%	6%	3%	4%
	Max	101	95	88	73	56	47	50	57	70	77	90	90
% change	5%	7%	9%	5%	5%	4%	6%	5%	9%	9%	4%	5%	
2010-2049 & RCP8.5	Median	61	61	54	46	39	36	36	37	40	46	51	58
	% change	4%	5%	5%	3%	3%	2%	2%	2%	4%	5%	4%	5%
	25th perc	55	55	49	41	37	35	34	35	37	41	45	50
	% change	4%	4%	4%	3%	2%	2%	1%	1%	3%	4%	4%	4%
	75th perc	69	68	61	50	43	38	37	39	44	52	58	66
	% change	5%	5%	6%	4%	4%	3%	2%	2%	5%	6%	5%	6%
	Max	102	95	87	74	57	47	50	57	70	77	93	92
% change	6%	7%	8%	6%	7%	6%	6%	6%	9%	9%	8%	7%	

Table 4.114: Summary statistics for daily water intake (L/hd/day) by month of year for Leeton for the historic period (1960-1999) and for each of three scenarios in 2050-2099. Summary statistics for the future period are derived from all five model outputs within each scenario. % changes are based on comparison to the same statistics from the historic period. perc = percentile.

Source	Measure	Month											
		1	2	3	4	5	6	7	8	9	10	11	12
1960-1999 (historic)	Min	35	38	34	32	31	31	30	31	31	32	31	33
	25th perc	53	53	47	40	36	34	34	35	36	40	44	48
	Median	59	59	52	44	38	36	35	36	39	43	49	55
	75th perc	66	65	57	48	41	37	36	38	42	49	55	63
	Max	96	89	81	69	54	45	47	54	64	71	87	86
2050-99 & RCP2.6	Median	63	62	55	46	39	37	36	37	41	46	53	58
	% change	7%	7%	7%	4%	3%	3%	2%	3%	5%	6%	8%	5%
	25th perc	56	55	49	42	37	35	34	35	38	41	46	51
	% change	5%	6%	5%	4%	3%	2%	1%	2%	4%	4%	6%	5%
	75th perc	71	70	62	51	43	38	37	40	45	52	61	66
	% change	8%	7%	7%	5%	4%	4%	3%	4%	7%	6%	10%	6%
	Max	102	100	88	74	57	48	50	61	72	77	95	94
% change	7%	12%	9%	6%	7%	9%	7%	13%	12%	9%	10%	9%	
2050-99 & RCP4.5	Median	63	63	56	47	40	37	36	38	41	48	53	60
	% change	8%	8%	9%	6%	5%	4%	4%	4%	7%	10%	9%	9%
	25th perc	56	56	50	42	37	35	35	36	38	42	47	52
	% change	6%	7%	7%	5%	4%	3%	3%	3%	5%	7%	8%	8%
	75th perc	72	71	63	52	44	39	38	40	46	54	62	69
	% change	9%	9%	10%	8%	7%	5%	5%	6%	10%	11%	11%	9%
	Max	103	102	90	76	59	50	52	63	75	82	97	98
% change	8%	14%	12%	10%	10%	12%	11%	17%	16%	16%	12%	15%	
2050-99 & RCP8.5	Median	66	66	60	49	41	38	37	39	43	50	56	62
	% change	13%	12%	15%	11%	8%	7%	6%	7%	12%	14%	14%	13%
	25th perc	59	58	53	44	38	36	35	36	39	44	49	54
	% change	11%	10%	13%	9%	6%	5%	4%	5%	9%	11%	11%	12%
	75th perc	75	74	67	55	45	41	39	42	48	57	65	72
	% change	14%	13%	16%	14%	10%	9%	7%	10%	15%	17%	17%	15%
	Max	110	107	97	82	62	53	55	68	82	88	104	104
% change	15%	20%	20%	19%	16%	19%	18%	26%	27%	25%	20%	21%	

Table 4.115: summary statistics for water intake at Leeton expressed as ML per thousand head per year, based on aggregating daily water intake estimates to produce an annual estimate.

Year	Model	Scenario	min	p25	median	p75	max
(ML / '000 head / year)							
1960-1999	None	None	16.0	16.5	16.7	17.1	17.8
2010-2049	Combined	RCP2.6	16.5	17.1	17.3	17.7	18.6
<i>% change from historic</i>			3%	3%	4%	3%	4%
	Combined	RCP4.5	16.5	17.1	17.4	17.7	18.6
<i>% change from historic</i>			3%	4%	4%	4%	5%
	Combined	RCP8.5	16.6	17.2	17.4	17.8	18.7
<i>% change from historic</i>			3%	4%	4%	4%	5%
2050-2099	Combined	RCP2.6	16.6	17.3	17.6	18.0	18.9
<i>% change from historic</i>			4%	4%	5%	6%	6%
	Combined	RCP4.5	17.0	17.7	18.0	18.4	19.4
<i>% change from historic</i>			6%	7%	8%	8%	9%
	Combined	RCP8.5	17.7	18.4	18.8	19.3	20.4
<i>% change from historic</i>			10%	11%	13%	13%	14%



Annual water intake at Leeton:
RCP8.5 (top), RCP4.5 (middle) & RCP2.6 (bottom) scenarios

Figure 4.52: Plot of annual water intake (ML/1000 head/year) at Leeton by year for each of three scenarios over two periods (1960-1999 and 2010-2099). Water intake for 2010-2099 shows the range from minimum to maximum annual values across the five models (shaded area) and the median (black line). The blue line shows a smoothed long-term average.

4.4.5 Narrogin

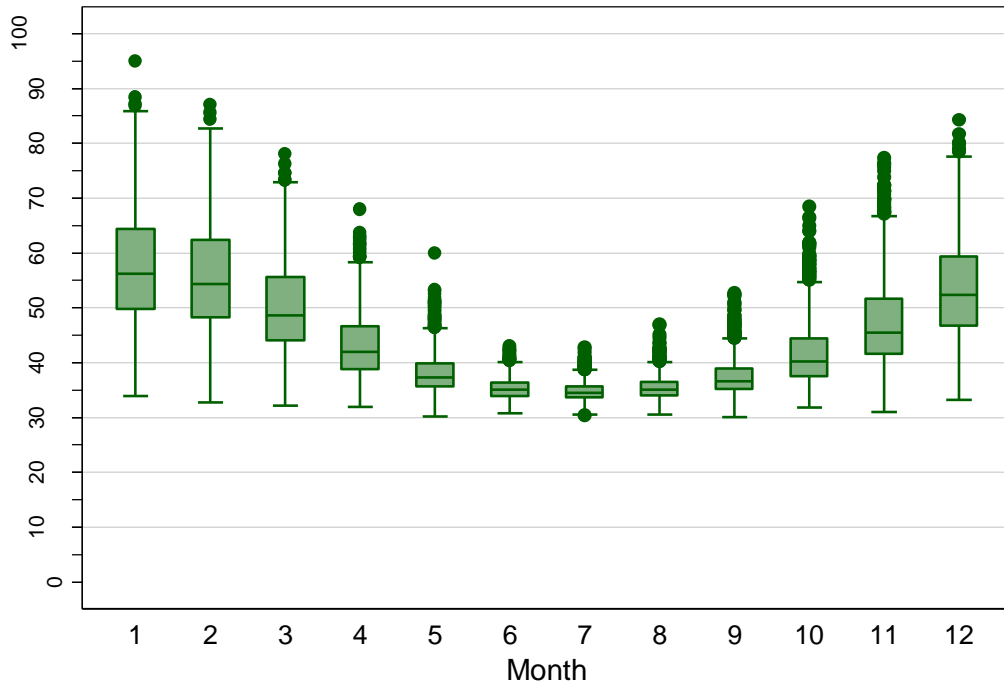


Figure 4.53: Box plot showing median water usage (L/hd/day) at Narrogin by month from daily predictions over the period 1960-1999.

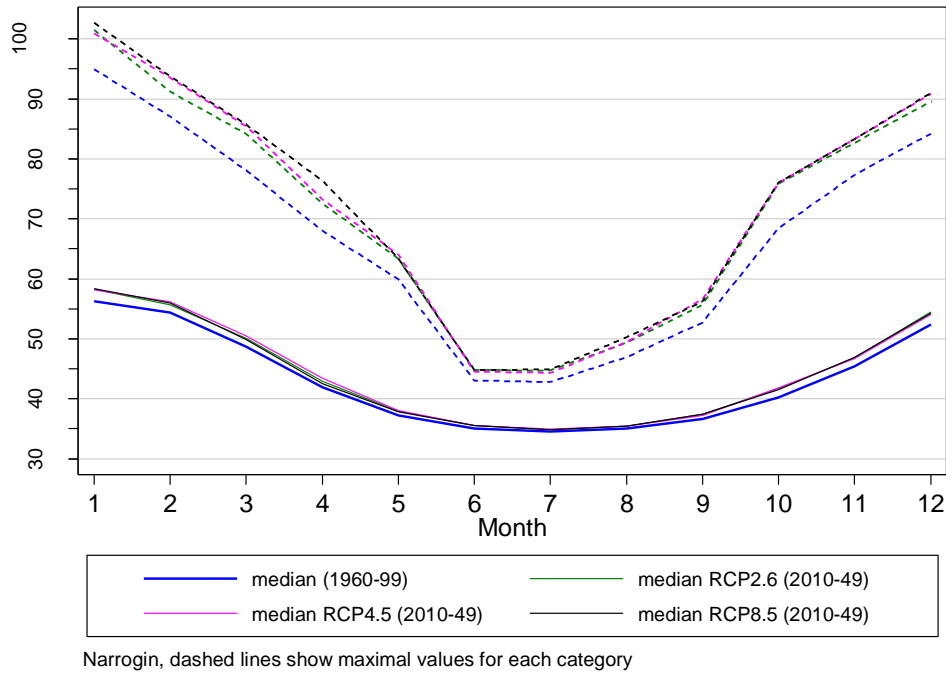


Figure 4.54: Predicted median daily water intake by month of year at Narrogin for the period from 2010-2049 (solid lines). The solid blue line is the median predicted water intake from the historic period (1960-1999), provided for comparative purposes. Dashed lines shows the maximum daily water intake for each month.

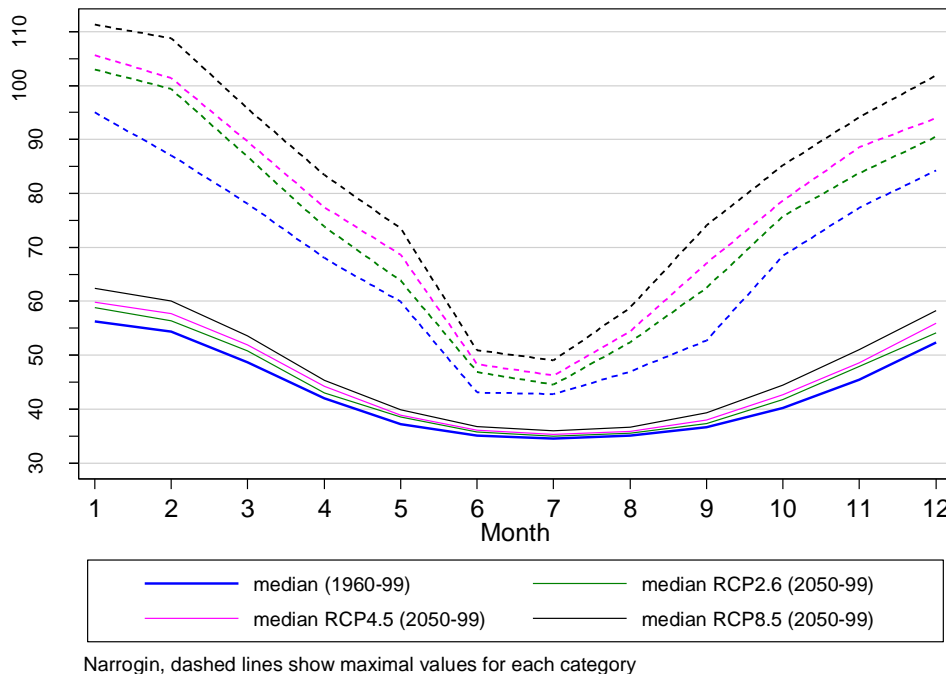


Figure 4.55: Predicted median daily water intake by month of year at Narrogin for the period from 2050-2099 (solid lines). The solid blue line is the median predicted water intake from the historic period (1960-1999), provided for comparative purposes. Dashed lines shows the maximum daily water intake for each month.

Table 4.116: Summary statistics for daily water intake (L/hd/day) by month of year for Narrogin for the historic period (1960-1999) and for each of three scenarios in 2010-2049. Summary statistics for the future period are derived from all five model outputs within each scenario. % changes are based on comparison to the same statistics from the historic period. perc = percentile.

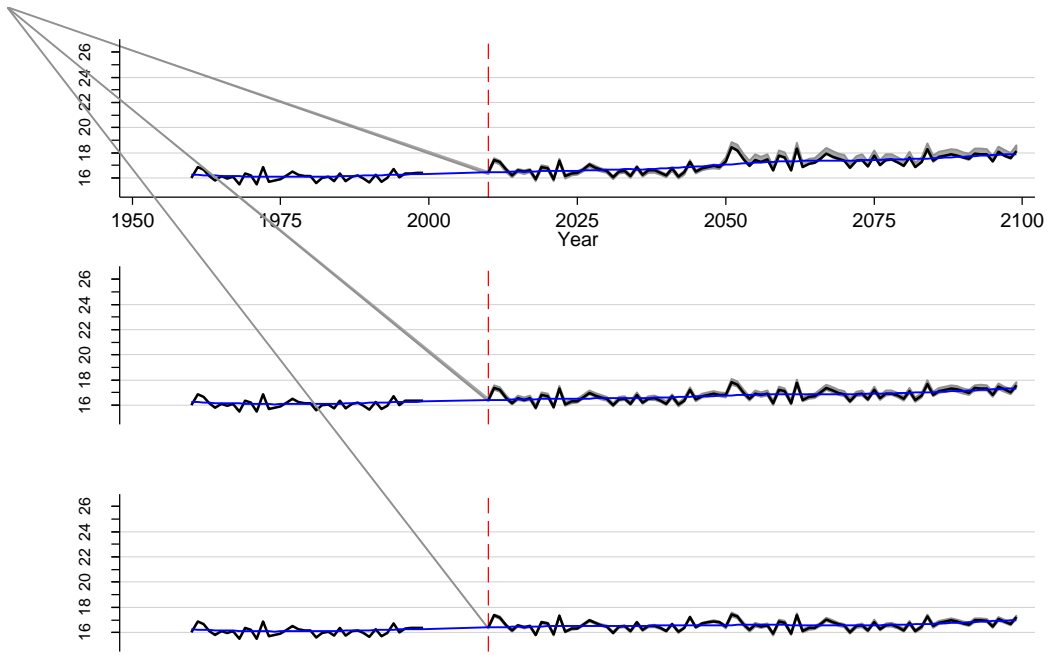
Source	Measure	Month											
		1	2	3	4	5	6	7	8	9	10	11	12
1960-1999 (historic)	Min	34	33	32	32	30	31	30	31	30	32	31	33
	25th perc	50	48	44	39	35	34	34	34	35	38	42	47
	Median	56	54	49	42	37	35	35	35	37	40	45	52
	75th perc	64	62	56	47	40	36	36	36	39	44	52	59
	Max	95	87	78	68	60	43	43	47	53	68	77	84
2010-2049 & RCP2.6	Median	58	56	50	43	38	35	35	35	37	42	47	54
	% change	4%	2%	3%	2%	2%	1%	1%	1%	2%	4%	3%	4%
	25th perc	51	49	45	39	36	34	34	34	36	39	43	48
	% change	3%	2%	2%	2%	1%	1%	1%	1%	2%	3%	2%	3%
	75th perc	67	64	58	48	41	37	36	37	40	47	54	62
	% change	4%	3%	3%	3%	3%	2%	1%	2%	3%	5%	4%	4%
	Max	100	90	82	71	63	44	44	49	56	74	81	89
% change	5%	4%	4%	5%	5%	3%	2%	4%	5%	8%	5%	6%	
2010-2049 & RCP4.5	Median	58	56	50	43	38	36	35	35	37	42	47	54
	% change	3%	3%	4%	4%	2%	1%	1%	1%	2%	4%	3%	3%
	25th perc	51	50	45	40	36	34	34	34	36	39	43	48
	% change	3%	3%	3%	3%	2%	1%	1%	1%	1%	3%	2%	3%
	75th perc	67	65	58	49	41	37	36	37	40	47	53	61
	% change	4%	4%	4%	4%	3%	2%	2%	1%	2%	5%	3%	4%
	Max	100	91	83	73	64	44	44	49	55	74	81	88
% change	5%	5%	6%	7%	6%	3%	3%	3%	4%	9%	5%	5%	
2010-2049 & RCP8.5	Median	58	56	50	43	38	36	35	35	37	42	47	54
	% change	4%	3%	3%	1%	1%	1%	1%	1%	2%	3%	3%	4%
	25th perc	51	49	45	39	36	34	34	34	36	38	43	48
	% change	3%	3%	2%	1%	1%	1%	1%	1%	2%	3%	3%	3%
	75th perc	67	65	57	48	41	37	36	37	40	46	54	62
	% change	4%	4%	3%	2%	2%	2%	1%	1%	3%	4%	4%	4%
	Max	100	91	81	70	62	44	44	49	56	74	82	89
% change	5%	4%	4%	3%	4%	3%	3%	3%	5%	8%	6%	5%	

Table 4.117: Summary statistics for daily water intake (L/hd/day) by month of year for Narrogin for the historic period (1960-1999) and for each of three scenarios in 2050-2099. Summary statistics for the future period are derived from all five model outputs within each scenario. % changes are based on comparison to the same statistics from the historic period. perc = percentile.

Source	Measure	Month											
		1	2	3	4	5	6	7	8	9	10	11	12
1960-1999 (historic)	Min	34	33	32	32	30	31	30	31	30	32	31	33
	25th perc	50	48	44	39	35	34	34	34	35	38	42	47
	Median	56	54	49	42	37	35	35	35	37	40	45	52
	75th perc	64	62	56	47	40	36	36	36	39	44	52	59
	Max	95	87	78	68	60	43	43	47	53	68	77	84
2050-99 & RCP2.6	Median	59	56	51	43	39	36	35	36	37	42	48	54
	% change	5%	4%	4%	2%	4%	2%	1%	1%	2%	4%	5%	3%
	25th perc	52	50	46	39	36	34	34	34	36	39	43	48
	% change	4%	3%	4%	2%	2%	1%	1%	1%	1%	3%	4%	3%
	75th perc	67	65	59	48	42	37	36	37	40	47	55	62
	% change	4%	3%	5%	3%	4%	2%	2%	1%	2%	5%	7%	4%
	Max	101	97	83	71	64	46	44	50	62	74	83	88
% change	7%	11%	6%	4%	6%	6%	3%	7%	17%	8%	7%	5%	
2050-99 & RCP4.5	Median	60	58	52	44	39	36	35	36	38	43	49	56
	% change	6%	6%	7%	5%	4%	3%	2%	2%	4%	6%	7%	7%
	25th perc	53	51	46	40	37	35	34	35	36	39	44	49
	% change	6%	5%	5%	4%	3%	2%	2%	2%	3%	5%	5%	6%
	75th perc	68	66	60	50	42	38	37	38	41	48	56	64
	% change	6%	6%	8%	7%	5%	4%	3%	3%	5%	8%	9%	8%
	Max	104	100	86	75	65	47	45	52	65	77	85	93
% change	9%	15%	10%	10%	9%	9%	5%	11%	23%	13%	10%	10%	
2050-99 & RCP8.5	Median	62	60	54	45	40	37	36	37	39	44	51	58
	% change	11%	10%	10%	8%	7%	5%	4%	4%	7%	10%	12%	11%
	25th perc	55	53	48	41	37	35	35	35	37	41	45	51
	% change	10%	9%	9%	7%	5%	4%	3%	3%	6%	8%	9%	9%
	75th perc	72	69	62	51	43	39	37	39	42	51	60	67
	% change	11%	11%	12%	10%	9%	6%	5%	6%	9%	14%	15%	13%
	Max	110	106	90	78	68	49	47	55	70	84	92	98
% change	16%	22%	15%	15%	14%	13%	9%	17%	34%	22%	19%	17%	

Table 4.118: summary statistics for water intake at Narrogin expressed as ML per thousand head per year, based on aggregating daily water intake estimates to produce an annual estimate.

Year	Model	Scenario	min	p25	median	p75	max
(ML / '000 head / year)							
1960-1999	None	None	15.5	15.9	16.1	16.4	16.9
2010-2049	Combined	RCP2.6	15.8	16.3	16.5	16.8	17.4
<i>% change from historic</i>			2%	3%	3%	3%	3%
	Combined	RCP4.5	15.9	16.3	16.6	16.8	17.4
<i>% change from historic</i>			2%	3%	3%	3%	3%
	Combined	RCP8.5	15.9	16.4	16.6	16.8	17.4
<i>% change from historic</i>			2%	3%	3%	3%	3%
2050-2099	Combined	RCP2.6	15.9	16.5	16.7	16.9	17.5
<i>% change from historic</i>			3%	4%	3%	3%	3%
	Combined	RCP4.5	16.2	16.8	17.0	17.3	17.8
<i>% change from historic</i>			4%	6%	5%	6%	6%
	Combined	RCP8.5	16.7	17.4	17.6	17.9	18.5
<i>% change from historic</i>			8%	9%	9%	10%	10%



Annual water intake at Narrogin:
RCP8.5 (top), RCP4.5 (middle) & RCP2.6 (bottom) scenarios

Figure 4.56: Plot of annual water intake (ML/1000 head/year) at Narrogin by year for each of three scenarios over two periods (1960-1999 and 2010-2099). Water intake for 2010-2099 shows the range from minimum to maximum annual values across the five models (shaded area) and the median (black line). The blue line shows a smoothed long-term average.

4.5 Effluent water runoff

Runoff was produced as a daily estimate from MEDLI hydrology models. Simple summary statistics for daily runoff values are provided in Section 4.2.4.

This section provides more detailed summaries of runoff to examine patterns of change in the potential for available effluent water under various climate change scenarios at each location.

Preliminary inspection indicated that runoff was slightly right skewed but inspection of median and mean estimates as summary statistics indicated there was very little difference between the two measures. As a result mean runoff estimates are used as the summary measure of runoff for this report.

As indicated in the methodology section, runoff was expected to be driven mainly by rainfall and this was confirmed in initial inspection of the output data.

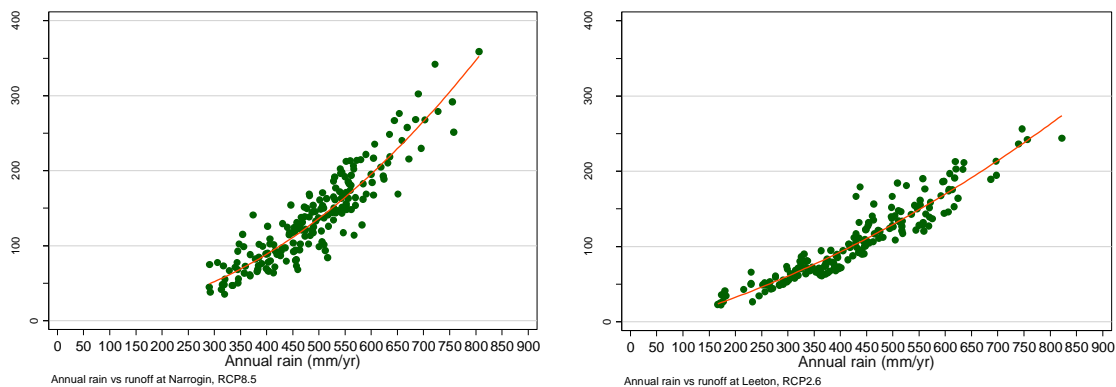


Figure 4.57: Scatterplots of annual rainfall (y-axis) and annual runoff (x-axis) for two representative modelling runs. The left plot shows average rainfall and runoff estimates derived from all model outputs at Narrogin for RCP8.5 and the right plot shows estimates derived from all model outputs at Leeton for RCP2.6. Lines are fitted quadratic regression lines.

Simple regression models (data not shown) were fitted with outcome being annual runoff (mm/year) and the explanatory variable being annual rainfall (mm/year). Separate models were fitted for each combination of location and RCP using data averaged over all five models within each combination of location and RCP. The r -squared values (coefficient of determination) provide a measure of the explanatory power of rainfall to predict runoff and may be interpreted as the proportion of variation in runoff that can be explained by rainfall. The r -squared values ranged from 0.81 to 0.89 and averaged 0.845 across all regression models.

Figure 4.58 shows the close pattern between annual rainfall and annual runoff using one modelling dataset as an example (Leeton, RCP2.6). The thin lines show annual average rainfall and runoff and show that there is very close agreement in the variability over time of rain and runoff. It is important to note that the scale of the two vertical axes is different and that runoff in general terms is about 30% of annual rainfall in mm/year.

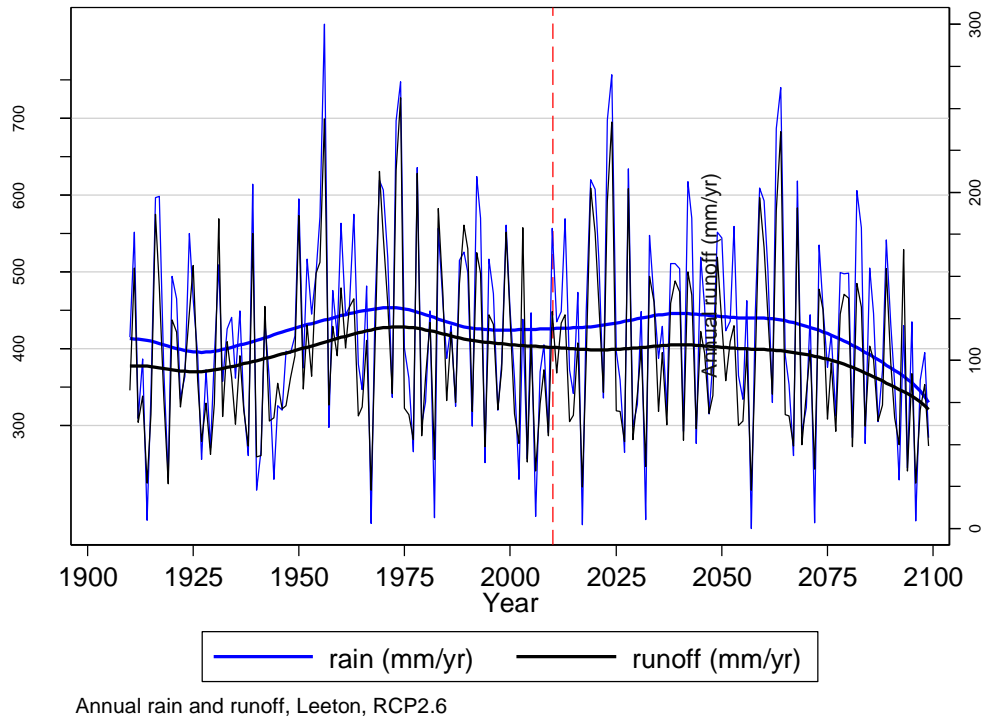


Figure 4.58: Plot of annual rainfall (left axis) and annual runoff (right axis) over time with smoothed averages of rainfall (thick blue line) and runoff (thick black line) overlaid.

The point of this initial exploratory reporting is to confirm that rainfall is the main driver of runoff and that the pattern over time of annual runoff (and even daily runoff) will mirror very closely the pattern of rainfall.

Preliminary modelling also indicated that there was relatively little variability in annual runoff measures between the different models (CNRM-CN5, GFDL-ESM2G, HadGEM2-ES, MIROC5, MRI-CGCM3) within one scenario (RCP level). This is shown in Figure 4.59 in an illustrative plot from one RCP (8.5) and location (Narrogin).

The left side of the plot shows the historic annual runoff estimates (mm/year) drawn from SILO data for this location. The right side of the plot (to the right of the vertical, red, dashed line at year=2010), shows the average of the five model runs for RCP8.5 at this location as the blue line. The area around the blue line shaded in gray shows the range from the minimum of the five model runs and the maximum of the five model runs for RCP8.5. The shaded area therefore shows the range between the five model-specific outputs.

The thick pink line is a smoothed, long-term average generated using a lowess plotting function.

In terms of method development, preliminary modelling suggested that the average of the five separate models for each RCP was a very good representation of the change in runoff over time under different climate change scenarios.

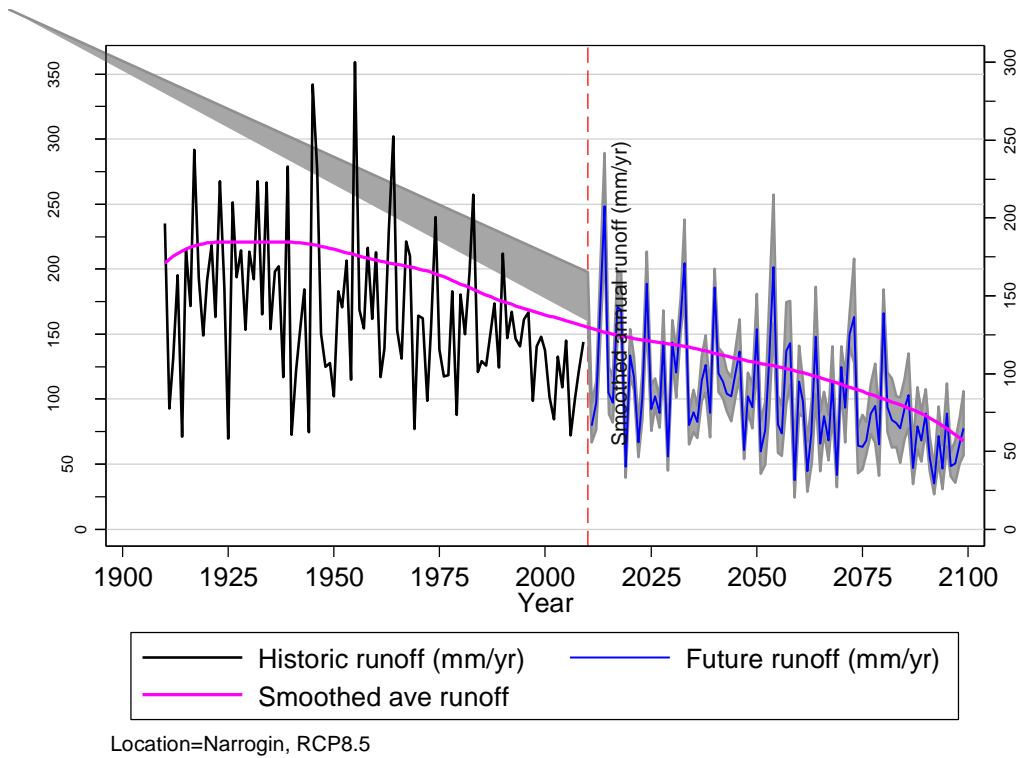


Figure 4.59: Example plot of annual runoff over time, from Narrogin and for RCP8.5.

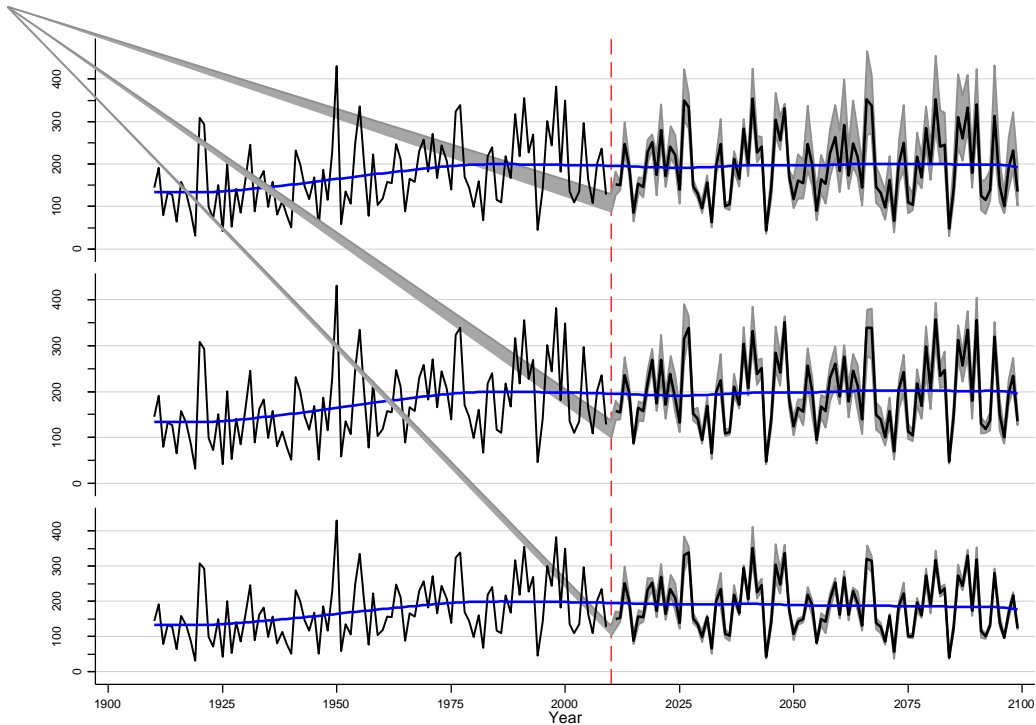
The remainder of this section provides detailed summary statistics and plots of runoff for each location and scenario.

4.5.1 Caroona

Table 4.119: Summary statistics for annual runoff at Caroona, CoV=coefficient of variation. The change in coefficient of variation is provided for 2050-2099 and is expressed as a % of the 2010-2049 values. The change in mean runoff is expressed as a % of the historic mean runoff.

Year	Model	Scenario	Mean mm/yr	Min	Max	CoV	Change in CoV % cf 2010-49	Change in mean cf hist % cf historic
1910-2009	None	None	173	31	431	0.49		
2010-2049	Combined	RCP2.6	196	43	352	0.40		13.1%
	Combined	RCP4.5	195	48	351	0.39		13.0%
	Combined	RCP8.5	195	43	354	0.40		12.9%
2050-2099	Combined	RCP2.6	182	41	330	0.41	2.3%	5.1%
	Combined	RCP4.5	198	48	357	0.40	3.4%	14.5%
	Combined	RCP8.5	196	48	352	0.40	-0.1%	13.5%

It is interesting to note that there was a rise in mean annual runoff (mm/yr) and little change in variability (CoV). Most of the rise appeared to occur in the first period (2010-2049) and then there was little change in the subsequent period for RCP4.5 and 8.5, while the runoff actually fell in the RCP2.6 scenario from the 2010-49 period to the 2050-2099 period.



Annual runoff, Carooona. RCP8.5 (top), RCP4.5 (mid), RCP2.6 (bottom)

Figure 4.60: Plot showing the annual runoff (mm/yr) at Carooona for the historic and predicted time periods. The predicted period incorporates a shaded area showing the range from the minimum to maximum value from the five models for each year and the block line shows the annual average for the five models. The blue line is a smoothed long-term average runoff estimate.

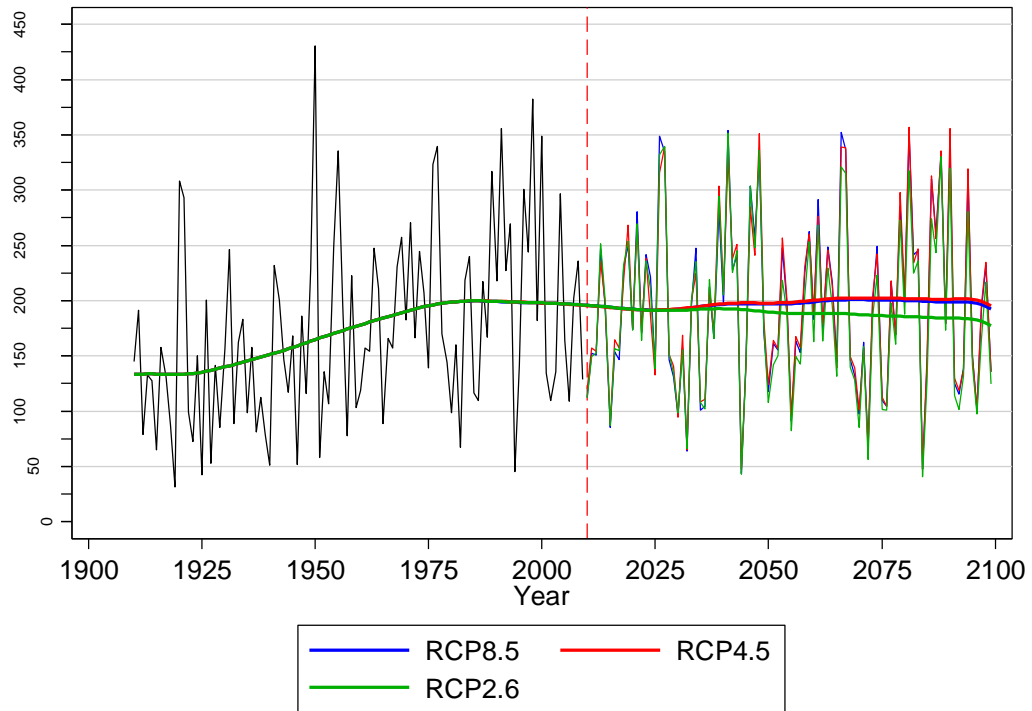


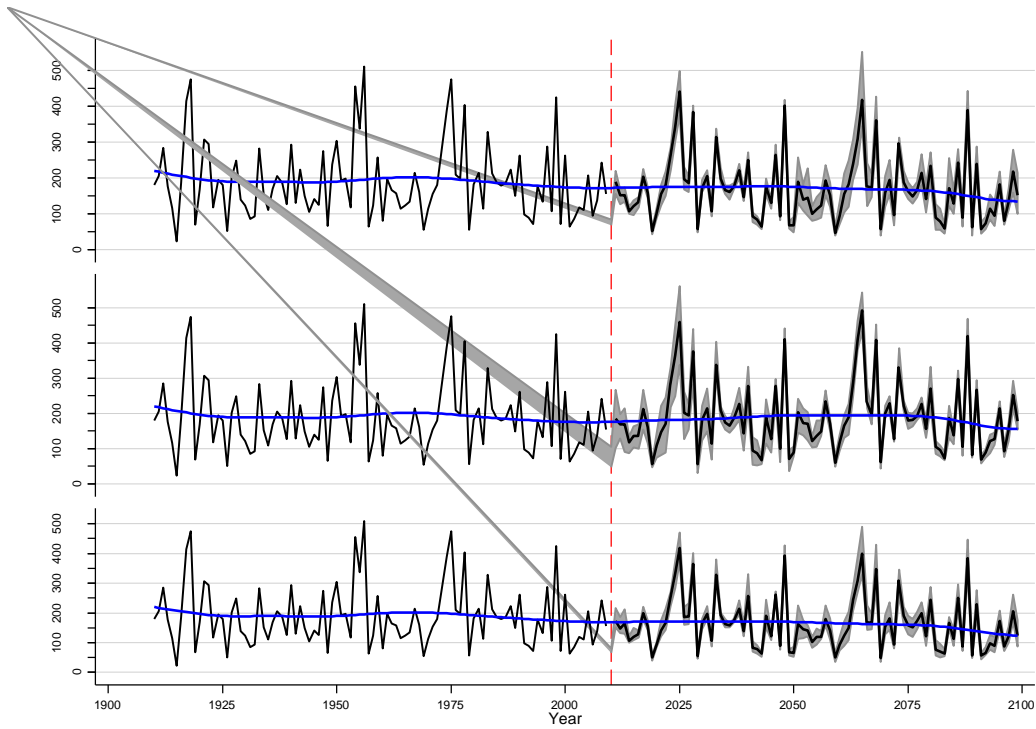
Figure 4.61: Plot showing annual runoff at Caroona from historic climate records (black line) and annual runoff for each of the three RCP levels. The thick coloured lines show smoothed long-term average runoff for each RCP.

4.5.2 Comet

Table 4.120: Summary statistics for annual runoff at Comet, CoV=coefficient of variation. The change in coefficient of variation is provided for 2050-2099 and is expressed as a % of the 2010-2049 values. The change in mean runoff is expressed as a % of the historic mean runoff.

Year	Model	Scenario	Mean	Min	Max	CoV	Change in CoV	Change in mean cf hist
			mm/yr				% cf 2010-49	% cf historic
1910-2009	None	None	189	23	510	0.54		
2010-2049	Combined	RCP2.6	174	49	418	0.53		-8.1%
	Combined	RCP4.5	186	57	459	0.52		-1.5%
	Combined	RCP8.5	178	51	441	0.53		-5.8%
2050-2099	Combined	RCP2.6	155	48	398	0.55	2.8%	-17.8%
	Combined	RCP4.5	189	60	492	0.52	-1.6%	0.0%
	Combined	RCP8.5	162	47	417	0.53	-1.0%	-14.4%

There was a general trend for a decline in annual runoff measures for all future scenarios based on % change compared to the historic mean. In contrast there was little change in variability based on the CoV.



Annual runoff, Comet. RCP8.5 (top), RCP4.5 (mid), RCP2.6 (bottom)

Figure 4.62: Plot showing the annual runoff (mm/yr) at Comet for the historic and predicted time periods. The predicted period incorporates a shaded area showing the range from the minimum to maximum value from the five models for each year and the block line shows the annual average for the five models. The blue line is a smoothed long-term average runoff estimate.

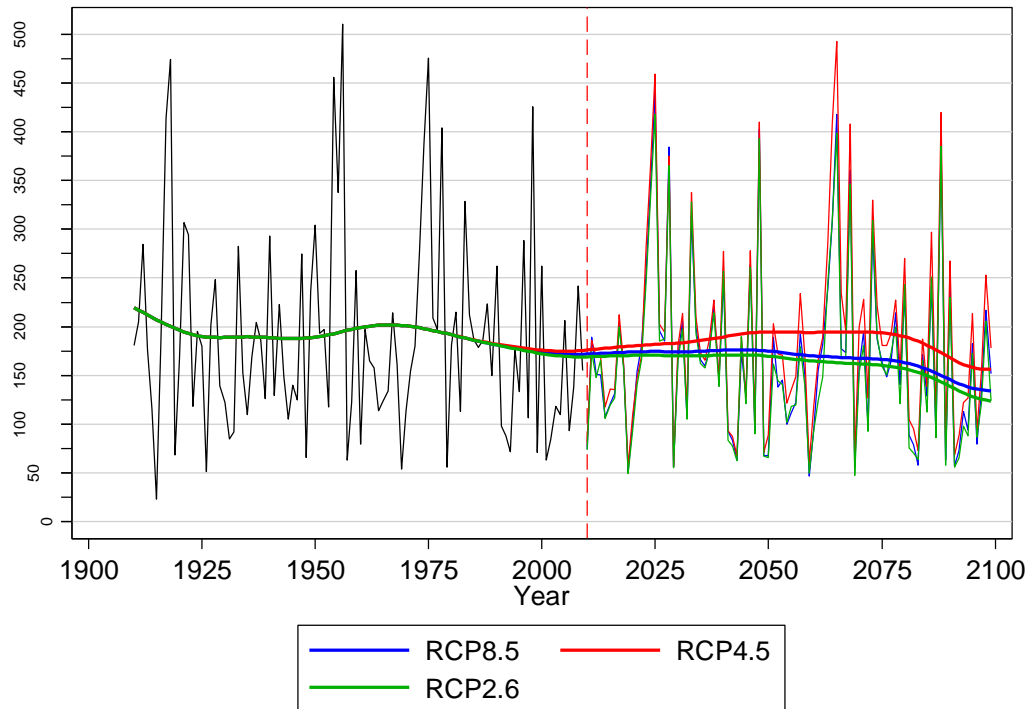


Figure 4.63: Plot showing annual runoff at Comet from historic climate records (black line) and annual runoff for each of the three RCP levels. The thick coloured lines show smoothed long-term average runoff for each RCP.

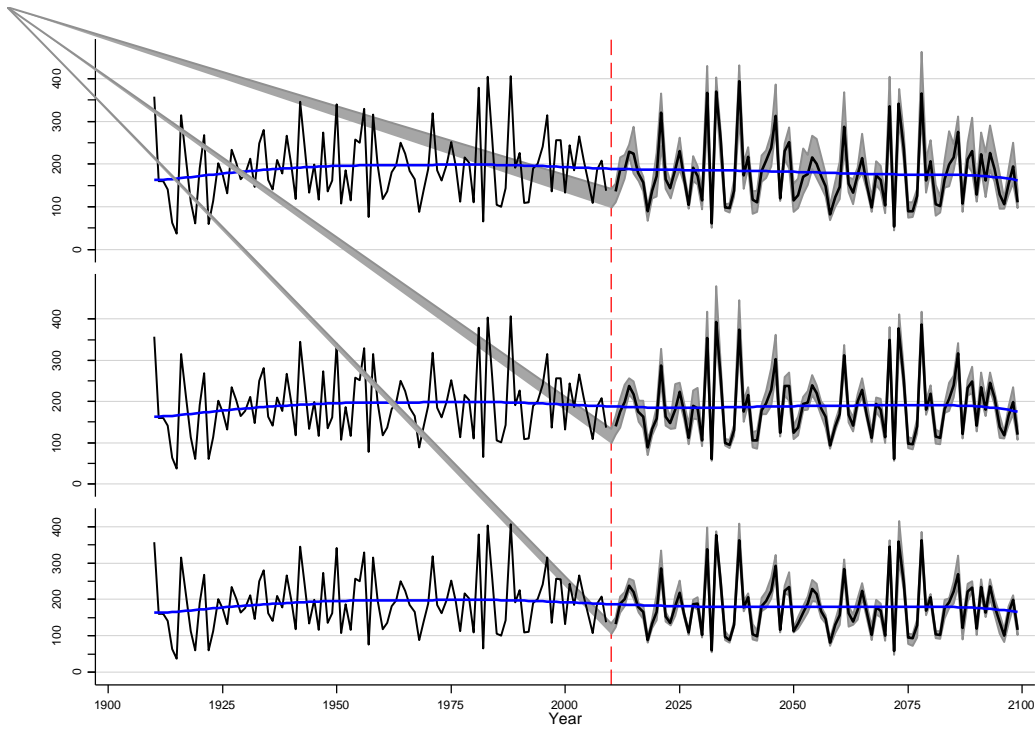
The long term trends are shown by the smoothed average lines. The lines show a more marked drop at the extreme part of the future time period but the progressive decline in available data means there is more uncertainty in smoothed means near the edges of the data. More data is required before the sudden drop in runoff after about 2080 could be viewed with any confidence.

4.5.3 Dalby

Table 4.121: Summary statistics for annual runoff at Dalby, CoV=coefficient of variation. The change in coefficient of variation is provided for 2050-2099 and is expressed as a % of the 2010-2049 values. The change in mean runoff is expressed as a % of the historic mean runoff.

Year	Model	Scenario	Mean	Min	Max	CoV	Change in CoV	Change in mean cf hist
								% cf 2010-49
			mm/yr					
1910-2009	None	None	192	37	407	0.41		
2010-2049	Combined	RCP2.6	183	60	376	0.41		-5.1%
	Combined	RCP4.5	186	60	394	0.42		-3.3%
	Combined	RCP8.5	189	61	395	0.42		-1.6%
2050-2099	Combined	RCP2.6	176	59	363	0.39	-4.2%	-8.6%
	Combined	RCP4.5	187	61	387	0.39	-7.1%	-2.7%
	Combined	RCP8.5	172	54	366	0.40	-5.9%	-10.9%

Results indicate a progressive decline in runoff for the future scenarios and also a decline in variability.



Annual runoff, Dalby. RCP8.5 (top), RCP4.5 (mid), RCP2.6 (bottom)

Figure 4.64: Plot showing the annual runoff (mm/yr) at Dalby for the historic and predicted time periods. The predicted period incorporates a shaded area showing the range from the minimum to maximum value from the five models for each year and the block line shows the annual average for the five models. The blue line is a smoothed long-term average runoff estimate.

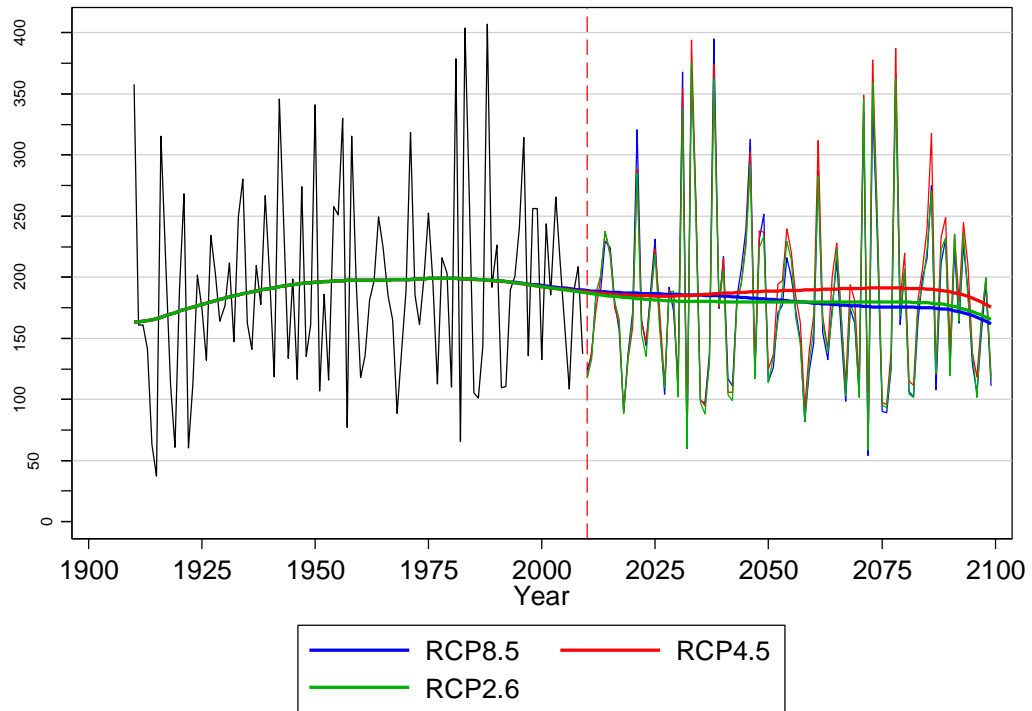


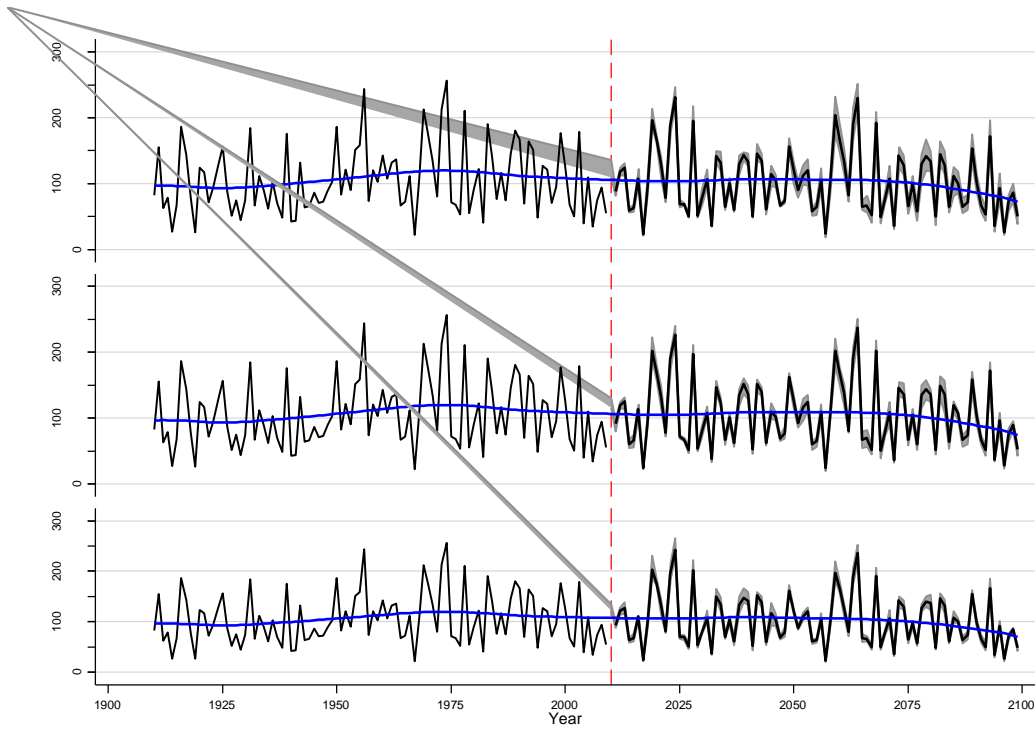
Figure 4.65: Plot showing annual runoff at Dalby from historic climate records (black line) and annual runoff for each of the three RCP levels. The thick coloured lines show smoothed long-term average runoff for each RCP.

4.5.4 Leeton

Table 4.122: Summary statistics for annual runoff at Leeton, CoV=coefficient of variation. The change in coefficient of variation is provided for 2050-2099 and is expressed as a % of the 2010-2049 values. The change in mean runoff is expressed as a % of the historic mean runoff.

Year	Model	Scenario	Mean	Min	Max	CoV	Change in	Change in
							CoV	mean cf hist
			mm/yr				% cf 2010-49	% cf historic
1910-2009	None	None	106	27	234	0.48		
2010-2049	Combined	RCP2.6	110	26	235	0.46		4.3%
	Combined	RCP4.5	108	25	232	0.45		2.4%
	Combined	RCP8.5	107	23	232	0.45		0.8%
2050-2099	Combined	RCP2.6	99	23	236	0.49	6.8%	-6.3%
	Combined	RCP4.5	103	25	237	0.48	7.2%	-2.9%
	Combined	RCP8.5	100	24	231	0.48	6.4%	-5.5%

The results show a decline in future runoff compared to the historic mean and at the same time a rise in the relative variability (CoV). This pattern is consistent with reduced average rainfall and more variability in rainfall.



Annual runoff, Leeton. RCP8.5 (top), RCP4.5 (mid), RCP2.6 (bottom)

Figure 4.66: Plot showing the annual runoff (mm/yr) at Leeton for the historic and predicted time periods. The predicted period incorporates a shaded area showing the range from the minimum to maximum value from the five models for each year and the block line shows the annual average for the five models. The blue line is a smoothed long-term average runoff estimate.

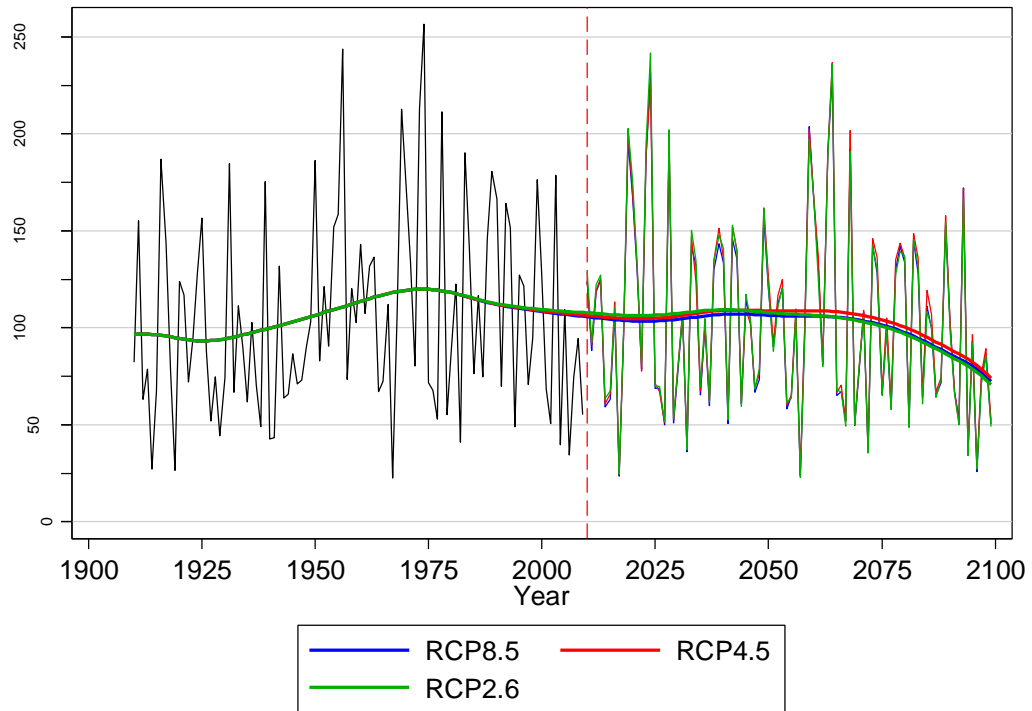


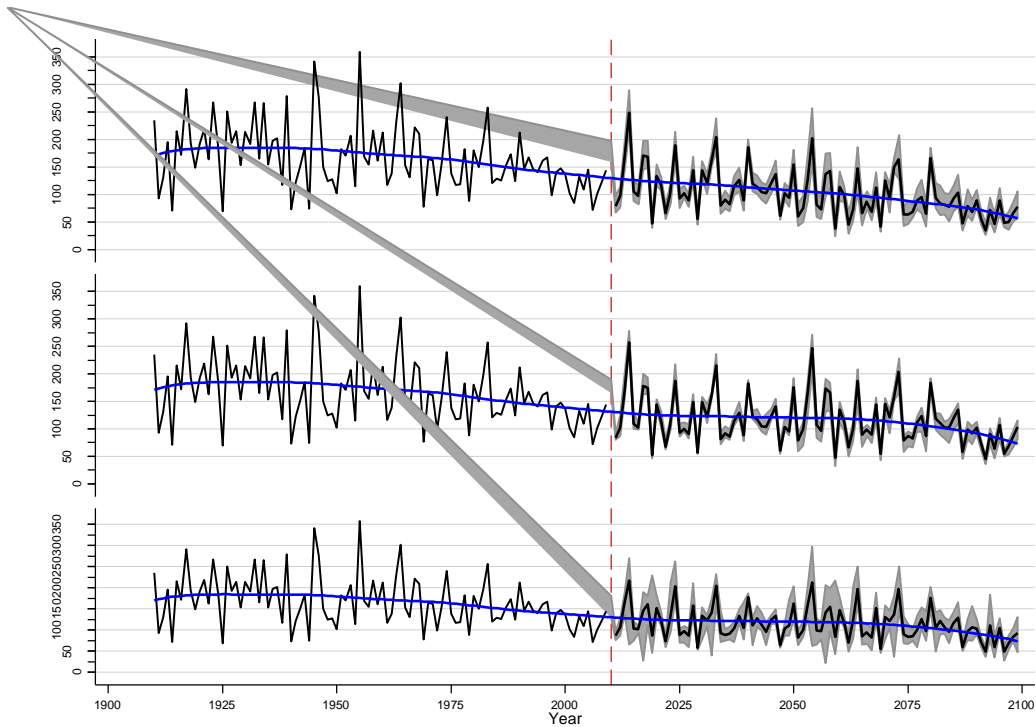
Figure 4.67: Plot showing annual runoff at Leeton from historic climate records (black line) and annual runoff for each of the three RCP levels. The thick coloured lines show smoothed long-term average runoff for each RCP.

4.5.5 Narrogin

Table 4.123: Summary statistics for annual runoff at Narrogin, CoV=coefficient of variation. The change in coefficient of variation is provided for 2050-2099 and is expressed as a % of the 2010-2049 values. The change in mean runoff is expressed as a % of the historic mean runoff.

Year	Model	Scenario	Mean	Min	Max	CoV	Change in CoV	Change in mean cf hist
			mm/yr				% cf 2010-49	% cf historic
1910-2009	None	None	167	69	359	0.36		
2010-2049	Combined	RCP2.6	122	58	218	0.31		-26.8%
	Combined	RCP4.5	123	52	258	0.36		-26.7%
	Combined	RCP8.5	120	48	248	0.36		-28.1%
2050-2099	Combined	RCP2.6	110	49	212	0.35	11.3%	-34.2%
	Combined	RCP4.5	111	45	247	0.39	6.8%	-33.7%
	Combined	RCP8.5	89	35	202	0.42	16.5%	-46.9%

Narrogin shows the most severe and progressive decline in runoff of all the locations. This change is consistent with a decline in expected rainfall as well. It is noticeable that while the mean runoff is declining the variability is increasing. Notice that variability is expressed using the CoV which expresses variation relative to the mean. This explains why the variation as viewed visually in the plot below appears to be reducing, when using the CoV (expressing variation relative to a declining mean) is increasing.



Annual runoff, Narrogin. RCP8.5 (top), RCP4.5 (mid), RCP2.6 (bottom)

Figure 4.68: Plot showing the annual runoff (mm/yr) at Narrogin for the historic and predicted time periods. The predicted period incorporates a shaded area showing the range from the minimum to maximum value from the five models for each year and the block line shows the annual average for the five models. The blue line is a smoothed long-term average runoff estimate.

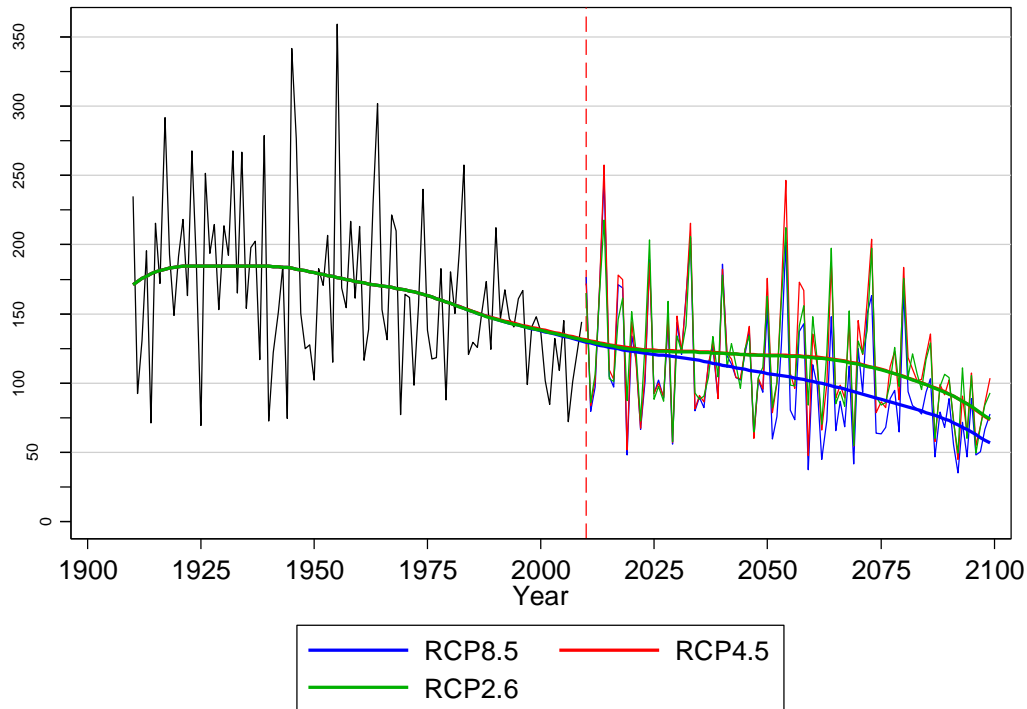


Figure 4.69: Plot showing annual runoff at Narrogin from historic climate records (black line) and annual runoff for each of the three RCP levels. The thick coloured lines show smoothed long-term average runoff for each RCP.

5 Discussion

This project involved several linked component activities combined to produce different types of outputs.

Five representative point locations across Australia were selected to represent the Australian feedlot industry recognising that the threat of climate change may be different in different parts of the country.

A structured review process resulted in the selection of the most appropriate climate models for generating predicted future climate files under different climate change scenarios for each of the locations.

Historic SILO records for climate variables recorded at daily intervals were sourced for each of the five selected locations for the period from 1900-2009 though different subsets of these historic records were used for different comparisons.

Predicted climate datasets were produced for the period 2010-2099, in two separate processes. One set of data was produced at a daily time-step, for use in feedlot hydrology modelling and in general descriptions of changes to climate at each location.

A second set of data was produced at an hourly time-step for use in modelling of accumulated heat load units as a representation of risk of heat stress in feedlot animals.

5.1 Changes to climate

A general pattern of rising temperatures over time was observed in all locations (see plots and tables in Section 4.1.1).

The mean temperature anomaly provides an indication of the expected rise in average temperature over time, compared to the average temperature for the period from 1961-1990 (Table 4.1). For the period 2010-2049, mean temperature anomaly estimates ranged from under 1 °C to just over 2 °C with most values lying between 0.96 °C and 1.3 °C. The exception to this was in Narrogin where temperature anomaly estimates for 2010-2049 showed a 2 °C rise.

The mean temperature anomaly for the period from 2050-2099 was higher (again compared to the 1961-1990 mean). Rises were between 1.3 to 4.3 °C depending on the scenario and location (Table 4.1).

There were rises in the number of days where the maximum daily temperature was greater than 35 °C or 40 °C (Section 4.1.1).

Rainfall patterns showed more variability over time.

The pattern of change for Carroona was variable. There were some situations where rainfall increased substantially and others where rainfall appeared to decline.

Some locations showed consistent changes in rainfall. Comet and Narrogin showed a decline in average rainfall that appeared to get progressively worse from historic to 2010-2049 and then to 2050-2099.

Dalby and Leeton also showed a decline in rainfall over time that was less obvious than Comet and Narrogin.

5.2 Feedlot hydrology

The key output from feedlot hydrology modelling using the MEDLI modelling framework was the estimates of pond overtopping frequency under different levels of climate change.

Pond overtopping is influenced by climate variables and particularly rainfall with additional influences from radiation and evaporation. It is also influenced by the design of the feedlot since a range of feedlot characteristics (pen design, pen cleaning, animal characteristics, feed type, use of irrigation and a range of other parameters) can all influence surface runoff.

Care was taken to define standard and representative feedlots in each location based on knowledge of the type of feedlots already in existence in each area. A detailed description of the approach to parameterising the MEDLI feedlot module is provided.

Figure 4.21 displays the mean overtopping rate and 95% confidence interval for each location and RCP, produced by averaging the five model outputs for each location-RCP combination.

There was no difference in overtopping rate over time at Comet and Dalby, suggesting that current approaches to determining pond dimensions are likely to be appropriate for the foreseeable future.

There was a substantial decline in pond overtopping rates at Leeton and Narrogin over time.

The pond overtopping rate at Carooona was interesting. For RCP2.6 and 4.5, there was no change in pond overtopping rate from the historic period to the 2000-2099 period. However, under the RCP8.5 scenario, there was a large increase in the rate of pond overtopping (from 9 per 100 years to 31 per 100 years, $p < 0.05$).

Rainfall records reported in Carooona

Table 4.23 and Table 4.24 for Carooona show that average annual rainfall increased in the 2050-2099 period and there was an increase in the number of days when heavier falls of rain were recorded compared to the historic period.

The findings suggest that there is little evidence to support changes in the guidelines with respect to holding pond dimensions. If the level of climate change experienced in the future is more consistent with the RCP8.5 scenario then there may be justification in revisiting the guidelines for some areas such as northern NSW (Carooona) because of possible risks of overtopping.

5.3 Heat load

There was considerable variation in heat load risk as measured by accumulated heat load units (AHLU) between the five different locations and the three different scenarios.

At all locations there was a progressive rise in AHLU measures from RCP2.6 through RCP4.5 and to RCP8.5.

Additional results are provided in the Appendices. As the number of days per year when AHL exceeded 100 units rose (Section 4.3) there were also rises in the number of heat load events per year and the median duration in days of heat load events (See separate appendices report for more detail).

There was considerable variation between different models and it is not possible to appreciate this variation in the plots of median days per year when AHL was above a threshold value (Section 4.3.1). Plots of cumulative AHL values over time are shown in detail in the separate report containing Appendices. Under some models and particularly CNRM-CM5, there were substantive increases in heat load and very high risk of severe heat stress and death in feedlot cattle, particularly under the severe RCP scenario.

A single extreme model run had very little impact on the median number of days when AHL exceeded a threshold as calculated across all models and displayed in the plots in Section 4.3.1.

When the number of days of AHL>100 was expressed as days per 10 years, it allowed direct comparison of the risk of heat load between locations and scenarios and under different mitigation strategies (see tables in Section 4.3.2).

In locations where CNRM-CM5 was producing heat load estimates that were substantially higher than other models, estimates were produced with and without CNRM-CM5 data included.

In all locations there was a rise in the number of heat load days per 10 years when moving from historic to RCP2.6, 4.5 and 8.5. In all cases mitigation at some level (mild, moderate or maximal) was sufficient to bring the heat load risk down to levels that were equivalent to or lower than the historic level. It is noteworthy that in several situations this required the exclusion of CNRM-CM5.

If the actual level of climate change is closer to the predictions from CNRM-CM5 than to the other four models then the level of heat load in Caroonna, Comet, Dalby and Leeton under the severe RCP scenario may be sufficient to cause serious adverse effects and increased mortality even in the presence of maximal mitigation. Given that CNRM-CM5 appeared to be producing predictions that were quite different to the other four models, this may be considered less likely than a pathway of change that is more consistent with the other four models.

The findings suggest that mitigation will be necessary, in some locations more than others and generally after 2050.

The simplest determination of the efficacy of mitigation is to look for a reduction in future heat load to the point where measures are similar to the historic period (Table 4.43).

At Dalby and Narrogin, there is very little change in heat load under RCP2.6 and RCP4.5 scenarios for the period from 2010-2049 and then there is a relatively small rise in heat load risk in the 2050-2099 period. For RCP8.5 at these locations there is an increased rise in heat load particularly after 2050 but much of this effect is due to the influence of the CNRM-CM5 model and when this model is filtered the rise is much less marked.

The results for Narrogin indicate that mild or moderate mitigation strategies will be sufficient to reduce heat load effects to historic levels, depending on the RCP scenario that is being considered.

The results for all other locations suggest that moderate or maximal mitigation strategies will be required to effectively manage heat load for the period from 2050-2099, and this is only effective when the results from CNRM-CM5 models are removed from the estimations.

It is strongly suggested that these findings be considered when revising guidelines and providing advice to feedlot managers.

5.4 Water intake

Cattle drinking water accounts for ~90% of total water usage on Australian feedlots. A detailed study involving water meter measurement of water usage in a Darling Downs feedlot reported smoothed average daily water intake levels ranging from a low of around 30 L/hd/day in June/July to a high of around 75 L/hd/day in February-March (Carter 2008). Individual daily records indicated that on

individual days in winter, daily water intake was capable of falling to levels as low as 11 L/hd/day. Very low water usage levels on a given day may be influenced by rainfall as well as other climatic, animal and feed related factors. The water usage records over an 11-month period was standardised to an annual estimate of 15 ML/1000 head/year, which compared favourably to the general industry estimate of allowing 24ML/1000 head/year as a measure of feedlot water requirements.

Our results were based on using a published model (Parker et al 2000) to predict water intake given daily climate inputs. Our findings were consistent with the actual water intake results reported by Carter (2008).

The same pattern was observed across all five locations: minimum water intake in June-July and maximal water intake between December-February. Median water intake levels for the historic period (1960-1999) ranged from a low of 35-45 L/hd/day to a summer high of 55-65 L/hd/day. There was least variability in water intake ranges in the winter and most variability in the summer. In summer months daily water intake varied from lows around 35-40 L/hd/day to maximal daily intakes of 85-95 L/hd/day.

There was a progressive rise in predicted daily water intake from historic to 2010-49 periods and again to the 2050-99 period at each location though the amount of the rise varied between locations and scenarios. The median daily water intake values for the period 2010-49 rose by 1-8% across all locations when compared to the 1960-99 period. The rise was smallest in the winter and generally highest in the summer months and the rise was generally smaller in the mild climate change scenario (RCP2.6) and larger in the most severe climate change scenario (RCP8.5). Peak water intake (represented by maximal daily intake estimates) rose by less than 10% compared to the historic period.

The same pattern was viewed in the 2050-99 period when compared to the historic period but the amount of increase in water intake was larger in the 2050-99 period compared to the increase in the 2010-49 period. There was a 3-17% increase in median daily water intake and peak daily water intake levels rose by up to 34% compared to historic levels.

Water intake was also expressed in ML per 1000 head per year in order to compare estimated water requirements to the general recommendation that feedlots should allow about 24 ML/1000 head/yr.

Median annual water intake estimates ranged from 17-22 ML/1000 head/yr across all scenarios and both time periods with the highest requirements occurring in the 2050-99 period and the RCP8.5 scenario.

In the 2010-49 period, median water requirements ranged from 17-20 ML/1000 head/yr and peak water requirements reached 21 ML/1000 head/yr at Comet while in all other locations peak requirements remained lower than 20 ML/1000 head/yr.

Peak water requirements were observed for Comet (24 ML/1000 head/yr) in 2050-99 and under the RCP8.5 scenario. There was not a lot of difference between the three scenarios for median and peak water requirements within any one location and at Comet under the RCP2.6 scenario, peak water requirements were 22 ML/1000 head/yr for the 2050-99 period.

The findings of this report indicate that water requirements will progressively rise over time under all scenarios. The rise in annual water requirements is progressively approaching the 24 ML/1000 head/yr level.

The national guidelines currently state that, *as a guide, a proposed feedlot would normally need to demonstrate access to approximately 24 ML of high-security water per annum per 1,000 SCU of feedlot capacity*. Our findings suggest that this requirement will need to be increased in the future.

5.5 Effluent water runoff

The volume of holding ponds is based primarily on the requirement for limiting overtopping and environmental contamination with water containing feedlot effluent.

It is recognised that holding ponds serve as a potential source of water, nutrients and organic matter that may be beneficial to pasture or crops. No precise guidelines are provided for the land application of feedlot effluent because of the diversity of possible soil, climate, cropping, pasture and management combinations which may exist at any one site.

It is unlikely that holding ponds can provide any more than a relatively minor and opportunistic (intermittent) contribution to land application purposes. Watts et al (2012) and Tucker et al (2010) have suggested that holding pond water may be best considered as a potential source of recycled water that might be used within the feedlot for cattle drinking water or sundry uses (trough cleaning, cattle washing etc), provided that treatment processes ensure water quality.

It is expected that if water supply becomes constrained either through cost or availability, there will be increasing interest in more efficient storage and use of all water on a feedlot, including the potential use of holding pond water through some form of recycling treatment so it can be used for other purposes.

In this report the daily MEDLI hydrological model was applied to estimate the frequency of pond overtopping given input assumptions about feedlot characteristics for each location, predicted climate data and location-specific holding pond dimensions based on national guidelines. The MEDLI model produces a range of outputs including a daily estimate of runoff from the feedlot into the effluent management system.

The daily volume of runoff was then analysed as an indicator of the potential change over time in runoff water availability at each location, by comparing runoff under various climate change scenarios for future time periods to the runoff estimates generated for the same location and using historic climate input data. The actual value of runoff is dependent in turn on input parameters about a wide range of feedlot characteristics (feedlot size, area of soft and hard feedlot pads, number of cattle of different market types, type of feed, DMI, management factors) as well as possible land application of holding pond water and climate factors. We set input parameters for these characteristics which meant that while the actual value of total runoff may be considered to be somewhat arbitrary, the change over time in response to different climate inputs while holding all the feedlot input parameters constant, provides a valid relative assessment of change in runoff availability. It is the proportion (or percentage) change either in volume of runoff or in variation that we are describing in this report.

There was a very close relationship between rainfall and runoff (as expected and noted previously) and in the absence of any precise information about runoff, the use of expected changes in rainfall at any location provides an excellent indication of the likely availability of runoff water.

Three of the five locations (Comet, Dalby and Narrogin) showed a progressive decline in water runoff volumes over time (compared to historic values). The decline ranged from 1-8% for Comet and Dalby and was far higher (~27% reduction compared to historic levels) for Narrogin.

Leeton showed a small increase in runoff volumes for 2010-49 followed by a decline in runoff for 2050-99.

Caroona showed a consistent increase in runoff over both time periods (13% rise in 2010-49 and 5-14% rise in 2050-99) compared to the historic period.

It was also noticeable that coefficient of variation for the 2050-99 period indicated a rise in the relative variation (standard deviation expressed as a proportion of the mean) in three of the five locations. Two locations showed a decline in variation but this was associated with a concomitant decline in mean annual runoff as well. A rise in CoV is interpreted as indicating increased variability in annual runoff with increased uncertainty about supply in any one year.

The findings suggest that with the exception of Caroona, all locations appear likely to experience a decline in annual runoff volumes over time and most of the locations are likely to have increased uncertainty about annual runoff volumes in any one year.

These findings are likely to be of value to feedlots considering future development plans that may involve potential land application of holding pond water or recycling of holding pond water for use within the feedlot.

6 Recommendations

1. It is recommended that current guidelines for management of waste and water runoff be maintained.

The findings of this report do not support change in the National Guidelines with respect to management of surface water runoff and the design of holding ponds.

2. It is recommended that efforts be directed at continuing to raise awareness amongst the feedlot industry about excessive heat load (EHL) and the importance of preventive and response measures including heat load mitigation strategies, monitoring and early detection of heat events and response plans to deal with short term heat events.
3. It is recommended that the feedlot industry review the national guidelines with respect to requirements for access to high-security water per 1,000 SCU of feedlot capacity for future feedlot developments.

7 References

- ACSC (Australian Centre for Sustainable Catchment), (2013). Impact of Increased Climate Variability on Feedlots. Technical Report. University of Southern Queensland, Toowoomba, Qld.
- Allen RG, LS Pereira, D Raes, and M Smith (1998). Crop evapotranspiration. Guidelines for computing crop water requirements. *FAO Irrigation and Drainage Paper 56*, 300 pp., FAO, Rome.
- Atzeni MG, Casey KD & Skerman A, (2001). A model to predict cattle feedlot runoff for effluent reuse application. In *Proceedings of MODSIM 2001*, Canberra, pp. 1871-1876.
- Barth CL, (1985a). Livestock Waste Characterisation - A New Approach, Agricultural Waste Utilisation and Management. *Proc. 5th Int. Symp. ASAE*, St Joseph MI, USA pp. 286-294.
- Barth CL, (1985b). The Rational Design Standard for Anaerobic Livestock Lagoons, Agricultural Waste Utilisation and Management. *Proc. 5th Int. Symp ASAE*, St Joseph, MI, USA pp. 660-671.
- Campbell GS (1985). Soil physics with BASIC transport models for soil-plant systems. Elsevier, Amsterdam, The Netherlands.
- Canterford RP, Pescod NR, Pearce HJ & Turner LH (2001). Design intensity-frequency-duration rainfall, in *Australian Rainfall and Runoff*, ed. Pilgrim DH, Institution of Engineers Australia, Barton, ACT.
- Carter WJ (2008). Investigation of lot fed cattle drinking water consumption. P.PIP.0171, Final report, Meat and Livestock Australia Limited, Sydney NSW.
- Casey KD, (1995). Computer design model of anaerobic lagoons for pig wastes. *Proc. 7th Int. Symp. ASAE*, Chicago, IL, USA pp. 521-531.
- Casey KD, Lunney CL, Watts PJ & Tucker RW, (1997). Odour emissions from feedlot retention ponds following heavy rainfall, in *National Workshop on Odour Measurement Standardisation*, ed. Jiang, J., University of New South Wales, Sydney, NSW., 20 – 22 August.
- Cordery I, (2001). Storm losses and design rainfall excess, in *Australian Rainfall and Runoff*, ed. Pilgrim DH, Institution of Engineers Australia, Barton, ACT.
- Davis RJ, Watts PJ & McGahan EJ (2012). *Quantification of feedlot manure output for BEEF-BAL model upgrade*, RIRDC Project No. PRJ-004377, Rural Industries Research and Development Corporation, Canberra.
- Dillon PJ, (1989). An analytical model of contaminant transport from diffuse sources in saturated porous media. *Water Resources Research*, 25(6), 1208–1218.
- Gardner EA & Davis R (eds.) (1998). *MEDLI Version 1.2 Technical Manual*, Department of Primary Industries, Queensland.
- Gaughan JB, Mader TL, Holt SM, Lisle A, (2008). A new heat load index for feedlot cattle. *Journal of Animal Science*, 86(1):226-34.

- Giorgi F, Hewitson BC, Christensen J, Hulme M, von Storch H, Whetton P, Jones R, Mearns L, Fu C (2001). Regional climate information – evaluation and projections. In *Climate Change 2001: The Scientific Basis*. Contribution of Working Group 1 to the Third Assessment Report of The Intergovernmental Panel on Climate Change, Houghton JT, Ding Y, Griggs DJ, Noguer M, van der Linden PJ (eds). Cambridge University Press: Cambridge, New York, USA; 881.
- Ham JM and TM DeSutter, (1999). Seepage losses and nitrogen export from swine-waste lagoons: A water balance study. *J. Environ. Qual.* 28:1090-1099.
- Harrold TI, Jones R (2003). Downscaling of GCM rainfall: a refinement of the perturbation method. Abstracts: EGS-AGU-EUG Joint Assembly, Nice, France, 6-11 April, 2003.
- Intergovernmental Panel on Climate Change (2007). *Climate Change 2007 - Impacts, Adaptation and Vulnerability*, Cambridge University Press, Cambridge.
- Knisel WG, (1980). CREAMS: A Fieldscale Model for Chemical, Runoff, and Erosion from Agricultural Management Systems. USDA, Science and Education Administration, Conservation Report No. 26, Washington, D.C.
- Littleboy M, Silburn DM, Freebairn DM, Woodruff DR and Hammer GL, (1989). PERFECT, A computer simulation model of Productivity, Erosion, Runoff Functions to Evaluate Conservation Techniques. Queensland Department of Primary Industries, Bulletin QB89005, 119 pp.
- Littleboy M, Silburn DM, Freebairn DM, Woodruff DR, Hammer GL and Leslie JK, (1992). Impact of soil erosion on production in cropping systems. I. Development and validation of a simulation model. *Australian Journal of Soil Research*, 30:757-774.
- Liu BYH, and RC Jordan (1960). The interrelationship and characteristic distribution of direct, diffuse and total solar radiation. *Solar Energy*, 4:1-19.
- Lorrimor JC, Powers W & Sutton A, (2000). Manure characteristics. In *Manure Management Systems Series MWPS-18*. Iowa State University, Ames Iowa.
- Lott S, (1994). Drainage, in *Designing Better Feedlots*, eds. Watts, P. and Tucker, R., Queensland Department of Primary Industries, Toowoomba, Qld., pp. 5.5-37.
- Lott S, (1995). Australian feedlot hydrology – Part 2 (modelling). In *Proceedings of National Feedlot Waste Management Conference*, Gold Coast, 11-14 June 1995.
- Lott SC, (1998). Feedlot hydrology, PhD thesis, University of Southern Queensland, Toowoomba, Qld.
- Maas EV & Hoffman GJ, (1977). Crop salt tolerance - current assessment. *J. Irrig. and Drainage Div.*, ASCE 103 (IR2): 115-134.
- Madden JM & Dornbush JN, (1971). Measurement of runoff and runoff carried waste from commercial feedlots. In *Livestock Waste Management and Pollution Abatement. Proceedings of the International Symposium on Livestock Wastes*, Columbus Ohio, American Society of Agricultural Engineers, St Joseph, MI, pp. 44-47.

- Maximo CC, McAvaney BJ, Pitman AJ, and Perkins SE (2008). Ranking the AR4 climate models over the Murray-Darling Basin using simulated maximum temperature, minimum temperature and precipitation. *International Journal of Climatology*, 28, 1097-1112.
- MLA, (2012). National Guidelines for Beef Cattle Feedlots in Australia, 3rd edition. Meat & Livestock Australia in association with the Australian Lot Feeders' Association and the Feedlot Industry Accreditation Committee.
- Mercado ML, Bellouin N, Sitch S, Boucher O, Huntingford C, Wild M, Cox MP (2009). Impact of changes in diffuse radiation on the global land carbon sink. *Nature*: Vol. 458. doi:10.1038/nature07949.
- Miner JR, (1980). Controlling odours from livestock production facilities: State of the art in livestock waste: A renewable resource. *Proceedings of the 4th International Symposium ASAE*. St Joseph, Michigan, pp 297-301.
- Mockus V, (1957). Use of storm and watersheds characteristics in synthetic hydrograph analysis and application, United States. Department of Agriculture Soil Conservation Service, Washington, DC.
- Mockus V, (1964). Estimation of Direct runoff from storm rainfall, in *National Engineering Handbook*, United States Department of Agriculture Soil Conservation Service, Washington, DC.
- Mockus V, (1969). Hydrologic soil-cover complexes, in *National Engineering Handbook*, United States Department of Agriculture Soil Conservation Service, Washington, DC.
- NSW Agriculture, Department of Land and Water Conservation, Department of Urban Affairs and Planning & Environment Protection Authority (1997). *The New South Wales feedlot manual*, NSW Agriculture, Orange.
- O'Loughlin GG & Robinson DK, (2001). Urban stormwater drainage, in *Australian Rainfall and Runoff*, ed. Pilgrim DH, Institution of Engineers Australia, Barton, ACT.
- Parker DB, DE Eisenhauer, DD Schulte, and DL Martin, (1999) Modeling seepage from an unlined beef cattle feedlot runoff storage pond. *Trans. of the ASAE*, 42(5):1437-1445.
- Parker DB, Perino LJ, Auvermann BW and Sweeten JM (2000). Water use and conservation at Texas high plans beef cattle feedyards. *Applied Engineering in Agriculture* 16(1):77-82.
- Pilgrim DH & Cordery I, (1993). Flood Runoff, in *Handbook of Hydrology*, ed. Maidment DR, McGraw-Hill, New York, NY.
- Pilgrim DH & Doran DG, (2001). Choice of flood estimation method, in *Australian Rainfall and Runoff*, ed. Pilgrim DH, Institution of Engineers Australia, Barton, ACT.
- Pilgrim DH, ed., (2001). *Australian Rainfall and Runoff*, Institution of Engineers Australia, Barton, ACT.
- Pittock AB, (2003). Climate Change: An Australian Guide to the Science and Potential Impacts, Australian Greenhouse Office, Canberra, Australia.

- QPIF (2004). *BEEFBAL - a nutrient mass balance model for beef cattle feedlots*, Department of Employment, Economic Development and Innovation, Queensland Primary Industries and Fisheries, accessed October 2009 < <http://www2.dpi.qld.gov.au/environment/1240.html> >.
- Ritchie JT, (1972). Model for predicting evaporation from a row crop with incomplete cover. *Water Resour. Res.* 8, 1204-1213.
- Sanders PR, Lott SC, Watts P, Tucker RW, Casey KD and Lyndon K (1994). Lot fed cattle water consumption. Report 12.A. Meat Research Corporation Project No. DAQ.079, Queensland Department of Primary Industries and Feedlot Services Australia, Jul 1994, Toowoomba, QLD.
- SCARM, (1997). National Guidelines for Beef Cattle Feedlots in Australia. Standing Committee on Agricultural and Resource Management, CSIRO, Collingwood, Vic.
- Sharpley AN, and JR Williams, (1990a). EPIC: Erosion/Productivity Impact Calculator 1. Model Documentation. *Technical Bulletin 1768*. U.S. Department of Agriculture.
- Sharpley AN, and JR Williams, (1990b). EPIC: Erosion/Productivity Impact Calculator 2. User Manual. *Technical Bulletin 1768*. U.S. Department of Agriculture.
- Shaw RJ & Thorburn PJ, (1985). Prediction of leaching fraction from soil properties, irrigation water and rainfall. *Irrigation Science*, 6:73–83.
- Sinclair SE (1997). Effects of ration modification on production and characteristics of manure from feedlot cattle - (1) Phosphorus levels. *Report to the Cattle and Beef Industry CRC Sub-Program 6 - Feedlot Waste Management*, Queensland Department of Primary Industries, Brisbane, Qld.
- Skerman A (2005). Reference manual for the establishment and operation of beef cattle feedlots in Queensland. Department of Primary Industries and Fisheries, QLD.
- Suppiah R, Hennessy KJ, Whetton PH, McInnes K, Macadam I, Bathols J, Ricketts J, and Page CM, (2007a). Australian climate change projections derived from the simulations performed by the IPCC 4th Assessment Report. *Aust. Met. Mag.*, 56, 131-152.
- Suppiah R, Macadam I and Whetton PH, (2007b). Climate Change Projections for the Tropical Rainforest Region of North Queensland. Unpublished report to the Marine and Tropical Sciences Research Facility. Reef and Rainforest Research Centre Limited, Cairns (38pp.).
- Taylor KE, RJ Stouffer, GA Meehl, (2012). An Overview of CMIP5 and the experiment design. *Bull. Amer. Meteor. Soc.*, 93, 485-498, doi:10.1175/BAMS-D-11-00094.1.
- Thompson RB, Ryden JC and Lockyer DR, (1987). Fate of nitrogen in cattle slurry following surface application or injection to grassland. *Journal of Soil Science*, 38: 689–700.
- Tucker RW, Davis RJ, Scobie MJ, Watts PJ, Trigger RZ, Poad GD and O’Keefe MF (2010). Determination of effluent volumes and reliability, effluent characterisation and feedlot water requirements. B.FLT.0348 Milestone 2 report, Meat and Livestock Australia Limited, Sydney NSW.

- USDA-SCS, (1972). National Engineering Handbook. Hydrology Section 4, Chapters 4-10. Washington, D.C.: USDA.
- USSL (United States Salinity Laboratory), (1954). Diagnosis and improvement of saline and alkali soils. *Agricultural Handbook No. 60*, US Department of Agriculture, US Government Printer, Washington.
- van Sliedregt H, McGahan EJ & Casey KD (2000), *Predicting waste production from feedlot cattle*, Unpublished Confidential Report prepared for Cattle and Beef CRC (Meat Quality) Sub-program 6 - Feedlot Waste Management, August 2000, DPI Intensive Livestock Environmental Management Services, Toowoomba, Qld.
- Vergara W, AM Deeb, AM Valencia, RS Bradley, B Francou, A Zarzar, A Grünwaldt, and S M. Haeussling (2007). Economic impacts of rapid glacier retreat in the Andes, *EOS transactions AGU*, 88, 261.
- Waichler SR, MS Wigmosta, (2003). Development of Hourly Meteorological Values From Daily Data and Significance to Hydrological Modeling at H. J. Andrews Experimental Forest. *Journal of Hydrometeorology*, 4(2): 251-263.
- Watts PJ, Gardner EA, Tucker RW & Casey KD, (1994). Mass-balance approach to design of nutrient management systems at cattle feedlots. Proceedings of the Great Plains Animal Waste Conference on Confined Animal Production and Water Quality: Balancing Animal Production and the Environment, Denver, Colorado, p 27-33.
- Watts PJ and McKay ME, (1986). Simulation of cattle feedlot hydrology. *Proceedings of the Conference on Agricultural Engineering*, Bundaberg, 1986. Pp. 393-398. Canberra, Australia: Institution of Engineers, Australia.
- Watts PJ, Ni Cheallaigh A, Valentine JG, Tucker RW and O'Keefe MF (2012). Environmental performance review of Australian feedlots. B.FLT.0468 Final report, Meat and Livestock Australia Limited, Sydney NSW.
- Weeks WD, (1983). The calculation of evaporation in Queensland. *I.E Aust. QLD Div. Tech. Papers*, 24 (4):1-5.
- Western Australian Lot Feeders' Association (2002). Guidelines for the environmental management of beef cattle feedlots in Western Australia. Bulletin (Western Australia. Dept. of Agriculture).
- Whetton PH, K McInnes, RN Jones, KJ Hennessy, R Suppiah, CM Page, J Bathols, and P Durack (2005). Climate change projections for Australia for impact assessment and policy application: A review. CSIRO Technical Paper. 001, Aspendale, Vic., CSIRO Marine and Atmospheric Research, 34p.
- Winchester CF and Morris MJ, (1956). Water intake rates of cattle. *Journal of Animal Science*, 15:722-740.

8 Appendices

A separate companion volume to this report has been prepared with appendices covering the following topics.

Appendix 1 provides additional material on the approach to selection of feedlot locations used for modelling.

Appendix 2 provides additional detailed material on the selection of climate models and their assessment for suitability for this project.

Appendix 3 provides a detailed description of the MEDLI modelling framework and the feedlot module.

Appendix 4 provides additional tables and plots of results from heat load modelling.